UNDERSTANDING THE COMPLEXITY OF IXODES SCAPULARIS AND AMBLYOMMA AMERICANUM TICK FEEDING THROUGH PROTEOMICS FOR A MULTI-ANTIGEN VACCINE DESIGN

A Dissertation

by

TAE KWON KIM

Submitted to the Office of Graduate and Professional Studies of
Texas A&M University
in partial fulfillment of the requirements for the degree of

DOCTOR OF PHILOSOPHY

Chair of Committee,	Albert Mulenga
Committee Members,	Leslie Garry Adams
	Karen Snowden
	Waithaka Mwangi
	Jon Skare
Head of Department,	Ramesh Vemulapalli

August 2019

Major Subject: Biomedical Sciences

ABSTRACT

Tick saliva proteins facilitate feeding success and transmission of tick-borne disease agents by ticks, and thus, they might serve as effective antigens for a tick vaccine. This dissertation for the first-time identifies saliva proteins that are secreted every 24 h during tick-feeding of two distantly-related and most medically important ticks species in the United States, *Ixodes scapularis* and *Amblyomma americanum*. Data in this dissertation reveal that tick feeding is a complex system that is dynamically changing in response to the host defenses. Understanding biological functional roles of tick saliva proteins is critical to developing novel methods to prevent tick-borne disease infections. Therefore, the second part of this dissertation defines the functional roles of three serine protease inhibitors (serpins: AAS19, AAS41 and AAS46), which are thought to control serine proteases that mediate host defense mechanisms. While these serpins are secreted into the host during feeding and are immunogenic, only AAS19 and AAS41 were functionally active, having anti-hemostatic or anti-inflammatory properties, respectively. The finding that despite being 97% identical to AAS41, AAS46 is apparently not an efficient inhibitor provides insights into how the tick might evade host defenses: it is possible that ticks secrete AAS46 as an immune decoy to protect the functional AAS41 from immune attack. Finally, information generated from this dissertation was utilized to formulate a cocktail anti-tick vaccine that included 13 recombinant tick saliva proteins. Although these antigens elicited an immune response in immunized cattle, they did not protect cattle against primary tick infestations; however, immunization enhanced the naturally acquired immunity against tick feeding that is elicited by repeated infestation. This dissertation contributes to a better understanding of the molecular basis of tick-feeding physiology, which is the needed first step before novel tick control methods can be developed. Results from

this dissertation have contributed to our understanding of the molecular basis of tick feeding physiology and will serve as foundation to formulate an effective tick-antigen based vaccine to prevent tick-borne disease transmission.

DEDICATION

This work is dedicated to my father, mother and brother who have supported me throughout the whole process. Without them this would not have been possible.

ACKNOWLEDGEMENTS

I would like to graciously thank my committee chair, Dr. Albert Mulenga for truly opening the doors for me to join his lab. It's been over 10 years since I began as an undergraduate research student in Dr. Mulenga's lab and I have gained a lot of skillsets and life lessons over these years. Dr. Mulenga has been a great mentor by providing me the guidance and wisdom not only in science but also in many aspects of life.

I would also like to thank my amazing committee members, Dr. Karen Snowden, who has been there for me since my master's training and continued to be a great mentor during my doctorate training. Dr. Garry Adams, for his one-one discussions to help dig deep down into the root of things to build me to think as a future scientist. Dr. Waithaika Mwangi for his great mentorship and advice on the immunological aspects of vaccine development. Dr. Jon Skare for his collaborations with the Mulenga lab and introducing me to the field of tick-borne disease agents. I have been very honored to have the guidance and support from a great group of scientists throughout the course of my doctorate training.

I could not have achieved this goal without the help of the College of Veterinary Medicine and Department of Veterinary Pathobiology at Texas A&M University. The faculty, advisors, staff and students have all been excellent in providing a great environment for graduate studies.

Most importantly, I would like to thank my mom for all the love, encouragement and support she has provided me to be who I am right now. She is a very strong-willed person and a great role model.

CONTRIBUTORS AND FUNDING SOURCES

Contributors:

This work was supervised by a dissertation committee consisting of Dr. Albert Mulenga, Dr. Leslie Gary Adams, and Dr. Karen Snowden from Texas A&M University, College of Veterinary Medicine, Department of Veterinary Pathobiology; Dr. Jon Skare, Texas A&M University, College of Medicine, Department of Microbial Pathogenesis and Immunology; and Dr. Waithaka Mwangi, Kansas State University, College of Veterinary Medicine.

The data collection for Chapter 2 was made possible by contributions from Dr. John Yates III, Dr. James Moresco, Dr. Antonio Pinto, and Dr. Jolene Diedrich from The Scripps Research Institute in La Jolla, CA; Dr. Lucas Tirloni, from Texas A&M University, College of Veterinary Medicine, Department of Veterinary Pathobiology; and Dr. Itabajara da Silva Vaz from Universidade Federal do Rio Grande do Sul, Porto Alegre, Brazil.

The data collection for Chapter 3 was made possible by contributions from Dr. Lucas Tirloni from Texas A&M University, College of Veterinary Medicine, Department of Veterinary Pathobiology; Dr. Markus Berger from Hospital de Clinicas de Porto Alegre, Centro de Pesquisa Experimental, Porto Alegre, Brazil; Dr. Carlos Logullo from Instiuto de Biodversidade e Sustentabilidade, Universidade Federal do Rio de Janeiro, Macae, Brazil; and Dr. Itabajara da Silva Vaz and Dr. Carlos Termignoni from Universidade Federal do Rio Grande do Sul, Porto Alegre, Brazil.

The animal handling for Chapter 4 was made possible by contributions from Dr. Clay Ashley, Norman Ellison, Destiny Taylor, Clint Taylor, Melissa Walker, Jud Perry, and Gene Wood at Texas A&M University, College of Veterinary Medicine, Veterinary Medical Park.

Animal work done using rabbits was made possible by contributions from Dr. Vincent Gresham, Andrea Moss, and Kelsey Johnson at Texas A&M University, Comparative Medicine Program, Laboratory Animal Resources and Research

All other work and analyses conducted for the dissertation was completed by the student independently.

Funding Sources

This work was financially supported by US Public Health Service/National Institutes of Health Grants and USDA, and Texas A&M AgriLife awarded to Dr. Albert Mulenga.

NOMENCLATURE

AAS4	*Amblyomma americanum* serpin 4
AAS6	*Amblyomma americanum* serpin 6
AAS19	*Amblyomma americanum* serpin 19
AAS27	*Amblyomma americanum* serpin 27
AAS41	*Amblyomma americanum* serpin 41
AAS46	*Amblyomma americanum* serpin 46
Ach	Acidic chitinase
AV422	Cross-species conserved tick saliva protein
CRT	Calreticulin
EMPRIN	Extracellular metalloprotease secretion inducing protein
HRF	Histamine release factor
IGFBP	Insulin growth factor binding protein-like
TCI	Tick carboxypeptidase inhibitor
Serpin	Serine protease inhibitor
TSP	Tick salivary protein

TABLE OF CONTENTS

CHAPTER I

INTRODUCTION

Ticks and Tick-Borne Diseases

Ticks are hematophagous obligate ectoparasites that have a wide range of hosts such as mammals, birds, reptiles, and amphibians (Sonenshine and Roe, 2014). With approximately 900 species identified, ticks are ubiquitously found throughout many regions of the world. They are classified in the Kingdom Animalia, Phylum Arthropoda, Class Arachnida, Subclass Acari, Superorder Parasitiformes, and Order Ixodida. Ticks are further divided into three Families as Ixodidae (hard-bodied ticks), Argasidae (soft-bodied ticks) and a single species containing Nuttalliellidae. Within the Family Ixodidae, hard ticks have been further divided into Prostriata and Metastriata groups based on the presence of a morphological feature termed the anal groove, which is located above the anus, for the former, and below, for the latter. The Prostriata comprise of only a single genus, *Ixodes*, while the remaining genera of hard ticks, *Amblyomma*, *Rhipicephalus* (*Boophilus*), *Dermacentor*, *Hyalomma*, *Haemaphysalis*, have been grouped in Metastriata. It has been proposed that host adaptation has played a major role in tick evolution leading to cospeciation between the tick and their hosts (Hoogstraal and Kim, 1982, Black and Peisman, 1994, Sonenshine and Roe, 2014). Of the three families, Ixodidae have been widely studied and have shown to transmit a great number of important pathogens including viruses, bacteria, protozoa and fungi that affect human and veterinary medicine (Jongejan and Uilenberg, 2004, Sonenshine and Roe, 2014).

Ticks have gained the attention in public health policy with a recent publication that advocated for One Health solutions listing 17 human tick-borne diseases (TBDs) among sources

of human health concerns (Dantas-Torres et al., 2012). Moreover, the dramatic rise related to ticks and TBDs have caught the attention of U.S. lawmakers, and recently passed the 21st Century Cures Act of 2016 which created the Tick-Borne Disease Working Group. Under the Cures Act, the Tick-Borne Disease Working Group was tasked with evaluating the impact of tick-borne diseases and required research to find solutions (www.hhs.gov).

In livestock production, ticks and TBDs have caused annual losses in billions of U.S. dollars globally (Grisi et al., 2014, Jongejan and Uilenberg, 2004). Likewise, of the 23 human vector borne diseases that are listed by the World Health Organization, six (Crimean-Congo haemorrhagic fever, Lyme disease, relapsing fever, rickettsial diseases (spotted fever and Q fever), tick-borne encephalitis, and tularemia) are tick-borne (http://www.who.int/news-room/fact-sheets/detail/vector-borne-diseases: reported on October 31 2017). In the United States of America (USA), two tick species, *Ixodes scapularis,* commonly known as the deer tick or blacklegged tick, and *Amblyomma americanum,* the lone star tick (focus organisms of this doctorate dissertation) are among important tick species of medical and veterinary health significance.

Ixodes scapularis is among the most medically important tick species known to transmit 6 of the 16 human TBD agents in the USA: *Borrelia burgdorferi* sensu stricto (Burgdorfer et al., 1982), *Anaplasma phagocytophilum* (Levin and Ross, 2004), *Borrelia miyamotoi* (Crowder et al., 2014), *Babesia microti* (Prusinski et al., 2014), *Ehrlichia* spp.-like (Pritt et al., 2011) and Powassan virus (Dupuis et al., 2013). Additionally, close relatives of this tick including *I. pacificus* on the west coast of the USA and *I. ricinus* in Europe are vectors of important human TBD agents including *B. burgdorferi* sensu lato isolates, *B. miyamotoi,* and *A. phagocytophilum* (Rizzoli et al., 2004).

Likewise, *A. americanum* is involved in transmission of multiple human and animal disease agents. In public health, *A. americanum* is the principal vector for *Ehrlichia chaffensis*, the causative agent of human monocytic ehrlichiosis (Anderson et al., 1993), and *E. ewingii*, which also causes ehrlichiosis in humans, referred to as human granulocytic ehrlichiosis (Murphy et al., 1998, Buller et al., 1999, Wolf et al., 2000). This tick also transmits *Francisella tularensis*, the causative agent for Tularemia (Hopla et al., 1953, Taylor et al., 1991), a yet to be described disease agent, suspected as *Borrelia lonestari*, which causes Lyme disease-like symptoms referred to as southern tick associated rash illness (STARI) (Armstrong et al., 2001, James et al., 2001), and also an *E. ruminantium*-like organism referred to as the Panola Mountain *Ehrlichia* (PME) (Reeves et al., 2008, Yabsley et al., 2008). There is also evidence that *A. americanum* may transmit *Rickettsia amblyommii*, *R. rickettsia, and R. parkeri*, the causative agent to rickettsiosis to humans (Apperson et al., 2008, Breitschwerdt, et al., 2011). This tick has also been reported to transmit the Heartland and Bourbon viruses to humans (McMullan et al., 2012, Savage et al., 2013). Most recently, this tick has been shown to be responsible for causing an α-gal allergy or mammalian meat allergy (MMA) to humans upon a tick bite (Steinke et al., 2015). In veterinary health, *A. americanum* transmits *Theileria cervi* to deer (Laird et al., 1988), and *E. ewingii* to dogs (Little et al., 2010). There are reports of mortality in deer fawns that were attributed to a combination of heavy *A. americanum* infestation and *T. cervi* infections (Yabsley et al., 2005). In livestock production, heavy infestations were thought to cause low productivity in cattle (Barnard 1985, Tolleson et al., 2010). With over 83% reported cases of human tick infestations, *A. americanum* is the most dominant tick species that bites humans in the Southern USA (Felz et al., 1996).

Tick Control and Prevention of Tick-Borne Diseases

In absence of effective vaccines against TBD agents, controlling ticks using acaricides remains the most reliable method (Piesman and Eisen, 2008, Hoen et al., 2009). Although effective in the short term, limitations of chemical acaricides such as selecting resistant tick populations, costs in new acaricide development, environmental and food contamination have necessitated the search for alternative tick control methods (Jongejan and Uilenberg, 1994, George et al., 2004). Immunization of animals has been advocated as a sustainable alternative tick control method (Allen and Humphreys, 1979, Mulenga et al., 2001, Willadsen, 2006). The rationale is that anti-tick vaccines will be effective against both acaricide susceptible and resistant tick populations (Mulenga et al., 1999, Mulenga et al., 2001, Willadsen, 2004, Merino et al., 2013). Commercialization of the vaccine against *Rhipicephalus* (*Boophilus*) *microplus*, the cattle tick, validated the feasibility of controlling ticks through immunization (Allen and Humphreys, 1979, Willadsen et al., 1995). Weaknesses of the *R. microplus* vaccine including effectiveness against one tick species (Rodriguez et al., 1995a, Rodriguez et al., 1995b, Garcia-Garcia et al., 2000), necessitates the search for effective target anti-tick vaccine antigens with potential to control multiple tick species (Mulenga et al., 2013).

The concept of immunization against tick feeding was borne out of a research study showing that repeated infestations with *D. variabilis* larvae and nymphs provoked tick feeding resistance in rabbits (Trager 1939a, 1939b). These findings were later confirmed by several investigators for other tick species that fed on different animals (Bowessidjaou et al., 1977, Brown and Knapp, 1981, Brown et al., 1984a, Latif et al., 1988, Brossard and Papateodorou, 1990, Barriga et al., 1991, Gebbia et al., 1995). Further work confirmed that immunization of animals with tick salivary gland extracts conferred protective immunity against tick feeding as revealed by reduced

tick fitness, reduced fecundity, and increased mortality in *A. americanum* (Brown et al., 1984b), *Dermacentor andersoni* (Wikel, 1981), *R. microplus* (Jittapalapong et al., 2008, Nikpay and Nabian, 2016), *Ornithodoros moubata*, *O. erraticus* (Astigarraga et al., 1995), and *Hyalomma anatolicum* (Manohar and Banerjee, 1992). The major limitation toward global adoption of anti-tick vaccines as an alternative tick control method is identification of effective target antigens. To create successful anti-tick vaccines, knowledge of the molecular mechanisms involved in tick feeding biology and physiology must advance. This knowledge will result in discovery of weak links in tick biology that can be targeted for tick vaccine development. For my doctorate dissertation, I was interested in understanding tick feeding physiology as a means to identify physiologically important proteins that can be targeted in tick vaccine development.

Tick Feeding Physiology

Ticks undergo three developmental stages; specifically, the larva, nymph, and adult. Depending on species, ticks have evolved to complete the developmental cycle by parasitizing one-, two-, or three- hosts (Sonenshine and Roe, 2014). *I. scapularis* and *A. americanum* are both three-host ticks in which they may acquire a different host after every developmental stage. Hard ticks generally share a similar behavioral sequence of events that has been mapped in to six broad phases to successfully feed and reproduce (Walade and Rice, 1982, Sonenshine, 1993). The behavioral process of tick feeding begins with the *pre-appetence phase*, when a newly hatched larva or newly molted nymph or an adult tick shows no desire to feed. Subsequently, over a period of days to weeks when conditions are optimal the tick transitions to the *appetence phase* where they attain appetence and begin to display host-seeking behaviors. Upon engaging the host, the tick transitions into the *pre-feeding phase*, when it probes around and select a suitable feeding site

on its host. Upon engaging the host, the tick feeding process proceeds through three broad phases: *preparatory feeding phase* during the first 24-36 h of attachment when the tick attaches onto the host by secreting tick saliva proteins into the host, along with an adhesive substance called tick cement, which aids in staying attached onto its host skin and in creating the feeding lesion. In the *prepartatory feeding phase* the tick takes in little to no blood meal and it is speculated that the tick conditions the host for TBD agent colonization. This is followed by the *slow feeding phase* (proceeds through 120 h of attachment) when the tick starts to take in host blood, transmit major TBD agents (Piesman et al., 1987, Ribeiro et al., 1987, Piesman et al., 1991, Katavolos et al., 1998, Ebel and Kramer 2004), undergoes neosomy (grow more tissue) to prepare its body for taking in massive amounts of blood for the *rapid feeding phase* when it feeds to repletion and detaches during the last 24 h of the feeding process.

Unlike other ectoparasites, hard ticks feed for days to weeks. Ticks feed by disrupting host tissue using a pair of shear-like apparatus termed the chelicerae and sucking up blood that accumulates into the feeding lesion. This in turn provokes host defense responses, including pain, hemostasis (to limit blood loss), inflammation, complement activation (to protect against invading microbial organisms), and tissue repair responses (to heal the feeding lesion) (Ribeiro, 1987, Ribeiro and Francischetti, 2003, Francischetti et al., 2009). To date, some proteins derived from tick saliva have been identified, which have a direct role at the feeding site, allowing the tick to fend off host defenses and successfully acquire its blood meal (Steen et al., 2006, Maritz-Olivier et al., 2007). For instance, serine proteases mediate some host defense pathways to tick feeding and are controlled by inhibitors belonging to serine protease inhibitors (serpins) family (Gettins, 2002, Huntington, 2006, Rau et al., 2007). From this perspective, it is proposed that ticks inject serpins into the host to mediate evasion from host defenses and thus they could be suitable targets

for anti-tick vaccines (Mulenga et al., 2001). Following a blood meal acquisition, it is also necessary that blood remains fluid for subsequent digestion, in which different tick proteins have been described acting as anticoagulant molecules in the tick midgut (Ricci et al., 2007, Anderson et al., 2008, Liao et al., 2009).

In addition to blood meal acquisition, tick saliva proteins are also involved with the transmission and acquisition of TBD agents (Nuttall and Labuda, 2004). Reports of reduced pathogen transmission to repeatedly tick infested animals that developed resistance to tick feeding (Bell et al., 1979, Jones and Nuttall, 1990, Nazario et al., 1998, Burke et al., 2005) provide credence to the importance of tick saliva proteins in tick vector competence. Thus, identification of tick saliva proteins will provide a basis for development of novel methods to interfere with tick feeding and prevention of pathogen transmission. On this basis, the *I. scapularis* genome was sequenced (Gulia-Nuss et al., 2016, Miller et al., 2018) and these data have provided opportunities for in-depth studies of biological adaptations that make ticks successful vectors of pathogens. These data were postulated to facilitate studies that will reveal biochemical targets that can be developed for novel tick control methods (Hill et al., 2005). Towards discovery of tick genes that regulate the initial stages of tick feeding, subtractive hybridization analysis was used to identify genes that were differentially up regulated in *A. americanum* (Mulenga et al., 2007), *I. scapularis* (Xu et al., 2005), *I. ricinus* (Leboulle et al., 2002, Rudenko et al., 2005), *R. microplus* (Lew-Tabor et al., 2010), and *R. haemaphysaloides* (Xiang et al., 2012) that were stimulated upon the start of feeding. With the advent of next-generation sequencing (NGS) technologies, tick salivary gland transcriptomes have been described (Francischetti et al., 2009, 2005, 2008a, 2008b, 2011, Karim et al., 2011, Karim and Ribeiro, 2015, Garcia et al., 2014, Kotsyfakis et al., 2015, Schwarz et al., 2013, 2014, Ribeiro et al., 2011, 2012, Moreira et al., 2017, Esteves et al., 2017, Antunes et al.,

2018). However, the major limitation of transcriptomic-based studies is that it does not inform on transcripts that encode for proteins that are secreted in tick saliva. In an interesting approach to identify secreted tick salivary proteins (TSPs), Mulenga et al., (1999) used antibodies from rabbits that were repeatedly infested with larvae, nymph and adult *H. longicornis* tick stages to screen phage display cDNA expression libraries. Similar screening approaches were used to identify immunodominant *I. scapularis* TSPs (Das et al., 2000, 2001). However, these studies were limited to identifying very few TSPs. To improve on identifying more immunogenic TSPs, Radulovic et al., (2014) and Lewis et al., (2015) used immunoscreening methods combined with high throughput NGS sequencing to identify 24-48 h *A. americanum* and 24 h *I. scapularis* immunogenic tick saliva proteins, respectively. In a related study, Edman degradation of *I. scapularis* saliva identified 15 proteins consisting of protease inhibitors, proteases, histamine binding proteins and proteins of unknown function (Valenzuela et al., 2002). Recently proteins in saliva of ixodid ticks from replete fed *Rhipicephalus sanguineus* (Oliveira et al., 2013), partial and replete fed *R. microplus* (Tirloni et al., 2014), three and five day fed *D. andersoni* (Mudenda et al., 2014), and replete fed adult and nymph *H. longicornis* (Tirloni et al., 2015) were identified. In argasid ticks, a lone study identified saliva proteins from twice fed *O. moubata* ticks with saliva collected after four months from feeding (Diaz-Martin et al., 2013). Whereas studies reviewed here identified proteins in saliva of ticks at one or two feeding time points, this dissertation focused on identifying proteins that *I. scapularis* and *A. americanum* ticks likely inject into animals every 24 h during feeding and toward the end of the tick feeding process. In the literature, apart from housekeeping proteins, amino acid identity levels between the Prostriata (*I. scapularis*) and Metastriata (*A. americanum*) are low. Therefore, identification of TSPs from two distantly related

tick species will provide an in-depth view of families of proteins and/or molecular systems that are conserved between *I. scapularis* and *A. americanum* ticks at the host interface.

Significance of Research

This doctorate degree dissertation research contributes by providing insight on the role(s) of TSPs in tick feeding physiology. To attempt at identifying important TSPs that might be important to all tick species, an approach to compare the salivary proteins utilized by the two distantly related tick species, *I. scapularis* and *A. americanum* was adopted. This dissertation provides comprehensive information on the molecules that play key roles in tick feeding, and thus sets a strong foundation toward identification of ideal targets to develop a tick-antigen based vaccine to prevent tick-borne disease infections.

References

Allen, J.R., Humphreys, S.J., 1979. Immunisation of guinea pigs and cattle against ticks. Nature 280, 491-493.

Anderson, B.E., Sims, K.G., Olson, J.G., Childs, J.E., Piesman, J.F., Happ, C.M., Maupin, G.O., Johnson, B.J., 1993. *Amblyomma americanum*: a potential vector of human ehrlichiosis. Am. J. Trop. Med. Hyg. 49, 239-244.

Anderson, J.M., Sonenshine, D.E., Valenzuela, J.G., 2008. Exploring the mialome of ticks: an annotated catalogue of midgut transcripts from the hard tick, *Dermacentor variabilis* (Acari: Ixodidae). BMC Genomics 9, 552.

Antunes, S., Couto, J., Ferrolho, J., Rodrigues, F., Nobre, J., Santos, A.S., Santos-Silva, M.M., de la Fuente, J., Domingos, A., 2018. *Rhipicephalus bursa* sialotranscriptomic response to blood feeding and *Babesia ovis* infection: identification of candidate protective antigens. Front. Cell. Infect. Microbiol. 8, 116.

Apperson, C.S., Engber, B., Nicholson, W.L., Mead, D.G., Engel, J., Yabsley, M.J., Dail, K., Johnson, J., Watson, D.W., 2008. Tick-borne diseases in North Carolina: is "*Rickettsia amblyommii*" a possible cause of rickettsiosis reported as Rocky Mountain spotted fever? Vector Borne Zoonotic Dis. 8, 597-606.

Armstrong, P.M., Brunet, L.R., Spielman, A., Telford, S.R.,3rd, 2001. Risk of Lyme disease: perceptions of residents of a Lone Star tick-infested community. Bull. World Health Organ. 79, 916-925.

Astigarraga, A., Oleaga-Perez, A., Perez-Sanchez, R., Encinas-Grandes, A., 1995. A study of the vaccinal value of various extracts of concealed antigens and salivary gland extracts against *Ornithodoros erraticus* and *Ornithodoros moubata*. Vet. Parasitol. 60, 133-147.

Barnard, D.R., 1985. Injury thresholds and production loss functions for the lone star tick, *Amblyomma americanum* (Acari: Ixodidae), on pastured, preweaner beef cattle, *Bos taurus*. J. Econ. Entomol. 78, 852-855.

Barriga, O.O., Andujar, F., Andrzejewski, W.J., 1991. Manifestations of immunity in sheep repeatedly infested with *Amblyomma americanum* ticks. J. Parasitol. 77, 703-709.

Bell, J.F., Stewart, S.J., Wikel, S.K., 1979. Resistance to tick-borne *Francisella tularensis* by tick-sensitized rabbits: allergic klendusity. Am. J. Trop. Med. Hyg. 28, 876-880.

Black, W.C.,4th, Piesman, J., 1994. Phylogeny of hard- and soft-tick taxa (Acari: Ixodida) based on mitochondrial 16S rDNA sequences. Proc. Natl. Acad. Sci. U. S. A. 91, 10034-10038.

Bowessidjaou, J., Brossard, M., Aeschlimann, A., 1977. Effects and duration of resistance acquired by rabbits on feeding and egg laying in *Ixodes ricinus* L. Experientia 33, 528-530.

Breitschwerdt, E.B., Hegarty, B.C., Maggi, R.G., Lantos, P.M., Aslett, D.M., Bradley, J.M., 2011. *Rickettsia rickettsii* transmission by a lone star tick, North Carolina. Emerg. Infect. Dis. 17, 873-875.

Brossard, M., Papatheodorou, V., 1990. Immunity against female *Ixodes ricinus* L.: effect on feeding and haemoglobin digestion. Ann. Parasitol. Hum. Comp. 65, 32-36.

Brown, S.J., Knapp, F.W., 1981. Response of hypersensitized guinea pigs to the feeding of *Amblyomma americanum* ticks. Parasitology 83, 213-223.

Brown, S.J., Barker, R.W., Askenase, P.W., 1984a. Bovine resistance to *Amblyomma americanum* ticks: an acquired immune response characterized by cutaneous basophil infiltrates. Vet. Parasitol. 16, 147-165.

Brown, S.J., Shapiro, S.Z., Askenase, P.W., 1984b. Characterization of tick antigens inducing host immune resistance. I. Immunization of guinea pigs with *Amblyomma americanum*-derived salivary gland extracts and identification of an important salivary gland protein antigen with guinea pig anti-tick antibodies. J. Immunol. 133, 3319-3325.

Buller, R.S., Arens, M., Hmiel, S.P., Paddock, C.D., Sumner, J.W., Rikhisa, Y., Unver, A., Gaudreault-Keener, M., Manian, F.A., Liddell, A.M., Schmulewitz, N., Storch, G.A., 1999. *Ehrlichia ewingii*, a newly recognized agent of human ehrlichiosis. N. Engl. J. Med. 341, 148-155.

Burgdorfer, W., Barbour, A.G., Hayes, S.F., Benach, J.L., Grunwaldt, E., Davis, J.P., 1982. Lyme disease-a tick-borne spirochetosis? Science 216, 1317-1319.

Burke, G., Wikel, S.K., Spielman, A., Telford, S.R., McKay, K., Krause, P.J., Tick-borne Infection Study Group, 2005. Hypersensitivity to ticks and Lyme disease risk. Emerg. Infect. Dis. 11, 36-41.

Crowder, C.D., Carolan, H.E., Rounds, M.A., Honig, V., Mothes, B., Haag, H., Nolte, O., Luft, B.J., Grubhoffer, L., Ecker, D.J., Schutzer, S.E., Eshoo, M.W., 2014. Prevalence of *Borrelia miyamotoi* in *Ixodes* ticks in Europe and the United States. Emerg. Infect. Dis. 20, 1678-1682.

Das, S., Marcantonio, N., Deponte, K., Telford, S.R.,3rd, Anderson, J.F., Kantor, F.S., Fikrig, E., 2000. SALP16, a gene induced in *Ixodes scapularis* salivary glands during tick feeding. Am. J. Trop. Med. Hyg. 62, 99-105.

Das, S., Banerjee, G., DePonte, K., Marcantonio, N., Kantor, F.S., Fikrig, E., 2001. Salp25D, an *Ixodes scapularis* antioxidant, is 1 of 14 immunodominant antigens in engorged tick salivary glands. J. Infect. Dis. 184, 1056-1064.

Dantas-Torres, F., Chomel, B.B., Otranto, D., 2012. Ticks and tick-borne diseases: a One Health perspective. Trends Parasitol. 28, 437-446.

Diaz-Martin, V., Manzano-Roman, R., Valero, L., Oleaga, A., Encinas-Grandes, A., Perez-Sanchez, R., 2013. An insight into the proteome of the saliva of the argasid tick *Ornithodoros*

moubata reveals important differences in saliva protein composition between the sexes. J. Proteomics 80, 216-235.

Dupuis, A.P.,2nd, Peters, R.J., Prusinski, M.A., Falco, R.C., Ostfeld, R.S., Kramer, L.D., 2013. Isolation of deer tick virus (Powassan virus, lineage II) from *Ixodes scapularis* and detection of antibody in vertebrate hosts sampled in the Hudson Valley, New York State. Parasit. Vectors 6, 185.

Ebel, G.D., Kramer, L.D., 2004. Short report: duration of tick attachment required for transmission of powassan virus by deer ticks. Am. J. Trop. Med. Hyg. 71, 268-271.

Esteves, E., Maruyama, S.R., Kawahara, R., Fujita, A., Martins, L.A., Righi, A.A., Costa, F.B., Palmisano, G., Labruna, M.B., Sa-Nunes, A., Ribeiro, J.M.C., Fogaca, A.C., 2017. Analysis of the salivary gland transcriptome of unfed and partially fed *Amblyomma sculptum* ticks and descriptive proteome of the saliva. Front. Cell. Infect. Microbiol. 7, 476.

Felz, M.W., Durden, L.A., Oliver, J.H.J., 1996. Ticks parasitizing humans in Georgia and South Carolina. J. Parasitol. 82,3, 505-508.

Francischetti, I.M., My Pham, V., Mans, B.J., Andersen, J.F., Mather, T.N., Lane, R.S., Ribeiro, J.M., 2005. The transcriptome of the salivary glands of the female western black-legged tick *Ixodes pacificus* (Acari: Ixodidae). Insect Biochem. Mol. Biol. 35, 1142-1161.

Francischetti, I.M., Sa-Nunes, A., Mans, B.J., Santos, I.M., Ribeiro, J.M., 2009. The role of saliva in tick feeding. Front. Biosci. (Landmark Ed) 14, 2051-2088.

Francischetti, I.M., Mans, B.J., Meng, Z., Gudderra, N., Veenstra, T.D., Pham, V.M., Ribeiro, J.M., 2008a. An insight into the sialome of the soft tick, *Ornithodorus parkeri*. Insect Biochem. Mol. Biol. 38, 1-21.

Francischetti, I.M., Meng, Z., Mans, B.J., Gudderra, N., Hall, M., Veenstra, T.D., Pham, V.M., Kotsyfakis, M., Ribeiro, J.M., 2008b. An insight into the salivary transcriptome and proteome of the soft tick and vector of epizootic bovine abortion, *Ornithodoros coriaceus*. J. Proteomics 71, 493-512.

Francischetti, I.M., Anderson, J.M., Manoukis, N., Pham, V.M., Ribeiro, J.M., 2011. An insight into the sialotranscriptome and proteome of the coarse bontlegged tick, *Hyalomma marginatum rufipes*. J. Proteomics 74, 2892-2908.

Garcia, G.R., Gardinassi, L.G., Ribeiro, J.M., Anatriello, E., Ferreira, B.R., Moreira, H.N., Mafra, C., Martins, M.M., Szabo, M.P., de Miranda-Santos, I.K., Maruyama, S.R., 2014. The sialotranscriptome of *Amblyomma triste, Amblyomma parvum* and *Amblyomma cajennense* ticks, uncovered by 454-based RNA-seq. Parasit. Vectors 7, 430.

Garcia-Garcia, J.C., Montero, C., Redondo, M., Vargas, M., Canales, M., Boue, O., Rodriguez, M., Joglar, M., Machado, H., Gonzalez, I.L., Valdes, M., Mendez, L., de la Fuente, J., 2000.

Control of ticks resistant to immunization with Bm86 in cattle vaccinated with the recombinant antigen Bm95 isolated from the cattle tick, *Boophilus microplus*. Vaccine 18, 2275-2287.

Gebbia, J.A., Bosler, E.M., Evans, R.D., Schneider, E.M., 1995. Acquired resistance in dogs to repeated infestation with *Ixodes scapularis* (Acari: Ixodidae) reduces tick viability and reproductive success. Exp. Appl. Acarol. 19, 593-605.

George, J.E., Pound, J.M., Davey, R.B., 2004. Chemical control of ticks on cattle and the resistance of these parasites to acaricides. Parasitology 129 Suppl, 353.

Gettins, P.G., 2002. Serpin structure, mechanism, and function. Chem. Rev. 102, 4751-4804.

Grisi, L., Leite, R.C., Martins, J.R., Barros, A.T., Andreotti, R., Cancado, P.H., Leon, A.A., Pereira, J.B., Villela, H.S., 2014. Reassessment of the potential economic impact of cattle parasites in Brazil. Rev. Bras. Parasitol. Vet. 23, 150-156.

Gulia-Nuss, M., Nuss, A.B., Meyer, J.M., Sonenshine, D.E., Roe, R.M., Waterhouse, R.M., Sattelle, D.B., de la Fuente, J., Ribeiro, J.M., Megy, K., Thimmapuram, J., Miller, J.R., Walenz, B.P., Koren, S., Hostetler, J.B., Thiagarajan, M., Joardar, V.S., Hannick, L.I., Bidwell, S., Hammond, M.P., Young, S., Zeng, Q., Abrudan, J.L., Almeida, F.C., Ayllon, N., Bhide, K., Bissinger, B.W., Bonzon-Kulichenko, E., Buckingham, S.D., Caffrey, D.R., Caimano, M.J., Croset, V., Driscoll, T., Gilbert, D., Gillespie, J.J., Giraldo-Calderon, G.I., Grabowski, J.M., Jiang, D., Khalil, S.M., Kim, D., Kocan, K.M., Koci, J., Kuhn, R.J., Kurtti, T.J., Lees, K., Lang, E.G., Kennedy, R.C., Kwon, H., Perera, R., Qi, Y., Radolf, J.D., Sakamoto, J.M., Sanchez-Gracia, A., Severo, M.S., Silverman, N., Simo, L., Tojo, M., Tornador, C., Van Zee, J.P., Vazquez, J., Vieira, F.G., Villar, M., Wespiser, A.R., Yang, Y., Zhu, J., Arensburger, P., Pietrantonio, P.V., Barker, S.C., Shao, R., Zdobnov, E.M., Hauser, F., Grimmelikhuijzen, C.J., Park, Y., Rozas, J., Benton, R., Pedra, J.H., Nelson, D.R., Unger, M.F., Tubio, J.M., Tu, Z., Robertson, H.M., Shumway, M., Sutton, G., Wortman, J.R., Lawson, D., Wikel, S.K., Nene, V.M., Fraser, C.M., Collins, F.H., Birren, B., Nelson, K.E., Caler, E., Hill, C.A., 2016. Genomic insights into the *Ixodes scapularis* tick vector of Lyme disease. Nat. Commun. 7, 10507.

Hill, C.A., Wikel, S.K., 2005. The *Ixodes scapularis* Genome Project: an opportunity for advancing tick research. Trends Parasiol. 21, 151-153.

Hoen, A.G., Rollend, L.G., Papero, M.A., Carroll, J.F., Daniels, T.J., Mather, T.N., Schulze, T.L., Stafford, K.C.,3rd, Fish, D., 2009. Effects of tick control by acaricide self-treatment of white-tailed deer on host-seeking tick infection prevalence and entomologic risk for *Ixodes scapularis*-borne pathogens. Vector Borne Zoonotic Dis. 9, 431-438.

Hoogstraal H, Aeschlimann A. (1982). Tick-host specificity. Mitt Schweiz Entomol Ges. 55:5–32.

Hopla CE, D.C., 1953. The isolation of *Bacterium tularense* from the tick *Amblyomma americanum.* J. Kans. Entomol. Soc. 26, 71-72.

Huntington, J.A., 2006. Shape-shifting serpins--advantages of a mobile mechanism. Trends Biochem. Sci. 31, 427-435.

James, A.M., Liveris, D., Wormser, G.P., Schwartz, I., Montecalvo, M.A., Johnson, B.J., 2001. *Borrelia lonestari* infection after a bite by an *Amblyomma americanum* tick. J. Infect. Dis. 183, 1810-1814.

Jittapalapong, S., Phichitrasilp, T., Chanphao, H., Rerkamnuychoke, W., Stich, R.W., 2008. Immunization with tick salivary gland extracts. Ann. N. Y. Acad. Sci. 1149, 200-204.

Jones, L.D., Nuttall, P.A., 1990. The effect of host resistance to tick infestation on the transmission of Thogoto virus by ticks. J. Gen. Virol. 71 (Pt 5), 1039-1043.

Jongejan, F., Uilenberg, G., 1994. Ticks and control methods. Rev. Sci. Tech. 13, 1201-1226.

Jongejan, F., Uilenberg, G., 2004. The global importance of ticks. Parasitology 129 Suppl, 3.

Karim, S., Ribeiro, J.M., 2015. An insight into the sialome of the lone star tick, *Amblyomma americanum*, with a glimpse on its time dependent gene expression. PLoS One 10, e0131292.

Karim, S., Singh, P., Ribeiro, J.M., 2011. A deep insight into the sialotranscriptome of the gulf coast tick, *Amblyomma maculatum*. PLoS One 6, e28525.

Katavolos, P., Armstrong, P.M., Dawson, J.E., Telford, S.R.,3rd, 1998. Duration of tick attachment required for transmission of granulocytic ehrlichiosis. J. Infect. Dis. 177, 1422-1425.

Kotsyfakis, M., Schwarz, A., Erhart, J., Ribeiro, J.M., 2015. Tissue- and time-dependent transcription in *Ixodes ricinus* salivary glands and midguts when blood feeding on the vertebrate host. Sci. Rep. 5, 9103.

Laird, J.S., Kocan, A.A., Kocan, K.M., Presley, S.M., Hair, J.A., 1988. Susceptibility of *Amblyomma americanum* to natural and experimental infections with *Theileria cervi*. J. Wildl. Dis. 24, 679-683.

Latif, A.A., Newson, R.M., Dhadialla, T.S., 1988. Feeding performance of *Amblyomma variegatum* (Acarina: Ixodidae) fed repeatedly on rabbits. Exp. Appl. Acarol. 5, 83-92.

Leboulle, G., Rochez, C., Louahed, J., Ruti, B., Brossard, M., Bollen, A., Godfroid, E., 2002. Isolation of *Ixodes ricinus* salivary gland mRNA encoding factors induced during blood feeding. Am. J. Trop. Med. Hyg. 66, 225-233.

Levin, M.L., Ross, D.E., 2004. Acquisition of different isolates of *Anaplasma phagocytophilum* by *Ixodes scapularis* from a model animal. Vector Borne Zoonotic Dis. 4, 53-59.

Lewis, L.A., Radulovic, Z.M., Kim, T.K., Porter, L.M., Mulenga, A., 2015. Identification of 24h *Ixodes scapularis* immunogenic tick saliva proteins. Ticks Tick Borne Dis. 6, 424-434.

Lew-Tabor, A.E., Moolhuijzen, P.M., Vance, M.E., Kurscheid, S., Valle, M.R., Jarrett, S., Minchin, C.M., Jackson, L.A., Jonsson, N.N., Bellgard, M.I., Guerrero, F.D., 2010. Suppressive subtractive hybridization analysis of *Rhipicephalus (Boophilus) microplus* larval and adult transcript expression during attachment and feeding. Vet. Parasitol. 167, 304-320.

Liao, M., Zhou, J., Gong, H., Boldbaatar, D., Shirafuji, R., Battur, B., Nishikawa, Y., Fujisaki, K., 2009. Hemalin, a thrombin inhibitor isolated from a midgut cDNA library from the hard tick *Haemaphysalis longicornis*. J. Insect Physiol. 55, 164-173.

Little, S.E., O'Connor, T.P., Hempstead, J., Saucier, J., Reichard, M.V., Meinkoth, K., Meinkoth, J.H., Andrews, B., Ullom, S., Ewing, S.A., Chandrashekar, R., 2010. *Ehrlichia ewingii* infection and exposure rates in dogs from the southcentral United States. Vet. Parasitol. 172, 355-360.

Manohar, G.S., Banerjee, D.P., 1992. Effects of immunization of rabbits on establishment, survival, and reproductive biology of the tick *Hyalomma anatolicum anatolicum*. J. Parasitol. 78, 77-81.

Maritz-Olivier, C., Stutzer, C., Jongejan, F., Neitz, A.W., Gaspar, A.R., 2007. Tick anti-hemostatics: targets for future vaccines and therapeutics. Trends Parasitol. 23, 397-407.

McMullan, L.K., Folk, S.M., Kelly, A.J., MacNeil, A., Goldsmith, C.S., Metcalfe, M.G., Batten, B.C., Albarino, C.G., Zaki, S.R., Rollin, P.E., Nicholson, W.L., Nichol, S.T., 2012. A new phlebovirus associated with severe febrile illness in Missouri. N. Engl. J. Med. 367, 834-841.

Merino, O., Alberdi, P., Perez de la Lastra, J M, de la Fuente, J., 2013. Tick vaccines and the control of tick-borne pathogens. Front. Cell. Infect. Microbiol. 3, 30.

Miller, J.R., Koren, S., Dilley, K.A., Harkins, D.M., Stockwell, T.B., Shabman, R.S., Sutton, G.G., 2018. A draft genome sequence for the *Ixodes scapularis* cell line, ISE6. F1000Res 7, 297.

Moreira, H.N.S., Barcelos, R.M., Vidigal, P.M.P., Klein, R.C., Montandon, C.E., Maciel, T.E.F., Carrizo, J.F.A., Costa de Lima, P H, Soares, A.C., Martins, M.M., Mafra, C., 2017. A deep insight into the whole transcriptome of midguts, ovaries and salivary glands of the *Amblyomma sculptum* tick. Parasitol. Int. 66, 64-73.

Mudenda, L., Pierle, S.A., Turse, J.E., Scoles, G.A., Purvine, S.O., Nicora, C.D., Clauss, T.R., Ueti, M.W., Brown, W.C., Brayton, K.A., 2014. Proteomics informed by transcriptomics identifies novel secreted proteins in *Dermacentor andersoni* saliva. Int. J. Parasitol. 44, 1029-1037.

Mulenga, A., Sugimoto, C., Sako, Y., Ohashi, K., Musoke, A., Shubash, M., Onuma, M., 1999. Molecular characterization of a *Haemaphysalis longicornis* tick salivary gland-associated 29-kilodalton protein and its effect as a vaccine against tick infestation in rabbits. Infect. Immun. 67, 1652-1658.

Mulenga, A., Sugino, M., Nakajim, M., Sugimoto, C., Onuma, M., 2001. Tick-Encoded serine proteinase inhibitors (serpins); potential target antigens for tick vaccine development. J. Vet. Med. Sci. 63, 1063-1069.

Mulenga, A., Blandon, M., Khumthong, R., 2007. The molecular basis of the *Amblyomma americanum* tick attachment phase. Exp. Appl. Acarol. 41, 267-287.

Mulenga, A., Kim, T.K., Ibelli, A.M., 2013. Deorphanization and target validation of cross-tick species conserved novel *Amblyomma americanum* tick saliva protein. Int. J. Parasitol. 43, 439-451.

Murphy, G.L., Ewing, S.A., Whitworth, L.C., Fox, J.C., Kocan, A.A., 1998. A molecular and serologic survey of *Ehrlichia canis*, *E. chaffeensis*, and *E. ewingii* in dogs and ticks from Oklahoma. Vet. Parasitol. 79, 325-339.

Nazario, S., Das, S., de Silva, A.M., Deponte, K., Marcantonio, N., Anderson, J.F., Fish, D., Fikrig, E., Kantor, F.S., 1998. Prevention of *Borrelia burgdorferi* transmission in guinea pigs by tick immunity. Am. J. Trop. Med. Hyg. 58, 780-785.

Nikpay, A., Nabian, S., 2016. Immunization of cattle with tick salivary gland extracts. J. Arthropod Borne Dis. 10, 281-290.

Nuttall, P.A., Labuda, M., 2004. Tick-host interactions: saliva-activated transmission. Parasitology 129 Suppl, 177.

Oliveira, C.J., Anatriello, E., de Miranda-Santos, I.K., Francischetti, I.M., Sa-Nunes, A., Ferreira, B.R., Ribeiro, J.M., 2013. Proteome of *Rhipicephalus sanguineus* tick saliva induced by the secretagogues pilocarpine and dopamine. Ticks Tick Borne Dis. 4, 469-477.

Piesman, J., Mather, T.N., Sinsky, R.J., Spielman, A., 1987. Duration of tick attachment and *Borrelia burgdorferi* transmission. J. Clin. Microbiol. 25, 557-558.

Piesman, J., Maupin, G.O., Campos, E.G., Happ, C.M., 1991. Duration of adult female *Ixodes dammini* attachment and transmission of *Borrelia burgdorferi*, with description of a needle aspiration isolation method. J. Infect. Dis. 163, 895-897.

Piesman, J., Eisen, L., 2008. Prevention of tick-borne diseases. Annu. Rev. Entomol. 53, 323-343.

Pritt, B.S., Sloan, L.M., Johnson, D.K., Munderloh, U.G., Paskewitz, S.M., McElroy, K.M., McFadden, J.D., Binnicker, M.J., Neitzel, D.F., Liu, G., Nicholson, W.L., Nelson, C.M., Franson, J.J., Martin, S.A., Cunningham, S.A., Steward, C.R., Bogumill, K., Bjorgaard, M.E., Davis, J.P., McQuiston, J.H., Warshauer, D.M., Wilhelm, M.P., Patel, R., Trivedi, V.A., Eremeeva, M.E., 2011. Emergence of a new pathogenic *Ehrlichia* species, Wisconsin and Minnesota, 2009. N. Engl. J. Med. 365, 422-429.

Prusinski, M.A., Kokas, J.E., Hukey, K.T., Kogut, S.J., Lee, J., Backenson, P.B., 2014. Prevalence of *Borrelia burgdorferi* (Spirochaetales: Spirochaetaceae), *Anaplasma phagocytophilum* (Rickettsiales: Anaplasmataceae), and *Babesia microti* (Piroplasmida: Babesiidae) in *Ixodes scapularis* (Acari: Ixodidae) collected from recreational lands in the Hudson Valley Region, New York State. J. Med. Entomol. 51, 226-236.

Radulovic, Z.M., Kim, T.K., Porter, L.M., Sze, S.H., Lewis, L., Mulenga, A., 2014. A 24-48 h fed *Amblyomma americanum* tick saliva immuno-proteome. BMC Genomics 15, 518.

Rau, J.C., Beaulieu, L.M., Huntington, J.A., Church, F.C., 2007. Serpins in thrombosis, hemostasis and fibrinolysis. J. Thromb. Haemost. 5 Suppl 1, 102-115.

Reeves, W.K., Loftis, A.D., Nicholson, W.L., Czarkowski, A.G., 2008. The first report of human illness associated with the Panola Mountain *Ehrlichia* species: a case report. J. Med. Case Rep. 2, 139.

Ribeiro, J.M., 1987. Role of saliva in blood-feeding by arthropods. Annu. Rev. Entomol. 32, 463-478.

Ribeiro, J.M., Mather, T.N., Piesman, J., Spielman, A., 1987. Dissemination and salivary delivery of Lyme disease spirochetes in vector ticks (Acari: Ixodidae). J. Med. Entomol. 24, 201-205.

Ribeiro, J.M., Francischetti, I.M., 2003. Role of arthropod saliva in blood feeding: sialome and post-sialome perspectives. Annu. Rev. Entomol. 48, 73-88.

Ribeiro, J.M., Anderson, J.M., Manoukis, N.C., Meng, Z., Francischetti, I.M., 2011. A further insight into the sialome of the tropical bont tick, *Amblyomma variegatum*. BMC Genomics 12, 136.

Ribeiro, J.M., Labruna, M.B., Mans, B.J., Maruyama, S.R., Francischetti, I.M., Barizon, G.C., de Miranda Santos, I K, 2012. The sialotranscriptome of *Antricola delacruzi* female ticks is compatible with non-hematophagous behavior and an alternative source of food. Insect Biochem. Mol. Biol. 42, 332-342.

Ricci, C.G., Pinto, A.F., Berger, M., Termignoni, C., 2007. A thrombin inhibitor from the gut of *Boophilus microplus* ticks. Exp. Appl. Acarol. 42, 291-300.

Rizzoli, A., Rosa, R., Mantelli, B., Pecchioli, E., Hauffe, H., Tagliapietra, V., Beninati, T., Neteler, M., Genchi, C., 2004. *Ixodes ricinus*, transmitted diseases and reservoirs. Parassitologia 46, 119-122.

Rodriguez, M., Massard, C.L., da Fonseca, A.H., Ramos, N.F., Machado, H., Labarta, V., de la Fuente, J., 1995a. Effect of vaccination with a recombinant Bm86 antigen preparation on natural infestations of *Boophilus microplus* in grazing dairy and beef pure and cross-bred cattle in Brazil. Vaccine 13, 1804-1808.

Rodriguez, M., Penichet, M.L., Mouris, A.E., Labarta, V., Luaces, L.L., Rubiera, R., Cordoves, C., Sanchez, P.A., Ramos, E., Soto, A., 1995b. Control of *Boophilus microplus* populations in grazing cattle vaccinated with a recombinant Bm86 antigen preparation. Vet. Parasitol. 57, 339-349.

Rudenko, N., Golovchenko, M., Edwards, M.J., Grubhoffer, L., 2005. Differential expression of *Ixodes ricinus* tick genes induced by blood feeding or *Borrelia burgdorferi* infection. J. Med. Entomol. 42, 36-41.

Savage, H.M., Godsey, M.S.,Jr, Lambert, A., Panella, N.A., Burkhalter, K.L., Harmon, J.R., Lash, R.R., Ashley, D.C., Nicholson, W.L., 2013. First detection of heartland virus (Bunyaviridae: Phlebovirus) from field collected arthropods. Am. J. Trop. Med. Hyg. 89, 445-452.

Schwarz, A., von Reumont, B.M., Erhart, J., Chagas, A.C., Ribeiro, J.M., Kotsyfakis, M., 2013. De novo *Ixodes ricinus* salivary gland transcriptome analysis using two next-generation sequencing methodologies. FASEB J. 27, 4745-4756.

Schwarz, A., Tenzer, S., Hackenberg, M., Erhart, J., Gerhold-Ay, A., Mazur, J., Kuharev, J., Ribeiro, J.M., Kotsyfakis, M., 2014. A systems level analysis reveals transcriptomic and proteomic complexity in *Ixodes ricinus* midgut and salivary glands during early attachment and feeding. Mol. Cell. Proteomics 13, 2725-2735.

Sonenshine, D.E., Roe, R.M., 2014. Biology of Ticks Volume 1. Oxford University Press, Oxford, United Kingdom.

Steen, N.A., Barker, S.C., Alewood, P.F., 2006. Proteins in the saliva of the Ixodida (ticks): pharmacological features and biological significance. Toxicon 47, 1-20.

Steinke, J.W., Platts-Mills, T.A., Commins, S.P., 2015. The alpha-gal story: lessons learned from connecting the dots. J. Allergy Clin. Immunol. 135, 96; quiz 597.

Taylor, J.P., Istre, G.R., McChesney, T.C., Satalowich, F.T., Parker, R.L., McFarland, L.M., 1991. Epidemiologic characteristics of human tularemia in the southwest-central states, 1981-1987. Am. J. Epidemiol. 133, 1032-1038.

Tirloni, L., Reck, J., Terra, R.M., Martins, J.R., Mulenga, A., Sherman, N.E., Fox, J.W., Yates, J.R.,3rd, Termignoni, C., Pino, A.F., Vaz Ida, S.,Jr, 2014. Proteomic analysis of cattle tick *Rhipicephalus (Boophilus) microplus* saliva: a comparison between partially and fully engorged females. PLoS One 9, e94831.

Tirloni, L., Islam, M.S., Kim, T.K., Diedrich, J.K., Yates, J.R.,3rd, Pinto, A.F., Mulenga, A., You, M.J., Da Silva Vaz, I.,Jr, 2015. Saliva from nymph and adult females of *Haemaphysalis longicornis*: a proteomic study. Parasit. Vectors 8, 338. 10.1186/s13071-015-0918-y

Tolleson, D.R., Teel, P.D., Stuth, J.W., Strey, O.F., Welsh, T.H., Jr, Carstens, G.E., Longnecker, M.T., Banik, K.K., Prince, S.D., 2010. Effects of a lone star tick (*Amblyomma americanum*) burden on performance and metabolic indicators in growing beef steers. Vet. Parasitol. 173, 99-106.

Trager, W., 1939a. Acquired immunity to ticks. J. Parasitol 25, 57-81.

Trager, W., 1939b. Further observations on acquired immunity to the tick *Dermacentor variabilis* Say. J. Parasitol. 25, 137-139.

Valenzuela, J.G., Francischetti, I.M., Pham, V.M., Garfield, M.K., Mather, T.N., Ribeiro, J.M., 2002. Exploring the sialome of the tick *Ixodes scapularis*. J. Exp. Biol. 205, 2843-2864.

Walade, S.M., Rice, M.J., 1982. The sensory basis of tick feeding behavior. Physiology of Ticks, pp. 71–118.

Wikel, S.K., 1981. The induction of host resistance to tick infestation with a salivary gland antigen. Am. J. Trop. Med. Hyg. 30, 284-288.

Willadsen, P., Bird, P., Cobon, G.S., Hungerford, J., 1995. Commercialisation of a recombinant vaccine against *Boophilus microplus*. Parasitology 110 Suppl, 43.

Willadsen, P., 2004. Anti-tick vaccines. Parasitology 129 Suppl, 367.

Willadsen, P., 2006. Vaccination against ectoparasites. Parasitology 133 Suppl, S25.

Wolf, L., McPherson, T., Harrison, B., Engber, B., Anderson, A., Whitt, P., 2000. Prevalence of *Ehrlichia ewingii* in *Amblyomma americanum* in North Carolina. J. Clin. Microbiol. 38, 2795.

Xiang, F., Zhou, Y., Zhou, J., 2012. Identification of differentially expressed genes in the salivary gland of *Rhipicephalus haemaphysaloides* by the suppression subtractive hybridization approach. J. Integr. Agric 11, 1528-1536.

Xu, Y., Bruno, J.F., Luft, B.J., 2005. Identification of novel tick salivary gland proteins for vaccine development. Biochem. Biophys. Res. Commun. 326, 901-904.

Yabsley, M.J., Quick, T.C., Little, S.E., 2005. Theileriosis in a white-tailed deer (*Odocoileus virginianus*) fawn. J. Wildl. Dis. 41, 806-809.

Yabsley, M.J., Loftis, A.D., Little, S.E., 2008. Natural and experimental infection of white-tailed deer (*Odocoileus virginianus*) from the United States with an *Ehrlichia* sp. closely related to *Ehrlichia ruminantium*. J. Wildl. Dis. 44, 381-387.

CHAPTER II*

DETERMINE *IXODES SCAPULARIS* AND *AMBLYOMMA AMERICANUM* TICK SALIVA PROTEOMES

Rationale

It is well established that multiple proteins that ticks inject into the host during feeding regulate successful tick feeding, transmission of TBD agents, and the colonization of host tissue by the transmitted TBD agents. Therefore, identification of proteins in tick saliva as pursued in this dissertation is expected to establish the foundation to understand the molecular basis of tick feeding. This information will in return be useful in studies to develop tick-antigen based vaccines to prevent transmission of tick-borne disease (TBD) agents by ticks. Until recently, the identification of proteins in tick saliva was hampered by the lack of technologies that is able to identify proteins from small amounts of samples. The recent demonstration that LC-MS/MS sequencing could identify proteins in tick saliva encouraged this objective. The goal of this chapter was to identify proteins that *Amblyomma americanum* and *Ixodes scapularis* sequentially injected into the host during feeding. The rationale is three-fold. **1)** *I. scapularis* and *A. americanum* ticks transmit the majority of human tick-borne disease (TBD) agents in the USA. **2)** Identification of tick saliva proteins sequentially injected into the host during feeding will reveal tick proteins that are injected into the host prior to TBD agent transmission by ticks, which represent targets in a tick-antigen based vaccine to prevent TBD infections. **3)** As *I. scapularis* and *A. americanum* are

---

*Reprinted with permission from *Ixodes scapularis* tick saliva proteins sequentially secreted every 24 h during blood feeding by Kim, T.K., Tirloni, L., Pinto, A.F., Moresco, J., Yates, J.R. III., da Silva Vaz Jr., I., and Mulenga A., 2016. PLoS Negl Trop Dis. 10(1): e0004323. https://doi.org/10.1371/journal.pntd.0004323. 2016.

respectively categorized as Protstriata and Metastriata groups, which are distantly related, comparing the two datasets will identify conserved tick saliva proteins used by both species during tick feeding. These potentially regulate critical conserved tick feeding functions and thus, might represent effective target antigens for tick vaccine development. This chapter tested the following hypothesis:

- H_0: *Ixodes scapularis* and *Amblyomma americanun* ticks will not sequentially secrete a varying mixture of different tick saliva proteins during feeding.

- H_1: *Ixodes scapularis* and *Amblyomma americanun* ticks will sequentially secrete a varying mixture of different tick saliva proteins during feeding.

The two parts of this chapter were successfully accomplished. Results from the first part of this chapter describes identification and bioinformatics analysis of tick and rabbit host proteins that *Ixodes scapularis* sequentially inject into the host every 24 h during feeding was published in the article below.

Part I*

Ixodes scapularis tick saliva proteins sequentially secreted every 24 h during blood feeding

Materials and Methods

Ethics statement

All experiments were done according to the animal use protocol approved by Texas A&M University Institutional Animal Care and Use Committee (IACUC) (AUP 2011-207 and 2011-189) that meets all federal requirements, as defined in the Animal Welfare Act (AWA), the Public Health Service Policy (PHS), and the Humane Care and Use of Laboratory Animals.

Ticks and saliva collection

I. scapularis ticks were purchased from the tick rearing facility at Oklahoma State University (Stillwater, OK, USA). Prior to feeding on rabbits, female ticks were paired with males to mate. Ticks were considered mated once males were detached from the females. Routinely, ticks were fed on rabbits as previously described (Ibelli et al., 2014). Mated *I. scapularis* ticks were restricted to feed onto the outer part of the ear of New Zealand rabbits with orthopedic stockinet's glued with Kamar adhesive (Kamar Products Inc., Zionsville, IN, USA). A total of 84 adult *I. scapularis* ticks (42 per ear) were placed into tick containment apparatus on three rabbits and allowed to attach.

To collect tick saliva, female ticks partially fed for 24 h (n = 43 ticks), 48 h (n = 40 ticks), 72 h (n = 40 ticks), 96 h (n = 40 ticks), 120 h (n = 40 ticks) as well as apparently fully fed but not detached from the host (BD, n = 8 ticks) and spontaneously detached ticks (SD, n = 6 ticks) were rinsed in Milli-Q water and dried on a paper towel. Rinsed ticks were placed dorsal-side down on

double-sided tape on a glass slide. Salivation was induced by injecting 1 – 3 µL of 2% pilocarpine hydrochloride in phosphate buffered saline (PBS, pH 7.4) on the ventral side adjacent to the fourth leg coxa using a 34 gauge/ 0.5 inches/ 45° angle beveled needle on a model 701 Hamilton syringe (Hamilton Company, Reno, NV, USA). Subsequently, saliva was collected every 15 – 30 min using a Hamilton syringe for approximately 4h at room temperature.

Protein digestion and sample preparation

Saliva of *I. scapularis* ticks (at least 2 µg total protein per run X3) for each specific feeding time point was digested in solution with trypsin. Saliva were diluted in 8 M urea/0.1 M Tris, pH 8.5, reduced with 5 mM Tris (2-carboxyethyl) phosphine hydrochloride (TCEP, Sigma-Aldrich, St Louis, MO, USA) and alkylated with 25 mM iodoaceamide (Sigma-Aldrich). Proteins were digested overnight at 37 °C in 2 M urea/0.1M Tris pH 8.5, 1 mM $CaCl_2$ with trypsin (Promega, Madison, WI, USA) with a final ratio of 1:20 (enzyme:substrate). Digestion reactions, in a final concentration of 0.15 µg/mL, were quenched with formic acid (5 % final concentration) and centrifuged for debris removal.

Pre-columns and analytical columns

Reversed phase pre-columns were prepared by first creating a Kasil frit at one end of a deactivated 250 µm ID/360 µm OD capillary (Agilent Technologies, Santa Clara, CA, USA). Kasil frits were prepared by dipping 20 cm capillary in 300 µL Kasil 1624 (PQ Corporation, Malvern, PA, USA) and 100 µL formamide solution, curing at 100 °C for 3 h and adjusting the length. Pre-columns were packed in-house (John Yates III's Laboratory, The Scripps Research Institute, La Jolla, CA, USA) with 2 cm of 5 µm ODS-AQ C18 (YMC America, Inc., Allentown, PA, USA)

particles from particle slurries in methanol. Analytical reversed phase columns were fabricated by pulling a 100 µm ID/360 µm OD silica capillary (Molex Polymicro Technologies, Austin, TX, USA) to a 5 µm ID tip. The same packing material was packed until 20 cm directly behind the pulled tip. Reversed phase pre-columns and analytical columns were connected using a zero-dead volume union (IDEX Corp., Upchurch Scientific, Oak Harbor, WA, USA).

LC-MS/MS

Peptide mixtures were analyzed by nanoflow liquid chromatography mass spectrometry using an Easy NanoLC II and a Q Exactive mass spectrometer (Thermo Scientific, Waltham, MA, USA). Peptides eluted from the analytical column were electrosprayed directly into the mass spectrometer. Buffer A and B consisted of 5 % acetonitrile/0.1 % formic acid and 80 % acetonitrile/0.1 % formic acid, respectively. The flow rate was set to 400 nL/min. Feeding time saliva samples (1.5 µg per injection) were separated in 155 min chromatographic runs, as follows: 1-10 % gradient of buffer B in 10 min, 10-40 % of buffer B in 100 min, 40-50 % of buffer B in 10 min and 50-90 % of buffer B in 10 min. Column was held at 90 % of buffer B for 10 min, reduced to 1 % of buffer B and re-equilibrated prior to next injection.

The mass spectrometer was operated in a data dependent mode, collecting a full MS scan from 400 to 1,200 m/z at 70,000 resolution and an AGC target of 1×10^6. The 10 most abundant ions per scan were selected for MS/MS at 17,500 resolution and AGC target of 2×10^5 and an underfill ratio of 0.1 %. Maximum fill times were 20 and 120 ms for MS and MS/MS scans, respectively, with dynamic exclusion of 15 s. Normalized collision energy was set to 25. The mass spectrometry proteomics data have been deposited to the ProteomeXchange Consortium (Vizcaino et al., 2014) via the PRIDE partner repository with the dataset identifier PXD003214.

Data Analysis

Tandem mass spectra were extracted from Thermo RAW files using RawExtract 1.9.9.2 (McDonald et al., 2004) and searched with ProLuCID (Xu et al., 2015) against a non-redundant database containing an Ixodidae database from National Center for Biotechnology Information (NCBI, www.ncbi.nlm.nih.gov) (62,246 entries) concatenated with *Oryctolagus cuniculus* from Uniprot (www.uniprot.org) reference database (21,148 entries) and reverse sequences of all entries. Database sequence redundancies were removed by FastaDBXtractor module from PatternLab for Proteomics platform (Carvalho et al., 2010). Searches were done using Integrated Proteomics Pipeline – IP2 (Integrated Proteomics Applications, Inc., San Diego, CA, USA). The search space included all fully-tryptic and half-tryptic peptide candidates. Carbamidomethylation of cysteine was used as static modification. Data was searched with 50 ppm precursor ion tolerance and 20 ppm fragment ion tolerance.

The validity of the peptide spectrum matches (PSMs) generated by ProLuCID (Xu et al., 2015) was assessed using Search Engine Processor (SEPro) module from PatternLab for Proteomics platform (Carvalho et al., 2010). Identifications were grouped by charge state and tryptic status, resulting in four distinct subgroups. For each group, ProLuCID XCorr, DeltaCN, DeltaMass, ZScore, number of peaks matched and secondary rank values were used to generate a Bayesian discriminating function. A cutoff score was established to accept a protein false discovery rate (FDR) of 1% based on the number of decoys. This procedure was independently performed on each data subset, resulting in a false-positive rate that was independent of tryptic status or charge state. Additionally, a minimum sequence length of six residues per peptide was required. Results were post processed to only accept PSMs with <10ppm precursor mass error.

Protein functional annotation and classification

BLASTP searches against several databases were performed to annotate the matched proteins. To check tick proteins identity, the following databases were used: non-redundant (NR), Acari and refseq-invertebrate from NCBI, Acari from Uniprot, the GeneOntology (GO) FASTA subset (Ashburner et al., 2000), MEROPS database (Rawlings et al., 2012), and the conserved domains database of NCBI (Marchler-Bauer et al., 2015) containing the COG (Tatusov et al., 2003), PFAM (Bateman et al., 2002), and SMART motifs (Schultz et al., 2000). To check rabbit proteins, the following databases were used: *Oryctolagus cuniculus* and refseq-vertebrates databases from NCBI, *O. cuniculus* from Uniprot, the GeneOntology (GO) FASTA subset (Ashburner et al., 2000) the conserved domains database of NCBI (Marchler-Bauer et al., 2015), containing the COG (Tatusov et al., 2003) , PFAM (Bateman et al., 2002), and SMART motifs (Schultz et al., 2000). To functionally classify the protein sequences, a program provided by Dr. José M. C Ribeiro written in Visual Basic 6.0 (Microsoft, Redmond, Washington, USA) was used (Karim et al., 2011). The functionally annotated catalog for each dataset was manually curated and input in a hyperlinked Excel spreadsheet (S1 and S2 Tables).

Relative abundance and graphical visualization

To determine the relative abundance of saliva proteins normalized spectral abundance factors (NSAF) were used. The NSAF value was validated as reliable in a label-free relative quantification approach (Zhu et al., 2010, Florens et al., 2006, Paoletti et al., 2006). Average NSAF of two or three replicates were used. To determine relative abundance, average NSAF for each protein functional class or an individual annotated protein was expressed as a percent (%) of total NSAF per time point. To visualize relative expression patterns on a heat map, % NSAF values

were normalized using Z-score statics using the formula $Z = \frac{X-\mu}{\sigma}$, where *Z i*s the Z-score, *X* is the NSAF for each protein per time point, μ is the mean throughout time points, σ is the standard deviation throughout time points. Normalized NSAF values were used to generate heat maps using the heatmap2 function from the gplots library in R (Warnes et al., 2013).

Phylogeny analysis

Amino acid sequences were used to construct a guide phylogeny tree using MacVector 12.7.3 (MacVector Inc Cary, NC, USA) software. Protein sequences were aligned using Muscle method in MacVector under default settings. Subsequently, the tree was constructed using the Neighbor Joining method with uncorrected ("p") distance setting. To estimate bootstrap values, replications were set to 1000.

Results and Discussion

Tick saliva collection

We successfully harvested pilocarpine-induced saliva of *I. scapularis* ticks that were partially fed on rabbits for 24, 48, 72, 96 and 120 h as well as those that were apparently engorged but not detached (BD), and those that had engorged and spontaneously detached (SD). During collection of saliva, we observed that saliva of 24 h fed ticks dried up quickly forming flakey white crystal-like residues, and to collect we dissolved these flakes in 2 µL sterile phosphate buffered saline (PBS, pH 7.4) batches. On the contrary, saliva droplet of ticks at subsequent feeding stages was visible within seconds to min after pilocarpine injection.

Protein composition in I. scapularis tick saliva changes every 24 h

S1 table lists tick and rabbit proteins that were identified in *I. scapularis* saliva. The search of extracted tandem mass spectra against the tick and rabbit protein database using ProLucid (Xu et al., 2015) and filtering using SEPro (Carvalho et al., 2010) produced hits to 769 tick and 130 rabbit proteins respectively with at least one peptide match per protein (S1 Table, please note the different tabs). When subjected to further analysis in BirdsEye View module from PatternLab for Proteomics platform (Carvalho et al., 2010), 582 of the 769 tick proteins were determined to be authentic as they were detected in two or all of the three runs, while the remaining 187 proteins detected in only one of the three runs were considered low confidence hits and not further discussed (S1 Table). Of the 130 rabbit proteins that were detected in *I. scapularis* tick saliva, 83 met the criteria for authentication. When subjected to auto-annotation (Karim et al., 2015), 582 tick and 83 rabbit high confidence proteins respectively classified into 24 (Table 1) and 18 (Table 2) functional protein classes. Specifically, tables 1 and 2 summarizes cumulative numbers of proteins that were identified in each functional class, apparent relative abundance at each time point, and time points at where class were not detected [represented by zero (0)].

Figs 1 and 2 gives a snap shot of relative abundance of tick (Fig 1) and rabbit (Fig 2) proteins in *I. scapularis* saliva every 24 h. In Fig 1, it is apparent that majority of *I. scapularis* tick proteins in this study belong to four predominant functional protein classes starting with proteins of unknown function, followed by protease inhibitors (PI), antimicrobial/immunity related, and heme binding proteins. This is followed by lowly abundant protein classes that account for 1-6% (cytoskeletal, glycine rich, and protein modification machinery) with the remaining protein classes being detected accounted for less than 1%. Of the four major protein classes, relative abundance of proteins of unknown function appear to increase with feeding, accounting for 33-58% of total

protein between 24-120 h before dropping to 13% in saliva of fully fed but not detached ticks (BD) as well as fully fed and spontaneously detached. Similarly, heme binding proteins increased from ~14% at 24 h to ~24% at 96 h, before dropping to 10% at 120 h, coming back up to 24% in BD and dropping to 8% in SD. On the other hand, PIs and antimicrobial/immunity related peptides decreased in abundance with feeding with the former dropping from 24.7% at 24 h to 17-8% at 48-120 h respectively, but increasing to 21% in BD and dropping to 7% in SD. Similarly, anti-microbial/immunity-related proteins decreased from 18% at 24 h to 17-5% at 48-120 h, before slightly rising to ~7% in BD and SD (Table 1 and Fig 1). Notable protein classes include proteases and lipocalins that appear to increase in abundance with feeding. Protease content increases from 0.5% at 24 h to 3-6% at 48, 96, and 120 h except for 72 h were content was at 0.5%, and 5-6% in BD and SD (Fig 1). Similarly lipocalin content increases from 0.3% at 24 h to ~6% at 120 h, not detected in BD, but accounted for ~3% of protein content in SD. Also notable in Table 1 and Fig 1, tick housekeeping-like proteins appear to increase with feeding.

Fig 2 summarizes relative abundance of rabbit proteins that were detected in *I. scapularis* saliva. It is interesting to note that of the 18 protein classes in Table 2, four protein classes: heme/iron, hemoglobin/RBC degradation products, antimicrobial/immune related, and keratin were found in all time points. It is notable that these four protein classes represented the most abundant rabbit proteins in tick saliva. Except at 72 h where rabbit heme/iron binding proteins accounted for 3%, this protein was among the most predominant in other time points accounting for 17-75% of total rabbit protein content in tick saliva. Similarly, hemoglobin/RBC-related proteins increased from 7.6% at 24 h to 50.2% in BD and 39.3% in SD. Immunity-related proteins of rabbits were most abundant at 48, 96, and 120 h saliva at 30%, 29.6%, and 27.6% respectively (Fig 2). Keratins detected at all time points could signal handling contamination of our samples.

Another interesting observation in Fig 2, fibrinogen the precursor to fibrin, which is involved in clot formation was detected toward the end of feeding, 0.25% in 96 h saliva increasing to 3.1% in SD. Could this suggest that the tick ingests fibrinogen during feeding and secretes it back into the host during the detachment phase to promote wound healing? Hard ticks create a wound in host skin from which they suck the blood, however this wound is completely healed when ticks detach.

Secretion dynamics of selected protein classes during I. scapularis tick feeding.

We are interested in understanding mechanisms that regulate early stage tick feeding, and thus the subsequent discussion of data is biased toward non-housekeeping-like tick derived proteins that were found in saliva from 24/48 h. We have discussed rabbit derived proteins separately, but highlight similarities and differences where appropriate. We used Z-statistics normalization of NSAF values (S3 Table) to develop heat maps in Figs 3-5. These data give insight into relative abundance of specific proteins during feeding: proteases (Fig 3A), protease inhibitors (Fig 3B), lipocalins/tick histamine-binding proteins/fatty acid binding proteins (Fig 4A), anti-microbial/immunity-related (Fig 4B), heme-binding proteins (Fig 4C), anti-oxidants (Fig 4D), proteins of unknown function (Fig 5A), glycine rich proteins (Fig 5B) and extracellular matrix proteins (Fig 5C).

Majority of proteases in I. scapularis saliva are metalloproteases

The *I. scapularis* genome encodes for at least 233 putatively active and 150 putatively inactive proteases belonging to serine, cysteine, aspartic, metallo, and threonine protease families (Mulenga and Erickson, 2011). In this study we found 33 proteases in four clans: serine- (n = 3), cysteine- (n = 3), aspartic- (n = 1), and metalloproteases (n = 26) (S2 Table). When searched

against the Merops database (Rawlings et al., 2012), the 26 metalloproteases belong to families M12 (n = 15), M20 (n = 4), M2 (n = 2), M28 (n = 2), M13 (n = 1), M17 (n = 1), and M49 (n = 1) (S2 Table), while serine, cysteine and aspartic proteases are classified in families S1, C1 and A1 respectively. Most of the proteases here are likely associated with tick feeding regulation in that 75% (25/33) were detected between 24-120 h during tick feeding except for seven that were identified only in SD (S2 Table). Nearly 40% of proteases in the *I. scapularis* genome are metalloproteases (Mulenga and Erikson, 2011). Whether or not the observation in this study that majority of proteases in *I. scapularis* tick saliva are metalloproteases reflects the protease composition in *I. scapularis* genome or it is a physiological event, is unknown at this point.

Z-score statistic analysis and visualization of normalized NSAF values of the 26 metalloproteases (Fig 3A) show that M12 and M2 metalloproteases were likely secreted in high abundance between 24-120 h during feeding respectively, which could indicate the importance of these proteins in regulating the first five days to tick feeding. The remaining metalloproteases in families M17, 20, 28 and 49, which were abundant in BD and SD (Fig 3A) are not likely associated with regulating tick feeding events.

The observation that *I. scapularis* predominantly secreted family M12 metalloproteases during feeding is suggestive of the importance of this protein class in tick feeding physiology. Emerging evidence indicate that this is the case. A recombinant protein of M12 protease (AAP22067.1, MCC Fig 3A) has gelatinase and fibrin(ogen)olytic activities (Francischetti et al., 2003), which is a pro-tick feeding event. In a related study, RNAi silencing of AAM93625.1 (MCC Fig 3A) and AAT92201.1 (MCF Fig 3A) homologs, Metis 1 and 2 (CAO000625 and CAO000626) in *I. ricinus* impaired blood meal feeding and egg laying with salivary gland protein extracts of these ticks not affecting host fibrinolysis (Decrem et al., 2008). In related studies, snake venom

M12 proteases were associated with hemorrhaging, edema, hypotension, hypovolemia, inflammation and necrosis (Weldon et al., 2012, Zhang et al., 2009, Fox et al., 2005) some of which will promote tick feeding. It will be interesting to characterize the role(s) of tick saliva proteases identified in this study.

Majority of protease inhibitors in I. scapularis saliva likely inhibit serine proteases

The first line of host defense to tick feeding such as inflammation, platelet aggregation, blood clotting, complement activation, and cellular immunity are mediated by proteases that are controlled by protease inhibitors (PI). From this perspective, it has been hypothesized that ticks could inject PIs into the host to evade host defense (Prevot et al., 2007, Maritz-Olivier et al., 2007, Mulenga et al., 2002, 2001, 2000). In this study, we identified 43 putative PIs (S1 Table), which according to the Merops database belong in eight families: I2 (Kunitz type serine protease inhibitors, n = 2), I4 (serine protease inhibitors, [serpins], n = 11), I8 (TIL domain serine protease inhibitors, n = 13), I25 (cystatins, cysteine protease inhibitors, n = 4), I31 (thyropins, cysteine protease inhibitors n = 2), I39 (α-2 macroglobulin, A2M, n = 9), I43 (Kazal type serine protease inhibitors, n = 1), and I68 (carboxypeptidase inhibitors, TCI, n = 1) were identified in *I. scapularis* saliva (S2 Table). It is notable that 84% (36/43) of PIs were detected in 24 and 48 h saliva (S2 Table), suggesting the potential for these proteins to regulate early stages of tick feeding. The observation here that majority of PIs in this study are likely inhibitors of serine proteases could signal the potential that most host defense pathways to tick feeding are likely serine protease mediated.

Similar to other protein classes in this study, relative abundance of PIs varied every 24 h (Fig 3B). Serpins show three secretion profiles: SCA proteins are abundant in first 48 h and

decrease with feeding, SCB are abundant at 96 h and increase in SD saliva, and SCC proteins increase in abundance from 24 to 120 h (Fig 3B1). Similarly, TIL domain PIs segregate in three clusters: those abundant during first 48 h of feeding but decrease with feeding in TCA, increase with feeding between 24-96 h in TCB, and those abundant in BD and SD saliva in TCC (Fig 3B2). In Fig 3B3, alpha-2-macroglobulins segregate in two clusters: those secreted in abundance between 24-120 h in αCA, and 48-SD in αCB. In Fig 3B4, cystatins cluster into CCA for those that increase in abundance with feeding and CCB for those that were secreted in high abundance at the 120 h time point.

There is evidence that some of the PIs identified in this study regulate important tick feeding functions. For instance serpin EEC19556.1 in SCA (Fig 3B1) is 98% identical to AID54718.1, an inhibitor of trypsin and thrombin that also inhibited blood clotting and platelet aggregation (Ibelli et al, 2014). Similarly *I. ricinus* serpin ABI94056, the homolog of *I. scapularis* serpin EEC14235.1 in this study (Fig 3B1 SCB) is an immunosuppressant, anti-inflammatory, and anti-hemostatic serpin (Palenikova et al., 2015, Chmelar et al., 2011, Kovarova et al., 2010). In other studies, *I. scapularis* cystatin AAY66685.1 in this study (Fig 3B4 CCA) known as Sialostatin L2 and its close relative Sialostatin L have immuno-modulatory functions, and suppressed cytokine production in absence (Lieskovska et al., 2015a, Horka et al.., 2012, Sa-Nunes et al., 2009, Kotsyfakis et al., 2007, Kotsyfakis et al., 2006) or presence of *B. burgdorferi* (Lieskovska et a., 2015b). It will be exciting to understand role(s) of PIs in *I. scapularis* feeding identified in this study.

Lipocalins/tick histamine-binding proteins (tHBP)/fatty acid binding proteins (FABP)

Lipocalins/HBP and FABPs belong to the calycin superfamily of hydrophobic ligand

binding extracellular proteins (Dart et al., 2011, Flower, 1996, 1994). The lipocalin protein family to which HBPs belong is a large group of proteins that bind and transport small hydrophobic molecules, and also associated with multiple functions including regulation of inflammation through binding of pro-inflammation molecules such as histamine (Mans et al., 2005, Paesen et al., 2000, 1999). Likewise the FABPs bind and transport hydrophobic ligands including long chain fatty acids, eicosanoids, bile salts and peroxisome proliferators (Smathers and Petersen, 2011). Tick lipocalins/histamine-binding proteins are thought to be involved with mediating the tick's evasion of the host's inflammation defense through sequestration of pro-inflammatory biogenic amines, lipids, histamine, serotonin and prostanoids (Ganfornina et al., 2000). Tick histamine binding proteins (tHBP) are a subset of lipocalins with two histamine-binding pockets (Paesen et al., 2000). Of the 18 proteins in S2 Table and Fig 4A, 14 are annotated as tHBPs, three as lipocalins, and one as FABP-like. Similar to other proteins, *I. scapularis* appears to selectively inject tHBPs/lipocalins into the host at specific time periods, with two tHBPs detected at 24 h in LCC, one at 48 h and three proteins each at 72 h and 96 h in LCD (Fig 4A). The highest numbers of tHBPs/lipocalins were identified at 120 h in LCA (n = 12) of which half were exclusive to this time point (S2 Table and Fig 4A). It is notable that two tHBPs and one each of lipocalin and FABP-like identified in this study were exclusive to SD saliva in LCB, which could suggest that these proteins are involved with events at the end of tick feeding.

A limited number of studies suggest that lipocalins/HBPs/FABP indeed perform tick-feeding functions. Three *R. appendiculatus* tHBPs were predicted to suppress inflammation during blood feeding as revealed by its ability to outcompete histamine receptors (Paesen et al., 1999). In other studies, *D. reticulatus* tHBP bound histamine and serotonin (Sangamnatdej et al., 2002), and *Ornithodoros moubata* tHBP, referred to as moubatin, demonstrated inhibition of collagen induced

platelet aggregation (Keller et al., 1993). In a recent study, lipocalins/HBPs/FABPs were identified among 24-48 h *A. americanum* immunogenic tick saliva proteins (Radulovic et al., 2014) suggesting that these proteins are part of the tick saliva proteins that confer anti-tick resistance in repeatedly infested animals. It is notable that in Radulovic et al., (2014), alongside lipocalins/HBPs, a leukotriene B4-like protease was also found among 24-48 h *A. americanum* immunogenic tick saliva proteins. It is interesting to note that *I. ricinus*, tHBP referred to as LIR6 bound leukotriene B4 (Beaufays et al., 2008), a pro-inflammatory mediator and a potent neutrophil chemoattractant.

I. scapularis tick saliva anti-microbial proteins

The tick feeding style of tearing up host tissue and sucking up blood from a wounded feeding site exposes the host to microbial infections. From this perspective ticks were postulated to inject anti-microbial peptides into the feeding site to prevent the feeding site from being infected (Francischetti et al., 2009, Valenzuela et al., 2002). Multiple anti-microbial peptides have been characterized in ticks, a majority of which are defensins (Wang et al., 2015, Tonk et al., 2014a, 2014b, Zheng et al., 2012, Chrudimska et al., 2011, Lu et al., 2010, Saito et al., 2009, Sonenshine et al., 2002, Nakajima etal., 2002), microplusin/microplusin-like (Esteves et al., 2009, Silva et al., 2009, Fogaca et al., 2004) and hebreain/hebreain-like (Lai et al., 2004). In this study seven of the 15 anti-microbial peptides in S2 Table and Fig 4B are microplusin-like, a single lysozyme, and the rest, are characterized by pathogen-recognition domains (n = 7). Fig 4B shows three secretion patterns, where ACA proteins were abundant during 24-120 h, ACB were only present in 48 h and ACC proteins increase from 48-96 h but highly abundant in BD and SD saliva. Except for microplusin (Fogaca et al., 2004), which was shown to stop *Micrococcus luteu*s and *Cryptococcus*

neoformans growth (Silva et al., 2011), nothing is known on the role(s) of most of the anti-microbial peptides in this study. It is notable that majority of anti-microbial peptides in this study are apparently injected into the host within the first 48 h of feeding (n = 11) (S2 Table and Fig 4B). Understanding functions of some of these antimicrobial peptides will reveal microbes that *I. scapularis* want to keep out of the feeding site.

Heme-binding proteins

When fully fed, hard ticks are estimated to imbibe host blood that is more than 100 times their original weight (Kaufman, 2007). Catabolism of this huge amount of blood generates high amounts of iron and heme (Toh et al., 2010, Ponka, 1999, 1997). Both iron and heme are needed for normal cell function (Ponka, 1999, 1997). However, if left unsecured, both iron and heme can cause cell damage through promotion of oxidative stress (Citelli et al., 2007, Graca-Souza et al., 2006). Ticks are postulated to prevent iron and heme mediated tick cell damage through expression of iron and heme binding proteins, which play two roles: bind and distribute to cells for normal physiology, and sequester excess iron or heme and prevent oxidative stress triggered cell damage (Toh et al., 2010).

One of the most notable observations in this study is that although heme-binding proteins represented ~2.6% (15/582) of proteins identified, they accounted for ~11-24% of total protein abundance (Table 1 and Fig 1). This could suggest that heme metabolism is potentially a "must-not-fail" tick physiological function. The observation that all 15 heme binding proteins in this study are likely injected into the host from within 24-48 h of the tick starting to feed (S2 Table) suggests that this mechanism is important from the start of tick feeding. In Fig 4B three secretion patterns are observable: HCA increases in abundance in 120 h-BD proteins, HCB abundant in 48

and 96 h, and HCC abundant in first 48 h but decrease with feeding. It is notable that the five heme binding proteins that were detected at all time points (S2 Table) cluster together in HCA (Fig 4C) with the exception of EEC13578.1. These proteins account for up to 38% of total NSAF within this class, which could suggest their significance in tick feeding physiology.

It is interesting to note that both iron and heme-binding proteins were also detected in high abundance in saliva of *D. andersoni* (Mudenda et al., 2014), *R. microplus* (Tirloni et al., 2014), and *H. longicornis* (Tirloni et al., 2015). However only the latter was detected in this study. Whether or not this is unique to *I. scapularis* or that iron-binding proteins were injected at below detectable levels needs further investigation. Published evidence has suggested that the tick may detoxify heme/iron through sequestration in digestive cells (hemosomes) (Galay et al., 2015, Lara et al., 2003) and hemolymph (Maya-Monteiro et al., 2004, 2000, Gudderra et al., 2000). Data in this study and others (Lewis et al., 2015, Tirloni et al., 2015, 2014, Radulovic et al., 2014, Graca-Souza et al., 2002) that show secretion of heme binding proteins in tick saliva suggest a third possibility of eliminating heme through tick saliva. Given that heme has pro-inflammatory functions (Dutra and Bozza, 2014), secretion of these proteins in tick saliva may be associated with heme sequestration, and thus allowing tick evasion of the host's inflammation defense. Iron sequestration is among the mammalian host's anti-microbial defense. To counter the host's iron sequestration defense, microbes have developed elaborate ways to bind iron from the environment (Dumas et al., 2013, Cornelis et al., 2011, Cornelis, 2010) and directly uptake heme, which is then digested to release associated iron (Ballouche et al., 2009). From this perspective it is possible that secretion of heme binding proteins is the tick's strategy to make heme available to transmitted pathogens at the tick-feeding site. It is important to note here that *B. burgdorferi*, the most

important *I. scapularis* transmitted human TBD agent, may not require iron to colonize the host (Posey and Gherardini, 2000).

Anti-oxidants

Tissue injury caused by tick feeding such as disrupting host tissue and then sucking blood from the wounded area will lead to production of reactive oxygen species (ROS), which will in turn damage host tissue and/or transmitted TBD agents (Narasimhan et al., 2007, Rojkind et al., 2002). Thus, it is expected that ticks would inject anti-oxidants into the feeding site as observed in this study. Fig 4D summarizes relative abundance of 36 putative anti-oxidant proteins, 23 of which were identified only in SD saliva (S2 Table), and are likely associated with events toward end of tick feeding. The remaining 13 proteins were identified between 24 h-BD and are likely associated with tick feeding regulation. The heat map in Fig 4D show that different anti-oxidants were detected in high abundance at different time points: ANCA in BD and SD, ANCB at 96 h, ANCC in SD, ANCD at 48 and 72 h, ANCE at 24 h and, ANCF at 120 h. It is interesting to note that some of the data in this study are consistent with previous observations. Glutathione peroxidase (AAK97814.1) previously found among immuno-dominant proteins in engorged *I. scapularis* (Das et la., 2001) is among the 23 anti-oxidants that were found in SD saliva only (S3 Table and Fig 4D).

The role(s) of antioxidants in tick physiology remain mostly unknown. In a recent study, thioredoxin peroxidase gene expression increased in organs of *B. burgdorferi* infected *I. ricinus* ticks (Rudenko et la., 2005) suggesting involvement in tick and pathogen interaction. It is interesting to note in this study thioredoxin peroxidase protein in non-infected ticks decreased with

feeding (S3 Table). It will be interesting to determine if anti-oxidant proteins identified from this study may play roles at the tick-host interface in TBD acquisition and transmission.

I. scapularis tick saliva proteins of unknown function

More than 30% of tick sequences in public databases are of unknown function (Karim and Ribeiro, 2015, Kotsyfakis et al., 2015, Xu et al., 2015, Schwarz et al., 2014, Francischetti et al., 2011, 2008, 2005, Karim et al., 2011, Ribeiro et al., 2011, Chmelar et al., 2008, Mulenga et al., 2007, Ribeiro et al., 2006, Valenzuela et al., 2002). In this study we have identified 129 tick saliva proteins (TSP) of unknown function (S2 Table). For clarity secretion profiles of the 112 TSPs of unknown function are summarized in Fig 5A, while the remaining 17 glycine-rich proteins, which are thought to be involved in tick cement formation (Kemp et al, 1982) are shown in Fig 5B. It is interesting to note that in S2 Table, 93.7% (105/112) of TSPs were detected in 24-120 h saliva which could indicate that these proteins are important to tick feeding physiology. The remaining 6.3% (7/112) were exclusive to BD and SD stages and are likely associated with events towards end of feeding. Some proteins were found at one time point: 48 (n = 12), 72 (n = 7), 96 (n = 5) and 120 h (n = 14) saliva (S2 Table). More than half (n = 62) of TSPs of unknown function were detected within the first 48 h of feeding. These could be crucial for tick feeding initiation and progression. Patterns in Fig 5A suggest that the tick may potentially selectively inject different proteins into its host every 24 h. In this way, the tick could successfully evade host immunity and acquire a blood meal. Seven clusters (UCA-UCG) of TSP of unknown function are observed (Fig 5A). Most notable is that TSP of unknown function that are highly abundant at 24 h (UCG Fig 5A), decrease with feeding indicating that these proteins could serve as pivotal proteins in commencing the tick feeding process. Other secretion patterns include proteins that are abundant

at 48, 72, 96, and 120 h in UCE, UCC, UCF, and UCA respectively, as these proteins could be important in maintaining different phases of the tick feeding process. Proteins in UCD and UCA could play important roles towards end of feeding such as in wound healing and detachment from its host or serve as markers for completion of tick feeding.

Like several other hard ticks, *I. scapularis* ticks secrete cement to securely anchor onto host skin during the prolonged tick-feeding period (Sonenshine and Roe, 2014, Sauer et al., 1995, Kemp et al., 1982). Chemical analysis studies have shown that tick cement has a high content of glycine-rich proteins (Kemp et al., 1982). On this basis, we speculate that glycine rich proteins in S2 Table could be associated with tick cement formation. The first layer of the tick cement cone is deposited within 5-30 min of the tick attaching, while the second layer starts to form from 24 h post attachment (Kemp et al., 1982). It is interesting to note that majority (n = 13) of the glycine rich proteins were identified in high abundance in 24 and 48 h saliva (S3 Table and Fig 5B). Secretion patterns of glycine rich proteins shown in Fig 5B suggest that the tick alternates secretion of these proteins during feeding. Most notably the proteins in GCA are most abundant in 24 h, GCB in 48 h, GCC in 96 h, GCD in BD-SD, and GCE in 72-120 h saliva (Fig 5B). The importance of glycine rich proteins detected in abundance towards the end of feeding is unknown at this point. However, there is a possibility for these proteins representing products of degenerated salivary glands. It will be interesting to determine the function of these proteins towards the end of feeding. When subjected to phylogeny analysis, 40.2% (45/112) of TSP of unknown function are unique in that they segregate individually, followed by 7.1% (8/112) that cluster in pairs, and the remaining 52.7% (59/112) segregate in five clusters (C) A-E (Fig 6). According to previously described classifications of *I. scapularis* proteins (Ribeiro et al., 2006), CA, CB, and CD clusters are respectively classified as basic tail (group 1, n = 15) or tailless proteins (group 2, n = 10),

GPIIb/IIIa antagonist (group 9, n = 7), and 7-9 kDa family (group 7, n = 11). TSPs in CC cluster (n = 7) have insulin binding-like proteins motifs (Mulenga and Khumthong, 2010), while CE cluster proteins are leucine rich (n = 9) as revealed by sequence inspection. On the basis of amino acid motifs, Ribeiro et al., (2006) classified basic tail and basic tailless proteins into types I-III. Of the 25 CA proteins, 44% (11/25) and 20% (5/25) fit to basic tail types I and II protein respectively, and the remaining 36% (9/25) fit to basic tailless proteins.

An interesting observation from our data is that proteins that segregated together in the (Fig 6), were identified at different time points (Figs 7A-E) suggesting that the tick could be selectively secreting these proteins during feeding. Similar to Figs 3-5, we used Z-statistics normalization of NSAF values (S3 Table) to develop heat maps in Figs 7A-E. Basic tail or tailless proteins segregated into five clusters according to secretion patterns starting with the lone protein in BCA that is abundant in SD, followed by proteins in BCB, BCC, BCD and BCE that are respectively abundant in 96, 48, 120, and 72 h saliva (Fig 7A). Likewise in Fig 7B, GPIIb/IIIa antagonist protein cluster in three groups: abundant from 72 h (GPCA), 24 and 48 h (GPCB), and 48 h only (GPCC). In Fig 7C, except for one protein, which is abundant in SD saliva (ICB), majority of these proteins are abundant in 24-72 h saliva (ICA). In Figs 7D and 7E, 7-9 kDa and Leucine rich proteins were identified at variable levels throughout feeding.

Putative GPIIb/IIIa in GPCB (Fig 7B) cluster are characterized by "RGD" motif and can potentially block platelet aggregation by blocking activated platelets from binding to fibrinogen (Heemskerk et al., 2002). In a recent study, peptides containing the "NGR" motif prevented resting platelets to bind to fibrinogen (Moriarty et al., 2015). It is interesting to note that four (AAY66799, AAY66507, AAY66621, and AAY66504) basic tail saliva proteins have this motif. Whether or not these proteins can functionally block platelet aggregation of resting platelets needs verification.

If functional, these could play key roles in tick feeding success in that at the start of tick feeding, the tick will encounter resting platelets. Surprisingly none of the four NGR motif proteins were detected in 24 h saliva when we expect resting platelets at the feeding site. Interestingly, except for AAY66507.1 (UCE) detected in 48 and 96 h saliva, the other three were detected at single time points: AAY66799.1 at 72 h (UCC), AAY66621.1 at 96 h (UCF), and AAY66504.1 at 120 h (UCB).

I. scapularis tick saliva extracellular matrix-like proteins

Similar to glycine-rich proteins, extracellular matrix proteins likely participate in tick cement formation and/or cell adhesion function. In this study we found 9 extracellular proteins (S2 Table) that included cuticle and chitinase-like proteins. Two secretion patterns are observed in Fig 5C, where ECB proteins were abundant from 24-96 h and ECA proteins were abundant in BD and SD saliva. No proteins were detected in 120 h saliva from this class. It is interesting to note that both the active and inactive forms of chitinase were identified in the first 48 h. The former is highlighted by a peritrophin-A chitin-binding domain, which is involved in remodeling the chitinous tick exoskeleton, particularly the mouthpart (Arkane and Muthukrishnan, 2010, Merzendorfer and Zimoch, 2003). The latter is highly identical to *A. americanum* tick feeding stimuli responsive acidic chitinase (Mulenga et al., 2007), which when silenced by RNAi caused ticks to loosely attach onto host skin (Kim et al., 2014). Blast2seq alignments revealed that the two *I. scapularis* inactive chitinases (EEC01936.1 and JAB70416.1) identified in both 24 and 48 h saliva are respectively 64 and 65% identical to *A. americanum* inactive chitinase (AIR95100.1). Whether or not *I. scapularis* inactive chitinases serves similar function during tick feeding needs further investigation.

Housekeeping proteins and other TSPs

In addition to anti-oxidants discussed above, housekeeping-like proteins identified in this study include those associated with metabolism of lipids (n = 15), carbohydrates (n = 20), intermediate (n =1), energy (n = 45), nucleotides (n = 14) and amino acids (n = 20) (S2 Table). Others are classified as cytoskeletal (n = 32), proteasome machinery (n = 10), protein modification (n = 49), protein synthesis (n = 24), protein export (n = 10), nuclear regulation (n = 7), signal transduction and apoptosis (n = 8), transcription machinery, (n = 8), and transporters and receptors (n = 19) (S2 Table). Cumulative NSAF as an index for protein abundance suggests that majority of housekeeping-like proteins were secreted toward the end of tick feeding in BD and SD saliva, respectively (Table 1).

The tick salivary gland starts to degenerate toward the end of tick feeding and is almost completed within four days of the tick detaching (Freitas et al., 2007, Sauer et al., 1995). Given that most housekeeping genes function inside the cell, one may argue that the high abundance of these proteins in BD and SD saliva may represent progressive SG degradation toward end of tick feeding. However, recent immuno-screening of phage display expression libraries with antibodies to 24 h *I. scapularis* (Lewis et al., 2015) and 24-48 h *A. americanum* (Radulovic et al., 2014) tick saliva proteins that identified housekeeping-like indicates that secretion of some of the housekeeping proteins starts way before tick salivary gland degeneration, and thus, these proteins likely play important role(s) in tick feeding regulation.

One remarkable tick adaptation is that although ticks feed from a wounded area in the host's skin, the feeding site is completely healed when ticks complete feeding and detach from host skin. There is a possibility that some of the proteins identified in BD and SD could be associated with speeding up wound healing. It is interesting to note that some cytoskeletal proteins including

actin (Rockey et al., 2013, Strudwick and Cowin, 2012, Cowin, 2006, Martin and Lewis, 1992, Doillon et al., 1987), profilin (Ho et al., 2014, Brock et al., 2012), alpha tubulin (Ho et al., 2014), calponin (Daimon et al., 2013, Appel et al., 2010), non-muscle myosin (Bond et al., 2011, Bement et al., 1993, Martin and Lewis, 1992), thymosin (Kim and Kwon et al., 2015), and tropomyosin (Lees et al., 2013) identified at high abundance in BD and SD saliva were associated with different aspects of wound healing. Could secretion of these proteins at high abundance be the tick's way to help the host heal?

Host proteins in I. scapularis saliva

When ticks feed on blood, they uptake thousands of host proteins. The observation in this study that *I. scapularis* secreted 83 out of thousands of host proteins suggests that the tick has a mechanism to selectively secrete host proteins in its saliva. Similar to secretion dynamics of tick-derived proteins, the tick appears to selectively secrete different rabbit proteins at different tick feeding time points (S1 Table). It is potentially possible that similar to tick-derived proteins, host proteins in tick saliva perform functions that are unique to different tick feeding phases. Proteins identified from 24/48 h saliva and other time points (immunity/antimicrobial function, heme/iron metabolism, hemoglobin, nuclear regulation, extracellular matrix, and collagen alpha-1 chain), likely aide the tick to feed. On the other hand, proteins identified in BD and SD saliva such as fibrinogen and protease inhibitors are likely associated with events toward the end of tick feeding. For instance, functionally annotated antimicrobial peptides: antimicrobial protein CAP18 (Larrick et al., 1995, Tossi et al., 1994) identified in all samples except 120 h saliva, neutrophil gelatinase-associated lipocalin (Nasioudis and Witkin, 2015, Miethke and Skerra, 2010), neutrophil granule protein (Borregaard et al., 2007, Brinkmann et al., 2004, Levy, 2000), protein S100-A12

(Santamaria-Kisiel et al., 2006), neutrophil antibiotic (Levy, 2000), and lysozyme C (Ibrahim et al., 2001, Laible and Germaine, 1985) that were identified in 48 h and other stage saliva (S2 Table) could aid the tick to clear microbes from the tick feeding site. It is interesting to note that we identified both tick- and rabbit- derived antimicrobial peptides at the same time points. It is most likely that these antimicrobial peptides target different microbes with tick-derived proteins clearing tick-derived microbes, whereas host-derived proteins clear microbes from the host. Cell free hemoglobin (Hb) was shown to possess antimicrobial activity through oxidative shock (Lee and Ding, 2013, Du et al., 2010), and thus there is a possibility that Hb detected in tick saliva could be providing antimicrobial function (Belmonte et al., 2012, Fogaca et al., 1999) at the tick-feeding site. In another study peptides derived from hemoglobin digestion by tick proteases have been described as antimicrobial peptides (Nakajima et al., 2003, Sforca et al. ,2005, Fogaca et al., 1999). It is also possible that secretion of Hb could just be an indication of blood meal digestion.

Similar to ticks (Fig 1), rabbit derived heme/iron metabolism associated proteins were the highly abundant at all time points (Fig 2). A notable difference is that whereas we exclusively identified heme-binding proteins for ticks, we identified a majority of iron binding proteins for rabbits (n = 6) and one heme binding protein (S2 Table). Could this mean that, *I. scapularis* uses host proteins to remove excess iron though its saliva? If so, it could be that *I. scapularis* tick-derived heme binding proteins are responsible for removing heme, but the tick engages host-iron binding proteins to remove excess iron. Except for haptoglobin (Dobryszycka, 1997), which was detected in SD saliva, all other iron binding proteins: serum albumin, histidine rich glycoprotein, lactotransferrin, and serotransferrin as well as the heme binding protein, hemopexin and serum albumin were identified from 24/48 h saliva and other stages during feeding (S2 Table). Based on our data, *I. scapularis* apparently could use host proteins to eliminate excess iron from the host

starting within 24-48 h. It is also interesting to note that human serum albumin was shown to suppress tumor necrosis factor-alpha (TNF) and complement component C5a triggered neutrophil respiratory burst (Schreiber et al., 2009, Nathan et al., 1993). It is possible the increased concentration of serum albumin at the tick-feeding site could serve other functions. Given that the host uses iron sequestration as the defense mechanism against microbes (Cassat and Skaar, 2013, Skaar, 2010, Ganz, 2009, Collins, 2008), it is possible that the tick's manipulation of the host to pump back iron into the feeding site could be an adaptation to aide TBD agents to colonize the host, with exception of organisms such as *B. burgdorferi,* which do not need iron for proliferation (Posey and Gherardini, 2000).

It is interesting to note that in this study we detected rabbit fibrinogen in BD and SD saliva. Fibrinogen is the source for fibrin needed to strengthen the blood clot (Mosesson, 2005, Davie et al., 1991). Could it be that the tick pumps back fibrinogen into the host to aide in sealing off the feeding site at the end of tick feeding? Given that high abundance of keratins are expressed in the skin (Kim and Coulombe, 2007, Fuchs and Cleveland, 1998), there is a possibility that keratin proteins identified in *I. scapularis* tick saliva could be due to sample handling or rabbit skin contamination. It is important to note that all keratin types that were identified in *I. scapularis* tick saliva in this study are associated with different layers of the skin (Moll et al., 2008, Schweizer et al., 2006), and thus there is a high chance we identified remnants on tick mouthparts. However the eight keratin proteins identified in this study represent less than a quarter of the 27 skin keratins (Moll et al., 2008). Does the tick selectively inject keratins, and for what purpose is an interesting question for future research.

Conclusion

The unique contribution of this study is that, we have for the first time attempted to identify tick- and host- derived proteins that are found in *I. scapularis* tick saliva every 24 h through the first five days of feeding as well as toward the end of feeding. This study provides identities of *I. scapularis* tick saliva proteins associated with regulation of: (i) early tick feeding events such as tick attachment onto host skin and creating the feeding lesion, which precede tick transmission of TBD agents, (ii) slow feeding phase when most TBD agents are transmitted and the tick prepares for rapid feeding phase, and (iii) rapid feeding phase when the tick feeds to repletion and detaches from the host. The impact of these data on future in depth tick feeding physiology studies is vast. For instance, transmission of most TBD agents occur at least 36-48 h post tick attachment (Gern, 2009, Konnai et al., 2007, Ebel et al., 2004, des Vignes et al., 2001, Katavolos et al., 1998). What happens if we immunize against 24-48 h tick saliva proteins, is TBD agent transmission stopped? On the other hand we have identified proteins that were apparently secreted at all time points. In future studies, it would be interesting to determine if these proteins regulate "must have" pathways? It will be interesting to validate the importance of such proteins using the RNAi silencing approach. Some proteins were found at single, two or three time points, could these regulate functions unique to that tick-feeding period?

An interesting recurring pattern observed in these data is that some functionally similar but antigenically unique proteins were identified at different feeding time points. We speculate that this could be the tick's strategy to protect essential pathways from immune response attack. For instance, host immune response against 24 h proteins will not affect functions of functionally similar but antigenically unique proteins at later feeding time points. Essentially the host immune defense against tick feeding will restart every so often, and in the end it will not be effective. In

this way key tick feeding physiological functions will continue uninterrupted. Could this mechanism be the tick's equivalent to antigenic variation used by parasites such as Trypanosomes to evade host immunity (Horn, 2014, Barry and McCulloch, 2001, Turner, 1984)? What happens if we target as a cluster of functionally similar but antigenically unique proteins that are injected into the host at different time points?

We would like to caution the reader on the inherent limitations of this study. First, in LC-MS/MS approaches, there is a possibility that predominant proteins will mask discovery of lowly expressed but important proteins, and thus the list of *I. scapularis* tick saliva proteins presented here may not be exhaustive. Second, we sequenced proteins in saliva that was collected by pilocarpine stimulation, and whether or not all detected proteins are secreted under physiological conditions remains to be investigated. However, we are encouraged by our findings that 13% (76/582) of *I. scapularis* tick saliva proteins in this study were reported in other tick saliva proteomes and immuno-transcriptome studies (S4 Table). Of the 76 proteins, 12 and 13 proteins were found among tick saliva immunogenic proteins that bound antibodies to 24 h *I. scapularis* (Lewis et al., 2015) and 24-48 h *A. americanum* tick saliva proteins (Radulovic et al., 2014) respectively. Additionally one protein was identified in *I. scapularis* nymphs as an immunogenic protein that bound to human serum from exposure to tick bites (Becker et al., 2015). The remaining proteins were found in saliva proteomes of *R. microplus* (n=28, (Tirloni et al., 2014)), *H. longicornis* (n=22, (Tirloni et al., 2015)), *D. andersoni* (n=2, (Mudenda et al., 2014)), *O. moubata* (n=5, (Diaz-Martin et al., 2013), sequencing of *I. scapularis* tick saliva by Edman degradation (n = 4) (Valenzuela et al., 2002), and others were verified as secreted in western blotting studies (Kim et al., 2015, Radulovic et al., 2015, Ibelli et al., 2014, Mulenga et al., 2013, Schuijt et al., 2011, Buresova et al., 2009, Narasimhan et al., 2002, Sanders et al., 1999).

I. scapularis proteins in S4 Table could represent highly conserved tick saliva proteins that regulate important functions, which if disrupted could affect the tick. These proteins could represent priority candidates in future studies. We would like to note that some of the protein sequences in this study are from *I. ricinus* and other tick species. Majority of these protein sequences have homologs in *I. scapularis*, which were eliminated as redundancies when we collapsed the local database. *I. ricinus* proteins in this study represent highly conserved proteins among *Ixodes* spp ticks.

References

Appel S, Allen PG, Vetterkind S, Jin JP, Morgan KG. (2010) H3/acidic calponin: An actin-binding protein that controls extracellular signal-regulated kinase 1/2 activity in nonmuscle cells. Mol Biol Cell 21(8): 1409-1422. 10.1091/mbc.E09-06-0451 [doi].

Arakane Y, Muthukrishnan S. (2010) Insect chitinase and chitinase-like proteins. Cell Mol Life Sci 67(2): 201-216. 10.1007/s00018-009-0161-9; 10.1007/s00018-009-0161-9.

Ashburner M, Ball CA, Blake JA, Botstein D, Butler H, et al. (2000) Gene ontology: Tool for the unification of biology. the gene ontology consortium. Nat Genet 25(1): 25-29. 10.1038/75556 [doi].

Ballouche M, Cornelis P, Baysse C. (2009) Iron metabolism: A promising target for antibacterial strategies. Recent Pat Antiinfect Drug Discov 4(3): 190-205. Abstract 02 for E.Pub [pii].

Barry JD, McCulloch R. (2001) Antigenic variation in trypanosomes: Enhanced phenotypic variation in a eukaryotic parasite. Adv Parasitol 49: 1-70.

Bateman A, Birney E, Cerruti L, Durbin R, Etwiller L, et al. (2002) The pfam protein families database. Nucleic Acids Res 30(1): 276-280.

Beaufays J, Adam B, Decrem Y, Prevot PP, Santini S, et al. (2008) *Ixodes ricinus* tick lipocalins: Identification, cloning, phylogenetic analysis and biochemical characterization. PLoS One 3(12): e3941. 10.1371/journal.pone.0003941 [doi].

Becker M, Felsberger A, Frenzel A, Shattuck WM, Dyer M, et al. (2015) Application of M13 phage display for identifying immunogenic proteins from tick (*Ixodes scapularis*) saliva. BMC Biotechnol 15: 43-015-0167-3. 10.1186/s12896-015-0167-3 [doi].

Belmonte R, Cruz CE, Pires JR, Daffre S. (2012) Purification and characterization of hb 98-114: A novel hemoglobin-derived antimicrobial peptide from the midgut of *Rhipicephalus (Boophilus) microplus*. Peptides 37(1): 120-127. 10.1016/j.peptides.2012.05.017 [doi].

Bement WM, Forscher P, Mooseker MS. (1993) A novel cytoskeletal structure involved in purse string wound closure and cell polarity maintenance. J Cell Biol 121(3): 565-578.

Bond JE, Ho TQ, Selim MA, Hunter CL, Bowers EV, et al. (2011) Temporal spatial expression and function of non-muscle myosin II isoforms IIA and IIB in scar remodeling. Lab Invest 91(4): 499-508. 10.1038/labinvest.2010.181 [doi].

Borregaard N, Sorensen OE, Theilgaard-Monch K. (2007) Neutrophil granules: A library of innate immunity proteins. Trends Immunol 28(8): 340-345. S1471-4906(07)00156-1 [pii].

Brinkmann V, Reichard U, Goosmann C, Fauler B, Uhlemann Y, et al. (2004) Neutrophil extracellular traps kill bacteria. Science 303(5663): 1532-1535. 10.1126/science.1092385 [doi].

Brock AR, Wang Y, Berger S, Renkawitz-Pohl R, Han VC, et al. (2012) Transcriptional regulation of profilin during wound closure in *Drosophila* larvae. J Cell Sci 125(Pt 23): 5667-5676. 10.1242/jcs.107490 [doi].

Buresova V, Hajdusek O, Franta Z, Sojka D, Kopacek P. (2009) IrAM-an alpha2-macroglobulin from the hard tick Ixodes ricinus: Characterization and function in phagocytosis of a potential pathogen *Chryseobacterium indologenes*. Dev Comp Immunol 33(4): 489-498. 10.1016/j.dci.2008.09.011 [doi].

Cassat JE, Skaar EP. (2013) Iron in infection and immunity. Cell Host Microbe 13(5): 509-519. 10.1016/j.chom.2013.04.010 [doi].

Carvalho PC, Yates Iii JR, Barbosa VC. (2010) Analyzing shotgun proteomic data with PatternLab for proteomics. Curr Protoc Bioinformatics Chapter 13: Unit 13.13.1-15. 10.1002/0471250953.bi1313s30 [doi].

Chmelar J, Oliveira CJ, Rezacova P, Francischetti IM, Kovarova Z, et al. (2011) A tick salivary protein targets cathepsin G and chymase and inhibits host inflammation and platelet aggregation. Blood 117(2): 736-744. 10.1182/blood-2010-06-293241.

Chmelar J, Anderson JM, Mu J, Jochim RC, Valenzuela JG, et al. (2008) Insight into the sialome of the castor bean tick, *Ixodes ricinus*. BMC Genomics 9: 233-2164-9-233. 10.1186/1471-2164-9-233 [doi].

Chrudimska T, Slaninova J, Rudenko N, Ruzek D, Grubhoffer L. (2011) Functional characterization of two defensin isoforms of the hard tick *Ixodes ricinus*. Parasit Vectors 4: 63-3305-4-63. 10.1186/1756-3305-4-63 [doi].

Citelli M, Lara FA, da Silva Vaz I,Jr, Oliveira PL. (2007) Oxidative stress impairs heme detoxification in the midgut of the cattle tick, *Rhipicephalus (Boophilus) microplus*. Mol Biochem Parasitol 151(1): 81-88. S0166-6851(06)00309-4 [pii].

Collins HL. (2008) Withholding iron as a cellular defence mechanism--friend or foe? Eur J Immunol 38(7): 1803-1806. 10.1002/eji.200838505 [doi].

Cornelis P, Wei Q, Andrews SC, Vinckx T. (2011) Iron homeostasis and management of oxidative stress response in bacteria. Metallomics 3(6): 540-549. 10.1039/c1mt00022e [doi].

Cornelis P. (2010) Iron uptake and metabolism in pseudomonads. Appl Microbiol Biotechnol 86(6): 1637-1645. 10.1007/s00253-010-2550-2 [doi].

Cowin AJ. (2006) Role of the actin cytoskeleton in wound healing and scar formation. Primary Intention 14(1): 39-42.

Daimon E, Shibukawa Y, Wada Y. (2013) Calponin 3 regulates stress fiber formation in dermal fibroblasts during wound healing. Arch Dermatol Res 305(7): 571-584. 10.1007/s00403-013-1343-8 [doi].

Dartt DA. (2011) Tear lipocalin: Structure and function. Ocul Surf 9(3): 126-138.

Das S, Banerjee G, DePonte K, Marcantonio N, Kantor FS, et al. (2001) Salp25D, an *Ixodes scapularis* antioxidant, is 1 of 14 immunodominant antigens in engorged tick salivary glands. J Infect Dis 184(8): 1056-1064. JID010466 [pii].

Davie EW, Fujikawa K, Kisiel W. (1991) The coagulation cascade: Initiation, maintenance, and regulation. Biochemistry 30(43): 10363-10370.

Decrem Y, Mariller M, Lahaye K, Blasioli V, Beaufays J, et al. (2008) The impact of gene knock-down and vaccination against salivary metalloproteases on blood feeding and egg laying by *Ixodes ricinus*. Int J Parasitol 38(5): 549-560. 10.1016/j.ijpara.2007.09.003.

des Vignes F, Piesman J, Heffernan R, Schulze TL, Stafford KC,3rd, et al. (2001) Effect of tick removal on transmission of *Borrelia burgdorferi* and *Ehrlichia phagocytophila* by *Ixodes scapularis* nymphs. J Infect Dis 183(5): 773-778. JID000708 [pii].

Diaz-Martin V, Manzano-Roman R, Valero L, Oleaga A, Encinas-Grandes A, et al. (2013) An insight into the proteome of the saliva of the argasid tick *Ornithodoros moubata* reveals important differences in saliva protein composition between the sexes. J Proteomics 80: 216-235. 10.1016/j.jprot.2013.01.015 [doi].

Dobryszycka W. (1997) Biological functions of haptoglobin--new pieces to an old puzzle. Eur J Clin Chem Clin Biochem 35(9): 647-654.

Doillon CJ, Hembry RM, Ehrlich HP, Burke JF. (1987) Actin filaments in normal dermis and during wound healing. Am J Pathol 126(1): 164-170.

Du R, Ho B, Ding JL. (2010) Rapid reprogramming of haemoglobin structure-function exposes multiple dual-antimicrobial potencies. EMBO J 29(3): 632-642. 10.1038/emboj.2009.380 [doi].

Dumas Z, Ross-Gillespie A, Kummerli R. (2013) Switching between apparently redundant iron-uptake mechanisms benefits bacteria in changeable environments. Proc Biol Sci 280(1764): 20131055. 10.1098/rspb.2013.1055 [doi].

Dutra FF, Bozza MT. (2014) Heme on innate immunity and inflammation. Front Pharmacol 5: 115. 10.3389/fphar.2014.00115 [doi].

Ebel GD, Kramer LD. (2004) Short report: Duration of tick attachment required for transmission of Powassan virus by deer ticks. Am J Trop Med Hyg 71(3): 268-271.

Esteves E, Fogaca AC, Maldonado R, Silva FD, Manso PP, et al. (2009) Antimicrobial activity in the tick *Rhipicephalus (Boophilus) microplus* eggs: Cellular localization and temporal expression of microplusin during oogenesis and embryogenesis. Dev Comp Immunol 33(8): 913-919. 10.1016/j.dci.2009.02.009 [doi].

Florens L, Carozza MJ, Swanson SK, Fournier M, Coleman MK, et al. (2006) Analyzing chromatin remodeling complexes using shotgun proteomics and normalized spectral abundance factors. Methods 40(4): 303-311. S1046-2023(06)00207-6 [pii].

Flower DR. (1996) The lipocalin protein family: Structure and function. Biochem J 318 (Pt 1)(Pt 1): 1-14.

Flower DR. (1994) The lipocalin protein family: A role in cell regulation. FEBS Lett 354(1): 7-11. 0014-5793(94)01078-1 [pii].

Fogaca AC, Lorenzini DM, Kaku LM, Esteves E, Bulet P, et al. (2004) Cysteine-rich antimicrobial peptides of the cattle tick *Boophilus microplus*: Isolation, structural characterization and tissue expression profile. Dev Comp Immunol 28(3): 191-200. S0145305X03001514 [pii].

Fogaca AC, da Silva PI, Jr, Miranda MT, Bianchi AG, Miranda A, et al. (1999) Antimicrobial activity of a bovine hemoglobin fragment in the tick *Boophilus microplus*. J Biol Chem 274(36): 25330-25334.

Fox JW, Serrano SM. (2005) Structural considerations of the snake venom metalloproteinases, key members of the M12 reprolysin family of metalloproteinases. Toxicon 45(8): 969-985. S0041-0101(05)00064-4 [pii].

Francischetti IM, Anderson JM, Manoukis N, Pham VM, Ribeiro JM. (2011) An insight into the sialotranscriptome and proteome of the coarse bontlegged tick, *Hyalomma marginatum rufipes*. J Proteomics 74(12): 2892-2908. 10.1016/j.jprot.2011.07.015 [doi].

Francischetti IM, Sa-Nunes A, Mans BJ, Santos IM, Ribeiro JM. (2009) The role of saliva in tick feeding. Front Biosci (Landmark Ed) 14: 2051-2088. 3363 [pii].

Francischetti IM, Meng Z, Mans BJ, Gudderra N, Hall M, et al. (2008) An insight into the salivary transcriptome and proteome of the soft tick and vector of epizootic bovine abortion, *Ornithodoros coriaceus*. J Proteomics 71(5): 493-512. 10.1016/j.jprot.2008.07.006 [doi].

Francischetti IM, My Pham V, Mans BJ, Andersen JF, Mather TN, et al. (2005) The transcriptome of the salivary glands of the female western black-legged tick *Ixodes pacificus* (Acari: Ixodidae). Insect Biochem Mol Biol 35(10): 1142-1161. S0965-1748(05)00123-2 [pii].

Francischetti IM, Mather TN, Ribeiro JM. (2003) Cloning of a salivary gland metalloprotease and characterization of gelatinase and fibrin(ogen)lytic activities in the saliva of the Lyme disease tick vector *Ixodes scapularis*. Biochem Biophys Res Commun 305(4): 869-875. S0006291X0300857X [pii].

Freitas DR, Rosa RM, Moura DJ, Seitz AL, Colodel EM, et al. (2007) Cell death during preoviposition period in *Boophilus microplus* tick. Vet Parasitol 144(3-4): 321-327. S0304-4017(06)00612-1 [pii].

Fuchs E, Cleveland DW. (1998) A structural scaffolding of intermediate filaments in health and disease. Science 279(5350): 514-519.

Galay RL, Umemiya-Shirafuji R, Mochizuki M, Fujisaki K, Tanaka T. (2015) Iron metabolism in hard ticks (Acari: Ixodidae): The antidote to their toxic diet. Parasitol Int 64(2): 182-189. 10.1016/j.parint.2014.12.005 [doi].

Ganfornina MD, Kayser H, Sanchez D. (2000) Lipocalins in arthropoda: Diversification and functional explorations. In: Madame Curie Bioscience Database [Internet] Austin (TX): Landes Bioscience.

Ganz T. (2009) Iron in innate immunity: Starve the invaders. Curr Opin Immunol 21(1): 63-67. 10.1016/j.coi.2009.01.011 [doi].

Gern L. (2009) Life cycle of *Borrelia burgdorferi* sensu lato and transmission to humans. Curr Probl Dermatol 37: 18-30. 10.1159/000213068 [doi].

Gudderra NP, Neese PA, Sonenshine DE, Apperson CS, Roe RM. (2001) Developmental profile, isolation, and biochemical characterization of a novel lipoglycoheme-carrier protein from the american dog tick, *Dermacentor variabilis* (Acari: Ixodidae) and observations on a similar protein in the soft tick, *Ornithodoros parkeri* (Acari: Argasidae). Insect Biochem Mol Biol 31(4-5): 299-311. S0965174800001223 [pii].

Graca-Souza AV, Maya-Monteiro C, Paiva-Silva GO, Braz GR, Paes MC, et al. (2006) Adaptations against heme toxicity in blood-feeding arthropods. Insect Biochem Mol Biol 36(4): 322-335. S0965-1748(06)00012-9 [pii].

Graca-Souza AV, Arruda MA, de Freitas MS, Barja-Fidalgo C, Oliveira PL. (2002) Neutrophil activation by heme: Implications for inflammatory processes. Blood 99(11): 4160-4165.

Heemskerk JW, Bevers EM, Lindhout T. (2002) Platelet activation and blood coagulation. Thromb Haemost 88(2): 186-193.

Ho S, Marcal H, Foster LJ. (2014) Towards scarless wound healing: A comparison of protein expression between human, adult and foetal fibroblasts. Biomed Res Int 2014: 676493. 10.1155/2014/676493 [doi].

Horka H, Staudt V, Klein M, Taube C, Reuter S, et al. (2012) The tick salivary protein sialostatin L inhibits the Th9-derived production of the asthma-promoting cytokine IL-9 and is effective in the prevention of experimental asthma. J Immunol 188(6): 2669-2676. 10.4049/jimmunol.1100529 [doi].

Horn D. (2014) Antigenic variation in African trypanosomes. Mol Biochem Parasitol 195(2): 123-129. 10.1016/j.molbiopara.2014.05.001 [doi].

Ibelli AM, Kim TK, Hill CC, Lewis LA, Bakshi M, et al. (2014) A blood meal-induced *Ixodes* scapularis tick saliva serpin inhibits trypsin and thrombin, and interferes with platelet aggregation and blood clotting. Int J Parasitol 44(6): 369-379. 10.1016/j.ijpara.2014.01.010 [doi].

Ibrahim HR, Matsuzaki T, Aoki T. (2001) Genetic evidence that antibacterial activity of lysozyme is independent of its catalytic function. FEBS Lett 506(1): 27-32. S0014-5793(01)02872-1 [pii].

Katavolos P, Armstrong PM, Dawson JE, Telford SR,3rd. (1998) Duration of tick attachment required for transmission of granulocytic Ehrlichiosis. J Infect Dis 177(5): 1422-1425.

Karim S, Ribeiro JM. (2015) An insight into the sialome of the lone star tick, *Amblyomma americanum*, with a glimpse on its time dependent gene expression. PLoS One 10(7): e0131292. 10.1371/journal.pone.0131292 [doi].

Karim S, Singh P, Ribeiro JM. (2011) A deep insight into the sialotranscriptome of the gulf coast tick, *Amblyomma maculatum*. PLoS One 6(12): e28525. 10.1371/journal.pone.0028525 [doi].

Kaufman WR. (2007) Gluttony and sex in female Ixodid ticks: How do they compare to other blood-sucking arthropods? J Insect Physiol 53(3): 264-273. S0022-1910(06)00171-5 [pii].

Keller PM, Waxman L, Arnold BA, Schultz LD, Condra C, et al. (1993) Cloning of the cDNA and expression of moubatin, an inhibitor of platelet aggregation. J Biol Chem 268(8): 5450-5456.

Kemp DH, Stone BF, Binnington KC. (1982) Tick attachment and feeding: Role of the mouthparts, feeding apparatus, salivary gland secretions and the host response. In: Obenchain F, Galun R, editors. Physiology of Ticks. Oxford, UK: Pergamon Press Ltd. pp. 138-139.

Kim S, Kwon J. (2015) Thymosin beta4 has a major role in dermal burn wound healing that involves actin cytoskeletal remodelling via heat-shock protein 70. J Tissue Eng Regen Med. 10.1002/term.2028 [doi].

Kim S, Coulombe PA. (2007) Intermediate filament scaffolds fulfill mechanical, organizational, and signaling functions in the cytoplasm. Genes Dev 21(13): 1581-1597. 21/13/1581 [pii].

Kim TK, Ibelli AM, Mulenga A. (2015) *Amblyomma americanum* tick calreticulin binds C1q but does not inhibit activation of the classical complement cascade. Ticks Tick Borne Dis 6(1): 91-101. S1877-959X(14)00194-0 [pii].

Kim TK, Curran J, Mulenga A. (2014) Dual silencing of long and short *Amblyomma americanum* acidic chitinase forms weakens the tick cement cone stability. J Exp Biol 217(Pt 19): 3493-3503. 10.1242/jeb.107979 [doi].

Konnai S, Yamada S, Imamura S, Simuunza M, Chembensof M, et al. (2007) Attachment duration required for *Rhipicephalus appendiculatus* to transmit *Theileria parva* to the host. Vector Borne Zoonotic Dis 7(2): 241-248. 10.1089/vbz.2006.0616 [doi].

Kotsyfakis M, Schwarz A, Erhart J, Ribeiro JM. (2015) Tissue- and time-dependent transcription in *Ixodes ricinus* salivary glands and midguts when blood feeding on the vertebrate host. Sci Rep 5: 9103. 10.1038/srep09103 [doi].

Kotsyfakis M, Karim S, Andersen JF, Mather TN, Ribeiro JM. (2007) Selective cysteine protease inhibition contributes to blood-feeding success of the tick *Ixodes scapularis*. J Biol Chem 282(40): 29256-29263. M703143200 [pii].

Kotsyfakis M, Sa-Nunes A, Francischetti IM, Mather TN, Andersen JF, et al. (2006) Antiinflammatory and immunosuppressive activity of sialostatin L, a salivary cystatin from the tick *Ixodes scapularis*. J Biol Chem 281(36): 26298-26307. M513010200 [pii].

Kovarova Z, Chmelar J, Sanda M, Brynda J, Mares M, et al. (2010) Crystallization and diffraction analysis of the serpin IRS-2 from the hard tick *Ixodes ricinus*. Acta Crystallogr Sect F Struct Biol Cryst Commun 66(Pt 11): 1453-1457. 10.1107/S1744309110032343 [doi].

Lai R, Takeuchi H, Lomas LO, Jonczy J, Rigden DJ, et al. (2004) A new type of antimicrobial protein with multiple histidines from the hard tick, *Amblyomma hebraeum*. FASEB J 18(12): 1447-1449. 10.1096/fj.03-1154fje [doi].

Laible NJ, Germaine GR. (1985) Bactericidal activity of human lysozyme, muramidase-inactive lysozyme, and cationic polypeptides against *Streptococcus sanguis* and *Streptococcus faecalis*: Inhibition by chitin oligosaccharides. Infect Immun 48(3): 720-728.

Lara FA, Lins U, Paiva-Silva G, Almeida IC, Braga CM, et al. (2003) A new intracellular pathway of haem detoxification in the midgut of the cattle tick *Boophilus microplus*: Aggregation inside a specialized organelle, the hemosome. J Exp Biol 206(Pt 10): 1707-1715.

Larrick JW, Hirata M, Balint RF, Lee J, Zhong J, et al. (1995) Human CAP18: A novel antimicrobial lipopolysaccharide-binding protein. Infect Immun 63(4): 1291-1297.

Lee SK, Ding JL. (2013) A perspective on the role of extracellular hemoglobin on the innate immune system. DNA Cell Biol 32(2): 36-40. 10.1089/dna.2012.1897 [doi].

Lees JG, Ching YW, Adams DH, Bach CT, Samuel MS, et al. (2013) Tropomyosin regulates cell migration during skin wound healing. J Invest Dermatol 133(5): 1330-1339. 10.1038/jid.2012.489 [doi].

Levy O. (2000) Antimicrobial proteins and peptides of blood: Templates for novel antimicrobial agents. Blood 96(8): 2664-2672.

Lieskovska J, Palenikova J, Sirmarova J, Elsterova J, Kotsyfakis M, et al. (2015a) Tick salivary cystatin sialostatin L2 suppresses IFN responses in mouse dendritic cells. Parasite Immunol 37(2): 70-78. 10.1111/pim.12162 [doi].

Lieskovska J, Palenikova J, Langhansova H, Chagas AC, Calvo E, et al. (2015b) Tick sialostatins L and L2 differentially influence dendritic cell responses to *Borrelia* spirochetes. Parasit Vectors 8: 275-015-0887-1. 10.1186/s13071-015-0887-1 [doi].

Lewis LA, Radulovic ZM, Kim TK, Porter LM, Mulenga A. (2015) Identification of 24h *Ixodes scapularis* immunogenic tick saliva proteins. Ticks Tick Borne Dis 6(3): 424-434. 10.1016/j.ttbdis.2015.03.012 [doi].

Lu X, Che Q, Lv Y, Wang M, Lu Z, et al. (2010) A novel defensin-like peptide from salivary glands of the hard tick, *Haemaphysalis longicornis*. Protein Sci 19(3): 392-397. 10.1002/pro.317 [doi].

Mans BJ. (2005) Tick histamine-binding proteins and related lipocalins: Potential as therapeutic agents. Curr Opin Investig Drugs 6(11): 1131-1135.

Marchler-Bauer A, Derbyshire MK, Gonzales NR, Lu S, Chitsaz F, et al. (2015) CDD: NCBI's conserved domain database. Nucleic Acids Res 43(Database issue): D222-6. 10.1093/nar/gku1221 [doi].

McDonald WH, Tabb DL, Sadygov RG, MacCoss MJ, Venable J, et al. (2004) MS1, MS2, and SQT-three unified, compact, and easily parsed file formats for the storage of shotgun proteomic spectra and identifications. Rapid Commun Mass Spectrom 18(18): 2162-2168. 10.1002/rcm.1603 [doi].

Maritz-Olivier C, Stutzer C, Jongejan F, Neitz AW, Gaspar AR. (2007) Tick anti-hemostatics: Targets for future vaccines and therapeutics. Trends Parasitol 23(9): 397-407. S1471-4922(07)00173-0 [pii].

Martin P, Lewis J. (1992) Actin cables and epidermal movement in embryonic wound healing. Nature 360(6400): 179-183. 10.1038/360179a0 [doi].

Maya-Monteiro CM, Alves LR, Pinhal N, Abdalla DS, Oliveira PL. (2004) HeLp, a heme-transporting lipoprotein with an antioxidant role. Insect Biochem Mol Biol 34(1): 81-88.

Maya-Monteiro CM, Daffre S, Logullo C, Lara FA, Alves EW, et al. (2000) HeLp, a heme lipoprotein from the hemolymph of the cattle tick, *Boophilus microplus*. J Biol Chem 275(47): 36584-36589. 10.1074/jbc.M007344200 [doi].

Merzendorfer H, Zimoch L. (2003) Chitin metabolism in insects: Structure, function and regulation of chitin synthases and chitinases. J Exp Biol 206(Pt 24): 4393-4412.

Miethke M, Skerra A. (2010) Neutrophil gelatinase-associated lipocalin expresses antimicrobial activity by interfering with L-norepinephrine-mediated bacterial iron acquisition. Antimicrob Agents Chemother 54(4): 1580-1589. 10.1128/AAC.01158-09 [doi].

Moll R, Divo M, Langbein L. (2008) The human keratins: Biology and pathology. Histochem Cell Biol 129(6): 705-733. 10.1007/s00418-008-0435-6 [doi].

Moriarty R, McManus CA, Lambert M, Tilley T, Devocelle M, et al. (2015) A novel role for the fibrinogen asn-gly-arg (NGR) motif in platelet function. Thromb Haemost 113(2): 290-304. 10.1160/TH14-04-0366 [doi].

Mosesson MW. (2005) Fibrinogen and fibrin structure and functions. J Thromb Haemost 3(8): 1894-1904. JTH1365 [pii].

Mudenda L, Pierle SA, Turse JE, Scoles GA, Purvine SO, et al. (2014) Proteomics informed by transcriptomics identifies novel secreted proteins in *Dermacentor andersoni* saliva. Int J Parasitol 44(13): 1029-1037. 10.1016/j.ijpara.2014.07.003 [doi].

Mulenga A, Kim TK, Ibelli AM. (2013) Deorphanization and target validation of cross-tick species conserved novel *Amblyomma americanum* tick saliva protein. Int J Parasitol 43(6): 439-451. 10.1016/j.ijpara.2012.12.012; 10.1016/j.ijpara.2012.12.012.

Mulenga A, Erikson K. (2011) A snapshot of the *Ixodes scapularis* degradome. Gene 482(1-2): 78-93. 10.1016/j.gene.2011.04.008 [doi].

Mulenga A, Khumthong R. (2010) Silencing of three *Amblyomma americanum* (L.) insulin-like growth factor binding protein-related proteins prevents ticks from feeding to repletion. J Exp Biol 213(Pt 7): 1153-1161. 10.1242/jeb.035204 [doi].

Mulenga A, Khumthong R, Blandon MA. (2007) Molecular and expression analysis of a family of the *Amblyomma americanum* tick lospins. J Exp Biol 210(Pt 18): 3188-3198. 10.1242/jeb.006494.

Mulenga A, Tsuda A, Sugimoto C, Onuma M. (2002) Blood meal acquisition by ticks; molecular advances and implications for vaccine development. Jpn J Vet Res 49(4): 261-272.

Mulenga A, Sugino M, Nakajim M, Sugimoto C, Onuma M. (2001) Tick-encoded serine proteinase inhibitors (serpins); potential target antigens for tick vaccine development. J Vet Med Sci 63(10): 1063-1069.

Mulenga A, Sugimoto C, Onuma M. (2000) Issues in tick vaccine development: Identification and characterization of potential candidate vaccine antigens. Microbes Infect 2(11): 1353-1361.

Nakajima Y, van der Goes van Naters-Yasui, A., Taylor D, Yamakawa M. (2002) Antibacterial peptide defensin is involved in midgut immunity of the soft tick, *Ornithodoros moubata*. Insect Mol Biol 11(6): 611-618. 372 [pii].

Nakajima Y, Ogihara K, Taylor D, Yamakawa M. (2003) Antibacterial hemoglobin fragments from the midgut of the soft tick, *Ornithodoros moubata* (Acari: Argasidae). J Med Entomol 40(1): 78-81.

Narasimhan S, Sukumaran B, Bozdogan U, Thomas V, Liang X, et al. (2007) A tick antioxidant facilitates the Lyme disease agent's successful migration from the mammalian host to the arthropod vector. Cell Host Microbe 2(1): 7-18. S1931-3128(07)00127-8 [pii].

Narasimhan S, Koski RA, Beaulieu B, Anderson JF, Ramamoorthi N, et al. (2002) A novel family of anticoagulants from the saliva of *Ixodes scapularis*. Insect Mol Biol 11(6): 641-650. 375 [pii].

Nasioudis D, Witkin SS. (2015) Neutrophil gelatinase-associated lipocalin and innate immune responses to bacterial infections. Med Microbiol Immunol. 10.1007/s00430-015-0394-1 [doi].

Nathan C, Xie QW, Halbwachs-Mecarelli L, Jin WW. (1993) Albumin inhibits neutrophil spreading and hydrogen peroxide release by blocking the shedding of CD43 (sialophorin, leukosialin). J Cell Biol 122(1): 243-256.

Paesen GC, Adams PL, Nuttall PA, Stuart DL. (2000) Tick histamine-binding proteins: Lipocalins with a second binding cavity. Biochim Biophys Acta 1482(1-2): 92-101. S0167-4838(00)00168-0 [pii].

Paesen GC, Adams PL, Harlos K, Nuttall PA, Stuart DI. (1999) Tick histamine-binding proteins: Isolation, cloning, and three-dimensional structure. Mol Cell 3(5): 661-671. S1097-2765(00)80359-7 [pii].

Palenikova J, Lieskovska J, Langhansova H, Kotsyfakis M, Chmelar J, et al. (2015) *Ixodes ricinus* salivary serpin IRS-2 affects Th17 differentiation via inhibition of the interleukin-6/STAT-3 signaling pathway. Infect Immun 83(5): 1949-1956. 10.1128/IAI.03065-14 [doi].

Paoletti AC, Parmely TJ, Tomomori-Sato C, Sato S, Zhu D, et al. (2006) Quantitative proteomic analysis of distinct mammalian mediator complexes using normalized spectral abundance factors. Proc Natl Acad Sci U S A 103(50): 18928-18933. 0606379103 [pii].

Prevot PP, Couvreur B, Denis V, Brossard M, Vanhamme L, et al. (2007) Protective immunity against *Ixodes ricinus* induced by a salivary serpin. Vaccine 25(17): 3284-3292. S0264-410X(07)00012-6 [pii].

Ponka P. (1997) Tissue-specific regulation of iron metabolism and heme synthesis: Distinct control mechanisms in erythroid cells. Blood 89(1): 1-25.

Ponka P. (1999) Cellular iron metabolism. Kidney Int Suppl 69: S2-11.

Posey JE, Gherardini FC. (2000) Lack of a role for iron in the Lyme disease pathogen. Science 288(5471): 1651-1653. 8561 [pii].

Radulovic ZM, Porter LM, Kim TK, Bakshi M, Mulenga A. (2015) *Amblyomma americanum* tick saliva insulin-like growth factor binding protein-related protein 1 binds insulin but not insulin-like growth factors. Insect Mol Biol 24(5): 539-550. 10.1111/imb.12180 [doi].

Radulovic ZM, Kim TK, Porter LM, Sze SH, Lewis L, et al. (2014) A 24-48 h fed *Amblyomma americanum* tick saliva immuno-proteome. BMC Genomics 15: 518-2164-15-518. 10.1186/1471-2164-15-518 [doi].

Rawlings ND, Barrett AJ, Bateman A. (2012) MEROPS: The database of proteolytic enzymes, their substrates and inhibitors. Nucleic Acids Res 40(Database issue): D343-50. 10.1093/nar/gkr987 [doi].

Ribeiro JM, Anderson JM, Manoukis NC, Meng Z, Francischetti IM. (2011) A further insight into the sialome of the tropical bont tick, *Amblyomma variegatum*. BMC Genomics 12: 136-2164-12-136. 10.1186/1471-2164-12-136 [doi].

Ribeiro JM, Alarcon-Chaidez F, Francischetti IM, Mans BJ, Mather TN, et al. (2006) An annotated catalog of salivary gland transcripts from *Ixodes scapularis* ticks. Insect Biochem Mol Biol 36(2): 111-129. 10.1016/j.ibmb.2005.11.005.

Rockey DC, Weymouth N, Shi Z. (2013) Smooth muscle alpha actin (Acta2) and myofibroblast function during hepatic wound healing. PLoS One 8(10): e77166. 10.1371/journal.pone.0077166 [doi].

Rojkind M, Dominguez-Rosales JA, Nieto N, Greenwel P. (2002) Role of hydrogen peroxide and oxidative stress in healing responses. Cell Mol Life Sci 59(11): 1872-1891.

Rudenko N, Golovchenko M, Edwards MJ, Grubhoffer L. (2005) Differential expression of *Ixodes ricinus* tick genes induced by blood feeding or *Borrelia burgdorferi* infection. J Med Entomol 42(1): 36-41.

Sa-Nunes A, Bafica A, Antonelli LR, Choi EY, Francischetti IM, et al. (2009) The immunomodulatory action of sialostatin L on dendritic cells reveals its potential to interfere with autoimmunity. J Immunol 182(12): 7422-7429. 10.4049/jimmunol.0900075 [doi].

Saito Y, Konnai S, Yamada S, Imamura S, Nishikado H, et al. (2009) Identification and characterization of antimicrobial peptide, defensin, in the taiga tick, *Ixodes persulcatus*. Insect Mol Biol 18(4): 531-539. 10.1111/j.1365-2583.2009.00897.x [doi].

Sanders ML, Glass GE, Nadelman RB, Wormser GP, Scott AL, et al. (1999) Antibody levels to recombinant tick calreticulin increase in humans after exposure to *Ixodes scapularis* (say) and are correlated with tick engorgement indices. Am J Epidemiol 149(8): 777-784.

Sangamnatdej S, Paesen GC, Slovak M, Nuttall PA. (2002) A high affinity serotonin- and histamine-binding lipocalin from tick saliva. Insect Mol Biol 11(1): 79-86. 311 [pii].

Santamaria-Kisiel L, Rintala-Dempsey AC, Shaw GS. (2006) Calcium-dependent and -independent interactions of the S100 protein family. Biochem J 396(2): 201-214. BJ20060195 [pii].

Sauer JR, McSwain JL, Bowman AS, Essenberg RC. (1995) Tick salivary gland physiology. Annu Rev Entomol 40: 245-267. 10.1146/annurev.en.40.010195.001333.

Schreiber A, Xiao H, Jennette JC, Schneider W, Luft FC, et al. (2009) C5a receptor mediates neutrophil activation and ANCA-induced glomerulonephritis. J Am Soc Nephrol 20(2): 289-298. 10.1681/ASN.2008050497 [doi].

Schuijt TJ, Narasimhan S, Daffre S, DePonte K, Hovius JW, et al. (2011) Identification and characterization of *Ixodes scapularis* antigens that elicit tick immunity using yeast surface display. PLoS One 6(1): e15926. 10.1371/journal.pone.0015926 [doi].

Schultz J, Copley RR, Doerks T, Ponting CP, Bork P. (2000) SMART: A web-based tool for the study of genetically mobile domains. Nucleic Acids Res 28(1): 231-234. gkd062 [pii].

Schwarz A, Tenzer S, Hackenberg M, Erhart J, Gerhold-Ay A, et al. (2014) A systems level analysis reveals transcriptomic and proteomic complexity in *Ixodes ricinus* midgut and salivary glands during early attachment and feeding. Mol Cell Proteomics 13(10): 2725-2735. 10.1074/mcp.M114.039289 [doi].

Schweizer J, Bowden PE, Coulombe PA, Langbein L, Lane EB, et al. (2006) New consensus nomenclature for mammalian keratins. J Cell Biol 174(2): 169-174. jcb.200603161 [pii].

Sforca ML, Machado A, Figueredo RC, Oyama S,Jr, Silva FD, et al. (2005) The micelle-bound structure of an antimicrobial peptide derived from the alpha-chain of bovine hemoglobin isolated from the tick *Boophilus microplus*. Biochemistry 44(17): 6440-6451. 10.1021/bi0475323 [doi].

Silva FD, Rezende CA, Rossi DC, Esteves E, Dyszy FH, et al. (2009) Structure and mode of action of microplusin, a copper II-chelating antimicrobial peptide from the cattle tick *Rhipicephalus (Boophilus) microplus*. J Biol Chem 284(50): 34735-34746. 10.1074/jbc.M109.016410 [doi].

Silva FD, Rossi DC, Martinez LR, Frases S, Fonseca FL, et al. (2011) Effects of microplusin, a copper-chelating antimicrobial peptide, against *Cryptococcus neoformans*. FEMS Microbiol Lett 324(1): 64-72. 10.1111/j.1574-6968.2011.02386.x [doi].

Skaar EP. (2010) The battle for iron between bacterial pathogens and their vertebrate hosts. PLoS Pathog 6(8): e1000949. 10.1371/journal.ppat.1000949 [doi].

Smathers RL, Petersen DR. (2011) The human fatty acid-binding protein family: Evolutionary divergences and functions. Hum Genomics 5(3): 170-191. 63W0473601481088 [pii].

Sonenshine DE, Roe RM. (2014) Biology of ticks volume 1. Oxford, United Kingdom: Oxford University Press. 370 p.

Sonenshine DE, Ceraul SM, Hynes WE, Macaluso KR, Azad AF. (2002) Expression of defensin-like peptides in tick hemolymph and midgut in response to challenge with *Borrelia burgdorferi*, *Escherichia coli* and *Bacillus subtilis*. Exp Appl Acarol 28(1-4): 127-134.

Strudwick XL, Cowin AJ. (2012) Cytoskeletal regulation of dermal regeneration. Cells 1(4): 1313-1327. 10.3390/cells1041313 [doi].

Tatusov RL, Fedorova ND, Jackson JD, Jacobs AR, Kiryutin B, et al. (2003) The COG database: An updated version includes eukaryotes. BMC Bioinformatics 4: 41. 10.1186/1471-2105-4-41 [doi].

Toh SQ, Glanfield A, Gobert GN, Jones MK. (2010) Heme and blood-feeding parasites: Friends or foes? Parasit Vectors 3: 108-3305-3-108. 10.1186/1756-3305-3-108 [doi].

Tonk M, Cabezas-Cruz A, Valdes JJ, Rego RO, Chrudimska T, et al. (2014a) Defensins from the tick *Ixodes scapularis* are effective against phytopathogenic fungi and the human bacterial pathogen *Listeria grayi*. Parasit Vectors 7: 554-014-0554-y. 10.1186/s13071-014-0554-y [doi].

Tonk M, Cabezas-Cruz A, Valdes JJ, Rego RO, Rudenko N, et al. (2014b) Identification and partial characterisation of new members of the *Ixodes ricinus* defensin family. Gene 540(2): 146-152. 10.1016/j.gene.2014.03.002 [doi].

Tirloni L, Islam MS, Kim TK, Diedrich JK, Yates JR,3rd, et al. (2015) Saliva from nymph and adult females of *Haemaphysalis longicornis*: A proteomic study. Parasit Vectors 8(1): 338. 10.1186/s13071-015-0918-y [doi].

Tirloni L, Reck J, Terra RM, Martins JR, Mulenga A, et al. (2014) Proteomic analysis of cattle tick *Rhipicephalus (Boophilus) microplus* saliva: A comparison between partially and fully engorged females. PLoS One 9(4): e94831. 10.1371/journal.pone.0094831 [doi].

Tossi A, Scocchi M, Skerlavaj B, Gennaro R. (1994) Identification and characterization of a primary antibacterial domain in CAP18, a lipopolysaccharide binding protein from rabbit leukocytes. FEBS Lett 339(1-2): 108-112. 0014-5793(94)80395-1 [pii].

Turner MJ. (1984) Antigenic variation in parasites. Parasitology 88 (Pt 4)(Pt 4): 613-621.

Vizcaino JA, Deutsch EW, Wang R, Csordas A, Reisinger F, et al. (2014) ProteomeXchange provides globally coordinated proteomics data submission and dissemination. Nat Biotechnol 32(3): 223-226. 10.1038/nbt.2839 [doi].

Valenzuela JG, Francischetti IM, Pham VM, Garfield MK, Mather TN, et al. (2002) Exploring the sialome of the tick *Ixodes scapularis*. J Exp Biol 205(Pt 18): 2843-2864.

Wang J, Bian G, Pan W, Feng T, Dai J. (2015) Molecular characterization of a defensin gene from a hard tick, *Dermacentor silvarum*. Parasit Vectors 8: 25-014-0625-0. 10.1186/s13071-014-0625-0 [doi].

Warnes GR, Bolker B, Bonebakker L, Gentleman R, Huber W, et al. (2013) Various R programming tools for plotting data. The comprehensive R archive network. Http://Cran R-Project Org .

Weldon CL, Mackessy SP. (2012) Alsophinase, a new P-III metalloproteinase with alpha-fibrinogenolytic and hemorrhagic activity from the venom of the rear-fanged puerto rican racer *Alsophis portoricensis* (Serpentes: Dipsadidae). Biochimie 94(5): 1189-1198. 10.1016/j.biochi.2012.02.006 [doi].

Xu T, Park SK, Venable JD, Wohlschlegel JA, Diedrich JK, et al. (2015) ProLuCID: An improved SEQUEST-like algorithm with enhanced sensitivity and specificity. J Proteomics. S1874-3919(15)30059-2 [pii].

Xu XL, Cheng TY, Yang H, Yan F, Yang Y. (2015) De novo sequencing, assembly and analysis of salivary gland transcriptome of *Haemaphysalis flava* and identification of sialoprotein genes. Infect Genet Evol 32: 135-142. 10.1016/j.meegid.2015.03.010 [doi].

Zhang P, Shi J, Shen B, Li X, Gao Y, et al. (2009) Stejnihagin, a novel snake metalloproteinase from *Trimeresurus stejnegeri* venom, inhibited L-type Ca2+ channels. Toxicon 53(2): 309-315. 10.1016/j.toxicon.2008.12.006 [doi].

Zheng H, Zhou L, Yang X, Wang D, Liu J. (2012) Cloning and characterization of a male-specific defensin-like antimicrobial peptide from the tick *Haemaphysalis longicornis*. Dev Comp Immunol 37(1): 207-211. 10.1016/j.dci.2011.10.004 [doi].

Zhu W, Smith JW, Huang CM. (2010) Mass spectrometry-based label-free quantitative proteomics. J Biomed Biotechnol 2010: 840518. 10.1155/2010/840518 [doi].

Part II

A systems biology identification of *Amblyomma americanum* tick saliva proteins injected into rabbits every 24 h through 8 days of tick feeding

Materials and Methods

Ethics statement

All experiments were done according to the animal use protocol approved by Texas A&M University Institutional Animal Care and Use Committee (IACUC) (AUP 2011-207 and 2011-189) that meets all federal requirements, as defined in the Animal Welfare Act (AWA), the Public Health Service Policy (PHS), and the Humane Care and Use of Laboratory Animals.

A. americanum tick saliva collection

A. americanum ticks were purchased from the tick rearing facility at Oklahoma State University (Stillwater, OK, USA). Routinely, ticks were fed on rabbits as previously described (Mulenga et al., 2013a, Kim et al., 2014). Ticks were restricted to feed on the outer part of the ear of New Zealand rabbits with orthopedic stockinette glued with Kamar adhesive (Kamar Products Inc., Zionsville, IN, USA). Male *A. americanum* ticks (15 per ear) were pre-fed for three days prior to placing female ticks onto rabbit ears to feed. A total of 50 female *A. americanum* ticks (25 per ear) were placed into the tick containment apparatus on each of the three rabbits and allowed to attach.

Collection of female *A. americanum* tick saliva was done as previously described (Kim et al., 2016, Tirloni et al., 2014). Tick saliva was collected to identify proteins from two preparation methods (In-gel and In-solution) using liquid chromatography tandem mass spectrometry (LC-

MS/MS). Briefly saliva was collected from ticks injected with 1-3 μL of 2% pilocarpine hydrochloride in phosphate buffered saline (PBS, pH 7.4) between the fourth coxa and leg. Saliva was collected every 15 - 30 min for 4 h at room temperature by washing the mouthparts with sterile 1x PBS pH 7.4 using a 34-gauge needle and a Hamilton microliter syringe (Hamilton Company, Reno, NV, USA). Tick saliva was kept on ice during collections and stored at -80ºC. For the in-gel LC-MS/MS analysis, tick saliva was collected from 30 ticks that fed for 24, 72, 120, and 168 h. Likewise for in-solution LC-MS/MS analysis, saliva was collected from 30 ticks that were fed for 24, 48, 72, 96, 120, 144, 168, and 192 h, respectively, and ten ticks that were fully fed but not detached from the host (BD) and six ticks that were spontaneously detached from the host (SD).

In gel LC-MS/MS identification of proteins in A. americanum tick saliva

Tick saliva proteins were identified from an in-gel preparation method using LC-MS/MS as previously described (Tirloni et al., 2014). Saliva from a pool of 30 ticks collected from 24, 72, 120, and 168 h fed were reduced in 4X sample buffer and heat denatured at 95°C for five minutes. Total tick saliva protein collections for each time point were resolved on a Novex 4-20% Tris-Glycine Mini Gels (Thermo, Waltham, MA, USA) and visualized by Coomassie Brilliant Blue staining and destaining procedures. Visible bands were excised using a sharp razor blade and placed into a 1.5 ml tube to destain in Coomassie destaining solution (50% acetonitrile, 50% 25mM NH_4HCO_3). Destained gel slices were cut into small pieces using a fine razor blade, rinsed with ultrapure water and then dehydrated using 100% acetonitrile for 10 min. Gel pieces were individually digested using trypsin as described (Shevchenko A. et al., 1996). The resulting peptides were analyzed using an electrospray ionization (ESI) quadrupole time-of-flight (Q-TOF) MicroTM mass spectrometer (Waters, Milford, MA, USA) coupled to a capillary liquid

chromatography system nanoACQUITY UPLC (Waters, Milford, MA, USA). The peptides were eluted from a reverse-phase C18 column toward the mass spectrometer. Charged peptide ions (+2 and +3) were automatically mass selected and dissociated in MS/MS experiments.

In solution LC-MS/MS identification of proteins in A. americanum tick saliva

A. americanum tick saliva proteins were identified from an in-solution preparation method using LC-MS/MS as previously described (Tirloni et al., 2014, 2017, Kim et al., 2016). Briefly, ~2 µg of total TSPs (in triplicate runs) per feeding time point was digested in solution overnight at 37°C with trypsin in 8 M urea/0.1 M Tris (pH 8.5), reduced with 5 mM Tris (2-carboxyethyl) phosphine hydrochloride (TCEP, Sigma-Aldrich, St Louis, MO, USA), and alkylated with 25 mM iodoaceamide (Sigma-Aldrich). Proteins were digested overnight at 37°C in 2 M urea/0.1M Tris pH 8.5, 1 mM $CaCl_2$ with trypsin (Promega, Madison, WI, USA) with a final ratio of 1:20 (enzyme:substrate). Digestion reactions, in a final concentration of 0.15 µg/mL, were quenched with formic acid (5% final concentration) and centrifuged for debris removal.

Pre-columns and analytical columns

Reversed phase pre-columns were prepared by first creating a Kasil frit at one end of a deactivated 250 µm ID/360 µm OD capillary (Agilent Technologies, Santa Clara, CA, USA). Kasil frits were prepared by dipping 20 cm capillary in 300 µL Kasil 1624 (PQ Corporation, Malvern, PA, USA) and 100 µL formamide solution, curing at 100°C for 3 h and adjusting the length. Pre-columns were packed in-house (John Yates III's Laboratory, The Scripps Research Institute, La Jolla, CA, USA) with 2 cm of 5 µm ODS-AQ C18 (YMC America, Inc., Allentown, PA, USA) particles from particle slurries in methanol. Analytical reversed phase columns were fabricated by

pulling a 100 µm ID/360 µm OD silica capillary (Molex Polymicro Technologies, Austin, TX, USA) to a 5 µm ID tip. The same packing material was packed until 20 cm directly behind the pulled tip. Reversed phase pre-columns and analytical columns were connected using a zero-dead volume union (IDEX Corp., Upchurch Scientific, Oak Harbor, WA, USA).

LC-MS/MS

Peptide mixtures were analyzed by nanoflow liquid chromatography mass spectrometry using an Easy NanoLC II and a Q Exactive mass spectrometer (Thermo Scientific, Waltham, MA, USA). Peptides eluted from the analytical column were electrosprayed directly into the mass spectrometer. Buffer A and B consisted of 5% acetonitrile/0.1% formic acid and 80% acetonitrile/0.1% formic acid, respectively. The flow rate was set to 400 nL/min. Feeding time saliva samples (1.5 µg per injection) were separated in 155 min chromatographic runs, as follows: 1-10% gradient of buffer B in 10 min, 10-40% of buffer B in 100 min, 40-50% of buffer B in 10 min and 50-90% of buffer B in 10 min. Column was held at 90% of buffer B for 10 min, reduced to 1% of buffer B and re-equilibrated prior to next injection.

The mass spectrometer was operated in a data dependent mode, collecting a full MS scan from 400 to 1,200 m/z at 70,000 resolutions and an AGC target of 1×10^6. The 10 most abundant ions per scan were selected for MS/MS at 17,500 resolution and AGC target of 2×10^5 and an underfill ratio of 0.1%. Maximum fill times were 20 and 120 ms for MS and MS/MS scans, respectively, with dynamic exclusion of 15 s. Normalized collision energy was set to 25.

Identification of proteins in A. americanum tick saliva

Proteins in *A. americanum* tick saliva were identified according to the pipeline described

in Kim et al., (2016, Tirloni et al., 2014). Mass spectra from the in-gel sequencing were analyzed using databases noted above using the Mascot software version 2.2 (Matrix Science, London, UK) with parameters set to: tryptic specificity, one missed cleavage and a mass measurement tolerance of 0.2 Da in MS mode and 0.2 Da for MS/MS ions. The carbamidomethylation of cysteine and methionine oxidation were set as respective fixed and variable modifications. The MS/MS based peptide and protein identifications were validated using The Scaffold software version 4.0.5 (Proteome Software Inc., Portland, OR). Peptide identifications using Mascot required ion scores higher than the associated identity scores of 20-doubly and 35-triply charged peptides. Protein identifications were considered when the peptide sequence was 100% identical and at least two peptides matched the assigned protein. To be included in this analysis, all peptide sequences had to have 100% identity with assigned proteins.

For in-solution sequencing, the tandem mass spectra were extracted from Thermo RAW files using RawExtract 1.9.9.2 (McDonald et al., 2004) and searched with ProLuCID (Xu et al., 2015) in the Integrated Proteomics Pipeline – IP2 (Integrated Proteomics Applications, Inc., San Diego, CA, USA) against a non-redundant database. The database comprised of in-house *A. americanum* protein sequences (n=110,587) concatenated with *Oryctolagus cuniculus* (domestic rabbit) from Uniprot (www.uniprot.org) (n=21,148) and reverse sequences of all entries. The search space included all fully-tryptic and half-tryptic peptide candidates. Carbamidomethylation of cysteine was used as static modification. Data was searched with 50-ppm precursor ion tolerance and 20-ppm fragment ion tolerance. A minimum number of two peptide matches were required to be considered a hit. A cutoff score was established to accept a protein false discovery rate (FDR) of 1% based on the number of decoys. This procedure was independently performed on each data subset, resulting in a false-positive rate that was independent of tryptic status or charge state.

Additionally, a minimum sequence length of six residues per peptide was required. Results were post processed to only accept PSMs with <10ppm precursor mass error. Finally, the protein matches from each sampled time points were concatenated into one file using Identification Compare (IDcompare) program on IP2- Integrated Proteomics Pipeline Ver.5.0.1 (access granted by Dr. John R. Yates III).

For functional annotation, both tick and rabbit proteins were searched against the following databases: non-redundant (NR), Acari and refseq-invertebrate from NCBI, Acari from Uniprot, the GeneOntology (GO) FASTA subset (Ashburner et al., 2000), MEROPS database (Rawlings et al., 2012), and the conserved domains database of NCBI (Marchler-Bauer et al., 2015) containing the COG (Tatusov et al., 2003), PFAM (Bateman et al., 2002), and SMART motifs (Schultz et al., 2000). Outputs from the blast searches were used in the classifier program in Dr. Ribeiro's program (Karim et al., 2011) for functional classification based on the best match from among all the blast screens. To check rabbit proteins, *Oryctolagus cuniculus* protein sequences were used from NCBI and Uniprot. The functionally annotated proteins were manually validated.

Relative abundance and graphical visualization secretion dynamics of A. americanum tick saliva proteins

Relative abundance and graphical visualization of secretion dynamics were determined as described (Kim et al., 2016) using normalized spectral abundance factors (NSAF) that were validated as reliable in a label-free relative quantification approach (Florens et al., 2006, Paaletti et al., 2006, Zhu et al., 2010). For each functional class or an individual protein, NSAF was expressed as a percent (%) of total NSAF for that time point. Percent NSAF values were

normalized using Z-score statistics using the formula $Z = \frac{X-\mu}{\sigma}$, where *Z i*s the Z-score, *X* is the NSAF for each protein per time point, μ is the mean throughout time points, σ is the standard deviation throughout time points. Normalized percent NSAF values were used to generate heat maps using the heatmap2 function from the gplots library in R (Warnes et al., 2013).

Identification of A. americanum saliva proteins found in other tick saliva proteomes

A. americanum TSPs in this study were searched against published tick saliva proteomes of *I. scapularis* (Kim et al., 2016), *H longicornis* (Tirloni et al., 2015), *R. microplus* (Tirloni et al., 2014), *R. sanguineus* (Oliveria et al., 2013), *O. moubata* (Diaz-Martin et al., 2013), and *D. andersoni* (Mudenda et al., 2014) using local blastp analysis. Databases of protein sequences reported for each tick saliva proteome were extracted from NCBI or Uniprot and screened by blastp using the *A. americanum* salivary proteome (from this study) as the query. Protein matches ≥70% identity was reported.

Results and Discussion

Protein profile and abundance are dynamic during A. americanum tick feeding

Adult *A. americanum* ticks complete feeding over a long period of up to 14 days (Sonenshine, 1993). There is evidence that the tick utilizes different proteins every 24 h to regulate tick feeding. Previous studies have demonstrated that protein profile and abundance in salivary glands of female *A. americanum* is dynamic and changes during the course of tick feeding (McSwain et al., 1982). To attempt at capturing changes in TSP profiles, we successfully used pilocarpine to induce and collect saliva of *A. americanum* ticks every 24 h during the first 8 days

of tick feeding as well as from ticks that had engorged but had not detached, and replete fed ticks as previously described (Tatchell, 1967, Kim et al., 2016).

The early feeding stages (24 - 72 h) of *A. americanum* saliva was observed as a white flake that accumulated on the mouthparts over time after injection with 2% pilocarpine solution. Tick saliva was more evident after 72 h of feeding, observed as droplets of liquid forming at the mouthparts. Proteins in tick saliva were identified by LC-MS/MS using two approaches: "In-Gel" and "In-Solution" digested tick saliva protein peptides.

In the "In-Gel" digestion approach, saliva of *A. americanum* ticks was collected from ticks that were partially fed for 24, 72, 120, and 168 h and were electrophoresed on a 4-20% Tris-Glycine SDS-PAGE and Coomassie blue stained. Subsequently, visible protein bands (n=157) (Fig. 1, please note that markings on the gel represent bands that were excised) were individually excised, processed for in-gel trypsinization and digested peptides identified by LC-MS/MS. The peptide MS/MS spectra were searched against a combined database (tick, rabbit protein, and human contaminants [i.e keratin] proteins) using the MASCOT software version 2.2 (Matrix Science, London, UK). This analysis identified a total of 76 proteins (294 peptides) in tick saliva of which 55 (229 peptides) and 21 (64 peptides) belonged to tick and rabbit respectively (Supplemental Table 1, please note that this table also includes peptides that were identified). Of the total 55 tick saliva proteins 23, 16, 41, and 19 were identified in respective 24, 72, 120 and 168 h feeding time points (Tables 1A, 1B, and 1C). Likewise, 1, 19, 8, and 4 rabbit proteins were identified in tick saliva at the feeding time points that were analyzed respectively (Tables 1A, 1B, and 1C).

In the "In-Solution digestion" approach, saliva that was collected at 24, 48, 72, 96, 120, 144, 168, and 192 h feeding time points as well as ticks that were apparently engorged but were

not detached from the host (BD) and those that had fed to repletion (SD) were subjected to LC-MS/MS. Peptide mass spectra were searched against the database as described above using the Prolucid search engine (Xu et al., 2015), an MS/MS-based database search program. This analysis identified a respective total of 623, 717, 583, 641, 484, 724, 725, 786, 424, and 655 proteins (Supplemental Table 2). From the total number of proteins identified for each respective time points, 470, 560, 435, 459, 346, 551, 491, 552, 324, and 336 were identified as tick proteins. Rabbit proteins for each respective time points consisted of 127, 130, 115, 147, 112, 140, 199, 198, 78, and 282. The remaining 26, 27, 33, 35, 26, 33, 35, 36, 22, and 37 proteins for each respective time points were considered as human contaminants. Overall, a total of 1214, 335, and, 30 proteins were tick, rabbit, and human contaminants respectively (Supplemental Table 2). The remaining 33 hits were reversed sequences that represent false identification, which translated to an error rate of 0.02% and gave us confidence in our data.

Tick and rabbit proteins in A. americanum tick saliva classify in 29 and 25 functional classes

Identified proteins were annotated by searching against entries in public databases (NCBI, Uniprot, and MEROPS). This analysis categorized the 55 tick and 21 rabbit proteins that were identified in the "In-Gel" digestion method (Tables 1A, 1B, and 1C) into 12 tick and 9 rabbit functional protein classes (Supplemental Table 1). Please note that all proteins that were identified in the "In-Gel digestion" approach were among proteins identified in the "In-Solution digestion" approach. Proteins identified in the "In-Solution digestion approach (1214 tick and 335 rabbit) was classified into a respective 29 (Table 2A and 2B) and 25 (Table 3A and 3B) functional protein classes.

The majority of tick proteins in *A. americanum* tick saliva were identified as TSPs of unknown function (28%), followed by protease inhibitors (PI) (14%), proteases (8%), lipocalins (7%), and glycine rich proteins (6%). Some notable protein classes that were ≤4% include cytoskeletal, antioxidant/detoxification, extracellular matrix, immune related, heme/iron binding, mucins, evasins, antimicrobials, and ixodegrin, (Tables 2A and 2B, and Supplemental Table 2). In contrast, the majority of rabbit proteins found in *A. americanum* tick saliva is cytoskeletal (19%), followed by keratin (13%), nuclear regulation (8%), immunity related (8%), globin/RBC degradation (6%), and protein classes that were ≤5% include antimicrobials, heme/iron binding, protease inhibitors, proteases, extracellular matrix, antioxidant/detoxification, fibrinogen and lipocalin (Tables 3A and 3B, and Supplemental Table 2).

Majority of A. americanum tick salivary proteins is of unknown function

Figures 2A and 2B illustrates the relative abundance of tick saliva proteins every 24 h during tick feeding as determined by normalized spectral abundance factor (NSAF), the index for relative protein abundance. As shown in Figure 2A, TSPs of unknown function were the most abundant ranging from 23-41% during feeding, followed by protease inhibitors (PI) (13-23%), heme/iron metabolism proteins (6-25%), and histamine binding proteins/lipocalins (1-24%). Other notable tick proteins at ≤10% in abundance include glycine rich proteins, antimicrobial peptides, evasins, and proteases. Likewise, for rabbit proteins in *A. americanum* tick saliva, the most predominant functional class was hemoglobin/red blood cell products (13-58%) followed by cytoskeletal (6-20%), heme/iron metabolism (~5-16%), keratin (2-30%), and nuclear regulation (2-20%) (Fig. 2B). It is notable that rabbit functional classes related to immunity, antimicrobial peptides, protease inhibitors and proteases were abundant at ≤8% throughout feeding. The findin

that the majority of proteins in this study is of unknown function is not unique to *A. americanum;* it is consistent with findings in saliva of *I. scapularis* (Kim et al., 2016, part I of this chapter) and other transcriptome sequencing studies (Valenzuela et al., 2002, Ribeiro et al., 2006, Karim and Ribeiro, 2015). This is potentially a reflection of how much less information exists on tick feeding physiology.

Majority of A. americanum tick salivary proteins is associated with the tick feeding phase

To gain insight into broad relationships of secretion dynamics of both tick and rabbit proteins with the tick feeding process, Z-score statistics normalized NSAF values were visualized on heat maps (Figs. 3A and 3B). The clustering patterns are influenced by cumulative relative abundance of protein class.The blue to red transition denotes low to high abundance. As shown in Figure 3A, the 29 tick protein functional classes clustered into four broad secretion patterns (A-D). Broadly, the majority of tick proteins is secreted at high abundance starting from 24 h of feeding (Fig. 3A, clusters B, C, and D) with exception four protein classes, evasins, proteases, lipocalin, and nuclear regulation proteins in cluster A, which are injected into the host at high abundance starting from day five of feeding. More than 50% (15/29 functional classes) of proteins are abundant in saliva starting from 24 h through 144 h feeding time point (clusters B, C, and D). Likewise in cluster C, ~11% (10/29) are injected at high abundance in saliva of 24-192 h fed ticks but also abundant from engorged but not detached ticks.

Similar to tick proteins, the majority of rabbit proteins (21 of the 25 functional classes) was detected at high abundance in saliva of *A. americanum* ticks during feeding (Fig. 3B). The 25 rabbit protein classes segregated into four clusters, A-D (Fig. 3B). Rabbit proteins that were secreted at high abundance starting from 24 h through 72 h of feeding are part of clusters A and

B. Five of the seven proteins in cluster A are highly abundant at 24 and 48 h feeding time points, while those in clusters C and D were less abundant in the first 48 h of feeding and showed varied abundance levels starting from 72 h of feeding.

Secretion dynamics of selected A. americanum tick salivary proteins

Supplemental Table 2 lists individual proteins that were identified in *A. americanum* tick saliva. Eleven classes of proteins (immunity related, heme/iron metabolism, extracellular matrix/cell adhesion, protease inhibitors, proteases, detoxification, lipocalin, evasin, antimicrobial, glycine rich and proteins of unknown function) (Tables 2 A and 2B) considered as non-housekeeping proteins accounted for 65% of proteins that were found in saliva, and contributed more than 80% in relative abundance. In the subsequent sections, we have discussed non-housekeeping tick proteins individually, and have highlighted housekeeping-like tick proteins and rabbit proteins as a group below. Our lab is interested in understanding functions of proteases and protease inhibitors, and our subsequent discussion below is biased.

a) A. americanum tick saliva contains a large diversity of protease inhibitors in nine families

Porter et al., (2017) documented at least 18 different families of protease inhibitors (PI) that might be expressed by *A. americanum* and other tick species. Here we found 165 PIs belonging to nine families including Kunitz-type inhibitors (I2, n=68), serine protease inhibitors (serpins, I4, n=25), trypsin-inhibitor like (TIL, I8, n=38), alpha-2-macroglobulins (α2M, I39, n=14), cysteine inhibitors (cystatin, I25, n=13), thyropins (I31, n=3), phosphatidylethanolamine-binding proteins (I51, n=2), a pro-eosinophil major basic protein (proMBP, I63, n=1), and a tick carboxypeptidase inhibitor (TCI, n=1). Of significant interest, a majority of PIs (124/165) in this study is secreted at

high abundance in 24-120 h saliva (Fig. 4A, and Supplemental Table 2), strongly suggesting that functions of tick saliva PIs are associated with early stages of the tick feeding process that are critical to the success of ticks as pests and vectors of tick-borne disease agents.

Of the PI families in this study, serpins are the most studied (Mulenga et al., 2007a, 2009, Porter et al., 2015, 2017, Blisnick et al., 2017, Chmelar et al, 2017). This is based on the fact that, to successfully feed and transmit tick-borne disease agents, ticks have to overcome serine protease mediated host defense pathways. On this basis, it was proposed that ticks might utilize serpins to evade host defenses (Mulenga et al., 2001). From this perspective, it is notable that all serpins were injected into host starting from 24-48 h of feeding (Fig. 4A) suggesting these proteins might be involved with regulating tick feeding within hours of the tick starting to feed. Another interesting finding in this study is that, *A. americanum* serpin 6 and 19, which were previously validated as inhibitors of host defense system proteases (Mulenga et al., 2013a, Kim et al., 2015) were found in this study.

At the time of drafting this manuscript, we did not find reported studies on functional analysis of *A. americanum* tick cystatins. However, several reported in other tick species indicated that cystatins play important roles in tick feeding physiology (Wang et al., 2015, Zavasnik-Bergant et al., 2017). For cystatins (family I25, Fig. 4B), three of 13 were secreted within 24 h of feeding, indicating that a majority of cystatins might be involved in regulating tick feeding functions after the tick has initiated feeding. In Figure 4C, the secretion dynamics of alpha-2-macroglobulins (α2M) is similar to cystatins, where a majority was injected into the host at high abundance toward the end of feeding. There are very few studies on α2M in tick feeding physiology. Two studies reported on functional roles of α2M in soft tick immune defense (Kopacek et al., 2000) and anti-microbial activity in *I. ricinus* (Buresova et al., 2009).

The secretion dynamics of Kunitz-type inhibitors (Fig. 4D) and Trypsin-inhibitor like proteins (Fig. 4E) are comparable and notable: the ticks appear to secrete a different set of these inhibitors every 24 h starting from first day of tick feeding. This suggests that functions of these inhibitors are required throughout the tick feeding process. It is also notable that a moderate number of Kunitz-type inhibitors and TILs was also detected in saliva of replete fed ticks, unlike the other three inhibitors in this study. This suggests that these two PI families could also be involved in regulating tick feeding functions toward the end of tick feeding.

b) A majority of proteases in A. americanum saliva is metalloproteases

At the time of this study, protease families that were encoded by *A. americanum* were not enumerated, presumably because its genome had not been sequenced. However, analysis of annotated sequences from *I. scapularis* showed that the tick might encode for all protease classes: aspartic, cysteine, serine, metallo, and threonine proteases (Mulenga and Erikson, 2011). Here, we found that *A. americanum* secretes at least 95 proteases in its saliva. These 95 proteases include four classes and classify into 15 families: aspartic (family A1, n=5), cysteine (n=13 in families C1, C2, and C13), metallo- (n=55 in families M12, M13, M14, M15, M17, M20, M28, and M49), and serine (n=22 in families S1, S10, and S28) proteases (Figs. 4F, 4G, and 4H, and Supplemental Table 2). Please note that the heatmap for aspartic proteases was not developed due to low numbers (secretion dynamics is presented in Supplemental Table 2). The heatmap (Figs. 4F, 4G, and 4H, and Supplemental Table 2) show that 65 of the 95 proteases are injected into the host various time points during the first 5 days of feeding demonstrating that some the proteases in this study are associated with tick feeding regulation.

The observation that metalloproteases are in the majority in saliva of *A. americanum* is

consistent with our previous findings on the *I. scapularis* proteome (Kim et al., 2016, part I of this chapter). It is also notable that similar to the *I. scapularis* proteome, metalloproteases that were secreted at high abundance during the first 72 h feeding time points are in families M12 and M13 (Fig. 4G), indicating that these proteases regulate initial tick feeding functions that are important to both tick species. Indirect evidence on snake venom M12 proteases anti-coagulant activity suggest that secretion of these proteases at high abundance when the tick is initiating feeding might be beneficial to tick feeding (Fox and Serrano, 2005, Kini, 2006). There is also evidence that RNAi silencing of M12 proteases significantly affected tick feeding efficiency (Decrem et al., 2008). Likewise, indirect evidence suggests that the ticks might utilize M13 proteases to regulate host immunity. In mammals, M13 proteases are involved in modulating neurotransmitter levels, controlling blood pressure, involved in reproduction and cancer progression (Turner and Cottrell, 2004).

Another notable similarity between *I. scapularis* (part I of this chapter) and *A. americanum* proteomes is that both tick species secreted a fewer number of S1 serine proteases, three and four respectively (Fig. 4G, and Supplemental Table 2). We are interested in S1 serine proteases, because of their functional roles in signal transduction as activators of protease activated receptors (Ewen et al., 2010, Cattaruzza et al., 2014). Therefore, it is likely that ticks could utilize these proteases to interfere with host defense signaling at the tick feeding site. The observation that *A. americanum* injected cysteine proteases at the beginning of feeding indicates that cysteine proteases might be playing some role(s) in the early stages of tick feeding. In mammals, these proteases are active at acidic pH in endo/lysosomes (Kopitar-Jerala, 2012); it will be interesting to investigate their functional roles at the tick feeding site, which is expected to be near the physiological pH of 7.

c) Lipocalins/ histamine binding proteins are alternately secreted during tick feeding

Host inflammatory response is among host defense pathways that ticks must evade to complete feeding. Histamine is one of the key mediators of inflammation in tissue damage, such as in the event of tick feeding (reviewed in Paesen, 1999). From this perspective, lipocalins/tick histamine binding proteins in tick saliva are suspected to be part of the tick machinery to evade the host's inflammatory defense response through sequestration of histamine that is released at the tick feeding site. In this study, we found 90 lipocalins/tick histamine binding proteins that show two broad secretion patterns: secreted at multiple feeding time points and those that were alternately secreted at single time points (Fig. 4I). Given that in addition to regulating inflammation, lipocalins/histamine binding proteins have other diverse functions such as antimicrobial effects (Fluckinger et al., 2004, Chan et al., 2009), glucose metabolism (Cho et al., 2011) and binding several other biogenic amines such as serotonin and fatty acids (Ganfornina et al., 2000, Smathers and Petersen, 2011), it is likely that these proteins might be involved in regulating several tick functions besides inflammation.

d) Heme binding proteins are secreted at high abundance throughout feeding

Like other animals, ticks require iron and heme (the iron-containing part of hemoglobin) for normal physiological functions. Female ticks that were artificially fed a diet not containing hemoglobin failed to lay viable tick eggs, demonstrating the importance of heme (Perner et al., 2016). Supplemental Table 2 lists a total of 17 heme/iron binding proteins (mainly comprised of hemelipoproteins and vitellogenins) and a single ferritin that collectively accounted for the third most abundant protein class in tick saliva throughout feeding (Fig. 2). The secretion dynamics summarized in Figure 4J revealed two broad secretion patterns, those that are injected into the host

from 24 h through 120 h of feeding (HCB and HCC) and those that injected into the host starting from 144 h of feeding through the end of tick feeding (HCD and HCA). Ticks acquire both iron and heme from host blood (Lara et al., 2005), and thus iron and heme binding proteins are important to normal tick physiology. On this basis, it is potentially possible that heme/iron binding proteins in tick saliva could also function inside the tick. While heme and iron are essential to animal physiology, free forms are toxic (Toh et al. 2010). It will be interesting to investigate if heme/iron binding proteins identified in this study sequester heme/iron to protect the tick from damage by free heme and iron. Hemelipoproteins and vitellogenin can also bind lipids (Donohue et al., 2009), and thus there is a possibility that heme binding proteins in this study might be involved in functions that are unrelated to heme metabolism.

e) Ticks inject multiple antioxidants into the feeding site

Feeding and digestion of extensive amounts of host blood exposes ticks to hydroxyl radicals and reactive oxygen species (ROS), which if left uncontrolled could damage tick tissue (Rojkind et al., 2002, Narasimhan et al., 2007). Tick expressed anti-oxidant proteins protect the tick during feeding and digestion of the blood meal. In fact, RNAi silencing of tick antioxidants caused deleterious effects to ticks and prevented them from obtaining a full blood meal (Adamson et al., 2014, Kumar et al., 2016). Previous work by others and from our lab has documented the presence of anti-oxidants in tick salivary glands (Das et al., 2001, Wu et al., 2010) and saliva (Radulovic et al., 2014, Tirloni et al., 2014, 2015, Lewis et al., 2015, Kim et al., 2016). In this study, we identified 41 putative antioxidant enzymes in tick saliva. These enzymes include glutathione, thioredoxin, superoxide dismutase, catalase, peroxinectin, arylsulfatase, aldehyde dehydrogenase, epoxide hydrolase, sulfotransferase, sulfhydryl oxidase and glycolate oxidase.

Figure 4K reveals three broad secretion patterns; those that are injected into the host starting from 24 h of feeding (ACA, ACF), variable time points from 48 h of feeding (ACE, ACG, ACH), and those that are injected into the host once at various feeding time points (ACB, ACC, ACD, ACE, ACG, ACI). Like heme/iron binding proteins, tick anti-oxidants are presumed to function inside the tick. The findings from this study that antioxidants are secreted in tick saliva indicate that these proteins may be playing roles to keep the feeding site neutral. Injury caused during creation of the tick feeding lesion by ticks could trigger release of oxidants such as ROS, therefore it is conceivble that tick salivary antioxidants function to cleanse the blood meal before it is ingested by ticks.

f) Glycine rich proteins and extracellular matrix/ Cell adhesion are secreted early during tick feeding

Within 5-30 min of attachment, the tick secretes an adhesive substance called cement that anchor ticks onto host skin during its protracted feeding period (Kemp et al., 1982). Tick cement is also suggested to protect the tick from host immune molecules (reviewed in Binnington and Kemp, 1980, Sonenshine, 1993) and has antimicrobial function (Alekseev et al., 1995) at the feeding site. Glycine rich proteins are among classes of tick proteins that are thought to play key roles in formation of tick cement (Kemp et al., 1982). From this perspective, glycine rich proteins are among tick proteins that have received significant research attention (Mulenga et al., 1999, Bishop et al., 2002, Bullard et al., 2016, Hollmann et al., 2018). In this study, we found a total of 72 glycine rich proteins, which represented the fifth largest class of proteins identified in tick saliva during feeding (Fig. 2). A majority of the glycine rich proteins was secreted within the first six days of feeding (Fig. 4L) (GCA, GCD, GCH, GCI, GCJ, GCL, and GCM). Tick cement deposition is completed during the first 96 h of tick feeding, and thus it is conceivable that some of the glycine

rich proteins in this study might be involved with tick cement formation (Kemp et al., 1982). Although glycine rich proteins are mostly known for their potential role in tick cement formation, indirect evidence in other organisms indicate these proteins might be involved in other functions such as host defense and stress response as in plants (Czolpinksa and Rurek, 2018). It is interesting to note that some of the glycine rich proteins that were identified from tick cement in our lab (Hollmann et al., 2017) and others (Bullard et al., 2016) were also found in this study (Supplemental Table 3). Some of the glycine rich proteins were secreted from the 144 h time point, long after tick cement formation, these might regulate other tick feeding functions.

Figure 4M summarize the secretion dynamics of extracellular matrix proteins (n=38) that were found in this study. Similar to glycine rich proteins, a majority (29/38) of the extracellular proteins was secreted within the first five days of feeding demonstrating their role in early stage tick feeding regulation. Our speculation is that some of these proteins will play roles in formation of tick cement. In a previous study, RNAi silencing of chitinase, also identified in this study, weakened the tick cement cone to the extent that host blood leaked around the mouthparts of attached ticks (Kim et al., 2014).

g) Antimicrobials, mucins, and immune related proteins are secreted throughout feeding process

Once the tick has anchored itself onto the host skin, and created its feeding lesion, it faces a difficult task of overcoming host humoral and cellular immunity, but also prevents microbes in the host skin from colonizing the tick-feeding site. Here we show that *A. americanum* secretes immunomodulatory and antimicrobial peptides starting in the early stages of the tick feeding process (Fig. 4N). We identified nine antimicrobials consisting of microplusins, lysozymes, and

defensins (Fig. 4N). Previous studies showed that microplusin has dual effects against fungi and Gram-positive bacteria (Silva et al., 2009, Rossi et al., 2011), lysozyme against Gram-positive bacteria (Pellegrini et al., 1992, Wild et al., 1997), and defensin effective against both Gram-positive and -negative bacteria (Nakjima et al., 2003). The heat map in Figure 4N shows that antimicrobials were injected into the host starting at 24 and 48 h (AMCA), from 72 h (AMCC), and from 120 h (AMCB). This secretion pattern suggests that the functions of antimicrobial peptides are needed throughout feeding.

Similar to antimicrobials, we identified mucins (n=12, Fig. 4O), with a majority of these proteins (7/12) being secreted at high abundance within 24-48 h of feeding. Functional roles of mucins in ticks have not been studied. However, indirect evidence in mammals suggests that mucins might be involved in antimicrobial activity in that human mucins were shown to encapsulate microbes (Petrou and Crouzier, 2018).

Among probable immunomodulatory proteins, we identified evasins (Fig. 4P), ixodegrins (Fig. 4Q) and mucins. Evasins (n=12, Fig. 4P) were shown to bind to chemokines (Hayward et al., 2017, Eaton et al., 2018) to reduce leukocyte recruitment to the tick feeding site and therefore contribute to tick evasion of the host's inflammatory defense. It is interesting to note that the 12 evasins identified in tick saliva were present after 24 h of feeding and continued to be secreted throughout feeding at variable levels, which suggests that these proteins might not be involved in regulating tick feeding functions during the first 24 h of tick feeding.

Figure 4Q summarizes the secretion pattern of ixodegrin-like proteins in this study. These proteins were first described in *I. scapularis* as inhibitors of platelet aggregation (Francischetti et al., 2005). Platelet aggregation is the first step in the blood clotting system (Smith et al., 2015), which ticks must overcome to successfully feed. Thus, the presence of ixodegrins in saliva of *A.*

americanum is likely to be beneficial to tick feeding. Finally, we also found proteins that show similarity to previously characterized immunomodulatory proteins (Fig. 4R), which have been validated in other tick species including p36, which inhibits cell proliferation and cytokine expression (Konnai et al., 2009).

h) Tick salivary proteins of unknown function are alternately secreted.

Over one-third of Ixodidae protein sequences deposited into GenBank are annotated as hypothetical, secreted, conserved and unknown proteins. However, some protein sequences are annotated based on sequence identities and conserved signature motifs, which include basic tail/tails proteins, 8.9 kDa protein family, and leucine rich proteins. Other proteins have been functionally characterized such as AV422, a tick saliva protein that is highly upregulated when ticks are stimulated to start feeding involved in mediating tick anti-hemostatic and anti-complement functions (Mulenga et al., 2007b, Mulenga et al., 2013b), and RGD motif proteins that may play roles in inhibition of platelet aggregation (Francischetti et al., 2005). In this study, we have identified a total of 341 (Fig. 4S) TSPs that fit the above description that we refer here to as TSPs of unknown functions. More than 97% (326/341) of the 341 total TSP proteins were identified within the first eight days of feeding indicating their potential roles in regulating tick feeding. TSPs have an interesting secretion pattern of where a majority of these proteins was alternately injected once during feeding. From the perspective of finding target antigens for tick vaccine development, TSPs represent a unique opportunity in that they do not share any homology to host proteins and might not cross-react with the host.

A. americanum secretes multiple housekeeping-like proteins in its saliva throughout the feeding process

Supplemental Table 2 lists 292 housekeeping-like proteins that were identified in this study. Finding these proteins in *A. americanum* saliva is not unexpected, as similar findings have been previously reported in tick saliva (Tirloni et al., 2014, 2015, Kim et al., 2016). The 292 housekeeping-like proteins were classified into 16 classes including those associated with metabolism of amino acids (n = 7), carbohydrates (n = 25), energy (n = 31), lipids (n = 31), intermediate (n=1), and nucleic acids (n = 33). Other protein classes include those involved in nuclear regulation (n = 16), protein export (n = 1), protein modification machinery (n = 21), proteasome machinery (n = 10), protein synthesis (n = 11), signal transduction (n = 22), transposable element (n = 3), transcription machinery (n = 7), transporter/receptors (n = 18), and cytoskeletal (n = 55). It is interesting to note that within the first 24 h of feeding, 15 of the 16 classes were identified at high abundance (Fig. 2, and Table 2A and 2B).

One feature of housekeeping-like tick proteins is that they have high sequence identity with mammalian housekeeping proteins, and for this reason they are discounted as potential target antigens for tick vaccine development. However, we think that these proteins play an important role in tick feeding regulation. Housekeeping-like proteins identified here mostly function intracellularly, and they serve as alarm signals to alert the host defense system to injury when secreted outside (Rock and Kono, 2008). There is evidence that in the extracellular space, some of the housekeeping proteins such as heat shock proteins, have anti-inflammatory functions (Zininga et al., 2018) while histone proteins have antimicrobial activity (Poirier et al., 2014). Given high sequence similarity with host proteins, it could be that some of the housekeeping-like proteins play roles in promoting tick feeding through anti-inflammatory and anti-microbial activity.

Secretion of rabbit host proteins in A. americanum tick saliva is not random

In this study, we identified 335 host proteins belonging into 25 different classes that include cytoskeletal (19%), keratin (13%), nuclear regulation (8%), immune related (8%), hemoglobin/RBC degradation (6%), transporters/ receptors (5%), protein modification (5%), and the number of protein classes below 4% included antimicrobials, extracellular matrix, heme/iron binding, detoxification/ antioxidants, metabolism (energy, carbohydrates, lipid, amino acid, and nucleic acids), protein export, protein synthesis, fibrinogen, protease inhibitors, proteases, signal transduction, transcription machinery, proteasome machinery, and lipocalin (Table 3A and 3B, Supplemental Table 2). Relative abundance as determined by NSAF indicated that the most abundant protein classes hemoglobin/RBC degradation products (58-13%), followed by heme/ iron binding host proteins (13-16%), and cytoskeletal (6-20%) (Fig. 3).

At a glance, the presence of rabbit host proteins in *A. americanum* tick saliva could be dismissed as contamination. This observation might be strengthened by the fact that some rabbit host proteins in tick saliva such keratin, nuclear regulation proteins, and host antimicrobial peptides increased in abundance as feeding progressed. This suggested that secretion of host proteins into tick saliva was a consequence of ticks taking in an increased amount of host blood, and that some of these proteins might leak or be regurgitated back into the host via saliva. When ticks feed, the blood is ingested into the midguts for digestion. Nutrients and proteins from the host blood is absorbed through the midguts into the hemolymph, which is exposed to other tick tissues such as the salivary gland. Our data suggest that the tick might be systematically utilizing host proteins to regulate its tick feeding site during feeding. For instance, fibrinogen, which among other functions plays important roles in wound healing, was identified in 144 h fed tick saliva and increased as feeding progressed (Mosesson et al., 2005). Although it is known that cellular

infiltrates accumulate at the tick feeding site over time after the tick has detached (Brown et al, 1984), upon immediate detachment the tick feeding lesion is sealed, without leakage of blood. It would be interesting to investigate if host proteins attribute the wound healing properties of tick saliva, in that increase abundance in fibrinogen that is secreted into the feeding site might help with wound healing as the tick completes feeding.

Different tick species might utilize similar proteins to regulate feeding

At the time of drafting of this study, several other tick saliva proteomes had been published. We took advantage of the availability of these data to test the hypothesis that key proteins that are important to tick feeding might be conserved in tick species. Thus, we compared data in this study to proteomes of *I. scapularis* (Kim et al., 2016), *H. longicornis* (Tirloni et al., 2015), *D. andersoni* (Mudenda et al, 2014), *R. microplus* (Tirloni et al., 2014), *O. moubata* (Diaz-Martin et al., 2013) and *R. sanguineus* (Oliveira et al., 2013). This analysis revealed that more than 24% (292/1214) of the *A. americanum* tick saliva proteins in this study have homologs in saliva proteomes of other tick species (Supplemental Table 4). Table 4 highlights 168, 142, 138, 96, 24, and 13 *A. americanum* tick saliva proteins in 23 classes that were >70% identical to proteins in saliva of *I. scapularis* (Kim et al., 2016), *H. longicornis* (Tirloni et al., 2015), *D. andersoni* (Mudenda et al, 2014), *R. microplus* (Tirloni et al., 2014), *O. moubata* (Diaz-Martin et al., 2013) and *R. sanguineus* (Oliveira et al., 2013) respectively. Of the 23 classes of proteins, immune related proteins were present in all tick salivary proteomes. Likewise, proteins from nine other classes (cytoskeletal, protein modification, detoxification, protease inhibitors, protease, signal transduction, carbohydrate metabolism, extracellular matrix, and heme/iron binding) from *A. americanum* saliva were present in five other tick salivary proteomes.

We would like the reader to note that with the exception of *I. scapularis* tick saliva proteome for which proteins were identified every 24 h during feeding (Kim et al., 2016) the other tick saliva proteomes were limited to a narrow range of tick feeding time points and/or fully engorged ticks. This might explain be the reason higher number of *A. americanum* tick saliva proteins were found compared to *I. scapularis* tick saliva proteome. Of importance, however, *A. americanum* and *I. scapularis* are biologically different as they belong to different tick lineages, prostriata and metastriata (Hoogstraal and Aeschilimann, 1982, Black and Piesman, 1994). Thus, tick saliva proteins that are shared between these two tick species could represent important targets.

Conclusion

This study has made a unique contribution toward understanding the molecular basis of tick feeding physiology. This study provides a good starting point toward discovery of effective targets for tick vaccine development. Our strategy to identify tick saliva proteins every 24 h during feeding has allowed us to map proteins to different phases of the tick feeding process. This is significant as it provides for the opportunity to focus on tick saliva proteins that regulate tick feeding events that precede critical events such as tick-borne disease agent transmission. The majority of tick-borne disease agents is transmitted after 48 h of tick attachment (des Vignes et al., 2001, Ebel and Kramer et al., 2004), and therefore proteins that are secreted from 24 and 48 h of tick feeding time points are prime candidates for tick vaccine research. It is important to acknowledge the fact that during the course of feeding, *A. americanum* ticks secreted more than 1500 tick and rabbit-host proteins. This diverse and complex nature of tick saliva could implicate that the tick has inbuilt systems to evade host immunity, and that it is going to be a challenge to actually find effective targets for tick vaccine development. However, the findings that nearly 300

A. americanum tick saliva proteins were secreted by other tick species is very encouraging as these might represent those proteins that the tick must have to successfully feed, and they represent potential targets for tick vaccine development. In summary, this study has established the foundation for in-depth studies to understanding *A. americanum* tick feeding physiology. As *A. americanum* vectors multiple tick-borne disease agents, findings in this study will have a significant impact toward the development of tick vaccines.

References

Adamson, S., Browning, R., Singh, P., Nobles, S., Villarreal, A., Karim, S., 2014. Transcriptional activation of antioxidants may compensate for selenoprotein deficiencies in *Amblyomma maculatum* (Acari: Ixodidae) injected with selK- or selM-dsRNA. Insect Mol. Biol. 23, 497-510.

Alekseev, A.N., Burenkova, L.A., Podboronov, V.M., Chunikhin, S.P., 1995. Bacteriocidal qualities of ixodid tick (Acarina: Ixodidae) salivary cement plugs and their changes under the influence of a viral tick-borne pathogen. J. Med. Entomol. 32, 578-582.

Ashburner, M., Ball, C.A., Blake, J.A., Botstein, D., Butler, H., Cherry, J.M., Davis, A.P., Dolinski, K., Dwight, S.S., Eppig, J.T., Harris, M.A., Hill, D.P., Issel-Tarver, L., Kasarskis, A., Lewis, S., Matese, J.C., Richardson, J.E., Ringwald, M., Rubin, G.M., Sherlock, G., 2000. Gene ontology: tool for the unification of biology. The Gene Ontology Consortium. Nat. Genet. 25, 25-29.

Bateman, A., Birney, E., Cerruti, L., Durbin, R., Etwiller, L., Eddy, S.R., Griffiths-Jones, S., Howe, K.L., Marshall, M., Sonnhammer, E.L., 2002. The Pfam protein families database. Nucleic Acids Res. 30, 276-280.

Binnington, K.C., Kemp, D.H., 1980. Role of tick salivary glands in feeding and disease transmission. Adv. Parasitol. 18, 315-339.

Bishop, R., Lambson, B., Wells, C., Pandit, P., Osaso, J., Nkonge, C., Morzaria, S., Musoke, A., Nene, V., 2002. A cement protein of the tick *Rhipicephalus appendiculatus*, located in the secretory e cell granules of the type III salivary gland acini, induces strong antibody responses in cattle. Int. J. Parasitol. 32, 833-842.

Black, W.C.,4th, Piesman, J., 1994. Phylogeny of hard- and soft-tick taxa (Acari: Ixodida) based on mitochondrial 16S rDNA sequences. Proc. Natl. Acad. Sci. U. S. A. 91, 10034-10038.

Blisnick, A.A., Foulon, T., Bonnet, S.I., 2017. Serine protease inhibitors in ticks: an overview of their role in tick biology and tick-borne pathogen transmission. Front. Cell. Infect. Microbiol. 7, 199.

Brown, S.J., Barker, R.W., Askenase, P.W., 1984. Bovine resistance to *Amblyomma americanum* ticks: an acquired immune response characterized by cutaneous basophil infiltrates. Vet. Parasitol. 16, 147-165.

Bullard, R., Allen, P., Chao, C.C., Douglas, J., Das, P., Morgan, S.E., Ching, W.M., Karim, S., 2016. Structural characterization of tick cement cones collected from in vivo and artificial membrane blood-fed Lone Star ticks (*Amblyomma americanum*). Ticks Tick Borne Dis. 7, 880-892.

Buresova, V., Hajdusek, O., Franta, Z., Sojka, D., Kopacek, P., 2009. IrAM-An alpha2-macroglobulin from the hard tick *Ixodes ricinus*: characterization and function in phagocytosis of a potential pathogen *Chryseobacterium indologenes*. Dev. Comp. Immunol. 33, 489-498.

Cattaruzza, F., Amadesi, S., Carlsson, J.F., Murphy, J.E., Lyo, V., Kirkwood, K., Cottrell, G.S., Bogyo, M., Knecht, W., Bunnett, N.W., 2014. Serine proteases and protease-activated receptor 2 mediate the proinflammatory and algesic actions of diverse stimulants. Br. J. Pharmacol. 171, 3814-3826.

Chan, Y.R., Liu, J.S., Pociask, D.A., Zheng, M., Mietzner, T.A., Berger, T., Mak, T.W., Clifton, M.C., Strong, R.K., Ray, P., Kolls, J.K., 2009. Lipocalin 2 is required for pulmonary host defense against *Klebsiella* infection. J. Immunol. 182, 4947-4956.

Chmelar, J., Kotal, J., Langhansova, H., Kotsyfakis, M., 2017. Protease inhibitors in tick saliva: the role of serpins and cystatins in tick-host-pathogen interaction. Front. Cell. Infect. Microbiol. 7, 216.

Cho, K.W., Zhou, Y., Sheng, L., Rui, L., 2011. Lipocalin-13 regulates glucose metabolism by both insulin-dependent and insulin-independent mechanisms. Mol. Cell. Biol. 31, 450-457.

Czolpinska, M., Rurek, M., 2018. Plant glycine-rich proteins in stress response: an emerging, still prospective story. Front. Plant. Sci. 9, 302.

Das, S., Banerjee, G., DePonte, K., Marcantonio, N., Kantor, F.S., Fikrig, E., 2001. Salp25D, an *Ixodes scapularis* antioxidant, is 1 of 14 immunodominant antigens in engorged tick salivary glands. J. Infect. Dis. 184, 1056-1064.

Decrem, Y., Mariller, M., Lahaye, K., Blasioli, V., Beaufays, J., Zouaoui Boudjeltia, K., Vanhaeverbeek, M., Cerutti, M., Brossard, M., Vanhamme, L., Godfroid, E., 2008. The impact of gene knock-down and vaccination against salivary metalloproteases on blood feeding and egg laying by *Ixodes ricinus*. Int. J. Parasitol. 38, 549-560.

des Vignes, F., Piesman, J., Heffernan, R., Schulze, T.L., Stafford, K.C.,3rd, Fish, D., 2001. Effect of tick removal on transmission of *Borrelia burgdorferi* and *Ehrlichia phagocytophila* by *Ixodes scapularis* nymphs. J. Infect. Dis. 183, 773-778.

Diaz-Martin, V., Manzano-Roman, R., Oleaga, A., Encinas-Grandes, A., Perez-Sanchez, R., 2013. Cloning and characterization of a plasminogen-binding enolase from the saliva of the argasid tick *Ornithodoros moubata*. Vet. Parasitol. 191, 301-314.

Donohue, K.V., Khalil, S.M., Sonenshine, D.E., Roe, R.M., 2009. Heme-binding storage proteins in the Chelicerata. J. Insect Physiol. 55, 287-296.

Eaton, J.R.O., Alenazi, Y., Singh, K., Davies, G., Geis-Asteggiante, L., Kessler, B., Robinson, C.V., Kawamura, A., Bhattacharya, S., 2018. The N-terminal domain of a tick evasin is critical for

chemokine binding and neutralization and confers specific binding activity to other evasins. J. Biol. Chem. 293, 6134-6146.

Ebel, G.D., Kramer, L.D., 2004. Short report: duration of tick attachment required for transmission of powassan virus by deer ticks. Am. J. Trop. Med. Hyg. 71, 268-271.

Ewen, D., Clarke, S.L., Smith, J.R., Berger, C., Salmon, G., Trevethick, M., Shute, J.K., 2010. The role of protease-activated receptors PAR-1 and PAR-2 in the repair of 16HBE 14o(-) epithelial cell monolayers in vitro. Clin. Exp. Allergy 40, 435-449.

Florens, L., Carozza, M.J., Swanson, S.K., Fournier, M., Coleman, M.K., Workman, J.L., Washburn, M.P., 2006. Analyzing chromatin remodeling complexes using shotgun proteomics and normalized spectral abundance factors. Methods 40, 303-311.

Fluckinger, M., Haas, H., Merschak, P., Glasgow, B.J., Redl, B., 2004. Human tear lipocalin exhibits antimicrobial activity by scavenging microbial siderophores. Antimicrob. Agents Chemother. 48, 3367-3372.

Fox, J.W., Serrano, S.M., 2005. Structural considerations of the snake venom metalloproteinases, key members of the M12 reprolysin family of metalloproteinases. Toxicon 45, 969-985.

Francischetti, I.M., My Pham, V., Mans, B.J., Andersen, J.F., Mather, T.N., Lane, R.S., Ribeiro, J.M., 2005. The transcriptome of the salivary glands of the female western black-legged tick *Ixodes pacificus* (Acari: Ixodidae). Insect Biochem. Mol. Biol. 35, 1142-1161.

Fu, L., Niu, B., Zhu, Z., Wu, S., Li, W., 2012. CD-HIT: accelerated for clustering the next-generation sequencing data. Bioinformatics 28, 3150-3152.

Ganfornina, M.D., Kayser, H., Sanchez, D., 2000. Lipocalins in Arthropoda: Diversification and Functional Explorations. In: Madame Curie Bioscience Database [Internet]. Austin (TX): Landes Bioscience .

Hayward, J., Sanchez, J., Perry, A., Huang, C., Rodriguez Valle, M., Canals, M., Payne, R.J., Stone, M.J., 2017. Ticks from diverse genera encode chemokine-inhibitory evasin proteins. J. Biol. Chem. 292, 15670-15680.

Hollmann, T., Kim, T.K., Tirloni, L., Radulovic, Z.M., Pinto, A.F.M., Diedrich, J.K., Yates, J.R.,3rd, da Silva Vaz, I.,Jr, Mulenga, A., 2018. Identification and characterization of proteins in the *Amblyomma americanum* tick cement cone. Int. J. Parasitol. 48, 211-224.

Hoogstraal H, Aeschlimann A. (1982). Tick-host specificity. Mitt Schweiz Entomol Ges. 55:5–32.

Karim, S., Ribeiro, J.M., 2015. An insight into the sialome of the lone star tick, *Amblyomma americanum*, with a glimpse on its time dependent gene expression. PLoS One 10, e0131292.

Karim, S., Singh, P., Ribeiro, J.M., 2011. A deep insight into the sialotranscriptome of the gulf coast tick, *Amblyomma maculatum*. PLoS One 6, e28525.

Katavolos, P., Armstrong, P.M., Dawson, J.E., Telford, S.R.,3rd, 1998. Duration of tick attachment required for transmission of granulocytic ehrlichiosis. J. Infect. Dis. 177, 1422-1425.

Kemp, D.H., Stone, B.F., Binnington, K.C., 1982. Tick attachment and feeding: role of the mouthparts, feeding apparatus, salivary gland secretions and the host response, in Obenchain, F., Galun, R. (Eds.), Physiology of Ticks. Pergamon Press Ltd., Oxford, UK, pp. 138-139.

Kim, T.K., Curran, J., Mulenga, A., 2014. Dual silencing of long and short *Amblyomma americanum* acidic chitinase forms weakens the tick cement cone stability. J. Exp. Biol. 217, 3493-3503.

Kim, T.K., Tirloni, L., Radulovic, Z., Lewis, L., Bakshi, M., Hill, C., da Silva Vaz, I.,Jr, Logullo, C., Termignoni, C., Mulenga, A., 2015. Conserved *Amblyomma americanum* tick Serpin19, an inhibitor of blood clotting factors Xa and XIa, trypsin and plasmin, has anti-haemostatic functions. Int. J. Parasitol. 45, 613-627.

Kim, T.K., Tirloni, L., Pinto, A.F., Moresco, J., Yates, J.R.,3rd, da Silva Vaz, I.,Jr, Mulenga, A., 2016. *Ixodes scapularis* tick saliva proteins sequentially secreted every 24 h during blood feeding. PLoS Negl Trop. Dis. 10, e0004323.

Kini, R.M., 2006. Anticoagulant proteins from snake venoms: structure, function and mechanism. Biochem. J. 397, 377-387.

Konnai, S., Nakajima, C., Imamura, S., Yamada, S., Nishikado, H., Kodama, M., Onuma, M., Ohashi, K., 2009. Suppression of cell proliferation and cytokine expression by HL-p36, a tick salivary gland-derived protein of *Haemaphysalis longicornis*. Immunology 126, 209-219.

Kopacek, P., Weise, C., Saravanan, T., Vitova, K., Grubhoffer, L., 2000. Characterization of an alpha-macroglobulin-like glycoprotein isolated from the plasma of the soft tick *Ornithodoros moubata*. Eur. J. Biochem. 267, 465-475.

Kopitar-Jerala, N., 2012. The role of cysteine proteinases and their inhibitors in the host-pathogen cross talk. Curr. Protein Pept. Sci. 13, 767-775.

Kumar, D., Budachetri, K., Meyers, V.C., Karim, S., 2016. Assessment of tick antioxidant responses to exogenous oxidative stressors and insight into the role of catalase in the reproductive fitness of the Gulf Coast tick, *Amblyomma maculatum*. Insect Mol. Biol. 25, 283-294.

Lara, F.A., Lins, U., Bechara, G.H., Oliveira, P.L., 2005. Tracing heme in a living cell: hemoglobin degradation and heme traffic in digest cells of the cattle tick *Boophilus microplus*. J. Exp. Biol. 208, 3093-3101.

Lewis, L.A., Radulovic, Z.M., Kim, T.K., Porter, L.M., Mulenga, A., 2015. Identification of 24h *Ixodes scapularis* immunogenic tick saliva proteins. Ticks Tick Borne Dis. 6, 424-434.

Marchler-Bauer, A., Derbyshire, M.K., Gonzales, N.R., Lu, S., Chitsaz, F., Geer, L.Y., Geer, R.C., He, J., Gwadz, M., Hurwitz, D.I., Lanczycki, C.J., Lu, F., Marchler, G.H., Song, J.S., Thanki, N., Wang, Z., Yamashita, R.A., Zhang, D., Zheng, C., Bryant, S.H., 2015. CDD: NCBI's conserved domain database. Nucleic Acids Res. 43, 222.

McDonald, W.H., Tabb, D.L., Sadygov, R.G., MacCoss, M.J., Venable, J., Graumann, J., Johnson, J.R., Cociorva, D., Yates, J.R.,3rd, 2004. MS1, MS2, and SQT-three unified, compact, and easily parsed file formats for the storage of shotgun proteomic spectra and identifications. Rapid Commun. Mass Spectrom. 18, 2162-2168.

McSwain, J.L., Essenberg, R.C., Sauer, J.R., 1982. Protein changes in the salivary glands of the female lone star tick, *Amblyomma americanum*, during feeding. J. Parasitol. 68, 100-106.

Mosesson, M.W., 2005. Fibrinogen and fibrin structure and functions. J. Thromb. Haemost. 3, 1894-1904.

Mudenda, L., Pierle, S.A., Turse, J.E., Scoles, G.A., Purvine, S.O., Nicora, C.D., Clauss, T.R., Ueti, M.W., Brown, W.C., Brayton, K.A., 2014. Proteomics informed by transcriptomics identifies novel secreted proteins in *Dermacentor andersoni* saliva. Int. J. Parasitol. 44, 1029-1037.

Mulenga, A., Sugimoto, C., Sako, Y., Ohashi, K., Musoke, A., Shubash, M., Onuma, M., 1999. Molecular characterization of a *Haemaphysalis longicornis* tick salivary gland-associated 29-kilodalton protein and its effect as a vaccine against tick infestation in rabbits. Infect. Immun. 67, 1652-1658.

Mulenga, A., Sugino, M., Nakajim, M., Sugimoto, C., Onuma, M., 2001. Tick-encoded serine proteinase inhibitors (serpins); potential target antigens for tick vaccine development. J. Vet. Med. Sci. 63, 1063-1069.

Mulenga, A., Khumthong, R., Blandon, M.A., 2007a. Molecular and expression analysis of a family of the *Amblyomma americanum* tick Lospins. J. Exp. Biol. 210, 3188-3198.

Mulenga, A., Blandon, M., Khumthong, R., 2007b. The molecular basis of the *Amblyomma americanum* tick attachment phase. Exp. Appl. Acarol. 41, 267-287.

Mulenga, A., Khumthong, R., Chalaire, K.C., 2009. *Ixodes scapularis* tick serine proteinase inhibitor (serpin) gene family; annotation and transcriptional analysis. BMC Genomics 10, 217.

Mulenga, A., Erikson, K., 2011. A snapshot of the *Ixodes scapularis* degradome. Gene 482, 78-93.

Mulenga, A., Kim, T., Ibelli, A.M., 2013a. *Amblyomma americanum* tick saliva serine protease inhibitor 6 is a cross-class inhibitor of serine proteases and papain-like cysteine proteases that delays plasma clotting and inhibits platelet aggregation. Insect Mol. Biol. 22, 306-319.

Mulenga, A., Kim, T.K., Ibelli, A.M., 2013b. Deorphanization and target validation of cross-tick species conserved novel *Amblyomma americanum* tick saliva protein. Int. J. Parasitol. 43, 439-451.

Nakajima, Y., Ishibashi, J., Yukuhiro, F., Asaoka, A., Taylor, D., Yamakawa, M., 2003. Antibacterial activity and mechanism of action of tick defensin against Gram-positive bacteria. Biochim. Biophys. Acta 1624, 125-130.

Narasimhan, S., Sukumaran, B., Bozdogan, U., Thomas, V., Liang, X., DePonte, K., Marcantonio, N., Koski, R.A., Anderson, J.F., Kantor, F., Fikrig, E., 2007. A tick antioxidant facilitates the Lyme disease agent's successful migration from the mammalian host to the arthropod vector. Cell. Host Microbe 2, 7-18.

Oliveira, C.J., Anatriello, E., de Miranda-Santos, I.K., Francischetti, I.M., Sa-Nunes, A., Ferreira, B.R., Ribeiro, J.M., 2013. Proteome of *Rhipicephalus sanguineus* tick saliva induced by the secretagogues pilocarpine and dopamine. Ticks Tick Borne Dis. 4, 469-477.

Paesen, G.C., Adams, P.L., Harlos, K., Nuttall, P.A., Stuart, D.I., 1999. Tick histamine-binding proteins: isolation, cloning, and three-dimensional structure. Mol. Cell 3, 661-671.

Paoletti, A.C., Parmely, T.J., Tomomori-Sato, C., Sato, S., Zhu, D., Conaway, R.C., Conaway, J.W., Florens, L., Washburn, M.P., 2006. Quantitative proteomic analysis of distinct mammalian Mediator complexes using normalized spectral abundance factors. Proc. Natl. Acad. Sci. U. S. A. 103, 18928-18933.

Pellegrini, A., Thomas, U., von Fellenberg, R., Wild, P., 1992. Bactericidal activities of lysozyme and aprotinin against Gram-negative and Gram-positive bacteria related to their basic character. J. Appl. Bacteriol. 72, 180-187.

Perner, J., Sobotka, R., Sima, R., Konvickova, J., Sojka, D., Oliveira, P.L., Hajdusek, O., Kopacek, P., 2016. Acquisition of exogenous haem is essential for tick reproduction. Elife 5, 10.7554/eLife.12318.

Petrou, G., Crouzier, T., 2018. Mucins as multifunctional building blocks of biomaterials. Biomater. Sci. 6, 2282-2297.

Piesman, J., Mather, T.N., Sinsky, R.J., Spielman, A., 1987. Duration of tick attachment and *Borrelia burgdorferi* transmission. J. Clin. Microbiol. 25, 557-558.

Piesman, J., Maupin, G.O., Campos, E.G., Happ, C.M., 1991. Duration of adult female *Ixodes dammini* attachment and transmission of *Borrelia burgdorferi*, with description of a needle aspiration isolation method. J. Infect. Dis. 163, 895-897.

Poirier, A.C., Schmitt, P., Rosa, R.D., Vanhove, A.S., Kieffer-Jaquinod, S., Rubio, T.P., Charriere, G.M., Destoumieux-Garzon, D., 2014. Antimicrobial histones and DNA traps in invertebrate immunity: evidences in *Crassostrea gigas*. J. Biol. Chem. 289, 24821-24831.

Porter, L.M., Radulovic, Z.M., Mulenga, A., 2017. A repertoire of protease inhibitor families in *Amblyomma americanum* and other tick species: inter-species comparative analyses. Parasit. Vectors 10, 1.

Porter, L., Radulovic, Z., Kim, T., Braz, G.R., Da Silva Vaz, I.,Jr, Mulenga, A., 2015. Bioinformatic analyses of male and female *Amblyomma americanum* tick expressed serine protease inhibitors (serpins). Ticks Tick Borne Dis. 6, 16-30.

Radulovic, Z.M., Kim, T.K., Porter, L.M., Sze, S.H., Lewis, L., Mulenga, A., 2014. A 24-48 h fed *Amblyomma americanum* tick saliva immuno-proteome. BMC Genomics 15, 518.

Rawlings, N.D., Barrett, A.J., Bateman, A., 2012. MEROPS: the database of proteolytic enzymes, their substrates and inhibitors. Nucleic Acids Res. 40, 343.

Ribeiro, J.M., Alarcon-Chaidez, F., Francischetti, I.M., Mans, B.J., Mather, T.N., Valenzuela, J.G., Wikel, S.K., 2006. An annotated catalog of salivary gland transcripts from *Ixodes scapularis* ticks. Insect Biochem. Mol. Biol. 36, 111-129.

Ribeiro, J.M., Mather, T.N., Piesman, J., Spielman, A., 1987. Dissemination and salivary delivery of Lyme disease spirochetes in vector ticks (Acari: Ixodidae). J. Med. Entomol. 24, 201-205.

Rock, K.L., Kono, H., 2008. The inflammatory response to cell death. Annu. Rev. Pathol. 3, 99-126.

Rojkind, M., Dominguez-Rosales, J.A., Nieto, N., Greenwel, P., 2002. Role of hydrogen peroxide and oxidative stress in healing responses. Cell Mol. Life Sci. 59, 1872-1891.

Rossi, D.C.P., Silva, F.D., Daffre, S., Martinez, L.R., Nosanchuk, J.D., Frases, S., Fonseca, F.L., Rodrigues, M.L., Campos, C.B.L., 2011. Effects of microplusin, a copper-chelating antimicrobial peptide, against *Cryptococcus neoformans*. FEMS Microbiol Lett. 324, 64-72.

Schultz, J., Copley, R.R., Doerks, T., Ponting, C.P., Bork, P., 2000. SMART: a web-based tool for the study of genetically mobile domains. Nucleic Acids Res. 28, 231-234.

Shevchenko, A., Wilm, M., Vorm, O., Mann, M., 1996. Mass spectrometric sequencing of proteins silver-stained polyacrylamide gels. Anal. Chem. 68, 850-858.

Silva, F.D., Rezende, C.A., Rossi, D.C., Esteves, E., Dyszy, F.H., Schreier, S., Gueiros-Filho, F., Campos, C.B., Pires, J.R., Daffre, S., 2009. Structure and mode of action of microplusin, a copper II-chelating antimicrobial peptide from the cattle tick *Rhipicephalus* (*Boophilus*) *microplus*. J. Biol. Chem. 284, 34735-34746.

Smathers, R.L., Petersen, D.R., 2011. The human fatty acid-binding protein family: evolutionary divergences and functions. Hum. Genomics 5, 170-191.

Smith, S.A., Travers, R.J., Morrissey, J.H., 2015. How it all starts: Initiation of the clotting cascade. Crit. Rev. Biochem. Mol. Biol. 50, 326-336.

Sonenshine, D.E., 1993. Biology of Ticks. Oxford University Press, Oxford.

Tatchell, R.J., 1967. A modified method for obtaining tick oral secretion. J. Parasitol. 53, 1106-1107.

Tatusov, R.L., Fedorova, N.D., Jackson, J.D., Jacobs, A.R., Kiryutin, B., Koonin, E.V., Krylov, D.M., Mazumder, R., Mekhedov, S.L., Nikolskaya, A.N., Rao, B.S., Smirnov, S., Sverdlov, A.V., Vasudevan, S., Wolf, Y.I., Yin, J.J., Natale, D.A., 2003. The COG database: an updated version includes eukaryotes. BMC Bioinformatics 4, 41. Epub 2003 Sep 11.

Tirloni, L., Islam, M.S., Kim, T.K., Diedrich, J.K., Yates, J.R.,3rd, Pinto, A.F., Mulenga, A., You, M.J., Da Silva Vaz, I.,Jr, 2015. Saliva from nymph and adult females of *Haemaphysalis longicornis*: a proteomic study. Parasit. Vectors 8, y.

Tirloni, L., Reck, J., Terra, R.M., Martins, J.R., Mulenga, A., Sherman, N.E., Fox, J.W., Yates, J.R.,3rd, Termignoni, C., Pinto, A.F., Vaz Ida, S.,Jr, 2014. Proteomic analysis of cattle tick *Rhipicephalus* (*Boophilus*) *microplus* saliva: a comparison between partially and fully engorged females. PLoS One 9, e94831.

Toh, S.Q., Glanfield, A., Gobert, G.N., Jones, M.K., 2010. Heme and blood-feeding parasites: friends or foes? Parasit. Vectors 3, 108.

Turner, A.J. and G.S. Cottrell (2004) Handbook of Proteolytic Enzymes (ed. Barrett, A.J. et al.) pp. 931, Elsevier Academic Press, San Diego.

Valenzuela, J.G., Francischetti, I.M., Pham, V.M., Garfield, M.K., Mather, T.N., Ribeiro, J.M., 2002. Exploring the sialome ofthe tick *Ixodes scapularis*. J. Exp. Biol. 205, 2843-2864.

Walade, S.M., Rice, M.J., 1982. The sensory basis of tick feeding behavior. Physiology of Ticks, pp. 71–118.

Wang, Y., Zhou, Y., Gong, H., Cao, J., Zhang, H., Li, X., Zhou, J., 2015. Functional characterization of a cystatin from the tick *Rhipicephalus haemaphysaloides*. Parasit. Vectors 8, 5.

Warnes, G.R., Bolker, B., Bonebakker, L., Gentleman, R., Huber, W., Liaw, A., Lumley, T., Maechler, M., Magnusson, A., Moeller, S., Schwartz, M., Venables, B., 2013. Various R programming tools for plotting data. The Comprehensive R Archive Network.

Wild, P., Gabrieli, A., Schraner, E.M., Pellegrini, A., Thomas, U., Frederik, P.M., Stuart, M.C., Von Fellenberg, R., 1997. Reevaluation of the effect of lysoyzme on *Escherichia coli* employing ultrarapid freezing followed by cryoelectronmicroscopy or freeze substitution. Microsc. Res. Tech. 39, 297-304.

Wu, J., Wang, Y., Liu, H., Yang, H., Ma, D., Li, J., Li, D., Lai, R., Yu, H., 2010. Two immunoregulatory peptides with antioxidant activity from tick salivary glands. J. Biol. Chem. 285, 16606-16613.

Xu, T., Park, S.K., Venable, J.D., Wohlschlegel, J.A., Diedrich, J.K., Cociorva, D., Lu, B., Liao, L., Hewel, J., Han, X., Wong, C.C., Fonslow, B., Delahunty, C., Gao, Y., Shah, H., Yates, J.R.,3rd, 2015. ProLuCID: An improved SEQUEST-like algorithm with enhanced sensitivity and specificity. J. Proteomics.

Zavasnik-Bergant, T., Vidmar, R., Sekirnik, A., Fonovic, M., Salat, J., Grunclova, L., Kopacek, P., Turk, B., 2017. Salivary tick cystatin OmC2 targets lysosomal cathepsins S and C in human dendritic cells. Front. Cell. Infect. Microbiol. 7, 288.

Zhu, W., Smith, J.W., Huang, C.M., 2010. Mass spectrometry-based label-free quantitative proteomics. J. Biomed. Biotechnol. 2010, 840518.

Zininga, T., Ramatsui, L., Shonhai, A., 2018. Heat shock proteins as immunomodulants. Molecules 23, 10.3390/molecules23112846.

CHAPTER III*†

DETERMINE FUNCTIONAL ROLES OF SELECTED SERINE PROTEASE INHIBITORS FOUND IN TICK SALIVA AT THE TICK FEEDING SITE

Rationale

The tick feeding style of injuring host tissue and sucking blood that accumulates into the feeding lesion is expected to trigger host defense mechanisms that are mostly serine protease-mediated pathways that are tightly controlled by serine protease inhibitors (serpins). From this perspective, it has been proposed that ticks could utilize serpins to regulate evasion of host defenses. Therefore, in this chapter the goal was to determine the functional roles of three saliva serpins that were identified in tick saliva within the first 24 h of feeding from chapter II. Two of the salivary serpins were identified as secreted in tick saliva in all feeding time points, and one of the saliva serpins was conserved in other tick species. These serpins were chosen due to the reasoning that candidate serpins that are secreted throughout the tick feeding process and/or are conserved in other tick species probably regulate critical tick feeding functions. The goal was to determine the mechanism through which the candidate serpins interact with the host immune

---

*Reprinted with permission from Conserved *Amblyomma americanum* tick Serpin19, an inhibitor of blood clotting factors Xa and XIa, trypsin and plasmin, has anti-haemostatic functions by Kim, T.K., Tirloni, L., Radulovic Z., Lewis L., Bakshi, M., Hill., C., da Silva Vaz Jr., I., Logullo, C., Termignoni, C., and Mulenga A., 2015. Int J Parasitol. Aug;45(9-10);613-27. doi: 10.1016/j.ijpara.2015.03.009.

†Reprinted with permission from Target validation of highly conserved *Amblyomma americanum* tick saliva serine protease inhibitor19 by Kim, T.K., Radulovic Z., and Mulenga A., 2016. Ticks Tick Borne Dis. Apr;7(3);405-14. doi: 10.1016/j.ttbdis.2015.12.017.

system, and in so doing contributes to tick evasion of host immunity against tick feeding. This chapter tested the following hypothesis:

- H_0: Serine protease inhibitors in tick saliva will not block host defenses to tick feeding.
- H_1: Serine protease inhibitors in tick saliva will block host defenses to tick feeding.

I successfully characterized three *A. americanum* tick saliva serpins: AAS19, AAS41, and AAS46. Data on AAS19 were published in two articles below.

Part IA*

Conserved *Amblyomma americanum* tick Serpin19, an inhibitor of blood clotting factors Xa and XIa, trypsin and plasmin, has anti-haemostatic functions

Materials and Methods

Ethics statement

All animal work was conducted and approved according to Texas A&M University Institutional Animal Care and Use Committee (AUP 2011-0207).

Tick feeding, dissections, total RNA extractions and cDNA synthesis

A. americanum ticks were purchased from the tick laboratory at Oklahoma State University (Stillwater, OK). Routinely, ticks were fed on rabbits according to animal use protocols approved by Texas A & M University Institutional Animal Care and Use Committee. Feeding was done as

previously described (Mulenga et al., 2013; Kim et al., 2014a). *A. americanum* ticks were restricted to feed onto the outer part of the ear of New Zealand rabbits with orthopedic stockinet's glued with Kamar Adhesive (Kamar Products Inc., Zionsville, IN, USA). Six male ticks were pre-fed for three days prior to introducing 15 female ticks in each of the ear stockinet (total of 30 female ticks per rabbit).

Ticks were collected and dissected as previously described (Mulenga et al., 2013). Five ticks were manually detached every 24h for five days (24-120h). Within the first hour of detachment, tick mouthparts were inspected to remove remnant tissue and washed in RNase inhibitor diethylpyrocarbonate (DEPC)-treated water to prepare for dissections. Dissected tick organs, salivary glands (SG), midguts (MG), ovary (OV), synganglion (SYN), Malpighian tubules (MT), and carcass (CA, the remnants after removal of other organs) were placed in RNA later (Life Technologies, Carlsbad, CA, USA) or 1 mL Trizol total RNA extraction reagent (Life Technologies) and stored at -80° C until total RNA extraction.

Total RNA was extracted using the Trizol reagent according to manufacturer's instructions (Life Technologies) and re-suspended in DEPC treated water. Total RNA was quantified using a UV-VIS Spectrophotometer DU-640B (Beckman Coulter, Brea, CA, USA) or the Infinite M200 Pro plate reader (Tecan, Männedorf, Switzerland). Up to 1 µg total RNA was used to synthesize cDNA using the Verso cDNA Synthesis Kit following the manufacturer's instructions (Thermo Scientific, Waltham, MA, USA).

Structural alignment, amino acid motif scanning, and comparative modeling

To get an insight into the relationship of AAS19 (accession#: GAYW01000076; Porter et al., 2015) protein from *Amblyomma americanum* tertiary structure to its homologs in other tick

species, amino acid sequences from UniProt in other tick species: *Rhipicephalus pulchellus* (L7LRY7), *Ixodes ricinus* (V5IHU3), *Amblyomma maculatum* (G3ML49 and G3ML50), *Rhipicephalus microplus* (V9VP22), *Ixodes scapularis* (B7QJF1), *Amblyomma triste* (A0A023GPF9) and *Amblyomma cajenense* (A0A023FM57) were subjected to structural based ClustalW alignment using AAS19 tertiary structure as template. The alignment sequences were subsequently viewed using the GeneDoc software (http://www.nrbsc.org/gfx/genedoc/ebinet.htm). Additionally AAS19 amino acid sequence was manually inspected for annotated glycosaminoglycan (GAG) binding motifs as previously reviewed (Hileman et al., 1998). To determine potential N- or O-linked glycosylation sites, AAS19 amino acid was scanned using NetNGlyc 1.0 and NetOGlyc 4.0 servers (www.cbs.dtu.dk).

The 3-D structure for AAS19 was predicted using comparative modeling approach. The serpin protein C inhibitor structure (2OL2) (Li and Huntington, 2008) was retrieved from Protein Data Bank (PDB) and used as a molecular template for AAS19 modeling based on 30% and 53% sequence identity and similarity, respectively. Sequence alignments were generated using ClustalW algorithm (Larkin et al., 2007) and used as input in the Modeller 9v14 program (Webb and Sali, 2014). Models generated were evaluated using QMEAN4 and PROCHECK to estimate model reliability and predict quality (Benkert et al., 2008; Morris et al., 1992). The electrostatic potential of AAS19 and protein C inhibitor (2OL2, positive control template) was calculated in two approaches. First using the Adaptive Poisson-Boltzmann Solver (APBS) and protonation states were assigned using parameters for solvation energy (PARSE) force field for each structure by PDB2PQR (Unni et al., 2011). Execution of APBS and visualization of resulting electrostatic potentials were performed by Visual Molecular Dynamics (VMD) program (Humphrey et al., 1996) at ±5 kT/e of positive and negative contour fields. In the second approach electrostatic

potential was computed using APBS and visualized in SWISS PDB viewer (Guex and Peitsch, 1997) (http://www.expasy.org/spdbv/) set to default parameters.

Temporal and spatial quantitative RT-PCR transcription analyses of AAS19

Transcription analysis was done by two-step quantitative (q) RT-PCR using Applied Biosystems 7300 Real Time PCR System (Life Technologies) as described (Kim et al., 2014a). AAS19 specific qRT-PCR primers (For: 5′-GACAAGACGCACGGCAAAA-3′ and Rev: 5′-GAAGTCCGGCGGCTCAT-3′) were used to determine transcript abundance in triplicate pools of cDNA of dissected salivary gland (SG), midgut (MG), and remnant tissues as carcass (CA) of unfed, 24 and 48 h fed (n = 15 ticks per pool), 72 and 96 h fed (n = 10 ticks per pool), and 120 h fed (n = five ticks). Cycling conditions were the following: stage one at 50°C for 2 min, stage two at 95°C for 10 min, and stage three contained two steps with 40 cycles of 95°C for 15s and 60°C for 1 min. Reaction volumes in triplicate contained ten-fold diluted cDNAs that was originally synthesized from 1 μg total RNA, 350 nM of forward and reverse AAS19 primers, and 2X SYBR Green Master Mix (Life Technologies). For internal reference control, a forward (5′-GGCGCCGAGGTGAAGAA-3′) and reverse (5′-CCTTGCCGTCCACCTTGAT-3′) primers targeting of 40S ribosomal protein S4 (RPS4; accession number GAGD01011247.1) which is stably expressed in *Ixodes scapularis* during feeding (Koci et al., 2013) was used. Relative quantification (RQ) of AAS19 transcript was determined using the comparative C_T ($2^{-\Delta\Delta Ct}$) method (Livak and Schmittgen, 2001) and adopted in (Kim et al., 2014a). The data was presented as percent mean (M) transcript abundance ± SEM per tissue.

Expression and affinity purification of recombinant AAS19

Recombinant (r) AAS19 protein was expressed using the *Pichia pastoris* and pPICZα

plasmid expression system (Life Technologies) as described previously (Mulenga et al., 2013; Kim et al., 2014b). Mature AAS19 protein open reading frame (Porter et al., 2015) was sub-cloned into pPICZαA *Eco*RI and *Not*I sites using forward (For: 5′**GAATTC**GCAGAGCCCGACGAAGATGGC3′) and reverse (Rev: 5′**GCGGCCGC**GAGGGCGTTAATTTCGCCCAG3′) primers with added restriction enzyme sites in bold. The pPICZαA-AAS19 expression plasmid was linearized with *PmeI* and electroporated into *Pichia pastoris* X-33 strain (Life Technologies) using ECM600 electroporator (BTX Harvard Apparatus Inc., Holliston, MA, USA) with parameters set to 1.5 kV, 25 uF, and 186 Ω. Transformed colonies were selected on Yeast Extract Peptone Dextrose Medium with Sorbitol (YPDS) agar plates with zeocin (100 µg/µl), and methanol utilization on Minimal Methanol (MM) agar plates, both incubated at 28°C. Positive transformants were inoculated in buffered glycerol-complex medium (BMGY) and grown overnight at 28°C with shaking (230-250 rpm). Subsequently the cells were used to inoculate buffered methanol-complex medium (BMMY) to A_{600} of 1 after which protein expression was induced by adding methanol to 0.5% final concentration every 24 h for five days. Recombinant AAS19 in spent culture media was precipitated by ammonium sulfate saturation (525 g/L of media) with stirring overnight at 4°C. The precipitate was pelleted at 11,200g for 1h at 4°C and re-suspended in, and dialyzed against 20 mM Tris-HCl buffer pH 7.4. To verify expression of rAAS19, western blotting analysis was performed using the horseradish peroxidase (HRP)-labeled antibody to the C-terminus hexa histidine tag (Life Technologies) diluted to 1:5000 in 5% blocking buffer (5% skim milk powder in PBS w/Tween-20). The positive signal was detected using metal enhanced DAB chromogenic substrate kit (Thermo Scientific). Subsequently, rAAS19 was affinity purified under native conditions using Hi-Trap Chelating HP Columns (GE Healthcare Bio-Sciences, Pittsburgh, PA,

USA). Affinity purified putative rAAS19 was dialyzed against 20 mM Tris-HCl buffer pH 7.4 for downstream assays. To verify purity and background contamination, affinity purified rAAS19 was resolved on a 10% SDS-PAGE gel and silver stained. Samples with least background were selected and concentrated by either ammonium sulfate precipitation or by centrifugation using MicroSep Centrifugal Concentration Devices (Pall Corporation, Port Washington, NY, USA).

N- and O- linked deglycosylation assay

Preliminary amino acid sequence analyses predicted N- and O-linked glycosylation sites in AAS19. To determine if rAAS19 was N-glycosylated and/or O-glycosylated, 5 µg affinity purified rAAS19 was treated with protein deglycosylation enzyme mix according to manufacturer's instructions (New England Biolabs, Ipswich, MA, USA). Deglycosylation was verified by western blotting analysis using the antibody to C-terminus hexa histidine-tag (Life Technologies) and the positive signal detected using HRP chromogenic substrate (Thermo Scientific).

Determining if native AAS19 is injected into the host during tick feeding

To determine if native AAS19 is injected into the host during feeding, glycosylated and deglycosylated affinity-purified rAAS19 was subjected to routine western blotting analyses using antibodies to replete-fed *A. americanum* tick saliva proteins. Antibodies to replete-fed tick saliva proteins used here were produced as previously described (Mulenga et al., 2013).

Protease inhibitor (PI) profiling

Inhibitory activity of rAAS19 was tested against a panel of 16 mammalian serine proteases

related to host defense pathways against tick feeding. Mammalian proteases (per reaction) tested were: bovine thrombin (43 U), pancreatic porcine elastase (21.6 nM), pancreatic bovine trypsin (24.6 nM), pancreatic bovine α-chymotrypsin (96 nM), pancreatic porcine kallikrein (33 U), human chymase (10 U), human tryptase (10 U), human plasmin (10 nM) (Sigma-Aldrich, St. Louis, MO, USA), human neutrophil cathepsin G (166 nM) (Enzo Life Sciences Inc., Farmingdale, NY, USA), human factor (f) XIa (3.68 nM), bovine fIXa (306 nM), human fXIIa (7.6 nM), human t-PA (32 nM), human u-PA (47.2 nM) (Molecular Innovations, Inc., Novi, MI, USA), fXa (5.8 nM) (New England Biolabs) and proteinase-3 (68 U) (EMD Millipore, Billerica, MA, USA). Substrates were used at 0.20 mM final concentration and purchased from Sigma-Aldrich: N α-benzoyl-DL-Arg-pNA for tryptase, N-Succinyl-Ala-Ala-Pro-Phe-pNA for chymase, cathepsin G and chymotrypsin, N-Benzoyl-Phe-Val-Arg-pNA for thrombin and trypsin, N-Succinyl-Ala-Ala-Ala-p-nitroanilide for elastase. The following substrates were purchased from Chromogenix a part of Diapharma Inc. (Philadelphia, PA, USA): Bz-Ile-Glu(γ-OR)-Gly-Arg-pNA for fXa, H-D-Val-Leu-Lys-pNA for plasmin, and H-D-Pro-Phe-Arg-pNA for kallikrein, fXIa and fXIIa. The substrate CH_3SO_2-D-CHG-Gly-Arg-pNA was purchased from Molecular Innovations and used for fIXa, u-PA and t-PA. The substrate N-Methoxysuccinyl-Ala-Ala-Pro-Val-pNA was purchased from Enzo Life Sciences and used for proteinase-3.

Reagents were mixed at room temperature in triplicate. One μM of rAAS19 was pre-incubated with indicated amounts of the enzyme for 15 minutes at 37°C in 20 mM Tris-HCl, 150 mM NaCl, BSA 0.1%, pH 7.4 buffer. The corresponding substrate for each enzyme was added in a 100 μL final reaction volume and substrate hydrolysis was measured at A_{405nm} every 11s for 30 min at 30ºC using the Infinite M200 Pro plate reader (Tecan). Acquired A_{405nm} data were subjected to one phase decay analysis in Prism 6 software (GraphPad Software, La Jolla, CA, USA) to

determine plateau values as proxy for initial velocity of substrate hydrolysis (V_{max}) or residual enzyme activity. The percent enzyme activity inhibition level was determined using the formula: 100 - $V_{max}(V_i)/V_{max}$ (V_0) X 100 where V_{max} (V_i) = activity in presence of, and V_{max} (V_0) = activity in absence of rAAS19. Data are presented as mean ± SEM of triplicate readings.

Stoichiometry of inhibition (SI)

We determined stoichiometry of inhibition (SI) indices against five proteases: trypsin, plasmin, fXa, fXIa, and fXIIa that were inhibited by more than 80% in the PI profiling assay above. Different molar ratios (serpin:protease) of rAAS19 were pre-incubated for 1 hour with constant concentration of trypsin (10 nM), fXa (5 nM), fXIa (5 nM), and plasmin (10 nM). The residual enzyme activity was measured using colorimetric substrates specific for each enzyme as described above. The data were plotted as the residual activity (V_i/V_0) versus the inhibitor to enzyme molar ratio. SI or the molar ration of rAAS19 to protease when enzyme activity is completely inhibited was determined by fitting data onto the linear regression line in PRISM.

rAAS19 and protease complex formation

In varying molar ratios, affinity purified rAAS19 was incubated with trypsin, plasmin, fXa and fXIa, in Tris-HCl reaction buffer (20 mM Tris-HCl, 150 mM, NaCl, pH 7.4) for 1 hour at 37°C. Denaturing sample buffer was added to the reaction mix, and incubated at 99.9°C for 5 min in thermocycler. Samples were subjected to SDS-PAGE electrophoresis on a 12.5% acrylamide gel and stained with Coomassie brilliant blue using routine protocols.

Anti-platelet aggregation function of rAAS19

Anti-platelet aggregation function(s) of rAAS19 was determined using platelet rich plasma (PRP) isolated from citrated (acid citrate dextrose) whole bovine blood (WBBL) as previously described (Horn et al., 2000; Berger et al., 2010). To prepare PRP, fresh citrated WBBL was centrifuged at 200g for 20 min at 18°C. Subsequently the PRP (top layer) was transferred into a new tube and centrifuged at 800g for 20 min at 18°C. The pellet containing platelets was washed and diluted with Tyrode buffer pH 7.4 (137mM NaCl, 2.7mM KCl, 12mM $NaHCO_3$, 0.42mM Na_2HPO_4, 1mM $MgCl_2$, 0.1% glucose, 0.25% BSA) until $A_{650} = 0.15$. To determine anti-platelet aggregation function, various amounts of rAAS19 (1, 0.5, 0.25, and 0 μM) were pre-incubated for 15 min at 37°C with agonist 10 NIH-U thrombin, 20 μM ADP, or 0.7 μM cathepsin G in a 50 μL reaction. Adding 100 μL of pre-warmed PRP triggered platelet aggregation. Vice versa PRP was pre-incubated with various amounts of rAAS19 prior to addition of the agonist. Platelet aggregation was monitored every 20 seconds over 30 min at A_{650nm} using the Infinite M200 Pro plate reader (Tecan). In this assay higher optical density (OD) was observed in our blank (platelet only), and increased platelet aggregation was correlated with reduction in OD. To determine % platelet aggregation inhibition, OD data was fit to the one phase decay equation in PRISM (GraphPad) to determine plateau OD. The percent reduction in platelet aggregation was calculated using this formula: $Y = 100 – (\Delta Pn)/\Delta PC)*100$, where Y = % reduction in platelet aggregation, ΔPn and ΔPC = a respective rAAS19 treated and positive control plateau OD subtracted from blank plateau OD. Data is presented as mean ± SEM of duplicate platelet aggregation assays.

Anti-blood clotting function of rAAS19

The effect of rAAS19 against blood clotting was assessed using modified recalcification

time (RCT), activated partial thromboplastin time (aPTT), thrombin time (TT), and prothrombin time (PT) to respectively measure the effect on the entire blood cascade, the intrinsic, extrinsic, and common blood clotting activation pathways as described (Mulenga et al., 2013). All assays were done in duplicate, with clotting time monitored at A_{650nm} using the Infinite M200Pro plate reader (Tecan) set to 37°C. In these assays, clot formation was directly proportional to increase in OD, and results presented as mean ± SEM.

In the RCT assay, 50 μL of universal coagulation reference human plasma [UCRP] (Thermo Scientific) was pre-incubated with 10, 5, 1.25, 0.625, 0 μM rAAS19 in 90 μL Tris-HCl reaction buffer (20 mM Tris-HCl, 150 mM NaCl, pH 7.4) for 15 min at 37°C. Adding 10 μL of pre-warmed 150 mM calcium chloride ($CaCl_2$) triggered plasma clotting. Plasma clotting was monitored at every 20 s for 30 min.

In the aPTT assay, various amounts of rAAS19 (indicated above) were pre-incubated for 15 min at 37°C with 50 μL UCRP diluted to 100 μL with 20 mM Tris-HCl, 150 mM NaCl, pH 7.4. Subsequently, 50 μL of the aPTT reagent (Thermo Scientific) was added to plasma and incubated at 37°C for an additional 5 min to activate the reaction. Addition of 50 μL 25 mM $CaCl_2$ to the reaction triggered clotting, and clot formation was monitored every 10 s for 5 min.

In the TT assay, various amounts of rAAS19 (indicated above) were pre-incubated at 37°C for 15 min with 25 μL of the TT reagent (Thermo Scientific) containing $CaCl_2$ in 50 μL Tris-HCl reaction buffer with (20 mM Tris-HCl, 150 mM NaCl, pH 7.4). Adding 50 μL of pre-warmed UCRP started plasma clotting and clotting time was monitored every 10 s for 5 min.

In the PT assay various rAAS19 amounts as above were pre-incubated at 37°C for 15 min with 100 μL PT reagent (Thermo Scientific) containing $CaCl_2$ diluted up to 150 μL with 20 mM

Tris-HCl, 150 mM NaCl, pH 7.4 reaction buffer. Adding 50 μL of the pre-warmed UCRP (Thermo Scientific) triggered plasma clotting and clotting time monitored every 10 s for 5 min.

Statistical analysis

Statistical software packages in PRISM version 6 (GraphPad Software Inc.) were used.

Results

AAS19 tertiary structure retains features of a typical serpin

AAS19 amino acid sequence is homologous to serpins from other tick species, being that its functional domain reactive center loop (RCL) is 100% conserved among the majority of ixodid tick species (Porter et al., 2015). In this study we conducted comparative amino acid motif and secondary structure analyses to determine the relationship of AAS19 to its homologues in other tick species (Fig. 1). Comparative modeling using protein C inhibitor tertiary structure (2OL2) as a template showed that AAS19 predicted tertiary structure retains the typical serpin fold formed by 9 α-helices, 3 β sheets (5 strands each in βsA and βsB, and 3 strands in βsC) (Fig. 1 and Fig. 2) (Gettins, 2002). Amino acid motif scanning analyses showed conservation of the "RGD" motif (positions 40-42, Fig. 1), which is the binding site to integrin GPIIb-IIIa (Srinivasan et al., 2010; Nurden, 2014). Additionally, two N-glycosylation sites at positions 97-99 and 198-200 in AAS19 and in majority of its homologues are conserved as shown in broken line boxes (Fig. 1). Visual inspection of the alignment in Fig. 1 revealed seven clusters of basic amino acid residues that show similarity to annotated glycosaminoglycan (GAG) binding sites (BS) (reviewed in Hileman et al., 1998). The seven clusters of basic residues (basic residues in bold, amino acid positions based on structural alignment in Fig. 1) in AAS19 are:

[^{59}**K**VLALF**R**EQLDAS**R**^{72}],

[^{117}**KK**GEEAVE**K**INNWVSD**K**T**H**G**K**I**RR**^{140}],

[^{151}**R**LILLNAVYY**K**GTWLYEFN**K**A**R**T**K**P**R**^{176}],

[^{185}**K**VLVPMM**K**M**K**^{194}],

[^{229}**R**NGLE**H**L**K**SVLTTQTLN**R**AIS**R**MYP**K**DM**K**F**R**MP**K**L**K**LDT**K**YTL**K**^{272}],

[^{281}**KKK**IFSADADLSGISGA**K**NLYVSDVL**HK**^{301}] and

[^{343}**K**VYVD**H**PFIFLI**R**^{355}].

To gain further insight about the possibility that clusters of basic amino acid residues in AAS19 form basic patches, we calculated surface electrostatic potentials on the AAS19 model (Fig. 2B). This analysis predicts that [K^{137}-R^{139}-R^{140}-K^{161}-K^{264}-K^{268}- K^{308}], [K^{8}-K^{236}-R^{246}-R^{250}], [R^{172}-K^{174}-R^{176}-K^{185}-K^{192}-K^{194}-K^{343}], and [K^{117}-K^{118}-R^{151}-K^{272}-K^{298}], respectively, interact to form putative GAG binding sites (GAGBS) 1-4 on AAS19 surface (Fig. 2B). This methodology was able to recover the GAGBS in PCI, a protein whose GAGBS was previously described (Fig. 2A) (Li and Huntington, 2008).

AAS19 mRNA is expressed in several tick tissue during feeding

To determine the relationship of AAS19 transcription with the *A. americanum* tick-feeding phase we determined its spatial and temporal transcription profile. Fig. 3 shows AAS19 mRNA is expressed during blood meal and in unfed ticks. AAS19 is transcribed in salivary gland (SG) (Fig. 3A), midgut (MG) (Fig. 3B) and other tissues (carcass, CA) (Fig. 3C). AAS19 transcription in salivary gland does not change from unfed to 120 fed ticks. Contrarily in midgut and carcass, AAS19 transcription increases (RPS4 was used for normalization) with feeding (Fig. 3B and C).

AAS19 protein is injected into the host during feeding

Fig. 4A and 4B summarize expression and affinity purification of recombinant (r) AAS19 in *P. pastoris*. To verify expression, daily samples of 1 mL yeast spent media were concentrated by ammonium sulfate saturation and subjected to western blotting analysis using a specific antibody to the C-terminus histidine tag (as summarized in Fig. 4A). For large-scale expression, ammonium sulfate- precipitated rAAS19 was affinity purified under native conditions and purity checked by SDS-PAGE with silver staining (Fig. 4B). Fractions, W2, E1, E2, and E4 in Fig. 4B, the fractions that showed the smallest amount of contaminating protein, were pooled, concentrated and dialyzed in appropriate buffer by spin columns and used for further assays. Fraction E3 was used in western blotting analysis assays summarized in Fig. 4C-4E. As shown in Fig. 4C, a 1:50 dilution of rabbit pre-immune serum did not recognize rAAS19, while a 1:250 dilution of antibodies against saliva proteins of fully engorged *A. americanum* (Fig. 4B), and against the C-terminus histidine tag (Fig 4E) recognize both glycosylated (lane 1) and de-glycosylated (lane 2) rAAS19. In Fig. 4D and 4E, there is smearing in lane 1 but not in lane 2. Additionally, there is a downward molecular weight shift in lane 2. This shift in molecular size and disappearance of smears following de-glycosylation validates that rAAS19 is glycosylated.

rAAS19 is a broad spectrum inhibitor of trypsin-like proteases

Protease inhibition profiling was done against 16 mammalian proteases that regulate host defenses against tick feeding such as hemostasis, wound healing/tissue remodeling, and inflammatory response (Table 1). Molar excess of rAAS19 inhibited the activity of trypsin and trypsin-like proteases associated with hemostasis (Fig. 5). Pre-incubation of 1 μM rAAS19 respectively inhibited approximately 80, 82, 86, 95, and 98% the activity of plasmin (34.8 nM),

fXIIa (7.62 nM), fXa (5.81 nM), fXIa (3.68 nM), and trypsin (24.6 nM) (Fig. 5A and 5B). Additionally, rAAS19 also inhibits thrombin (43 U), tryptase (10 U), fIXa (30.6 nM), and chymotrypsin (96 nM) by approximately 13, 16, 20, and 28% respectively.

To evaluate rAAS19 inhibitory efficiency, we determined the stoichiometry of inhibition (SI) of proteases that were inhibited by more than 80% by rAAS19. Fig. 6A, C, E, and G show the kinetic of the hydrolysis of specific substrates by these enzymes in the absence (a) and in the presence (b-g) of rAAS19 at various concentrations. These data were fit to a linear regression, as shown in Fig. 6B, D, F, and H. The rAAS19 SI index was estimated from the X-axis intercept (Y = 0), for trypsin, plasmin, fXa, and fXIa at 5, 9, 23, and 28, respectively. The SI index for fXIIa was estimated at 103 (not shown). The rAAS19 mechanism of action as a typical inhibitory serpin was confirmed by the inability of heating and SDS (Huntington et al., 2000) to dissociate it from trypsin (Fig. 7A), fXa (Fig. 7B), and fXIa (Fig. 7C). Irreversible complex between rAAS19 and the target enzyme was observed only at inhibitor enzyme molar ratios (Fig. 7A lane 1-3, Fig. 7B lane 1-2, and Fig. 7C lane 1-6) where enzyme activity inhibition was observed (Fig. 6A, 6E and 6G).

rAAS19 inhibits thrombin triggered platelet aggregation

Platelet rich plasma was used in platelet aggregation assays using three agonists: thrombin (0.03 U/μL), ADP (20 μM), and cathepsin G (0.7 μM). rAAS19 inhibited thrombin activated platelet aggregation (Fig. 8). In data shown in Fig. 8A, we did not observe platelet aggregation without addition of the agonist (a). However with platelets activated by thrombin that was pre-incubated with 1 (b), 0.5 (c), 0.25 (d), and 0 μM (e) rAAS19 showed variable levels of platelet aggregation. Pre-incubating 3U of thrombin with 1 μM and 0.5 μM rAAS19, platelet aggregation was reduced by 56% and 27%, respectively, while at 0.25 μM rAAS19 did not have any effect

(Fig. 8B). The rAAS19 did not have any effects in ADP and cathepsin G activated platelet aggregation. On the other hand, pre-incubation of rAAS19 with platelets prior to addition of the agonist did not affect platelet aggregation.

rAAS19 delays plasma clotting

Plasma clotting time (CT), recalcification time (RCT), activated partial thromboplastin time (aPTT), and thrombin time (TT) were delayed by rAAS19 in a dose-response manner (Fig. 9). However, rAAS19 did not affect prothrombin time (PT). In the RCT assay, to measure the effect of rAAS19 on the entire blood clotting activation system, 0.625, 1.25, and 5 μM (arrowhead R-CT2), and 10 μM (arrowhead R-CT3) dose responsively delayed RCT-CT by ~100 and 250 seconds when compared to clotting time in absence of rAAS19 (arrowhead R-CT1, 0 μM) (Fig. 9A). In the aPTT assay to measure effect on the intrinsic blood clotting activation pathway (Fig. 9B), 0.625 and 1.25 μM rAAS19 did not have any effect (arrowhead A- CT1, while 5 and 10 μM rAAS19 delayed aPTT-CT by ~20 (A-CT2) and 40 (A-CT3) seconds respectively. In the TT assay (Fig. 9C) 0.625 μM rAAS19 was not different from control (arrowhead T-CT1), while 1.25 and 5 μM rAAS19 (arrowhead T-CT2), and 10 μM rAAS19 (arrowhead T-CT3) delayed clotting by ~180 and 250 seconds respectively.

rAAS19 delays plasma clotting

Plasma clotting time (CT), recalcification time (RCT), activated partial thromboplastin time (aPTT), and thrombin time (TT) were delayed by rAAS19 in a dose-response manner (Fig. 9). However, rAAS19 did not affect prothrombin time (PT). In the RCT assay, to measure the effect of rAAS19 on the entire blood clotting activation system, 0.625, 1.25, and 5 μM (arrowhead

R-CT2), and 10 μM (arrowhead R-CT3) dose responsively delayed RCT-CT by ~100 and 250 seconds when compared to clotting time in absence of rAAS19 (arrowhead R-CT1, 0 μM) (Fig. 9A). In the aPTT assay to measure effect on the intrinsic blood clotting activation pathway (Fig. 9B), 0.625 and 1.25 μM rAAS19 did not have any effect (arrowhead A- CT1, while 5 and 10 μM rAAS19 delayed aPTT-CT by ~20 (A-CT2) and 40 (A-CT3) seconds respectively. In the TT assay (Fig. 9C) 0.625 μM rAAS19 was not different from control (arrowhead T-CT1), while 1.25 and 5 μM rAAS19 (arrowhead T-CT2), and 10 μM rAAS19 (arrowhead T-CT3) delayed clotting by ~180 and 250 seconds respectively.

Discussion

This study was prompted by the characteristic high conservation of AAS19 in all ixodid tick species, for which data are available (Porter et al., 2015). We were particularly interested in AAS19 because of its functional domain RCL being 100% conserved in other ixodid ticks, suggesting this serpin has a role regulating proteolytic pathways crucial to all ixodid tick species. The observation that AAS19 motifs and secondary structure are conserved in AAS19 homologues in several tick species further suggests this protein has a potential to regulate processes that are important to ixodid ticks.

In proposing that tick use serpins to evade host defense, the assumption is tick inject serpins into the host during feeding. Although several serpin cDNAs have been cloned, only few reports confirm that saliva truly contains serpins (Mulenga et al., 2013; Ibelli et al., 2014; Mudenda et al., 2014; Tirloni et al., 2014a). Thus, observations in this study demonstrating native AAS19 is injected into the host during tick feeding and its activity inhibiting proteases participating in host defenses reinforces the idea that inhibitory serpins have a role in tick-host relationship. Based on

the rAAS19 inhibitory activity against trypsin and trypsin-like proteases including, plasmin and blood clotting factors Xa and XIa we conclude this serpin inhibits proteases involved in host defenses against tick feeding. Albeit at low rate, it is notable that rAAS19 also inhibits other blood clotting enzymes including fXIIa, fIIa (thrombin) and fIXa, as well as chymotrypsin and tryptase, further confirming that AAS19 has broad-spectrum of inhibitory functions. Although AAS19 inhibits these enzymes, we are cautious about these enzymes being physiological targets for AAS19 because the stoichiometry of inhibition (SI) indices estimated in this study were not near 1:1, as will be expected for an inhibition by serpins (Irving et al., 2000; Silverman et al., 2001). However, we note here that the observed high SI indices are not unique for rAAS19. For instance, a SI index of 10 was estimated for *Drosophila melanogaster* Spn1, which inhibits trypsin activity by 96% (Fullaondo et al., 2011). A high SI index could also be explained by the possibility that AAS19 requires a co-factor to enhance inhibition. Indeed, nearly all serpin acting upon the blood clotting activation cascade and fibrinolysis (antithrombin III, heparin-cofactor II, plasminogen activator inhibitor 1, protein C inhibitor, and protease nexin inhibitor) need to bind glycosaminoglycans in order to accelerate inhibition rate, which can be up to 10,000-fold higher, compared to the unbound native serpin (Rein et al., 2011). According, Z-protein dependent inhibitor (ZPI) has been shown to accelerate the inhibitory effect of ZPI upon fXa by 1000-fold (Broze, Jr., 2001; Munoz and Linhardt, 2004). Our demonstration that AAS19 has four putative GAG binding sites suggests its activity could be modulated by heparin or another glycosaminoglycan. Studies to investigate the effects of heparin on rAAS19 function are underway.

From the perspective of tick feeding physiology the AAS19 inhibition activity upon trypsin, fXa and fXIa could rationally be explained. Trypsin mostly known for its role as digestive

enzyme (Rawlings and Barrett, 1994) is also associated with inflammation in the skin (Meyer-Hoffert et al., 2004; Cattaruzza et al., 2014), while blood clotting factors Xa and XIa are critical proteases of the blood clotting activation cascade (Monroe and Hoffman, 2006; Roberts et al., 2006). On the other hand AAS19 inhibition of plasmin can at a glance be viewed as contradictory since plasmin is mostly known for its role digesting blood clot (fibrinolysis) (Angles-Cano, 1994; Angles-Cano et al., 1994), an activity that seems to beneficial to tick feeding. Similarly, plasmin also degrades and inactivates blood-clotting factors V, VIII, IX, and X *in vitro*, suggesting plasmin have anti-coagulant functions (Hoover-Plow, 2010) and thus beneficial to tick feeding. On the other hand, plasmin has also been reported to participate in several processes such as pro-inflammatory cytokines releasing (Syrovets et al., 2001), inducing monocytes and dendritic cells chemotaxis (Li et al., 2010), modifying IL-8 producing a potent attractant of neutrophils (Mortier et al., 2011), tissue remodeling and wound healing (Shen et al., 2012), all of which can negatively impair tick-feeding success. From this perspective, AAS19 inhibition of plasmin seems to contribute for blood feeding.

Given that AAS19 is injected in the host during tick feeding and because of its inhibitory activity in blood clotting factors we investigated its action in platelet aggregation and plasma clotting. Platelet aggregation is important to stop bleeding in injured small blood vessels, as observed in tick feeding (Francischetti et al., 2009). Platelet aggregation is activated by multiple agonists, including thrombin, collagen, ADP, and cathepsin G (Selak et al., 1988; Ohlmann et al., 2000; Brass, 2003). Since thrombin is considered the most efficient platelet aggregation agonist (Furman et al., 1998; Davi and Patrono, 2007), the observation that rAAS19 reduced thrombin-activated platelet aggregation by up to 56 ± 14% suggests that AAS19 may play a crucial role in tick modulation of platelet function. Thrombin activates platelet aggregation through activation of

Protease Activated Receptors (PAR) 1, 3, and 4 (Kahn et al., 1999; Asokananthan et al., 2002), and thus it is plausible that native AAS19 may contribute toward binding and inhibiting thrombin at the tick feeding site, preventing the formation of the platelet plug, thus impairing the integrity of the blood clot. The observation that pre-incubating rAAS19 with platelets for 15 min prior to addition of the agonist had minimal effect suggest that the observed rAAS19 anti-platelet aggregation effects were mediated through inhibition of thrombin activity. However, it is interesting to note that the "RGD" motif, which is known to interfere with platelet aggregation binding the integrin GPIIb-IIIa on activated platelets (Varon et al., 1993; Katada et al., 1997) is conserved in AAS19 and its homologues. If this motif was functional, pre-incubation with platelets should interfere with platelet aggregation function.

Platelet aggregation is followed by fibrin clot formation, which reinforces the platelet plug (Clemetson, 2012). Blood clotting can be activated via the extrinsic pathway initiated upon release of tissue factor from injured tissue or via the intrinsic pathway when factors XII, XI, IX, and VIII are converted into their active forms. These pathways converge into the common pathway when fXa activates prothrombin to thrombin, which in turn catalyzes formation of the fibrin clot (Hoffman and Monroe, III, 2001; Hoffman, 2003; Monroe and Hoffman, 2006). Routinely, to address the general effect of anti-blood clotting agents is assayed using the recalcification time (RCT) assay, while effects on the extrinsic, intrinsic and common blood clotting activation pathway are assayed using prothrombin time (PT), activated partial thromboplastin time (aPTT), and thrombin time (TT) assays (Davie et al., 1991), as were done in this study. Eight of the 11 blood clotting factors are serine proteases (Walsh and Ahmad, 2002). Thus, although empirical evidence is needed, it is conceivable that the observed rAAS19 anticoagulant function could be attributed to its inhibitory activity against five (fIIa, fIXa, fXa, fXIa, and fXIIa) of the eight-serine

protease mediators of the blood clotting activation cascade. Except for fVIII, the other four blood clotting factors (IXa, Xa, XIa, and XIIa) in the intrinsic pathway (aPTT assay) are serine proteases, all of which were inhibited by rAAS19, and this could explain the observation of up to 40s plasma clotting time delay in the aPTT assay. Similarly in the TT (common pathway) assay, the observed 250s delay in plasma clotting time could be explained by rAAS19 inhibitory activity against thrombin. The discrepancy of 250s delay in the TT assay and ~14% inhibition of thrombin activity in substrate hydrolysis is interesting, and raises questions for further investigation. There is a possibility that the observed significant clotting time delay in the TT assay could be explained by a possibility of a yet unknown factor in host serum that potentiate AAS19 anti-thrombin activity. Given that AAS19 has four putative heparin binding sites, it is conceivable that GAGs in serum binding to AA19 could potentiate its activity against thrombin. Experiments to resolve this question are underway.

We would like to note here that arthropods do have hemolymph-clotting cascades that are also controlled by serpins (Agarwala et al., 1996; Iwanaga et al., 1998; Kanost, 1999). Thus, there is a possibility that native AAS19 could be a well-conserved regulator of the tick's hemolymph clotting in ticks and the observed anti-coagulant function in this study could be an artifact. However, the observation in this study that native AAS19 was injected into the host during tick feeding strongly suggests the role for this protein at the tick-feeding site. Alternatively AAS19 may function both in the tick and at the tick-feeding site. It is important to note here that based on transcript abundance, AAS19 is predominant in the tick midgut, which could strongly indicate a role for this protein in the midgut. Tick digestion of the blood meal nutrients is intracellular (Lara et al., 2005; Franta et al., 2010), and for this to happen, host blood must remain in the unclotted

state. Could it be that AAS19 anticoagulant function is part of the mechanism in the midgut to prevent host blood from clotting before digestion commences?

In conclusion, data in this study contribute toward our understanding of the molecular basis of tick feeding physiology. Data here contribute to the growing list of tick saliva proteins that potentially regulate tick evasion of the mammalian host's defenses to tick feeding as well as have role(s) in other tick physiologic systems. On the basis of AAS19 being highly conserved, coupled with the fact that its RCL being 100% conserved, we conclude that tick physiological processes regulated by AAS19 are evolutionary conserved in all tick species. From the perspective of our long-term interest to find target anti-tick vaccine antigens, AAS19 represent an interesting candidate. Human and animal tick borne diseases are transmitted by different species of ticks, and thus developing universal anti-tick vaccines based on highly conserved proteins such as AAS19 has been advocated for (Fragoso et al., 1998; Mulenga et al., 2001; de la Fuente and Kocan, 2006; Azhahianambi et al., 2009; Parizi et al., 2012; Mulenga et al., 2013). Work toward validating the anti-tick vaccine efficacy of rAAS19 is warranted.

References

Agarwala, K.L., Kawabata, S., Miura, Y., Kuroki, Y., Iwanaga, S., 1996. Limulus intracellular coagulation inhibitor type 3. Purification, characterization, cDNA cloning, and tissue localization. J.Biol.Chem. 271, pp. 23768-23774.

Algermissen, B., Hermes, B., Feldmann-Boeddeker, I., Bauer, F., Henz, B.M., 1999a. Mast cell chymase and tryptase during tissue turnover: analysis on in vitro mitogenesis of fibroblasts and keratinocytes and alterations in cutaneous scars. Exp.Dermatol. 8, pp. 193-198.

Algermissen, B., Laubscher, J.C., Bauer, F., Henz, B.M., 1999b. Purification of mast cell proteases from murine skin. Exp.Dermatol. 8, pp. 413-418.

Angles-Cano, E., 1994. Overview on fibrinolysis: plasminogen activation pathways on fibrin and cell surfaces. Chem.Phys.Lipids 67-68, pp. 353-362.

Angles-Cano, E., Hervio, L., Rouy, D., Fournier, C., Chapman, J.M., Laplaud, M., Koschinsky, M.L., 1994. Effects of lipoprotein(a) on the binding of plasminogen to fibrin and its activation by fibrin-bound tissue-type plasminogen activator. Chem.Phys.Lipids 67-68, pp. 369-380.

Asokananthan, N., Graham, P.T., Fink, J., Knight, D.A., Bakker, A.J., McWilliam, A.S., Thompson, P.J., Stewart, G.A., 2002. Activation of protease-activated receptor (PAR)-1, PAR-2, and PAR-4 stimulates IL-6, IL-8, and prostaglandin E2 release from human respiratory epithelial cells. J.Immunol. 168, pp. 3577-3585.

Azhahianambi, P., Ray, D.D., Chaudhuri, P., Gupta, R., Ghosh, S., 2009. Vaccine Efficacy of Bm86 Ortholog of *H. a. anatolicum*, rHaa86 Expressed in Prokaryotic Expression System. J.Parasitol.Res. 2009.

Belaaouaj, A., 2002. Neutrophil elastase-mediated killing of bacteria: lessons from targeted mutagenesis. Microbes.Infect. 4, pp. 1259-1264.

Benkert, P., Tosatto, S.C., Schomburg, D., 2008. QMEAN: A comprehensive scoring function for model quality assessment. Proteins 71, pp. 261-277.

Berger, M., Reck, J., Jr., Terra, R.M., Pinto, A.F., Termignoni, C., Guimaraes, J.A., 2010. *Lonomia obliqua* caterpillar envenomation causes platelet hypoaggregation and blood incoagulability in rats. Toxicon 55, pp. 33-44.

Brass, L.F., 2003. Thrombin and platelet activation. Chest 124, pp. 18S-25S.

Broze, G.J., Jr., 2001. Protein Z-dependent regulation of coagulation. Thromb.Haemost. 86, pp. 8-13.

Carmo, A.A., Costa, B.R., Vago, J.P., de Oliveira, L.C., Tavares, L.P., Nogueira, C.R., Ribeiro, A.L., Garcia, C.C., Barbosa, A.S., Brasil, B.S., Dusse, L.M., Barcelos, L.S., Bonjardim, C.A.,

Teixeira, M.M., Sousa, L.P., 2014. Plasmin induces in vivo monocyte recruitment through protease-activated receptor-1-, MEK/ERK-, and CCR2-mediated signaling. J.Immunol. 193, pp. 3654-3663.

Cattaruzza, F., Amadesi, S., Carlsson, J.F., Murphy, J.E., Lyo, V., Kirkwood, K., Cottrell, G.S., Bogyo, M., Knecht, W., Bunnett, N.W., 2014. Serine proteases and protease-activated receptor 2 mediate the proinflammatory and algesic actions of diverse stimulants. Br.J.Pharmacol. 171, pp. 3814-3826.

Caughey, G.H., 2007. Mast cell tryptases and chymases in inflammation and host defense. Immunol.Rev. 217, pp. 141-154.

Chao, J., Shen, B., Gao, L., Xia, C.F., Bledsoe, G., Chao, L., 2010. Tissue kallikrein in cardiovascular, cerebrovascular and renal diseases and skin wound healing. Biol.Chem. 391, pp. 345-355.

Clemetson, K.J., 2012. Platelets and primary haemostasis. Thromb.Res. 129, pp. 220-224.

Collen, D., 1999. The plasminogen (fibrinolytic) system. Thromb.Haemost. 82, pp. 259-270.

Davi, G., Patrono, C., 2007. Platelet activation and atherothrombosis. N.Engl.J.Med. 357, pp. 2482-2494.

Davie, E.W., Fujikawa, K., Kisiel, W., 1991. The coagulation cascade: initiation, maintenance, and regulation. Biochemistry 30, pp. 10363-10370.

de la Fuente, J., Kocan, K.M., 2006. Strategies for development of vaccines for control of ixodid tick species. Parasite Immunol. 28, pp. 275-283.

Fragoso, H., Rad, P.H., Ortiz, M., Rodriguez, M., Redondo, M., Herrera, L., de la Fuente, J., 1998. Protection against *Boophilus annulatus* infestations in cattle vaccinated with the B. microplus Bm86-containing vaccine Gavac. off. Vaccine 16, pp. 1990-1992.

Francischetti, I.M., Sa-Nunes, A., Mans, B.J., Santos, I.M., Ribeiro, J.M., 2009. The role of saliva in tick feeding. Front Biosci.(Landmark.Ed) 14, pp. 2051-2088.

Franta, Z., Frantova, H., Konvickova, J., Horn, M., Sojka, D., Mares, M., Kopacek, P., 2010. Dynamics of digestive proteolytic system during blood feeding of the hard tick *Ixodes ricinus*. Parasit.Vectors. 3, p. 119.

Fullaondo, A., Garcia-Sanchez, S., Sanz-Parra, A., Recio, E., Lee, S.Y., Gubb, D., 2011. Spn1 regulates the GNBP3-dependent Toll signaling pathway in *Drosophila melanogaster*. Mol.Cell Biol. 31, pp. 2960-2972.

Furman, M.I., Liu, L., Benoit, S.E., Becker, R.C., Barnard, M.R., Michelson, A.D., 1998. The cleaved peptide of the thrombin receptor is a strong platelet agonist. Proc.Natl.Acad.Sci.U.S.A 95, pp. 3082-3087.

Gartner, T.K., Williams, D.C., Minion, F.C., Phillips, D.R., 1978. Thrombin-induced platelet aggregation is mediated by a platelet plasma membrane-bound lectin. Science 200, pp. 1281-1283.

Gettins, P.G., 2002. Serpin structure, mechanism, and function. Chem.Rev. 102, pp. 4751-4804.

Guex, N., Peitsch, M.C., 1997. SWISS-MODEL and the Swiss-PdbViewer: an environment for comparative protein modeling. Electrophoresis 18, pp. 2714-2723.

Hallgren, J., Pejler, G., 2006. Biology of mast cell tryptase. An inflammatory mediator. FEBS J. 273, pp. 1871-1895.

Hileman, R.E., Fromm, J.R., Weiler, J.M., Linhardt, R.J., 1998. Glycosaminoglycan-protein interactions: definition of consensus sites in glycosaminoglycan binding proteins. Bioessays 20, pp. 156-167.

Hoffman, M., 2003. A cell-based model of coagulation and the role of factor VIIa. Blood Rev. 17 Suppl 1, p. S1-S5.
Hoffman, M., Monroe, D.M., III, 2001. A cell-based model of hemostasis. Thromb.Haemost. 85, pp. 958-965.

Hoover-Plow, J., 2010. Does plasmin have anticoagulant activity? Vasc.Health Risk Manag. 6, pp. 199-205.

Horn, F., Dos Santos, P.C., Termignoni, C., 2000. *Boophilus microplus* anticoagulant protein: an antithrombin inhibitor isolated from the cattle tick saliva. Arch.Biochem.Biophys. 384, pp. 68-73.

Humphrey, W., Dalke, A., Schulten, K., 1996. VMD: visual molecular dynamics. J.Mol.Graph. 14, pp. 33-38.

Huntington, J.A., Read, R.J., Carrell, R.W., 2000. Structure of a serpin-protease complex shows inhibition by deformation. Nature 407, pp. 923-926.

Ibelli, A.M., Kim, T.K., Hill, C.C., Lewis, L.A., Bakshi, M., Miller, S., Porter, L., Mulenga, A., 2014. A blood meal-induced *Ixodes scapularis* tick saliva serpin inhibits trypsin and thrombin, and interferes with platelet aggregation and blood clotting. Int.J.Parasitol. 44, pp. 369-379.

Irving, J.A., Pike, R.N., Lesk, A.M., Whisstock, J.C., 2000. Phylogeny of the serpin superfamily: implications of patterns of amino acid conservation for structure and function. Genome Res. 10, pp. 1845-1864.

Iwanaga, S., Kawabata, S., Muta, T., 1998. New types of clotting factors and defense molecules found in horseshoe crab hemolymph: their structures and functions. J.Biochem.

Kahn, M.L., Nakanishi-Matsui, M., Shapiro, M.J., Ishihara, H., Coughlin, S.R., 1999. Protease-activated receptors 1 and 4 mediate activation of human platelets by thrombin. J.Clin.Invest 103, pp. 879-887.

Kanost, M.R., 1999. Serine proteinase inhibitors in arthropod immunity. Dev.Comp Immunol. 23, pp. 291-301.

Katada, J., Hayashi, Y., Sato, Y., Muramatsu, M., Takiguchi, Y., Harada, T., Fujiyoshi, T., Uno, I., 1997. A novel peptide motif for platelet fibrinogen receptor recognition. J.Biol.Chem. 272, pp. 7720-7726.

Kessenbrock, K., Dau, T., Jenne, D.E., 2011. Tailor-made inflammation: how neutrophil serine proteases modulate the inflammatory response. J.Mol.Med.(Berl) 89, pp. 23-28.

Kessenbrock, K., Frohlich, L., Sixt, M., Lammermann, T., Pfister, H., Bateman, A., Belaaouaj, A., Ring, J., Ollert, M., Fassler, R., Jenne, D.E., 2008. Proteinase 3 and neutrophil elastase enhance inflammation in mice by inactivating antiinflammatory progranulin. J.Clin.Invest 118, pp. 2438-2447.

Kim, T.K., Curran, J., Mulenga, A., 2014a. Dual silencing of long and short *Amblyomma americanum* acidic chitinase forms weakens the tick cement cone stability. J.Exp.Biol. 217, pp. 3493-3503.

Kim, T.K., Ibelli, A.M., Mulenga, A., 2014b. *Amblyomma americanum* tick calreticulin binds C1q but does not inhibit activation of the classical complement cascade. Ticks.Tick.Borne.Dis. 6, pp. 91-101.

Koci, J., Simo, L., Park, Y., 2013. Validation of internal reference genes for real-time quantitative polymerase chain reaction studies in the tick, *Ixodes scapularis* (Acari: Ixodidae). J.Med.Entomol. 50, pp. 79-84.
Korkmaz, B., Moreau, T., Gauthier, F., 2008. Neutrophil elastase, proteinase 3 and cathepsin G: physicochemical properties, activity and physiopathological functions. Biochimie 90, pp. 227-242.

Lara, F.A., Lins, U., Bechara, G.H., Oliveira, P.L., 2005. Tracing heme in a living cell: hemoglobin degradation and heme traffic in digest cells of the cattle tick *Boophilus microplus*. J.Exp.Biol. 208, pp. 3093-3101.

Larkin, M.A., Blackshields, G., Brown, N.P., Chenna, R., McGettigan, P.A., McWilliam, H., Valentin, F., Wallace, I.M., Wilm, A., Lopez, R., Thompson, J.D., Gibson, T.J., Higgins, D.G., 2007. Clustal W and Clustal X version 2.0. Bioinformatics. 23, pp. 2947-2948.

Li, H.J., Yin, H., Yao, Y.Y., Shen, B., Bader, M., Chao, L., Chao, J., 2007. Tissue kallikrein protects against pressure overload-induced cardiac hypertrophy through kinin B2 receptor and glycogen synthase kinase-3beta activation. Cardiovasc.Res. 73, pp. 130-142.

Li, W., Huntington, J.A., 2008. The heparin binding site of protein C inhibitor is protease-dependent. J.Biol.Chem. 283, pp. 36039-36045.

Li, X., Syrovets, T., Genze, F., Pitterle, K., Oberhuber, A., Orend, K.H., Simmet, T., 2010. Plasmin triggers chemotaxis of monocyte-derived dendritic cells through an Akt2-dependent pathway and promotes a T-helper type-1 response. Arterioscler.Thromb.Vasc.Biol. 30, pp. 582-590.

Li, X., Syrovets, T., Simmet, T., 2012. The serine protease plasmin triggers expression of the CC-chemokine ligand 20 in dendritic cells via Akt/NF-kappaB-dependent pathways. J.Biomed.Biotechnol. 2012, p. 186710.

Livak, K.J., Schmittgen, T.D., 2001. Analysis of relative gene expression data using real-time quantitative PCR and the 2(-Delta Delta C(T)) Method. Methods 25, pp. 402-408.

Mak, P., Pohl, J., Dubin, A., Reed, M.S., Bowers, S.E., Fallon, M.T., Shafer, W.M., 2003. The increased bactericidal activity of a fatty acid-modified synthetic antimicrobial peptide of human cathepsin G correlates with its enhanced capacity to interact with model membranes. Int.J.Antimicrob.Agents 21, pp. 13-19.

Mancek-Keber, M., 2014. Inflammation-mediating proteases: structure, function in (patho) physiology and inhibition. Protein Pept.Lett. 21, pp. 1209-1229.

Matsunaga, Y., Kido, H., Kawaji, K., Kamoshita, K., Katunuma, N., Ogura, T., 1994. Inhibitors of chymotrypsin-like proteases inhibit eosinophil peroxidase release from activated human eosinophils. Arch.Biochem.Biophys. 312, pp. 67-74.

Matsunaga, Y., Shono, M., Takahashi, M., Tsuboi, Y., Ogawa, K., Yamada, T., 2000. Regulation of lymphocyte proliferation by eosinophils via chymotrypsin-like protease activity and adhesion molecule interaction. Br.J.Pharmacol. 130, pp. 1539-1546.

Meyer-Hoffert, U., Rogalski, C., Seifert, S., Schmeling, G., Wingertszahn, J., Proksch, E., Wiedow, O., 2004. Trypsin induces epidermal proliferation and inflammation in murine skin. Exp.Dermatol. 13, pp. 234-241.

Monroe, D.M., Hoffman, M., 2006. What does it take to make the perfect clot? Arterioscler.Thromb.Vasc.Biol. 26, pp. 41-48.

Morris, A.L., MacArthur, M.W., Hutchinson, E.G., Thornton, J.M., 1992. Stereochemical quality of protein structure coordinates. Proteins 12, pp. 345-364.

Mortier, A., Gouwy, M., Van, D.J., Proost, P., 2011. Effect of posttranslational processing on the in vitro and in vivo activity of chemokines. Exp.Cell Res. 317, pp. 642-654.

Mudenda, L., Pierle, S.A., Turse, J.E., Scoles, G.A., Purvine, S.O., Nicora, C.D., Clauss, T.R., Ueti, M.W., Brown, W.C., Brayton, K.A., 2014. Proteomics informed by transcriptomics identifies novel secreted proteins in *Dermacentor andersoni* saliva. Int.J.Parasitol. 44, pp. 1029-1037.

Mulenga, A., Kim, T., Ibelli, A.M., 2013. *Amblyomma americanum* tick saliva serine protease inhibitor 6 is a cross-class inhibitor of serine proteases and papain-like cysteine proteases that delays plasma clotting and inhibits platelet aggregation. Insect Mol.Biol. 22, pp. 306-319.

Mulenga, A., Sugino, M., Nakajim, M., Sugimoto, C., Onuma, M., 2001. Tick-Encoded serine proteinase inhibitors (serpins); potential target antigens for tick vaccine development. J.Vet.Med.Sci. 63, pp. 1063-1069.

Munoz, E.M., Linhardt, R.J., 2004. Heparin-binding domains in vascular biology. Arterioscler.Thromb.Vasc.Biol. 24, pp. 1549-1557.

Nurden, A.T., 2014. Platelet membrane glycoproteins: a historical review. Semin.Thromb.Hemost. 40, pp. 577-584.

Ohlmann, P., Eckly, A., Freund, M., Cazenave, J.P., Offermanns, S., Gachet, C., 2000. ADP induces partial platelet aggregation without shape change and potentiates collagen-induced aggregation in the absence of Galphaq. Blood 96, pp. 2134-2139.

Olszewska-Pazdrak, B., Hart-Vantassell, A., Carney, D.H., 2010. Thrombin peptide TP508 stimulates rapid nitric oxide production in human endothelial cells. J.Vasc.Res. 47, pp. 203-213.

Parizi, L.F., Githaka, N.W., Logullo, C., Konnai, S., Masuda, A., Ohashi, K., Da Silva, V.I., Jr., 2012. The quest for a universal vaccine against ticks: cross-immunity insights. Vet.J. 194, pp. 158-165.

Porter, L., Radulovic, Z., Kim, T., Braz, G.R., Da Silva, V.I., Jr., Mulenga, A., 2015. Bioinformatic analyses of male and female *Amblyomma americanum* tick expressed serine protease inhibitors (serpins). Ticks.Tick.Borne.Dis. 6, pp. 16-30.

Rawlings, N.D., Barrett, A.J., 1994. Families of serine peptidases. Methods Enzymol. 244, pp. 19-61.

Reimers, H.J., Kinlough-Rathbone, R.L., Cazenave, J.P., Senyi, A.F., Hirsh, J., Packham, M.A., Mustard, J.F., 1976. In vitro and in vivo functions of thrombin-treated platelets. Thromb.Haemost. 35, pp. 151-166.

Rein, C.M., Desai, U.R., Church, F.C., 2011. Serpin-glycosaminoglycan interactions. Methods Enzymol. 501, pp. 105-137.

Renesto, P., Chignard, M., 1993. Enhancement of cathepsin G-induced platelet activation by leukocyte elastase: consequence for the neutrophil-mediated platelet activation. Blood 82, pp. 139-144.

Renesto, P., Halbwachs-Mecarelli, L., Nusbaum, P., Lesavre, P., Chignard, M., 1994. Proteinase 3. A neutrophil proteinase with activity on platelets. J.Immunol. 152, pp. 4612-4617.

Roberts, H.R., Hoffman, M., Monroe, D.M., 2006. A cell-based model of thrombin generation. Semin.Thromb.Hemost. 32 Suppl 1, pp. 32-38.

Selak, M.A., Chignard, M., Smith, J.B., 1988. Cathepsin G is a strong platelet agonist released by neutrophils. Biochem.J. 251, pp. 293-299.

Shen, Y., Guo, Y., Du, C., Wilczynska, M., Hellstrom, S., Ny, T., 2012. Mice deficient in urokinase-type plasminogen activator have delayed healing of tympanic membrane perforations. PLoS.One. 7, p. e51303.

Silverman, G.A., Bird, P.I., Carrell, R.W., Church, F.C., Coughlin, P.B., Gettins, P.G., Irving, J.A., Lomas, D.A., Luke, C.J., Moyer, R.W., Pemberton, P.A., Remold-O'Donnell, E., Salvesen, G.S., Travis, J., Whisstock, J.C., 2001. The serpins are an expanding superfamily of structurally similar but functionally diverse proteins. Evolution, mechanism of inhibition, novel functions, and a revised nomenclature. J.Biol.Chem. 276, pp. 33293-33296.

Srinivasan, R., Marchant, R.E., Gupta, A.S., 2010. In vitro and in vivo platelet targeting by cyclic RGD-modified liposomes. J.Biomed.Mater.Res.A 93, pp. 1004-1015.

Syrovets, T., Jendrach, M., Rohwedder, A., Schule, A., Simmet, T., 2001. Plasmin-induced expression of cytokines and tissue factor in human monocytes involves AP-1 and IKKbeta-mediated NF-kappaB activation. Blood 97, pp. 3941-3950.

Tirloni, L., Reck, J., Terra, R.M., Martins, J.R., Mulenga, A., Sherman, N.E., Fox, J.W., Yates, J.R., III, Termignoni, C., Pinto, A.F., Vaz Ida S Jr, 2014. Proteomic analysis of cattle tick *Rhipicephalus (Boophilus) microplus* saliva: a comparison between partially and fully engorged females. PLoS.One. 9, p. e94831.

Unni, S., Huang, Y., Hanson, R.M., Tobias, M., Krishnan, S., Li, W.W., Nielsen, J.E., Baker, N.A., 2011. Web servers and services for electrostatics calculations with APBS and PDB2PQR. J.Comput.Chem. 32, pp. 1488-1491.

Varon, D., Lider, O., Dardik, R., Shenkman, B., Alon, R., Hershkoviz, R., Kapustina, G., Savion, N., Martinowitz, U., Greenspoon, N., 1993. Inhibition of integrin-mediated platelet aggregation, fibrinogen-binding, and interactions with extracellular matrix by nonpeptidic mimetics of Arg-Gly-Asp. Thromb.Haemost. 70, pp. 1030-1036.

Walsh, K.A., Kauffman, D.L., Kumar, K.S., Neurath, H., 1964. On the structure and function of bovine trypsinogen and trypsin. Proc.Natl.Acad.Sci.U.S.A 51, pp. 301-308.

Walsh, P.N., Ahmad, S.S., 2002. Proteases in blood clotting. Essays Biochem. 38, pp. 95-111.

Webb, B., Sali, A., 2014. Comparative Protein Structure Modeling Using MODELLER. Curr.Protoc.Bioinformatics. 47, p. 5.

White, M.J., Glenn, M., Gomer, R.H., 2013. Trypsin potentiates human fibrocyte differentiation. PLoS.One. 8, p. e70795.

Part IB†

Target validation of highly conserved *Amblyomma americanum* tick saliva serine protease inhibitor19

Materials and Methods

Ethics statement

All animal work was conducted and approved according to Texas A&M University Institutional Animal Care and Use Committee (AUP 2011-0207).

Tick feeding, dissection, and protein extractions

A. americanum ticks used in this study were purchased from Oklahoma State University tick laboratory (Stillwater, OK, USA). Ticks were maintained in 85% humidity chamber at 25°C before placing them on rabbits to feed. To feed, *A. americanum* ticks were placed onto the outer portion of the ear of specific pathogen-free (SPF) New Zealand rabbits and restricted in this location using orthopedic stockinettes adhered on the rabbit ear with Kamar Adhesive (Kamar Products Inc., Zionsville, IN, USA). To initiate feeding, 10 male ticks were placed into each ear stocking three days prior to adding 15 female ticks in each ear stocking (total of 30 female ticks per rabbit). To prepare tick protein extracts, five ticks from unfed and manually detached at 24, 72 and 120 h post tick attachment were rinsed in sterile 1X phosphate buffered saline (PBS) pH 7.4 and processed for dissections. Ticks were placed on a sterile glass slide and cut on the extreme anterior, posterior and lateral ends using a sterile razor blade. Tick organs including salivary glands (SG), midguts (MG), synganglion (SYN), Malpighian tubule (MT), ovary (OVR) and the remnants labeled as carcass (CA) were isolated and placed into IP lysis buffer with protease inhibitor

cocktail (Thermo Scientific, Waltham, MA, USA). Protein extracts were homogenized and stored in -80°C.

RNAi silencing of AAS19 mRNA

RNAi-mediated silencing was performed as described (Mulenga et al., 2013, Kim et al., 2014). Double stranded RNA (dsRNA) was synthesized using the Megascript RNAi kit (Thermo Scientific) targeting position 327-971 of AAS19 nucleotide sequence (NCBI Accession# GAYW01000076). The 644 base pair dsRNA target sequence was searched against tick sequences in GenBank to verify specificity. Using 2 μg of purified PCR product as template, dsRNA was synthesized using primers with added T7 promoter sequence in bold (For: 5′-**TAATACGACTCACTATAGGG**GTACGCCCTGGACGTCGCCAACG-3′ and Rev 5′-**TAATACGACTCACTATAGGG**GAGAGGTCGGCGTCAGCGGAG-3′). PCR primers for enhanced green fluorescent protein coding cDNA (EGFP; accession number JQ064510.1) with added T7 promoter sequence (Kim et al., 2014) were used to synthesize control EGFP-dsRNA. Two test groups of 15 female *A. americanum* ticks were injected with 0.5 – 1 μL (~3 μg/μL) EGFP-dsRNA or AAS19-dsRNA in nuclease free water as described (Kim et al., 2014). Injected ticks were kept for 24 h at 25°C in 85% humidity to recover before being placed on SPF New Zealand rabbits to feed.

The effect of AAS19 mRNA disruption on tick feeding success was investigated by assessing tick attachment and mortality rates, time to feed to repletion, engorgement weight (EW) as an index for amount of blood taken in by tick, and egg mass conversion ratio (EMCR) as measure of utilizing blood meal to produce eggs as described. Tick phenotypes during feeding were documented daily using the Canon EOS Rebel XS camera attached to a Canon Ultrasonic EF 100mm 1:2:8 USM Macro Lens (Canon USA Inc., Melville, NY, USA).

Validation of RNAi silencing

Disruption of AAS19 mRNA was verified by quantitative RT-PCR as described (Kim et al., 2014). Three ticks each that were injected with EGFP-dsRNA and AAS19-dsRNA were sampled at 48 h post-attachment by manual detachment. Ticks were processed individually. Tick organs (SG, MG, SYN, MT, OVR, CA) were dissected as described above. Extraction of mRNA using the Dynabead mRNA Direct Kit (Thermo Scientific) were performed following the manufacturer's instructions. The extracted mRNA was quantified using the Infinite M200 Pro plate reader (Tecan, Männedorf, Switzerland). Template cDNA was synthesized from ~200 ng of mRNA using the Verso cDNA Synthesis Kit following the manufacturer's instructions (Thermo Scientific). Approximately 50 ng cDNA and AAS19 forward (5′-GACAAGACGCACGGCAAAA-3′) and reverse (5′-GAAGTCCGGCGGCTCAT- 3′) primers in a final concentration of 900 nM each, were mixed with 2X SYBR Green Master Mix (Thermo Scientific) in triplicates and was subjected to qRT-PCR. For an internal control, *A. americanum* 40S ribosomal protein S4 (accession number GAGD01011247.1) (Koci et al., 2013) was used. Relative quantification (RQ) of AAS19 transcript was determined as described (Kim et al., 2014). AAS19 mRNA suppression was determined using the formula, $S = 100\text{-}(RQ^T/RQ^C \text{ X } 100)$ where S = mRNA suppression, RQ^T and RQ^C = RQ of tissues in AAS19-dsRNA injected and EGFP-dsRNA injected ticks, respectively. Data are presented as the mean (M) AAS19 mRNA suppression ± SEM.

Immunization of rabbits with recombinant (r) AAS19 and tick challenge infestation

SPF New Zealand white rabbits of approximately 10 - 12 weeks of age were immunized with TiterMax Gold adjuvant (Sigma, St. Louis, MO) or 514 μg of rAAS19 antigen in 1X PBS pH

7.4 mixed with an equivalent volume of adjuvant to 1 mL. Expression and purification of the immunizing antigen, rAAS19, in *Pichia pastoris* (X-33) was previously described in Kim et al., (2015a). Two immunizations were administered at days 0 and 30. Rabbits were inoculated subcutaneously and intradermally with ~200 µL of rAAS19: adjuvant or PBS: adjuvant mix into five injection sites. Two weeks after immunization, serum was collected to verify antibody response to rAAS19 by ELISA. Following immunization, rabbits were challenge infested with 40 adult female ticks (20 ticks per ear). In order to determine if repeated tick infestation of animals immunized with recombinant tick saliva proteins such as rAAS19 enhanced anti-tick immunity, rabbits were re-infested with 40 ticks at two weeks after the first infestation. Each rabbit received 20 ticks per ear. The effect(s) of immunization against tick feeding parameters were determined as described in RNAi silencing (section 2.3).

ELISA and western blotting analysis

Routine ELISA and western blotting analysis verified rabbit antibody response to rAAS19. For ELISA, 0.5 µg affinity purified rAAS19 was coated on 96 well plates overnight in coating buffer (0.1M sodium carbonate pH 9.5). Coated wells were subsequently blocked with 300 µL of 5% skim milk in PBS-Tween20 for 1h at room temperature (RT). Following appropriate incubations with pre-immune or immune sera (1:1000 to 1:320000), goat anti-rabbit IgG Horseradish Peroxidase (HRP) conjugated secondary antibody (Millipore, Billerica, MA, USA) and appropriate washes, wells were incubated with 1-Step Ultra TMB ELISA Substrate (Thermo Scientific) for 8 min at RT to detect antibody binding. Adding 2 M sulfuric acid stopped the reaction and OD was determined at A_{450nm} using the Infinite M200 Pro plate reader (Tecan).

To determine if rAAS19 rabbit antisera specifically bound native AAS19, total protein extracts from dissected tick organs were subjected to routine western blotting analyses using

antibodies to rAAS19. Given that the immunizing antigen was glycosylated (Kim et al., 2015a), we investigated if the observed antibody response was directed toward glycans on rAAS19 by including three controls: yeast expressed deglycosylated and non-deglycosylated (Kim et al., 2015a) and bacteria expressed rAAS19 (described below). Samples were loaded and resolved on a 10% SDS-PAGE gel and transferred onto a PVDF membrane. Membranes were blocked overnight at 4ºC in 5% skim milk in PBS-Tween20. Following appropriate incubations with pre-immune or immune sera (1:10,000), the secondary Clean-Blot™ IP Detection Reagent HRP conjugated (1:40) (Thermo Scientific) antibody, and appropriate washes, membranes were incubated in Amersham ECL Prime Western Blotting Detection Reagent for 5 min and exposed on X-ray films for 10 and 30 min before developing films.

Recombinant AAS19 was expressed in bacteria using BL21 (DE3) pLysS *Escherichia coli* strain and the pRSETA plasmid expression system (Thermo Scientific) as previously described (Chalaire et al., 2011). Mature AAS19 protein open reading frame (Porter et al., 2015) was uni-directionally sub-cloned into pRSETA in *BamHI* and *EcoRI* sites using forward (5′-**GGATTC**GCAGAGCCCGACGAAGATGGCCG-3′) and reverse (5′-**GAATTC**TTAGAGGGCGTTAATTTCGCCCAG-3′) primers with added restriction enzyme sites in bold. Bacteria expressed rAAS19 were purified by eluting from PVDF membranes as described in Szewczyk et al. (1998) with slight modifications. To elute the protein off of the PVDF membrane, excised membrane was incubated with elution buffer (1% Triton X-100/2% SDS in 50mM Tris-HCl, pH 9.5) in 0.5 mL tubes for 30 minutes at RT with rapid shaking. Eluted proteins were collected, then transferred into a fresh tube and concentrated by acetone precipitation. Precipitates were re-suspended in 1X PBS pH 7.4.

Statistical analysis

Unpaired student t-test and Mann-Whitney analysis were used to determine if differences between AAS19-dsRNA and EGFP-dsRNA injected ticks were significant. One Way ANOVA and Tukey HSD, Fisher exact and Chi-Square test analyses were used to determine if tick-feeding performance on control and immunized rabbits were significantly different using the Prism 6 software (GraphPad Software, La Jolla, CA, USA). Data are reported as Mean ± SEM.

Results

AAS19 silencing causes tick deformities and reduces tick blood meal size

Figures 1 and 2 demonstrate that AAS19 is important to *A. americanum* tick feeding success as revealed by RNAi silencing analysis. Quantitative RT-PCR indicate that in three randomly sampled ticks, AAS19 mRNA suppression of 95-97%, 67-95%, 17-97%, 26-45%, 0-76%, and 0-12% in SG, MG, SY, MT, OV, and CA, respectively (Fig. 1), was achieved. Spontaneously detached ticks (Fig. 2A) were weighed to determine engorgement weight (EW) as an index for blood meal size. Mean EW of AAS19-dsRNA injected ticks (0.257 ± 0.04g) was ~50% smaller than EGFP-dsRNA injected ticks (0.504 ± 0.054g) with differences being statistically significant ($P < 0.01$) as revealed by unpaired student t-test (Fig. 2B). It is interesting to note that 75% (6/8) of the AAS19-dsRNA injected ticks were deformed (asterisks marked, Fig. 2A).

Native AAS19 protein is present in multiple tick organs

Immunization of rabbits with rAAS19 provoked antibody titers of more than 1:320,000 (not shown). Figure 3A shows that the antibody to rAAS19 specifically bound the

immunizing antigen (glycosylated, lane rY-) and the two controls: yeast expressed deglycosylated (rY+) and bacteria expressed non-glycosylated (rB) forms, indicating that the antibody response may be directed at glycan and/or the protein backbone epitopes. Likewise, in figure 3B we observed a single native AAS19 protein band within the expected size range at below 50 kDa. It is interesting to note that, we detected higher molecular weight diffuse protein bands (asterisks marked), which we suspect could be glycosylated forms of native AAS19. The expected mature AAS19 is 388 amino acids long with 43 kDa calculated molecular weight (Porter et al., 2015). Based on data in figure 3, native AAS19 protein is constitutively present in multiple tick organs (SG, MG, OVR, SYN, CA, MT, and CA). We would like to note here that in figure 3C, serum of the pre-immune control bound some non-specific bands ~60 kDa in MG and CA. Additionally, a non-specific band of ~50 kDa was found in the CA in unfed and 24 h samples, but not in other stages. The serum from rabbit injected with PBS-adjuvant control did not bind anything (Fig. 3D).

Immunization with rAAS19 enhances tick immunity induced by repeated tick infestation

Figure 4 summarizes A_{450nm} $\log^{10}$ of 1:20000 dilutions of immune sera to rAAS19 in tick-infested rabbits: control (filled circle) and immunized rabbits 1 and 2 (filled square and triangle respectively) collected at: (1) pre-immune (2) two weeks after the last immunization, (3) two and (4) four weeks post-first infestation, and (5) two weeks after second infestation. In the control rabbit, antibodies to rAAS19 increased with feeding from background at ~$\log^{10}$ of 0.001 to $\log^{10}$ of more than 0.01 after the second infestation. On the other hand repeated tick infestation of immunized rabbits did not result in increased antibody levels in immunized rabbits. While there was a nearly ten-fold increase between first and second infestations of control rabbits, there was a slight decrease in immunized rabbits after the second infestation (Fig. 4). Comparing data points

five (two weeks after second tick infestation) of control and immunized rabbits, it is apparent that immunization of rabbits with rAAS19 boosted antibody levels to AAS19 by nearly a 100-fold.

Figures 5 and 6 summarize the effects of rAAS19 immunization on *A. americanum* success during the first and second infestations. Immunization of rabbits with rAAS19 caused ticks to feed faster, but obtain smaller blood meal sizes overall (Figs. 5 and 6). In the first infestation, chi-square (and Fisher exact) test indicated that 91% of ticks that completed feeding within 15 days on immunized rabbit (R)1 ($P = 0.0038$) was statistically significant different from 79% of ticks that completed feeding on the control rabbit, while 85% of ticks completed feeding on R2 were apparently faster but not significantly different from the control (solid line) (Fig. 5A). Similarly in the second infestation, the observed 91% and 97% of ticks that completed feeding within 15 days on R1 and R2 respectively were different ($P = 0.0285$ and 0.0244, respectively) from 68% of ticks that completed feeding on the control rabbit (Fig. 5B). Despite feeding faster, ticks that fed on immunized rabbits obtained smaller blood meals as revealed by tick engorgement weight (EW) (Fig. 6). In the first infestation, One Way ANOVA [$F (2, 84) = 11.87$, $P < 0.0001$] and Tukey HSD analysis indicated that R1 Mean EW (599.2 ± 29.26) was not different from the control (607.1 ± 41.18), however R2 ticks were smaller with Mean EW (396.9 ± 30.91) significantly smaller [$P < 0.0002$] (Fig. 6A) than control. In the second infestation both R1 (287.2 ± 28.65 mg) and R2 (311.7 ± 24.27 mg) mean EW are apparently smaller, but not significantly different from control mean EW (336.3 ± 38.71mg) (Fig. 6B). It is notable that in figure 6B EW of ticks that fed on the control rabbit in the second infestation was smaller than the first infestation, which could point to the rabbit becoming resistant due to repeated infestations.

The egg mass of ticks that fed on R2 (134.4 ± 17.71 mg) was significantly lower ($P<0.0001$), whereas R1 (283.4 ± 23.20 mg) was apparently lower but not significantly different

than the control (308.1 ± 280.68 mg) (Fig. 6C), as revealed by Tukey HSD analysis. In the second infestation there were no significant differences in egg weight between all groups (Fig. 6D). The effect of rAA19 immunization on the tick's ability to convert the blood meal to eggs was inconclusive (Figs. 5E and 5F). The egg mass conversion ratio (EMCR) for ticks that fed on R2 (0.314 ± 0.023 mg) was significantly lower ($P<0.0001$) than the control (0.465 ± 0.026 mg) (Fig. 5E), however there was no effect on ticks that fed on R1 in both first and second infestations, and for ticks that fed on R2 in the second infestation (Figs. 6E and 6F).

Data summarized in table 1 show that while immunization did not apparently affect the ability of ticks to lay eggs in the first infestation, significantly more ticks that fed on immunized rabbits failed to lay eggs in the second infestation. Chi-square (Fisher exact) test revealed that the observed 61% ($P = 0.0167$) R1 and 68% ($P = 0.0010$) R2 of ticks that did not lay eggs in the second infestation were significantly higher than the 48% from the control rabbit. Other parameters summarized in table 1 were not different from the control. Although we placed equal numbers of ticks on the control and rAAS19-immunized rabbits, there was a difference in the number of engorged ticks per rabbit. We observed that some engorged ticks were crushed after they detached from the host and before we were able to collect them, which caused the differences in the number of engorged ticks.

Discusssion

We previously reported that AAS19 was a highly conserved serine protease inhibitor (serpin) that was characterized by its functional domain reactive center loop being 100% conserved in ixodid ticks where we could find data (Porter et al., 2015). In another study we showed that AAS19 mRNA was expressed in multiple tick organs, and that native AAS19 was an immunogenic tick saliva protein as indicated by antibodies to replete fed tick saliva proteins specifically binding

yeast expressed rAAS19. Further, we showed that rAAS19 has anti-haemostatic functions and that it is an inhibitor of trypsin-like proteases including five of the eight serine proteases in the blood clotting cascade (Kim et al., 2015a). These earlier findings collectively suggested the potential for AAS19 to regulate important functions in tick feeding success. In this study we confirm that AAS19 plays important roles in tick feeding physiology and overall tick fitness as revealed by the observed deformities and significant reductions in blood meal sizes of AAS19 dsRNA injected ticks. The cause of the observed deformations in AAS19-dsRNA injected ticks is unknown at this point. However, we speculate that uncontrolled activities of a yet unknown host and/or tick derived protease that is under control of AAS19 caused this. Similar to observations in this study, silencing of a serpin in *D.* melanogaster impaired arthropod morphology (Hashimoto et al., 2003). The role of inhibitory serpins is to terminate protease actions beyond what is physiologically allowable. Several lines of research have demonstrated that uncontrolled protease activity do destroy self-tissue, particularly in disease situations (Owen and Campbell, 1999, Nakatani et al., 2001, Straka, 2011). We hypothesize that the protease that is controlled by AAS19 is important to tick physiology, but if left uncontrolled it impairs in biochemical homeostasis, and identifying the AAS19 controlled protease is highly desirable.

The long-term goal of our research is to find target antigens for tick vaccine development. Thus, a goal of this study was to investigate immunogenicity and anti-tick vaccine efficacy rAAS19. The observation that rAAS19 provoked titers of up to 1:320000 confirmed immunogenicity of this antigen. There is evidence that antibodies to glycosylated immunogens such as rAAS19 may predominantly be directed to glycans on the protein, and not the protein backbone (Tellam et al., 1992, Rodriguez-Valle et al., 2001, Eberl et al., 2001, Kariuki et al., 2008). The observation that antibodies to yeast expressed rAAS19, also reacted with bacteria

expressed AAS19 rules this out. Of significant interest to us, the antibody response to rAAS19 also reacted with epitopes on glycosylated and non-glycosylated forms of native AAS19 as revealed by western blotting analysis data. The observation that native AAS19 protein is present in multiple tick organs and the fact that ticks inject this protein into the host during feeding (Kim et al., 2015a) suggests that this protein may function inside the tick and at the tick-feeding site. This observation is not unique to AAS19. Similar characteristics have been observed for multiple other tick saliva proteins including AV422 (Mulenga et al., 2013, Radulovic et al., 2014, Tirloni et al., 2014, 2015), insulin-like growth factor binding protein-related protein 1 (Radulovic et al., 2015), calreticulin (Sanders et al., 1999, Kim et al., 2015b), and tick histamine release factor (Mulenga et al., 2003). Functions of AAS19 in the tick and at the tick-feeding site are not well established other than previously reported anti-haemostatic properties (Kim et al., 2015a). Identifying AAS19 native targets in the tick and the tick-host interface would be the next step to better understand the role(s) of AAS19 in tick feeding physiology.

Trager (1939a, 1939b) observed that repeated infestations with *Dermacentor variabilis* larvae provoked tick-feeding resistance in rabbits (Trager et al., 1939a, 1939b). Over the years several lines of research have attempted to replicate these studies through immunization of animals with crude tick saliva gland protein extracts (Brown et al, 1984, Shapiro et al., 1989, Nyindo et al., 1989, Banerjee et al., 1990, Kovar, 2004, Willadsen, 2006, Narasimhan et al., 2007, Jittapalapong et al., 2008) and since the 1990s with recombinant tick saliva proteins (Tsuda et al., 2001, Mulenga et al., 1999, You, 2005, Dai et al., 2009, Guo et al., 2009). The common practice in tick vaccine efficacy studies is to challenge infests immunized animals once (Tsuda et al., 2001, Mulenga et al., 1999, You, 2005, Dai et al., 2009, Guo et al., 2009, Galay et al., 2014). In this study, a different approach was used. We challenge infested the control and immunized rabbits twice. Given the fact

that AAS19 is injected into animals during tick feeding (Kim et al., 2015a), we reasoned that repeated inoculation of native AAS19 could serve as a booster and enhance protective tick immunity conferred by rAAS19 immunization. It is interesting to note that, although in the first infestation, most tick feeding parameters were not affected except for smaller tick blood meal sizes observed on one of the two rAAS19-immunized rabbits. The effects of immunization in the second infestation were dramatic as ticks that fed on both immunized rabbits were not only smaller but majority of these ticks failed to lay eggs. The implication of this observation is that over time, immunization of animals with rAAS19 could reduce the tick population. The other practical implication could be toward finding ways to immunize wildlife against tick feeding. Traditional immunization protocols that require primary and booster injections are impractical in wildlife because of the difficulty to identify animals that require booster injections. Thus discovery of antigens such as rAAS19 in which tick infestation of immunized animals will serve as a booster will make it practical to deliver anti-tick vaccines to wildlife. In this way we can deliver tick vaccine antigens such as rAAS19 to wildlife once, and subsequent tick infestations will serve as booster and potentially the level of protection increasing with each subsequent infestation. Wildlife is central to both animal and human TBDs epidemiology as wild animals serve both as blood meal sources of vector ticks and reservoirs for TBD agents. For instance, white tailed deer is the major blood meal source for *A. americanum* and *Ixodes scapularis,* the two medically important tick species that transmit 9 of the 14 reportable human TBD agents listed by USA Centers for Disease Control (www.cdc.gov). There is evidence that deer populations were associated with human cases of TBDs in several localities around in the USA (Piesman et al., 1979, Nieto et al., 2012, Raizman et al., 2013, Wiznia et al., 2013, Mays et al., 2014). In the US livestock industry, the threat of *R. microplus* and *R. annulatus* including its vectored deadly *Babesia* cattle parasites have been

eradicated for more than 50 years (Walker, 2011, Giles et al., 2014). Re-establishment of *R. microplus* and *R. annulatus* ticks and their associated parasites are prevalent in Mexico (Lohmeyer et al., 2011; Busch et al., 2014). Re-increasing deer population threatens continued success of preventing *R. microplus* from Mexico establishing in the USA (Lohmeyer et al., 2011, Pound et al., 2010). Deer infested with acaricide resistant ticks from Mexico were found inside the USA border (Busch et al., 2014, Rodriguez-Vivas et al., 2014). Thus finding ways to effectively immunize deer against ticks could make significant contributions toward controlling human TBDs, which encourages the need to develop alternative control methods such as effective anti-tick vaccines.

The expected effect of anti-tick immunization on tick feeding success would be slowing down tick feeding efficiency. It was surprising to note in this study that majority of ticks that fed on the immunized rabbits detached from the host quicker than the control. The implication of ticks that fed on rAAS19 completing to feed at a much faster pace is unknown at the moment. It is notable that despite feeding faster, these ticks were able to oviposit. Unfortunately, we were not able to evaluate the egg hatching to validate if eggs that were laid by ticks that engorged faster were viable. Consistent with previous data (Merino et al., 2011, Almazan et al., 2010), we also observed that antibody titers to rAAS19 increased with tick feeding in control rabbits. In contrast, we observed an interesting phenomenon in rAAS19-immunized rabbits, that antibody titers to rAAS19 dropped following tick infestation before rising back up at four weeks post infestation.

Another interesting observation from our study was that, while RNAi silencing caused morphological deformities in AAS19 dsRNA injected ticks; ticks that engorged on rAAS19-immunized rabbits were normal albeit smaller. The discrepancy of this effect cannot be explained at this point. It is potentially possible that we achieved more suppression of protein function with

RNAi silencing than with antibodies to rAAS19. Given that we used a long, 644 base pair dsRNA, there is a possibility that the observed deformities could also be due to off target effects. In RNAi silencing, off target effects can occur if the target sequence has a match of as little as 11 contiguous nucleotides with another sequence (Qiu et al., 2005, Jackson et al., 2003). However, we believe that the possibility for off target effects is remote in that when subjected to phylogeny analysis with 120 other *A. americanum* serpins, AAS19 amino acid sequence segregated alone (Porter et al., 2015) indicating that this protein did not have a close relative among *A. americanum* serpins. Furthermore, when scanned against tick sequence entries in GenBank, AAS19 dsRNA target sequence did not return matches that were more than 21 nucleic acids long.

In conclusion, this study builds on the biology of AAS19, a uniquely highly conserved tick serpin that likely play yet unknown important roles both in the tick and at the tick-feeding site. Based on tick vaccine efficacy data in this study, rAAS19 is partially protective as a standalone target antigen. However, it represents a potential component of a cocktail tick vaccine antigen. Efforts to test tick vaccine efficacy of rAAS19 in a cocktail antigen mixture are underway.

References

Almazan, C., Lagunes, R., Villar, M., Canales, M., Rosario-Cruz, R., Jongejan, F., de la Fuente, J., 2010. Identification and characterization of Rhipicephalus (Boophilus) microplus candidate protective antigens for the control of cattle tick infestations. Parasitol. Res. 106, 471-479.

Banerjee, D.P., Momin, R.R., Samantaray, S., 1990. Immunization of cattle (Bos indicus X Bos taurus) against Hyalomma anatolicum anatolicum using antigens derived from tick salivary gland extracts. Int. J. Parasitol. 20, 969-972.

Brown, S.J., Shapiro, S.Z., Askenase, P.W., 1984. Characterization of tick antigens inducing host immune resistance. I. Immunization of guinea pigs with Amblyomma americanum-derived salivary gland extracts and identification of an important salivary gland protein antigen with guinea pig anti-tick antibodies. J. Immunol. 133, 3319-3325.

Busch, J.D., Stone, N.E., Nottingham, R., Araya-Anchetta, A., Lewis, J., Hochhalter, C., Giles, J.R., Gruendike, J., Freeman, J., Buckmeier, G., Bodine, D., Duhaime, R., Miller, R.J., Davey, R.B., Olafson, P.U., Scoles, G.A., Wagner, D.M., 2014. Widespread movement of invasive cattle fever ticks (Rhipicephalus microplus) in southern Texas leads to shared local infestations on cattle and deer. Parasit. Vectors 7, 188-3305-7-188.

Chalaire, K.C., Kim, T.K., Garcia-Rodriguez, H., Mulenga, A., 2011. Amblyomma americanum (L.) (Acari: Ixodidae) tick salivary gland serine protease inhibitor (serpin) 6 is secreted into tick saliva during tick feeding. J. Exp. Biol. 214, 665-673.

Dai, J., Wang, P., Adusumilli, S., Booth, C.J., Narasimhan, S., Anguita, J., Fikrig, E., 2009. Antibodies against a tick protein, Salp15, protect mice from the Lyme disease agent. Cell. Host Microbe 6, 482-492.

Eberl, M., Langermans, J.A., Vervenne, R.A., Nyame, A.K., Cummings, R.D., Thomas, A.W., Coulson, P.S., Wilson, R.A., 2001. Antibodies to glycans dominate the host response to schistosome larvae and eggs: is their role protective or subversive? J. Infect. Dis. 183, 1238-1247.

Galay, R.L., Miyata, T., Umemiya-Shirafuji, R., Maeda, H., Kusakisako, K., Tsuji, N., Mochizuki, M., Fujisaki, K., Tanaka, T., 2014. Evaluation and comparison of the potential of two ferritins as anti-tick vaccines against Haemaphysalis longicornis. Parasit. Vectors 7, 482-014-0482-x.

Giles, J.R., Peterson, A.T., Busch, J.D., Olafson, P.U., Scoles, G.A., Davey, R.B., Pound, J.M., Kammlah, D.M., Lohmeyer, K.H., Wagner, D.M., 2014. Invasive potential of cattle fever ticks in the southern United States. Parasit. Vectors 7, 189-3305-7-189.

Guo, X., Booth, C.J., Paley, M.A., Wang, X., DePonte, K., Fikrig, E., Narasimhan, S., Montgomery, R.R., 2009. Inhibition of neutrophil function by two tick salivary proteins. Infect. Immun. 77, 2320-2329.

Hashimoto, C., Kim, D.R., Weiss, L.A., Miller, J.W., Morisato, D., 2003. Spatial regulation of developmental signaling by a serpin. Dev. Cell. 5, 945-950.

Jackson, A.L., Bartz, S.R., Schelter, J., Kobayashi, S.V., Burchard, J., Mao, M., Li, B., Cavet, G., Linsley, P.S., 2003. Expression profiling reveals off-target gene regulation by RNAi. Nat. Biotechnol. 21, 635-637.

Jittapalapong, S., Phichitrasilp, T., Chanphao, H., Rerkamnuychoke, W., Stich, R.W., 2008. Immunization with tick salivary gland extracts. Ann. N. Y. Acad. Sci. 1149, 200-204.

Kariuki, T.M., Farah, I.O., Wilson, R.A., Coulson, P.S., 2008. Antibodies elicited by the secretions from schistosome cercariae and eggs are predominantly against glycan epitopes. Parasite Immunol. 30, 554-562.

Kim, T.K., Curran, J., Mulenga, A., 2014. Dual silencing of long and short Amblyomma americanum acidic chitinase forms weakens the tick cement cone stability. J. Exp. Biol. 217, 3493-3503.

Kim, T.K., Tirloni, L., Radulovic, Z., Lewis, L., Bakshi, M., Hill, C., da Silva Vaz, I.,Jr, Logullo, C., Termignoni, C., Mulenga, A., 2015a. Conserved Amblyomma americanum tick Serpin19, an inhibitor of blood clotting factors Xa and XIa, trypsin and plasmin, has anti-haemostatic functions. Int. J. Parasitol. 45, 613-627.

Kim, T.K., Ibelli, A.M., Mulenga, A., 2015b. Amblyomma americanum tick calreticulin binds C1q but does not inhibit activation of the classical complement cascade. Ticks Tick Borne Dis. 6, 91-101.

Koci, J., Simo, L., Park, Y., 2013. Validation of internal reference genes for real-time quantitative polymerase chain reaction studies in the tick, Ixodes scapularis (Acari: Ixodidae). J. Med. Entomol. 50, 79-84.

Kovar, L., 2004. Tick saliva in anti-tick immunity and pathogen transmission. Folia Microbiol. (Praha) 49, 327-336.

Lohmeyer, K.H., Pound, J.M., May, M.A., Kammlah, D.M., Davey, R.B., 2011. Distribution of Rhipicephalus (Boophilus) microplus and Rhipicephalus (Boophilus) annulatus (Acari: Ixodidae) infestations detected in the United States along the Texas/Mexico border. J. Med. Entomol. 48, 770-774.

Mays, S.E., Hendricks, B.M., Paulsen, D.J., Houston, A.E., Trout Fryxell, R.T., 2014. Prevalence of five tick-borne bacterial genera in adult Ixodes scapularis removed from white-tailed deer in western Tennessee. Parasit. Vectors 7, 473-014-0473-y.

Merino, O., Almazan, C., Canales, M., Villar, M., Moreno-Cid, J.A., Estrada-Pena, A., Kocan, K.M., de la Fuente, J., 2011. Control of Rhipicephalus (Boophilus) microplus infestations by the

combination of subolesin vaccination and tick autocidal control after subolesin gene knockdown in ticks fed on cattle. Vaccine 29, 2248-2254.

Mulenga, A., Kim, T.K., Ibelli, A.M., 2013. Deorphanization and target validation of cross-tick species conserved novel Amblyomma americanum tick saliva protein. Int. J. Parasitol. 43, 439-451.

Mulenga, A., Sugimoto, C., Sako, Y., Ohashi, K., Musoke, A., Shubash, M., Onuma, M., 1999. Molecular characterization of a Haemaphysalis longicornis tick salivary gland-associated 29-kilodalton protein and its effect as a vaccine against tick infestation in rabbits. Infect. Immun. 67, 1652-1658.

Mulenga, A., Macaluso, K.R., Simser, J.A., Azad, A.F., 2003. The American dog tick, Dermacentor variabilis, encodes a functional histamine release factor homolog. Insect Biochem. Mol. Biol. 33, 911-919.

Nakatani, K., Takeshita, S., Tsujimoto, H., Kawamura, Y., Sekine, I., 2001. Inhibitory effect of serine protease inhibitors on neutrophil-mediated endothelial cell injury. J. Leukoc. Biol. 69, 241-247.

Narasimhan, S., Deponte, K., Marcantonio, N., Liang, X., Royce, T.E., Nelson, K.F., Booth, C.J., Koski, B., Anderson, J.F., Kantor, F., Fikrig, E., 2007. Immunity against Ixodes scapularis salivary proteins expressed within 24 hours of attachment thwarts tick feeding and impairs Borrelia transmission. PLoS One 2, e451.

Nieto, N.C., Teglas, M.B., Stewart, K.M., Wasley, T., Wolff, P.L., 2012. Detection of relapsing fever spirochetes (Borrelia hermsii and Borrelia coriaceae) in free-ranging mule deer (Odocoileus hemionus) from Nevada, United States. Vector Borne Zoonotic Dis. 12, 99-105.

Nyindo, M., Essuman, S., Dhadialla, T.S., 1989. Immunization against ticks: use of salivary gland antigens and infestations with Rhipicephalus appendiculatus (Acari: Ixodidae) in rabbits. J. Med. Entomol. 26, 430-434.

Owen, C.A., Campbell, E.J., 1999. The cell biology of leukocyte-mediated proteolysis. J. Leukoc. Biol. 65, 137-150.

Piesman, J., Spielman, A., Etkind, P., Ruebush, T.K.,2nd, Juranek, D.D., 1979. Role of deer in the epizootiology of Babesia microti in Massachusetts, USA. J. Med. Entomol. 15, 537-540.

Porter, L., Radulovic, Z., Kim, T., Braz, G.R., Da Silva Vaz, I.,Jr, Mulenga, A., 2015. Bioinformatic analyses of male and female Amblyomma americanum tick expressed serine protease inhibitors (serpins). Ticks Tick Borne Dis. 6, 16-30.

Pound, J.M., George, J.E., Kammlah, D.M., Lohmeyer, K.H., Davey, R.B., 2010. Evidence for role of white-tailed deer (Artiodactyla: Cervidae) in epizootiology of cattle ticks and southern

cattle ticks (Acari: Ixodidae) in reinfestations along the Texas/Mexico border in south Texas: a review and update. J. Econ. Entomol. 103, 211-218.

Qiu, S., Adema, C.M., Lane, T., 2005. A computational study of off-target effects of RNA interference. Nucleic Acids Res. 33, 1834-1847.

Radulovic, Z.M., Kim, T.K., Porter, L.M., Sze, S.H., Lewis, L., Mulenga, A., 2014. A 24-48 h fed Amblyomma americanum tick saliva immuno-proteome. BMC Genomics 15, 518-2164-15-518.

Radulovic, Z.M., Porter, L.M., Kim, T.K., Bakshi, M., Mulenga, A., 2015. Amblyomma americanum tick saliva insulin-like growth factor binding protein-related protein 1 binds insulin but not insulin-like growth factors. Insect Mol. Biol. 24, 539-550.

Raizman, E.A., Holland, J.D., Shukle, J.T., 2013. White-tailed deer (Odocoileus virginianus) as a potential sentinel for human Lyme disease in Indiana. Zoonoses Public. Health. 60, 227-233.

Rodriguez Valle, M., Montero, C., Machado, H., Joglar, M., de la Fuente, J., Garcia-Garcia, J.C., 2001. The evaluation of yeast derivatives as adjuvants for the immune response to the Bm86 antigen in cattle. BMC Biotechnol. 1, 2.

Rodriguez-Vivas, R.I., Perez-Cogollo, L.C., Rosado-Aguilar, J.A., Ojeda-Chi, M.M., Trinidad-Martinez, I., Miller, R.J., Li, A.Y., de Leon, A.P., Guerrero, F., Klafke, G., 2014. Rhipicephalus (Boophilus) microplus resistant to acaricides and ivermectin in cattle farms of Mexico. Rev. Bras. Parasitol. Vet. 23, 113-122.

Sanders, M.L., Glass, G.E., Nadelman, R.B., Wormser, G.P., Scott, A.L., Raha, S., Ritchie, B.C., Jaworski, D.C., Schwartz, B.S., 1999. Antibody levels to recombinant tick calreticulin increase in humans after exposure to Ixodes scapularis (Say) and are correlated with tick engorgement indices. Am. J. Epidemiol. 149, 777-784.

Shapiro, S.Z., Voigt, W.P., Ellis, J.A., 1989. Acquired resistance to ixodid ticks induced by tick cement antigen. Exp. Appl. Acarol. 7, 33-41.

Straka, M., 2011. Oral manifestations of diabetes mellitus and influences of periodontological treatment on diabetes mellitus. Bratisl. Lek. Listy 112, 416-420.

Szewczyk, B., Pilat, Z., Bienkowska-Szewczyk, K., Summers, D.F., 1998. Elution of glycoproteins from replicas of sodium dodecyl sulfate-polyacrylamide gel electrophoresis gels. Electrophoresis 19, 220-223.

Tellam, R.L., Smith, D., Kemp, D.H., and Willadsen, P., 1992. Vaccination against ticks. Yong, W.K. (Ed.), In Animal Parasite Control Utilizing Biotechnology. CRC Press, Boca Raton, pp. 303.

Tirloni, L., Islam, M.S., Kim, T.K., Diedrich, J.K., Yates, J.R.,3rd, Pinto, A.F., Mulenga, A., You, M.J., Da Silva Vaz, I.,Jr, 2015. Saliva from nymph and adult females of Haemaphysalis longicornis: a proteomic study. Parasit. Vectors 8, 338-015-0918-y.

Tirloni, L., Reck, J., Terra, R.M., Martins, J.R., Mulenga, A., Sherman, N.E., Fox, J.W., Yates, J.R.,3rd, Termignoni, C., Pinto, A.F., Vaz Ida, S.,Jr, 2014. Proteomic analysis of cattle tick Rhipicephalus (Boophilus) microplus saliva: a comparison between partially and fully engorged females. PLoS One 9, e94831.

Trager, W., 1939a. Further observations on acquired immunity to the tick Dermacentor variabilis Say. J. Parasitol. 25, 137-139.

Trager, W., 1939b. Acquired Immunity to Ticks. J. Parasitol 25, 57-81.

Tsuda, A., Mulenga, A., Sugimoto, C., Nakajima, M., Ohashi, K., Onuma, M., 2001. cDNA cloning, characterization and vaccine effect analysis of Haemaphysalis longicornis tick saliva proteins. Vaccine 19, 4287-4296.

Walker, A.R., 2011. Eradication and control of livestock ticks: biological, economic and social perspectives. Parasitology 138, 945-959.

Willadsen, P., 2006. Vaccination against ectoparasites. Parasitology 133 Suppl, S9-S25.

Wiznia, D.H., Christos, P.J., LaBonte, A.M., 2013. The use of deer vehicle accidents as a proxy for measuring the degree of interaction between human and deer populations and its correlation with the incidence rate of Lyme disease. J. Environ. Health 75, 32-39.

You, M.J., 2005. Immunization of mice with recombinant P27/30 protein confers protection against hard tick Haemaphysalis longicornis (Acari: Ixodidae) infestation. J. Vet. Sci. 6, 47-51.

Part II

Amblyomma americanum serpin 41 (AAS41) is a tick salivary anti-inflammatory protein that targets chymase, while its homolog AAS46 is non-functional

Materials and Methods

Ethics statement

All experiments were done according to the animal use protocol approved by Texas A&M University Institutional Animal Care and Use Committee (IACUC# 2018-0001 ([continued from 2014-0310 and 2014-0311]) that meets all federal requirements, as defined in the Animal Welfare Act (AWA), the Public Health Service Policy (PHS), and the Humane Care and Use of Laboratory Animals and the Ethical Committee on Research Animal Care in Universidade Federal do Rio Grande do Sul, Brazil (register number 28371/2015).

Tick feeding, dissections, total RNA extractions, cDNA synthesis, and protein extractions

A. americanum ticks (egg, larva, nymph, and adult) were purchased from the tick laboratory at Oklahoma State University (Stillwater, OK) or obtained from BEI Resources (Manassas, VA, USA). Routinely, ticks were fed on rabbits as previously described (Mulenga et al., 2013, Kim et al., 2014). *A. americanum* ticks were restricted to feed onto the outer part of the ear of New Zealand rabbits with orthopedic stockinette glued with Kamar Adhesive (Kamar Products Inc., Zionsville, IN, USA). Six male ticks were pre-fed for three days prior to introducing 15 female ticks in each of the ear stockinette (total of 30 female ticks per rabbit).

Ticks were collected and dissected as previously described (Mulenga et al., 2013). Five ticks were manually detached every 24 h for five days (24-120 h). Within the first hour of

detachment, tick mouthparts were inspected to remove remnant host tissues and washed in RNase inhibitor diethylpyrocarbonate (DEPC)-treated water to prepare for dissections. Dissected tick organs, salivary glands (SG), midguts (MG), ovary (OV), synganglion (SYN), Malpighian tubules (MT), and carcass (CA, the remnants after removal of other organs) were placed in RNA*later*™ Stablization Solution (Thermo Fisher Scientific) or 1 mL Trizol total RNA extraction reagent (Thermo Fisher Scientific) and stored at -80° C until total RNA extraction.

Total RNA was extracted using the Trizol reagent according to manufacturer's instructions (Thermo Fisher Scientific) and re-suspended in diethyl pyrocarbonate (DEPC) treated water. Total RNA was quantified using a nanodrop plate reader Synergy H1 Hybrid Multi-Mode Microplate Reader (BioTek Instruments Inc., Winooski, VT, USA) and/or the Infinite M200 Pro plate reader (Tecan Group Ltd., Männedorf, Zürich, Switzerland). Up to 1 µg total RNA was used to synthesize cDNA using the Verso cDNA Synthesis Kit (Thermo Fisher Scientific) following the manufacturer's instructions.

To extract native proteins from specified tissues noted above, tissues were placed into sterile 1.5 ml tubes and sheared using fine scissors in IP/Clean Blot Lysis buffer containing protease inhibitor cocktail (Thermo Fisher Scientific). Crude protein extracts from 22 days post-oviposted eggs, and whole immatures (larvae and nymphs), and adult ticks were flash frozen in liquid nitrogen and extracted in 1x PBS (pH 7.4) containing a protease inhibitor cocktail comprised of 1mM phenylmethylsulfonyl fluoride (PMSF), 1mM E-64, 10mM ethylenediaminetetraacetic acid (EDTA), pH 7.4 (Research Products International, Mount Prospect, IL, USA) by crushing using a pestle or shearing using fine scissors. All protein extracts were sonicated on ice at 50% amplitude, centrifuged at 10,000 xg for 30 min at 4°C, and the supernatant was separated and

stored in -80C. The proteins in supernatant fractions were quantified using BCA assay (Thermo Fisher Scientific).

Temporal and spatial quantitative RT-PCR transcription analyses of selected serpins

Transcription analysis was done by two-sep quantitative (q) RT-PCR using Applied Biosystems 7300 Real Time PCR System (Thermo Fisher Scientific) or CFX96 Touch Real-Time PCR Detection System (Bio-Rad Laboratories Inc., Hercules, CA, USA) as previously described (Kim et. al., 2014). Forward (5′-GCAGCGACGACGAAGGCG-3′) and reverse (5′-GCCTGAAGATGTGCGTG-3′) qRT-PCR primers were designed using the Primer3 software (http://bioinfo.ut.ee/primer3-0.4.0/) for AAS41 and 46. The serpin amplicon target size was ~100 base pairs (bp). To verify if primer pairs are specific to these serpins, nucleotide sequences for each primer were subjected to Blastn (https://blast.ncbi.nlm.nih.gov/Blast.cgi) searches against the Ixodidae database. To determine transcript abundance, triplicate pools of cDNA of dissected salivary gland (SG), midgut (MG), and remnant tissues as carcass (CA) of unfed, 24 and 48 h fed (n = 15 ticks per pool), 72 and 96 h fed (n = 10 ticks per pool), and 120 h fed (n = five ticks) were used. Cycling conditions were set to the following: stage one at 50°C for 2 min, stage two at 95°C for 10 min, and stage three contained two steps with 40 cycles of 95°C for 15 s and 55°C for 1 min. Reaction volumes in triplicate contained ten-fold diluted cDNAs that were originally synthesized from 1 μg total RNA, an optimized concentration of 350 nM of forward and reverse selected serpin primers each, and 2x SYBR Green Master Mix (Thermo Fisher Scientific). For internal reference control, a forward (5′-GGCGCCGAGGTGAAGAA-3′) and reverse (5′-CCTTGCCGTCCACCTTGAT-3′) primers targeting of *A. americanum* 40S ribosomal protein S4 (RPS4: accession number GAGD01011247.1) which is stably expressed in *I. scapularis* during

feeding (Koci et al., 2013) was used. Relative quantification (RQ) of selected serpin transcripts was determined using the comparative C_T ($2^{-\Delta\Delta Ct}$) method (Livak and Schmittgen, 2001) and adopted in (Kim et al., 2014). The data were presented as percent mean (M) transcript abundance ± SEM per tissue.

Expression and affinity purification of selected recombinant serpins

Recombinant (r) AAS41 and 46 serpin proteins were expressed using the *Pichia pastoris* and pPICZα plasmid expression system (Thermo Fisher Scientific) as described previously (Mulenga et al., 2013, Kim et al., 2014). The mature protein open reading frame (Porter et al., 2015) was sub-cloned into pPICZα-C using forward (5′-**ATCGAT***G*CAAGAGGAGGACAAGGTGAC-3′) and reverse primers (5′-**GCGGCCGC**TTAGTGGTGGTGGTGGTGGTGAAGATGGTTCACTTGACCCGCGA-3′) with added respective *ClaI* and *NotI* restriction enzymes sites (in bold), an extra nucleotide guanine (italics) to put in-frame with the expression vector in the forward primer, and addition of a hexahistidine tag (underlined) in the reverse primer. The pPICZα C-rAAS41 and 46 expression plasmid was linearized with *PmeI* and electroporated into *Pichia pastoris* X-33 strain (Thermo Fisher Scientific) using ECM600 electroporator (BTX Harvard Apparatus Inc., Holliston, MA, USA) with parameters set to 1.5 kV, 25 μF, and 186 Ω. Transformed colonies were selected on Yeast Extract Peptone Dextrose Medium with Sorbitol (YPDS) agar plates with zeocin (100 μg/μl) incubated at 28°C. Positive transformants were inoculated in buffered glycerol-complex medium (BMGY) and grown overnight at 28°C with shaking (230-250 rpm). Subsequently the cells were used to inoculate buffered methanol-complex medium (BMMY) to A_{600} of 1 after which protein expression was induced by adding methanol to 0.5% final concentration every 24 h for five days.

Recombinant serpin in spent culture media was precipitated by ammonium sulfate saturation (525 g/L of media) with stirring overnight at 4°C. The precipitate was pelleted at 12,000 xg for 1 h at 4°C and re-suspended in and dialyzed against 20 mM Tris-HCl buffer pH 7.4. To verify expression of rAAS41 and 46, western blot analysis was performed using the horseradish peroxidase (HRP)-labeled antibody to the C-terminus hexa-histidine tag (Thermo Fisher Scientific) diluted to 1:5000 in 5% blocking buffer (5% skim milk powder in PBS w/Tween-20). The positive signal was detected using the chromogenic Metal Enhanced DAB Substrate Kit (Thermo Fisher Scientific) or Amersham ECL Prime Western Blotting Chemiluminescent Reagent (GE Healthcare Bio-Sciences, Pittsburgh, PA, USA). For chemiluminescent detection, the ChemiDoc Imaging System was used (Bio-rad). A negative control of pPICZα-C was included under same procedures. Subsequently, rAAS41 and 46 were affinity purified under native conditions using Hi-Trap Chelating HP Columns (GE Healthcare Bio-Sciences). Affinity purified putative rAAS41 and 46 were dialyzed against 20 mM Tris-HCl buffer pH 7.4 for downstream assays. To verify purity and background contamination, affinity purified rAAS41 and 46 were resolved on a 10% SDS-PAGE gel and silver stained. Samples with least background were selected and concentrated by centrifugation using Microsep Advance Centrifugal Concentration Devices with Omega Membrane at 10 kDa molecular weight cut-off (Pall Corporation, Port Washington, NY, USA).

Prediction and detection of post-translational glycosylation

Post-translational glycosylation in eukaryotes is involved in promoting protein folding and improves protein stability thereby serving in biological functions. Amino acid sequences of AAS41 and 46 were scanned for potential N-linked and O-linked glycosylation sites using the software NetNGlyc 1.0 Server (http://www.cbs.dtu.dk/services/NetNGlyc/) and NetOGlyc 4.0

Server (http://www.cbs.dtu.dk/services/NetOGlyc/), respectively. Analyzing rAAS41 and rAAS46 amino acid sequences, both showed three N-linked and six O-linked glycoslyation sites, therefore they were treated with protein deglycosylation enzyme mix according to manufacturer's instructions (New England Biolabs, Ipswich, MA, USA). Deglycosylation was verified by western blotting analysis using the antibody to C-terminus hexa histidine-tag (Thermo Fisher Scientific) and the positive signal detected using HRP chromogenic substrate (Thermo Fisher Scientific).

Validate if selected native serpins are injected into the host during tick feeding

To confirm that AAS41 and 46 identified from the *A. americanum* saliva proteomic data (chapter II) are secreted in saliva during feeding, native tick protein extracts were subjected to western blot analyses using antibodies to TSPs from rabbits that were repeatedly infested with *A. americanum* females until replete feeding (Mulenga et al., 2013). To reduce background binding, monospecific antibodies to candidate recombinant serpins using cyanogen bromide-activated-Sepharose 4B (Sigma-Aldrich Corp.) were used under manufacturer's instructions with some modifications. Recombinant AAS41 or 46 were bound to the cyanogen bromide-activated-Sepharose 4B (Sigma-Aldrich Corp.). Subsequently, rabbit antibodies to replete-fed tick saliva proteins were reacted with the rAAS41 or 46 bound on the matrix. After appropriate incubations and washing, bound monospecific antibodies were eluted with 0.1 M Glycine buffer (pH 2.4) and immediately neutralized with 1M Tris. Neutralized monospecific antibodies were dialyzed in 1x PBS pH 7.4 and stored at -80°C until use. The quality of the mono-specific antibodies was confirmed by western blotting analysis against rAAS41 and rAAS46.

To determine if native AAS41 and AAS46 are present in different tick live stages, three micrograms of total tick protein extracts from eggs, larvae, nymphs and adults (male and female)

were resolved by 10% SDS-PAGE and transferred on a PVDF membrane. Likewise, native tick protein samples extracted from salivary glands (SG), midguts (MG) and carcass (remnants after SG and MG were removed) from adult females were resolved by 10% SDS-PAGE and transferred on a PVDF membrane. Membranes were exposed to monospecific antibodies to rAAS41 and rAAS46 (1 mg/ml) at 1:500 dilution or pre-immune serum as controls, for 1 h at RT and washed using 1x PBS Tween-20. A secondary IP Clean Blot anti-rabbit IgG-HRP conjugated antibody (Thermo Fisher Scientific) was used to expose membranes for 1 h, and after appropriate washes with 1x PBS Tween-20, membranes were developed using Amersham ECL Prime Western Blotting Chemiluminescent Reagent (GE Healthcare Bio-Sciences). The bands were visualized using the ChemiDoc Imaging System (Bio-rad). Deglycosylated and glycosylated forms of rAAS41 and rAAS46 were included as controls using monospecific antibodies to rAAS41 and rAAS46 (1 mg/ml) at 1:2000 dilution.

To determine if AAS41 and AAS46 elicits an immune response in animals, rAAS41 and rAAS46 were first deglycosylated to expose antibodies to the mature protein backbone. Both deglycosylated and glysoylated protein samples were resolved by 10% SDS-PAGE, and then transferred to a PVDF membrane to screen by western blot analysis using serum from rabbits that had been repeatedly infested with *A. americanum* adult ticks every 24 or 48h and replete feeding (Radulovic et al., 2014, Mulenga et al., 2013). To determine if AAS41 and AAS46 homolog is present in *I. scapularis*, both deglycosylated and glycosylated rAAS41 and rAAS46 were screened with serum from repeatedly infested *I. scapularis* adults that fed until repletion or replete fed uninfected and *Borrelia burgdorferi* senu stricto infected nymphs (available in lab). All western blots included a pre-immune serum control.

Protease inhibitor (PI) profiling of selected rSerpins

Inhibitory activity of rAAS41 and rAAS46 were tested against a panel of commercially available mammalian serine proteases related to host defense pathways against tick feeding and substrate listed in Table 1.

Given that the commericially purchased human chymase is a recombinant protein expressed in *Pichia pastoris*, we wanted to explore other sources for native chymase. Therefore, mouse and rat native chymase were extracted from peritoneal cells containing mast cells (source of chymase) from sentinel animals provided by Texas A&M University, Comparative Medicine Program (CMP), Laboratory Animal Research and Resources (LARR) facility. To obtain the peritoneal cells, animals were first euthanized according to American Veterinary Medical Association (AVMA) Guidelines for the Euthanasia of Animals, and sterilized by dipping into 70% ethanol. Using sterile scissors and forceps, the outer skin of the peritoneum was excised and gently pulled back to expose the inner skin lining (the peritoneal cavity). A 25 ml volume of ice-cold 1x PBS pH 7.4 was injected using a 27-gauge needle and syringe into the peritoneal cavity and gently massaged the peritoneum to release any attached cells into the PBS solution. Using a 25-gauge needle and syringe, the peritoneal fluids were collected and centrifuged at 400 xg for 8 min at 4°C to obtain the cells (pellet). The cells were resuspended in 20 mM Tris-HCl, 1.5M, NaCl pH7.4 (binding buffer), disrupted by sonication (50% amplitude), and centrifuged at 12,000 xg for 15 min at 4°C to obtain the supernatant containing mast cell proteases, including chymase. To purify chymase from the supernatant, a Benzamidine sepharose 4 Fast Flow HiTrap Benzamindine FF column (GE Healthcare Bio-Sciences) was used according to the manufacturer's instructions. The column was equilibriated using the binding buffer and the supernatant was passed through the column. The column was washed up to 15 different fractions using 5 column volumes of the

binding buffer, and eluted up to 10 different fractions using 1 column volume of 0.1 M glycine-HCl pH 2.4, which was immediately neutralized with 1M Tris to a final pH of 7.4. The eluted chymase fractions were verified by silver stain and pure fractions were pooled together and dialyzed in 20 mM Tris-HCl, 150 mM NaCl, pH 7.4 reaction buffer. The BCA quantification assay (Thermo Fisher Scientific) was used to determine the final protein concentration and samples were stored at -80°C until use.

Reagents were mixed at room temperature in triplicate. One µM of rAAS41 or rAAS46 were pre-incubated with optimized amounts of the enzyme for 15 minutes at 37°C in 20 mM Tris-HCl, 150 mM NaCl, BSA 0.1%, pH 7.4 buffer. The corresponding substrate (200 µM) for each enzyme was added in a 100 µL final reaction volume and substrate hydrolysis was measured at A_{405nm} every 11s for 30 min at 30ºC using the Synergy H1 Hybrid Multi-Mode Microplate Reader (BioTek Instruments Inc.). Acquired A_{405nm} data was subjected to one phase decay analysis in Prism 6 software (GraphPad Software, La Jolla, CA, USA) to determine plateau values as proxy for initial velocity of substrate hydrolysis (V_{max}) or residual enzyme activity. The percent enzyme activity inhibition level was determined using the formula: $100 - \left(\frac{\text{Vmax(Vi)}}{\text{Vmax (V0)}} * 100\right)$ where V_{max} (V_i) = activity in presence of rSerpin, and V_{max} (V_0) = activity in absence of rSerpin. Data were presented as mean ± SEM of triplicate readings.

Stoichiometry of inhibition (SI)

The stoichiometry of inhibition (SI) indices was determined for human chymase and pancreatic bovine α-chymotrypsin to rAAS41 (protease:rSerpin) combinations as they were inhibited by more than 80% in the PI profiling assay above. Different molar ratios of rAAS41:protease ranging from 0:1, 0.625:1, 1.25:1, 2.5:1, 5:1, and 10:1 were pre-incubated for 1

hour with constant concentration of a protease. The residual enzyme activity was measured using colorimetric substrates specific for each enzyme as described above. The data were plotted as the residual activity ($\frac{Vi}{V0}$) versus the inhibitor to enzyme molar ratio. SI or the molar ratio of rAAS41:protease when enzyme activity is completely inhibited was determined by fitting data onto the linear regression line in Prism 6 software (GraphPad). The SI for rAAS46 was not determined, as PI profiling did not show inhibition above 80%.

rSerpins and protease complex formation

To determine if the rAAS41 forms a heat- and detergent-stable irreversible complex with its target protease, affinity purified rSerpin (in varying molar ratios indicated for SI assay above) was incubated with human chymase or pancreatic bovine α-chymotrypsin in Tris-HCl reaction buffer (20 mM Tris-HCl, 150 mM, NaCl, pH 7.4) for 1 hour at 37°C. Samples were then deglycosylated (noted above) and denaturing sample buffer was added to the reaction mix, and incubated at 99.9°C for 5 min in a thermal cycler. Samples were subjected to SDS-PAGE electrophoresis on a 12.5% acrylamide gel and stained with silver stain using routine protocols. The complex formation assay was not performed for rAAS46, as PI profiling did not show inhibition above 80%.

Anti-platelet aggregation function of rSerpin

Anti-platelet aggregation function(s) of rAAS41 or rAAS46 were determined using platelet rich plasma (PRP) isolated from citrated (acid citrate dextrose) whole bovine blood (WBBL) as previously described (Horn et al., 2000, Berger et al., 2010). To prepare PRP, fresh citrated WBBL was centrifuged at 200 xg for 20 min at 18°C. Subsequently the PRP (top layer) was transferred

into a new tube and centrifuged at 800 xg for 20 min at 18°C. The pellet containing platelets was washed and diluted with ice cold Tyrode buffer pH 7.4 (137mM NaCl, 2.7mM KCl, 12mM $NaHCO_3$, 0.42mM Na_2HPO_4, 1mM $MgCl_2$, 0.1% glucose, 0.25% BSA) until a spectrophotometric reading of A_{650} = 0.15 was achieved, which accounts for sufficient number of platelets for this assay. To determine anti-platelet aggregation function, various amounts of rSerpin (1, 0.5, 0.25, and 0 μM) were pre-incubated for 15 min at 37°C with agonist thrombin, ADP, or cathepsin G in a 50 μL reaction. The addition of 100 μL of pre-warmed PRP triggered the platelet aggregation. Vice versa PRP was pre-incubated with various amounts of rSerpin prior to addition of the agonist. Platelet aggregation was monitored every 20 seconds over 30 min at A_{650nm} using the Infinite M200 Pro plate reader (Tecan Group Ltd.) or Synergy H1 Hybrid Multi-Mode Microplate Reader (BioTek Instruments Inc.). In this assay, higher optical density (OD) was observed in the blank (platelet only), and increased platelet aggregation was correlated with reduction in the OD. To determine percent platelet aggregation inhibition, OD data were fit to the one phase decay equation in Prism 6 (GraphPad) to determine plateau OD. The percent reduction in platelet aggregation was calculated using this formula: $Y = 100 - (\frac{\Delta Pn}{\Delta PC})*100$, where Y = percent reduction in platelet aggregation, ΔPn= rSerpin treated plateau OD, and ΔPC = positive control plateau OD subtracted from blank plateau OD. Data were presented as mean ± SEM of duplicate platelet aggregation assays.

Anti-blood clotting function of rSerpin

The effect of rAAS41 and rAAS46 against blood clotting was assessed using modified recalcification time (RCT), activated partial thromboplastin time (aPTT), thrombin time (TT), and prothrombin time (PT) to respectively measure the effect on the entire blood cascade, the intrinsic,

extrinsic, and common blood clotting activation pathways as described (Nazareth et al., 2006, Liao et al., 2009, Mulenga et al., 2013). All assays were done in duplicate, with clotting time monitored at A_{650nm} using the Infinite M200Pro plate reader (Tecan Group Ltd.) or Synergy H1 Hybrid Multi-Mode Microplate Reader (BioTek Instruments Inc.) set to 37°C. In these assays, clot formation was directly proportional to increase in OD, and results were presented as mean ± SEM. It is expected that plasma clotting will increase the turbidity in the reaction mix, which will increase the A_{650nm} values, indicating the light path resistance.

In the RCT assay, 50 μL of universal coagulation reference human plasma [UCRP] (Thermo Fisher Scientific) was pre-incubated with 10, 5, 1.25, 0.625, or 0 μM rSerpin in 90 μL Tris-HCl reaction buffer (20 mM Tris-HCl, 150 mM NaCl, pH 7.4) for 15 min at 37°C. Adding 10 μL of pre-warmed 150 mM calcium chloride ($CaCl_2$) triggered plasma clotting. Plasma clotting was monitored at every 20 s for 30 min at A_{650nm} using the Infinite M200Pro plate reader (Tecan Group Ltd.) or Synergy H1 Hybrid Multi-Mode Microplate Reader (BioTek Instruments Inc.) set to 37°C.

In the aPTT assay, various amounts of rSerpin (indicated above) were pre-incubated for 15 min at 37°C with 50 μL UCRP diluted to 100 μL with 20 mM Tris-HCl, 150 mM NaCl, pH 7.4. Subsequently, 50 μL of the aPTT reagent (Thermo Fisher Scientific) was added to plasma and incubated at 37°C for an additional 5 min to activate the reaction. Adding 50 μL 25 mM $CaCl_2$ to the reaction triggered clotting. The clot formation was monitored every 10 s for 5 min at A_{650nm} using the Infinite M200Pro plate reader (Tecan Group Ltd.) or Synergy H1 Hybrid Multi-Mode Microplate Reader (BioTek Instruments Inc.) set to 37°C.

In the TT assay, various amounts of rSerpin (indicated above) were pre-incubated at 37°C for 15 min with 25 μL of the TT reagent (Thermo Fisher Scientific) containing $CaCl_2$ in 50 μL

Tris-HCl reaction buffer with (20 mM Tris-HCl, 150 mM NaCl, pH 7.4). Adding 50 μL of pre-warmed UCRP started plasma clotting. The clotting time was monitored every 10 s for 5 min at A_{650nm} using the Infinite M200Pro plate reader (Tecan Group Ltd.) or Synergy H1 Hybrid Multi-Mode Microplate Reader (BioTek Instruments Inc.) set to 37°C.

In the PT assay, various rSerpin amounts as above were pre-incubated at 37°C for 15 min with 100 μL PT reagent (Thermo Fisher Scientific) containing $CaCl_2$ diluted up to 150 μL with 20 mM Tris-HCl, 150 mM NaCl, pH 7.4 reaction buffer. Adding 50 μL of the pre-warmed UCRP (Thermo Fisher Scientific) triggered plasma clotting. The clotting time was monitored every 10 s for 5 min at A_{650nm} using the Infinite M200Pro plate reader (Tecan Group Ltd.) or Synergy H1 Hybrid Multi-Mode Microplate Reader (BioTek Instruments Inc.) set to 37°C.

Paw edema and vascular permeability assay

Adult male Wistar rats were supplied by the Central Animal Facility (CREAL), Universidade Federal do Rio Grande do Sul, UFRGS, Brazil. Rats were housed in plastic cages (4 rats per cage) within a temperature-controlled room (22–23°C, on a 12 h light/dark cycle) and had free access to water and food. For paw edema assay, compound 48/80-induced rat paw edema models were used to investigate the potential anti-inflammatory role of rAAS41 as described in Landucci et al., (1995) with slight modifications. Paw volume was measured using a digital plethysmometer (Insight, Ribeirão Preto, SP, Brazil). Before paw volume measurement, the rat paw was marked at the ankle to immerse the rat paw at the same point for plethysmometer readings. Subsequently, 50 μL of compound 48/80 (1 μg total in saline) was administered by intraplantar injection in the right paw in the absence or presence of endotoxin-free rAAS41 (25 μg per paw in saline). The left paw was used as a control and received the same volume of saline. As a control,

each group of rats received the same volume of saline (vehicle) in the presence of serpin only (25 µg per paw). As an index of edema formation, paw volume (in millimeters) was measured at 0, 30, 60 and 120 min. The density of the paw was measured by reading the plethysmometer volume in triplicates. The increase in paw volume was calculated by subtracting the average volume of the right paw by the average volume of the left paw at each time point.

The vascular permeability assay was performed as described in Muller et al. (2009). Male Wistar rats (weighting between 250 – 400 g) were anesthetized with intraperitoneal injection of xylazine (10 mg/kg) and ketamine (75 mg/kg). Under anesthesia, rats were injected intravenously (tail vein) with 700 µL of Evans blue dye (50 mg/kg in saline). After 5 min, rats were injected intradermally on the dorsal region (100 µL final volume) with: (i) saline, (ii) 1 µg of compound 48/80 in saline, (iii) 1 µg of compound 48/80 coinjected with 25 µg of rAAS41 in saline, or (iv) 25 µg of rAAS41 in saline. Two spots of each treatment were performed per animal (n=6; 12 spots per treatment). After 60 min, animals were euthanized and an area of skin that included the entire injection sites was carefully removed and photographed. Evans blue dye spots on visible in the skin injection sites were excised and the dye was extracted incubating the skin with 2.5 mL of 50% formamide for 24 h at 55°C. After centrifugation at 1500 xg for 10 min, the absorbance of the supernatant was measured at 620 nm using a spectrophotometer. Unpaired t-test was used for statistical analysis in which $p \leq 0.05$ was considered statistically significant.

RNAi silencing of selected serpins mRNA

RNAi-mediated silencing was performed for AAS41 and AAS46 tick salivary serpins as previously described (Mulenga et al., 2013, Kim et al., 2014). Multiple sequence alignments of AAS41 and AAS46 showed more than 97% identities at the nucleotide and amino acid levels.

Therefore, primers were designed to synthesize double stranded RNA (dsRNA) that targeted both AAS41 and AAS46, referred here to as AAS41/46. To synthesize dsRNA, the Megascript RNAi kit (Thermo Fisher Scientific) was used according to manufacturer's instructions. The dsRNA target sequence was searched against tick sequences in GenBank to verify specificity. Using 2 μg of purified PCR product as template, dsRNA was synthesized for each specific serpin using forward (5′-**TAATACGACTCACTATAGGG**CTGCACGAGACTCTGGGTTA-3′) and reverse (5′-**TAATACGACTCACTATAGGG**GGTAGACGTGGACATGATGC-3′) primers with added T7 promoter sequence (in bold). PCR primers for an unrelated tick gene, enhanced green fluorescent protein coding cDNA (EGFP: accession number JQ064510.1) with added T7 promoter sequence (Kim et al., 2014) were used to synthesize the control EGFP-dsRNA. Due to the high transcript expression of AAS41/46 determined by qRT-PCR, a strategy to deplete AAS41/46 mRNA was performed. Three adult *A. americanum* ticks were injected with 0.5 – 1 μL (~3 μg/μL) EGFP-dsRNA or AAS41/46-dsRNA as described (Kim et al., 2014), including a non-injected control and incubated for up to 3 weeks at 25°C with >85% humidity. Total RNA from individual ticks were extracted using Trizol methods and 1 μg was used for cDNA synthesis to determine the levels of AAS41/46 transcripts depleted after day 3, and 1, 2, and 3 weeks post-injections by qualitative PCR analysis using the primers for recombinant protein expression noted above.

For RNAi studies, two test groups of 15 female *A. americanum* ticks were injected with 0.5 – 1 μL (~3 μg/μL) EGFP-dsRNA or AAS41/46-dsRNA in nuclease free water as described above. Injected ticks were kept at 25°C with >85% humidity for three weeks and then placed on SPF New Zealand white rabbits to feed. The effect(s) of selected serpins mRNA disruption on tick feeding success was investigated by assessing tick attachment and mortality rates, time to feed to repletion, engorgement weight (EW) as an index for amount of blood taken in by tick, and egg

mass conversion ratio (EMCR) as measure of utilizing blood meal to produce eggs as described (Kim et al., 2014). Tick phenotypes during feeding were documented daily using the Canon EOS Rebel XS camera attached to a Canon Ultrasonic EF 100mm 1:2:8 USM Macro Lens (Canon USA Inc., Melville, NY, USA).

Validation of RNAi silencing

Disruption of AAS41/46 mRNA was verified by quantitative (q) RT-PCR as described (Kim et al., 2014). Three ticks that were injected with the control EGFP-dsRNA or AAS41/46-dsRNA were manually detached from the rabbit ears 72 h post-attachment. Ticks were processed individually for single tick analysis as opposed to pooling tick due to the limitation of dsRNA delivery in that although the same volume of dsRNA is delivered, not all ticks will obtain the same amount as there is some leakage of fluids during injections. Tick organs (SG, MG, SYN, MT, OVR, CA) were dissected as described above. Extraction of mRNA using the Dynabead mRNA Direct Kit (Thermo Fisher Scientific) were performed following the manufacturer's instructions. The extracted mRNA was quantified using the Infinite M200 Pro plate reader (Tecan Group Ltd.) or Synergy H1 Hybrid Multi-Mode Microplate Reader (BioTek Instruments Inc.). Template cDNA was synthesized from ~200 ng of mRNA using the Verso cDNA Synthesis Kit following the manufacturer's instructions (Thermo Fisher Scientific). Approximately 10-fold diluted cDNA and AAS41/46 350nM forward and reverse primers each from qRT-PCR (above) were mixed with 2X SYBR Green Master Mix (Thermo Fisher Scientific) in triplicates and were subjected to qRT-PCR. For an internal control, *A. americanum* 40S ribosomal protein S4 (accession number GAGD01011247.1) (Koci et al., 2013) was used. Relative quantification (RQ) of selected serpin transcripts was determined as described (Kim et al., 2014). Selected serpins mRNA suppression

was determined using the formula, $S = 100 - (\frac{RQT}{RQC} * 100)$ where S = mRNA suppression, *RQT* and *RQC* = RQ of tissues in selected serpin-dsRNA injected and EGFP-dsRNA injected ticks, respectively. Data was presented as the mean (M) of selected serpin mRNA suppression ± SEM.

Statistical analysis

Statistical software packages in PRISM version 6 (GraphPad Software Inc.) were used. Unpaired student t-test and Mann-Whitney analysis were used to determine if differences between AAS41/46-dsRNA and EGFP-dsRNA injected ticks are significant.

Results

A. americanum serpin (AAS) 41/46 are highly expressed in unfed and 24 h fed ticks

A. americanum serpins (AAS) 41 and 46 are nearly identical with differences restricted within the functional reactive center loop domain (Fig. 1). We initially identified AAS46 from our "In-Gel" digestion approach (part of Chapter II); we identified AAS41 in the process of constructing the expression plasmid for recombinant (r)AAS46. At the time of expression analysis, qRT-PCR primers were designed for AAS46, but we subsequently found that we targeted both AAS46 and AAS41. For this reason, the expression analysis in Figure 2 is likely for both AAS41 and AAS46 (AAS41/46).

Results from qRT-PCR analysis show that AAS41/46 mRNA is highly transcribed in salivary glands (SG), midguts (MG), and carcass (CA, tissue remnant after removal of SG and MG) of unfed ticks followed by fed ticks (Fig. 2A). We would like to advise the reader to note units on the Y-axis indicate the fold change in relative expression levels for AAS41/46 mRNA compared to the 120 h time point (as the calibrator), where the transcript expression levels were

the lowest. Figures 2A1, 2A2, and 2A3 show that AAS41/46 in the unfed tick the expression levels are up to 35-fold higher in the SG, 12-fold in MG, and 70-fold in CA compared to the 120 h time point. During feeding (24h -96 h) the transcript is reduced, showing up to 5-fold in SG, 4-fold in MG, and 10-fold in CA, compared to the 120 h time point.

Figure 2B summarizes native AAS41/AAS46 protein expression pattern during in unfed and partially fed ticks. We had previously determined proteomes of unfed ticks that were not stimulated to feed (taken from incubator), those that were stimulated to start feeding on rabbits, dogs, and humans (Tirloni et al., 2017), and those that had fed on rabbits (Chapter II of this dissertation). Inspecting the normalized spectral abundance factors (NSAF, index for relative protein abundance) in saliva proteomes revealed that AAS41/46 protein levels were enhanced when ticks were stimulated to start feeding on any host, and were expressed at high levels during the first three days of feeding and subsequently reduced with feeding (Fig. 2B).

Recombinant AAS41 and AAS46 are expressed as glycoproteins and present in major tick organs and all life stages

We successfully expressed and affinity purified both recombinant (r)AAS41 and rAAS46 in *Pichia pastoris* (Figs. 3A and 3B, respectively). The calculated molecular weight of both rAAS41 and rAAS46 with an added fusion tag was around 46 kDa. However, both recombinant proteins migrated at around 50 kDa. Amino acid sequence analysis predicted that both rAAS41 and rAAS46 have three N-linked and six O-linked glycosylsation sites. When treated with glycosidases, rAAS41 migrated lower than non-treated controls confirming that the observed high molecular weight was due to glycosylation (Fig. 3C).

Monospecific IgG antibodies to rAAS41/46 were purified and the quality and specificity was confirmed by western blot analysis that showed to be directed at both the deglycosylated and glycosylated forms or rAAS41 and rAAS46 (Fig. 3D). Consistent with the saliva proteome data (Chapter II), AAS41/46 appear to be most abundant in all tick tissues (SG, MG, and CA) in the unfed stage and decreases with feeding (Figs. 3E, 3F, and 3G). Using the purified rAAS41/46 monospecific antibody, western blot analyses of native proteins from egg, larvae, nymphs and adults (male and female) show binding between the 37 and 50 kDa molecular weight ladder (~45 kDa), which is the expected size of the mature rAAS41/46 (Fig. 3H). This indicates that native AAS41/46 are present in all life stages with higher abundance in the adult stages (Fig. 3H). Pre-immune controls show no binding to rAAS41/46 or native AAS41/46 in tick tissues and life stages (Figs. 3I, 3J, 3K, 3L, and 3M).

A. americanum rAAS41 and rAAS46 are immunogenic and cross-react to serum of rabbits repeatedly infested with Ixodes scapularis

Given that rAAS41 and rAAS46 are secreted in saliva, we determined if these serpins were immunogenic. Figure 4 shows that affinity purified rAAS41 and rAAS46 that were treated with deglycosylation enzyme mix (+) or without treatment (-), both bound to antibodies to tick saliva proteins from serum of rabbits that were repeatedly infested with *A. americanum* ticks for 24 h (Fig. 4A), 48 h (Fig. 4B), replete fed (Fig. 4C), but not pre-immune serum control (Fig. 4D) at 1:500 dilution. Likewise, both deglycosylated and glycosylated rAAS41 and rAAS46 are recognized by antibodies to tick saliva proteins from serum of rabbits that were repeatedly infested with *I. scapularis* tick adults replete fed (Fig. 4E), replete fed nymphs (Fig. 4F), replete fed nymphs that were infected with *Borrelia burgdorferi* sensu stricto (Fig. 4G), but not pre-immune serum

control (Fig. 4H) at 1:50 dilution. It is interesting to note that when screening with antibodies to 24 h, 48 h or replete fed *A. americanum* tick feeding, all the deglycosylated forms provided a band signal at ~46 kDa, indicating the detection of the expected mature protein molecular weight. However, when screening with rabbit serum to *I. scapularis*, only the serum to one-time fed *I. scapularis* nymphs that were infected with *B. burgdorferi* recognized the deglycosylated rAAS41 and rAAS46. On the contrary, the rabbit serum from rabbits that were repeatedly infested with uninfected nymphs and adults bound to the glycosylated form of rAAS41 and rAAS46, but not deglycosylated forms. The implication is that there may be a homolog to AAS41 and AAS46 in *I. scapularis* nymphs that are secreted in tick saliva during feeding under the influence of *B. burgdorferi* infection.

Recombinant AAS41 is an inhibitor of chymase and chymotrypsin, but rAAS46 is not

To gain insight into probable functional roles of rAAS41 and AAS46 at the tick feeding site, we screened their inhibitory profile against 19 mammalian serine proteases related to host defense pathways as described (Kim et al., 2015, Tirloni et al., 2016). This analysis revealed that rAAS41 (1 µM) inhibited activity of human chymase by 95%, rat and mouse chymase (peritoneal mast cell extract) by a respective 100 and 96%, bovine pancreatic α-chymotrypsin by 99%, papain by 60%, cathepsin G by 23%, and pancreatic elastase by 19% (Fig. 5A). In contrast rAAS46 (1 µM) inhibited activity of human chymase by 11.6%, mouse chymase (peritoneal mast cell extract) by 6%, bovine pancreatic α-chymotrypsin by 16%, papain by 62%, cathepsin G by 29%, human neutrophil proteinase 3 by 36%, and pancreatic elastase by 19% (Fig. 5B).

To check the inhibitory efficiency, we calculated stoichiometry of inhibition (SI) index of rAAS41 against human chymase and bovine pancreatic α-chymotrypsin. Accordingly, the SI index for rAAS41 was 3.8 against bovine pancreatic chymotrypsin (Fig. 6A) and 3.23 against human

chymase (Fig. 6B). A typical inhibitory serpin will form an SDS and heat stable complex with its target protease (Huntington et al., 2000, Gettins, 2002). We show that rAAS41 formed stable complexes with human chymase (Fig. 7A) and bovine α-chymotrypsin (Fig. 7B) as revealed by high molecular weight complexes that were stable with SDS and heat treatment (indicated by arrow head). These irreversible complexes between rAAS41 and the target proteases were observed at similar molar ratios comparable to SI.

We next determined association rate constant (k_a) of rAAS41 with human chymase was measured under pseudo-first order conditions using a discontinuous assay (Horvath et al., 2011) to gauge insight rate of action of rAAS41 against chymase. The k_a for the interaction of rAAS41

Recombinant AAS41 is an anti-inflammatory protein

Mast cell secreted chymase is a key mediator of inflammation (Caughey, 2007, Pejler et al., 2010, Dai and Korthuis, 2011), and thus, the observation that rAAS41 inhibited chymase suggested that this serpin might interfere with inflammation. We evaluated the effects of rAAS41 in a rat model of acute inflammation induced by compound 48/80 (an agonist of mast cell degranulation [Horsfield, 1965, Vassimon and Rothschild, 1990]). Injection of compound 48/80 induced acute inflammation that was characterized by edema formation as revealed by increase in paw thickness reaching a maximum 1 h post injection for formalin (Fig. 9A). When co-injected with rAAS41 (25 µg/paw) edema formation was significantly reduced by 38% ($p = 0.0142$) at 30 min, 72% ($p = 0.0009$) at 60 min, and 55% ($p = 0.0072$) at 120 min post-injections (Fig. 9A).

Intradermally, inflammation increases vascular permeability into the subcutaneous tissue and can be estimated using the Miles assay by measuring Evans blue dye fluid extravasation in rat skin (Muller et al., 2009). When compared to saline injection, compound 48/80 significantly

increased the vascular permeability into skin subcutaneous tissue. However, co-injection with rAAS41 (25 µg/spot) significantly reduced the amount of blue dye that was secreted ($p = 0.0033$) (Figs. 9B and 9C).

Recombinant AAS41 and rAAS46 are not involved with platelet aggregation or hemostasis

Cathepsin G and thrombin are potent agonists of platelet aggregation (Puri and Colman, 1993), and ADP is responsible for causing primary and secondary aggregation of platelets (Puri and Colman, 1997). The PI profiling for both rAAS41 and rAAS46 showed less than 40% inhibition of cathepsin G. We tested to see if rAAS41 and rAAS46 had any effect in delaying cathepsin G- or ADP-induced platelet aggregation. Overall there was no effect in delaying or stopping cathepsin G- or ADP-induced platelet aggregation when comparing to the positive control (data not shown).

Likewise, preventing blood clotting is one of the key functions of tick saliva proteins to allow the tick to ingest a blood meal. Therefore, we tested the ability of rAAS41 and rAAS46 to delay or inhibit blood clotting from human serum by RCT, APTT, PT, and TT assays. Consistent with the PI profile where rAAS41 or rAAS46 did not inhibit proteases involved in blood clotting (thrombin, trypsin, plasmin, t-PA, u-PA and blood clotting factors), there was no delay or inhibition of blood clotting when using these serpins (data not shown).

RNAi silencing of AAS41/46 significantly reduces the tick blood meal size

To gain insight on functional importance of AAS41/46 in tick feeding, we assessed the effects of RNAi silencing on *A. americanum* feeding summarized in Figure 10. Given the fact that AAS41/46 were highly expressed in unfed ticks, we first depleted the AAS41/46 transcript from

unfed ticks before assessing the effects of RNAi silencing on tick feeding. The rationale for depletion of target mRNA from unfed ticks is to prevent ticks from expressing the cognate protein when placed on rabbits to feed.

To deplete mRNA, unfed ticks that were injected with AAS41/46-dsRNA were analyzed using qualitative RT-PCR for cognate mRNA expression at 3, 7, and 21 days post dsRNA injection (Fig. 10A). As shown in Figure 10A, most of AAS41/46 mRNA was disrupted by day 21 after injecting dsRNA. Subsequently dsRNA injected ticks were incubated for three weeks before assessing the effects of RNAi silencing on tick feeding. To validate target mRNA suppression in ticks that had attached to feed, we sampled four ticks per treatment at 72 h of post-attachment and confirmed that AAS41/46 transcript was suppressed by 16-53%, 59-74%, and 68-84% in SG, MG and CA respectively (Fig. 10B).

To assess the impact of disrupting AAS41/46 mRNA of feeding success, ticks were allowed to feed to repletion. Overall, RNAi silencing did not affect tick feeding rate as both control (GFP-dsRNA injected ticks) and treatment ticks completed feeding within the same time frame (not shown). Replete fed ticks were photographed to document physical phenotypes (Fig. 10C). Subsequently, replete fed ticks were weighed to measure the engorgement mass as an index for the amount of blood ingested by the tick. This analysis showed that RNAi silencing significantly (p = 0.0376) reduced the amount of blood taken in by ticks (Fig. 10D1). Replete fed ticks were incubated at 22°C with >85% relative humidity to allow for egg laying. Our data show that, though not statistically significant, RNAi silencing caused a reduction in amount of eggs that were laid (Fig. 10D2), and the ability of fed ticks to convert the blood meal into eggs (Fig. 10D3).

Discussion

This study describes biological and functional characterization of two immunogenic *A. americanum* tick saliva serpins, AAS41 and AAS46, with high sequence homology, but that are functionally distinct. Host inflammation response to tick feeding is one of the cardinal host defenses that the tick must modulate to successfully feed and transmit tick-borne diseases. While anti-inflammatory properties of tick saliva are documented (Rodrigues et al., 2018, Banajee et al., 2016), the molecular identities of mediators of *A. americanum* saliva anti-inflammation effect are not fully known. In this study, we demonstrate that AAS41 is likely among proteins that *A. americanum* utilizes to evade the host's inflammation defense against tick feeding.

Given high sequence similarity between AAS41 and AAS46, we are interpreting our biological analysis on mRNA and protein expression with caution; we do not know if data presented here are for one of the serpins or for both. Despite this limitation, our qRT-PCR data showing that AAS41/46 mRNA are expressed in multiple tick organs and the finding that AAS41/46 protein is injected into the host during tick feeding suggested one or both of these proteins played significant roles in tick physiology. The finding that AAS41/46 protein is immunogenic and highly abundant in unfed and early stage feeding (24-72 h feeding timepoints) make these two proteins attractive candidates for tick vaccine development. From the standpoint of identifying cross species conserved tick saliva proteins that could be targeted for an anti-tick vaccine to stop pathogen transmission, it is interesting to note that the protein backbone of rAAS41 cross-reacts to rabbit serum from once fed *B. burgdorferi*-infected *I. scapularis* nymphs, but did not bind to rabbit serum from uninfected *I. scapularis* nymphs feeding. This could indicate that AAS41 homolog in *I. scapularis* could be secreted in saliva of only *B. burgdorferi* infected ticks. The 24-72 h tick feeding timepoints coincides with key tick feeding processes; creating the tick

feeding lesion (through first 24-36 h of feeding [Sonenshine 1993, Walade and Rice, 1982], and starting to transmit tick-borne disease agents (after first 48 h of feeding, des Vignes et al., 2001, Ebel and Kramer et al., 2004). From this perspective it was encouraging to note that RNAi silencing of AAS41/46 mRNA significantly reduced the feeding efficiency resulting in reduced blood meal feeding and fecundity. These findings gave us confidence to target AAS41/46 proteins in tick vaccine development (Chapter IV of this dissertation).

Another requirement to improve on design of tick vaccines is to understand functions of candidate antigens in tick feeding. Here, we have provided evidence to show that AAS41 is likely one of the tick saliva proteins that *A. americanum* utilizes to evade the host's inflammation defense by targeting the chymase inflammatory pathway (Caughey, 2007, Pejler et al., 2010, Dai and Korthuis, 2011). There is evidence that mast cells play critical roles in host response to tick feeding and comprise of 10% of the cutaneous cellular responses at the tick feeding site from cattle that were fed by *A. americanum* (Brown, 1984). Two studies demonstrated that mast cell deficient mice could not develop resistance against *Haemaphysalis longicornis* larvae tick feeding (Matsuda et al., 1985), while wild type mice with intact mast cell response expressed tick feeding resistance by massive degranulation of these cells at the feeding site (Ushio et al., 1993). On this basis, our findings that rAAS41 inhibited chymase that was purified from mast cells strongly suggest a role for native AAS41 to suppress inflammation in response to tick feeding by inhibiting chymase that is secreted by degranulating mast cells.

The tick accomplishes feeding by creating a wound in the skin and ingesting blood that accumulates in the wound (Sonenshine, 1993). The expected host response is tissue repair, which if successful will prevent the tick from successful feeding. Chymotrypsin and trypsin play critical roles in tissue repair (Shah and Mital, 2018), such as might be required at the tick feeding site.

Following injury, α1-antitrypsin and α2-macroglobulin, inhibitors of both trypsin and chymotrypsin are secreted, and if left uncontrolled could lead to delayed wound healing (Shah and Mital, 2018). As rAAS41 is also a strong inhibitor of chymotrypsin, it is conceivable that *A. americanum* native AAS41 might interfere with the host's tissue repair response by disrupting chymotrypsin kinetics at the tick feeding site. It is notable that native AAS41/46 were injected at secreted high levels through 168 h feeding when the tick is preparing to complete feeding, and the tick might no longer need to control inflammation (Fig. 1B). It is notable from data in Chapter II of this dissertation that, *A. americanum* tick saliva contained high levels of rabbit α1-antitrypsin and α2-macroglobulin, which also play roles in disrupting the host's tissue repair response.

One of the interesting lessons from this study is that we might not infer function of tick serpins based on sequence homology. It is noteworthy that despite high sequence similarity between AAS41 and AAS46, the two proteins were functionally different. We were pleasantly surprised that a two amino acid sequence difference within the reactive center loop affected functions of the two serpins. The function of serpins is influenced by the amino acid residue at the P1 position (Huntington et al., 2000, Gettins, 2002). The difference in function between rAAS41 and rAAS46 might be explained by the fact the former has a Leucine at its P1 site, while the latter has a Threonine amino acid residue. In conclusion, this study has made significant contributions toward understanding the molecular basis of tick feeding physiology. These findings are expected to influence design of tick vaccines.

In conclusion, this chapter has contributed toward understanding the molecular basis of tick feeding physiology. Three *A. americanum* tick salivary serpins, AAS19, AAS41, and AAS46 were successfully characterized. Data in this chapter indicate that AAS19 and AAS41 might function in mediating *A. americanum* tick evasion of the host's tissue repair response. The tick-

feeding style of creating a wound in host skin and then ingestion of host blood that accumulates into the lesion is expected to trigger the host's tissue repair response to close the wound and stop blood loss. If the host was successful, the tick will fail to feed. The repair process broadly involves four overlapping phases: blood clotting system, inflammation, cell proliferation, and tissue remodeling (Krafts, 2010, Shah and Mital, 2018). Data in this chapter strongly support the concept that AAS19 functions in facilitating tick evasion of the host's inflammation and blood clotting system as it inhibits trypsin and blood clotting factors (Stormorken, 1956, Davie and Fujikawa, 1975, Schmaier, 2007). On the other hand, AAS41 could be involved in facilitating tick evasion of host inflammation via its activity against chymotrypsin and chymase. RNAi silencing data confirmed the three *A. americanum* tick saliva serpins in this chapter regulated important tick feeding physiology functions in that disrupting their functions significantly reduced tick feeding success. On this basis, all three serpins were selected for analysis as potential target antigens in the fourth chapter of this dissertation.

References

Banajee, K.H., Verhoeve, V.I., Harris, E.K., Macaluso, K.R., 2016. Effect of *Amblyomma maculatum* (Acari: Ixodidae) Saliva on the acute cutaneous immune response to *Rickettsia parkeri* infection in a murine model. J. Med. Entomol. 53, 1252-1260.

Berger, M., Reck, J.,Jr, Terra, R.M., Beys da Silva, W. O., Santi, L., Pinto, A.F., Vainstein, M.H., Termignoni, C., Guimaraes, J.A., 2010. *Lonomia obliqua* venomous secretion induces human platelet adhesion and aggregation. J. Thromb. Thrombolysis 30, 300-310.

Brown, S.J., Barker, R.W., Askenase, P.W., 1984. Bovine resistance to *Amblyomma americanum* ticks: an acquired immune response characterized by cutaneous basophil infiltrates. Vet. Parasitol. 16, 147-165.

Caughey, G.H., 2007. Mast cell tryptases and chymases in inflammation and host defense. Immunol. Rev. 217, 141-154.

Dai, H., Korthuis, R.J., 2011. Mast cell proteases and inflammation. Drug Discov. Today Dis. Models 8, 47-55.

Davie, E.W., Fujikawa, K., 1975. Basic mechanisms in blood coagulation. Annu. Rev. Biochem. 44, 799-829.

des Vignes, F., Piesman, J., Heffernan, R., Schulze, T.L., Stafford, K.C.,3rd, Fish, D., 2001. Effect of tick removal on transmission of *Borrelia burgdorferi* and *Ehrlichia phagocytophila* by *Ixodes scapularis* nymphs. J. Infect. Dis. 183, 773-778.

Ebel, G.D., Kramer, L.D., 2004. Short report: duration of tick attachment required for transmission of powassan virus by deer ticks. Am. J. Trop. Med. Hyg. 71, 268-271.

Gettins, P.G., 2002. Serpin structure, mechanism, and function. Chem. Rev. 102, 4751-4804.

Horn, F., dos Santos, P.C., Termignoni, C., 2000. *Boophilus microplus* anticoagulant protein: an antithrombin inhibitor isolated from the cattle tick saliva. Arch. Biochem. Biophys. 384, 68-73.

Horsfield, G.I., 1965. The effect of compound 48/80 on the rat mast cell. J. Pathol. Bacteriol. 90, 599-605.

Horvath, A.J., Lu, B.G., Pike, R.N., Bottomley, S.P., 2011. Methods to measure the kinetics of protease inhibition by serpins. Methods Enzymol. 501, 223-235.

Huntington, J.A., Read, R.J., Carrell, R.W., 2000. Structure of a serpin-protease complex shows inhibition by deformation. Nature 407, 923-926.

Ibelli, A.M., Kim, T.K., Hill, C.C., Lewis, L.A., Bakshi, M., Miller, S., Porter, L., Mulenga, A., 2014. A blood meal-induced *Ixodes scapularis* tick saliva serpin inhibits trypsin and thrombin, and interferes with platelet aggregation and blood clotting. Int. J. Parasitol. 44, 369-379.

Kim, T.K., Curran, J., Mulenga, A., 2014. Dual silencing of long and short *Amblyomma americanum* acidic chitinase forms weakens the tick cement cone stability. J. Exp. Biol. 217, 3493-3503.

Kim, T.K., Tirloni, L., Radulovic, Z., Lewis, L., Bakshi, M., Hill, C., da Silva Vaz, I., Jr, Logullo, C., Termignoni, C., Mulenga, A., 2015. Conserved *Amblyomma americanum* tick Serpin19, an inhibitor of blood clotting factors Xa and XIa, trypsin and plasmin, has anti-haemostatic functions. Int. J. Parasitol. 45, 613-627.

Koci, J., Simo, L., Park, Y., 2013. Validation of internal reference genes for real-time quantitative polymerase chain reaction studies in the tick, *Ixodes scapularis* (Acari: Ixodidae). J. Med. Entomol. 50, 79-84.

Krafts, K.P., 2010. Tissue repair: The hidden drama. Organogenesis 6, 225-233.

Landucci, E.C., Antunes, E., Donato, J.L., Faro, R., Hyslop, S., Marangoni, S., Oliveira, B., Cirino, G., de Nucci, G., 1995. Inhibition of carrageenin-induced rat paw oedema by crotapotin, a polypeptide complexed with phospholipase A2. Br. J. Pharmacol. 114, 578-583.

Liao, M., Zhou, J., Gong, H., Boldbaatar, D., Shirafuji, R., Battur, B., Nishikawa, Y., Fujisaki, K., 2009. Hemalin, a thrombin inhibitor isolated from a midgut cDNA library from the hard tick *Haemaphysalis longicornis*. J. Insect Physiol. 55, 164-173.

Livak, K.J., Schmittgen, T.D., 2001. Analysis of relative gene expression data using real-time quantitative PCR and the 2(-Delta Delta C(T)) Method. Methods 25, 402-408.

Matsuda, H., Fukui, K., Kiso, Y., Kitamura, Y., 1985. Inability of genetically mast cell-deficient W/Wv mice to acquire resistance against larval *Haemaphysalis longicornis* ticks. J. Parasitol. 71, 443-448.

Mulenga, A., Kim, T.K., Ibelli, A.M., 2013. Deorphanization and target validation of cross-tick species conserved novel *Amblyomma americanum* tick saliva protein. Int. J. Parasitol. 43, 439-451.

Muller, F., Mutch, N.J., Schenk, W.A., Smith, S.A., Esterl, L., Spronk, H.M., Schmidbauer, S., Gahl, W.A., Morrissey, J.H., Renne, T., 2009. Platelet polyphosphates are proinflammatory and procoagulant mediators in vivo. Cell 139, 1143-1156.

Nazareth, R.A., Tomaz, L.S., Ortiz-Costa, S., Atella, G.C., Ribeiro, J.M., Francischetti, I.M., Monteiro, R.Q., 2006. Antithrombotic properties of Ixolaris, a potent inhibitor of the extrinsic pathway of the coagulation cascade. Thromb. Haemost. 96, 7-13.

Pejler, G., Ronnberg, E., Waern, I., Wernersson, S., 2010. Mast cell proteases: multifaceted regulators of inflammatory disease. Blood 115, 4981-4990.

Porter, L., Radulovic, Z., Kim, T., Braz, G.R., Da Silva Vaz, I.,Jr, Mulenga, A., 2015. Bioinformatic analyses of male and female *Amblyomma americanum* tick expressed serine protease inhibitors (serpins). Ticks Tick Borne Dis. 6, 16-30.

Puri, R.N., Colman, R.W., 1993. Thrombin- and cathepsin G-induced platelet aggregation: effect of protein kinase C inhibitors. Anal. Biochem. 210, 50-57.

Puri, R.N., Colman, R.W., 1997. ADP-induced platelet activation. Crit. Rev. Biochem. Mol. Biol. 32, 437-502.

Radulovic, Z.M., Kim, T.K., Porter, L.M., Sze, S.H., Lewis, L., Mulenga, A., 2014. A 24-48 h fed *Amblyomma americanum* tick saliva immuno-proteome. BMC Genomics 15, 518.

Rodrigues, V., Fernandez, B., Vercoutere, A., Chamayou, L., Andersen, A., Vigy, O., Demettre, E., Seveno, M., Aprelon, R., Giraud-Girard, K., Stachurski, F., Loire, E., Vachiery, N., Holzmuller, P., 2018. Immunomodulatory effects of *Amblyomma variegatum* saliva on bovine cells: characterization of cellular responses and identification of molecular determinants. Front. Cell. Infect. Microbiol. 7, 521.

Schmaier, A.H., 2007. Coagulation Factors. xPharm: The Comprehensive Pharmacology Reference, 1-6.

Shah, D., Mital, K., 2018. The Role of trypsin:chymotrypsin in tissue repair. Adv. Ther. 35, 31-42.

Sonenshine, D.E., 1993. Biology of Ticks. Oxford University Press, Oxford.

Stormorken, H., 1956. The effect of trypsin on blood coagulation and the mechanism of its action. J. Lab. Clin. Med. 48, 519-528.

Tirloni, L., Kim, T.K., Pinto, A.F.M., Yates, J.R.,3rd, da Silva Vaz, I.,Jr, Mulenga, A., 2017. Tick-Host Range Adaptation: Changes in protein profiles in unfed adult *Ixodes scapularis* and *Amblyomma americanum* saliva stimulated to feed on different hosts. Front. Cell. Infect. Microbiol. 7, 517.

Tirloni, L., Kim, T.K., Coutinho, M.L., Ali, A., Seixas, A., Termignoni, C., Mulenga, A., da Silva Vaz, I.,Jr, 2016. The putative role of *Rhipicephalus microplus* salivary serpins in the tick-host relationship. Insect Biochem. Mol. Biol. 71, 12-28.

Ushio, H., Watanabe, N., Kiso, Y., Higuchi, S., Matsuda, H., 1993. Protective immunity and mast cell and eosinophil responses in mice infested with larval *Haemaphysalis longicornis* ticks. Parasite Immunol. 15, 209-214.

Vassimon, C.S., Rothschild, A.M., 1990. Compound 48/80-induced secretion of histamine from rat peritoneal mast cells depends on a tryptase controlled step also leading to chymase activity. Agents Actions 30, 150-152.

Walade, S.M., Rice, M.J., 1982. The sensory basis of tick feeding behavior. Physiology of Ticks, pp. 71–118.

CHAPTER IV

IMMUNIZATION OF CATTLE USING A COCKTAIL MIXTURE OF SELECTED RECOMBINANT TICK SALIVA PROTEINS TO DETERMINE PROTECTION FROM TICK FEEDING

Rationale

This chapter is the extension of findings in the second and third chapter of this dissertation. The rationale was to mimic host immunity that is observed in repeatedly infested animals that acquire resistance against tick feeding (Bowessidjaou et al., 1977, Brown and Knapp, 1981, Brown et al., 1984, Latif et al., 1988, Brossard and Papateodorou, 1990, Barriga et al., 1991, Gebbia et al., 1995). This immunity is elicited by several TSPs as evidenced by western blot analysis, which show multiple tick saliva proteins reacting to immune sera of rabbits that were repeatedly infested with ticks. Therefore, to mimic naturally acquired tick feeding resistance, the goal was to test if a cocktail vaccine containing multiple tick salivary antigens could mimic immunity of repeatedly infested animals and protect cattle against tick infestation. This chapter tested the following hypothesis:

- H_0: Immunization of cattle with multiple recombinant tick saliva proteins will not mimic immunity against tick feeding that is induced by repeated tick infestation of animals.
- H_1: Immunization of cattle with multiple recombinant tick saliva proteins will mimic immunity against tick feeding that is induced by repeated tick infestation of animals.

Materials and Methods

Ethics statement

All animal work was conducted and approved according to Texas A&M University Institutional Animal Care and Use Committee (AUP: 2017-0250) that meets all federal requirements, as defined in the Animal Welfare Act (AWA), the Public Health Service Policy (PHS), and the Humane Care and Use of Laboratory Animals.

Selection of candidate vaccine antigens for immunization of cattle

Candidate tick saliva proteins for a vaccine cocktail were selected based on two criteria: (1) the protein was identified within the first 72 h of feeding in tick saliva, and (2) targets must be among genes that were upregulated in *A. americanum* that were stimulated to start feeding on cattle (Mulenga et al., 2007) and were also confirmed as immunogenic (Radulovic et al., 2014) including a putative extracellular metalloprotease secretion inducing protein [EMPRIN] and tick carboxypeptidase inhibitor [TCI]. Other immunogenic proteins that have been previously validated as secreted into the host in early stages of tick feeding in saliva include: calreticulin ([CRT] Jaworski et al., 1995), histamine release factor, ([HRF] Mulenga and Azad, 2005), *A. americanum* serpin 6 ([AAS6] Chalaire et al., 2011), a cross-species conserved protein ([AV422] Mulenga et al., 2013), acidic chitinase ([Ach] Kim et al., 2014), insulin-like growth factor binding protein- related protein 1 ([IGFBP] Radulovic et al., 2015), *A. americanum* serpin 27 ([AAS27] Tirloni et al., *submitted*), and *A. americanum* serpin 4 ([AAS4] Porter et al., *in preparation*) were included in the vaccine cocktail. *A. americanum* serpins [AAS19, AAS41, and AAS46] characterized from the second objective were also included in the vaccine cocktail. A total of 13 candidate tick saliva proteins (noted above) were selected for the vaccine cocktail.

To determine and confirm immunogenicity of the 13 candidate tick saliva proteins, the antibody epitope prediction program from IEDB Analysis Resource server (http://tools.iedb.org/main/bcell/) was used to detect linear epitopes from protein sequences. The amino acid sequences of the 13 candidate antigens were entered in the search bar and the "Bepipred Linear Epitope Prediction" method was selected. This method predicts the B-cell epitopes using both the Markov model and propensity scales method (Larsen et al, 2006).

Expression of 13 recombinant tick saliva proteins in Pichia pastoris

Thirteen TSPs with predicted B-cell epitopes were expressed using the *Pichia pastoris*, X-33, and pPICZα plasmid expression system (Thermo Fisher Scientific) as described in Chapter III. Of the 13 TSPs, six (AAS6, AAS19, Ach, AV422, CRT, and IGFBP) were previously expressed and functionally characterized by our lab and are published, four (AAS4, AAS27, AAS41, and AAS46) are in preparation for publication, and the remaining three (EMPRIN, HRF, and TCI) were expressed for this study. Therefore, the frozen stocks for 10 of the candidate antigens were available in the lab to proceed to large-scale protein expression. For EMPRIN, HRF and TCI, the mature protein open reading frames (Mulenga et al.,2007) were sub-cloned into respective pPICZα plasmid expression system (Thermo Fisher Scientific) as described in Chapter III. All recombinant proteins were affinity purified and were dialyzed in 1x PBS pH 7.4. The total protein concentration was determined using the BCA quantification assay (Thermo Fisher Scientific). Expression of recombinant proteins for immunization was verified by western blot analysis using antibody to hexahistidine-HRP. The purity was confirmed by resolving the recombinant proteins by SDS-PAGE and visualized by silver staining procedures.

Immunization of cattle with recombinant tick saliva proteins

Holstein steers (*Bos taurus*) ~3 months of age were placed in a tick-free pasture during immunizations at Texas A&M University, College of Veterinary Medicine and Biomedical Science, Veterinary Medical Park (TAMU-VMP). Animals were immunized in three groups: (1) buffer and adjuvant control consisting of 1x PBS pH 7.4 with equal volume of TiterMax Gold adjuvant (Sigma-Aldrich Corp., St. Louis, MO, USA), (2) a low (up to 100 μg per antigen) and (3) high dosage (up to 300 μg per antigen) of a cocktail mixture of 13 recombinant tick saliva proteins (rTSP) noted above, with TiterMax Gold adjuvant (Sigma-Aldrich Corp.). Animals were inoculated subcutaneously and/or intradermally with equal volumes of PBS:adjuvant or rTSPs:adjuvant mixtures. Immunizations were administered at day 0, booster at day 21, and a second booster at day 42. The second booster antigen concentrations were reduced three-fold. Blood was collected for serum preparation prior to administering the first immunization and subsequently every week thereafter for ELISA verification of host antibody response against each antigen.

Tick challenge infestation on adjuvant injected and rTSPs-adjuvant immunized cattle

Following immunizations of animals, tick challenge infestations were performed as previously described (Mulenga et al., 2007). Individual cattle were restrained in independent stanchions housed in a well-ventilated roof-covered area during tick infestations. An enlarged orthopedic stockinette used to contain ticks during feeding, was glued using Kamar adhesive (Kamar Products Inc. Zionsville, IN, USA) on the right and left sides of the back (chine) of the cattle. Adult (n=40 females and 20 males) and nymph (n=110-120) *A. americanum* ticks were placed into separate feeding stockinettes and daily monitored for tick feeding parameters such as

percent attached, percent feeding to engorgement, engorgement weight, percent egg laid (adults), egg mass (adults), egg mass conversion ratio (EMCR-indices for amount of blood meal converted for egg production), percent molted (nymphs) and record the feeding dynamics (rate of detachment). In order to determine if repeated tick infestation of animals that were immunized with recombinant TSPs enhances anti-tick immunity, animals were re-infested with ticks five weeks after the first infestation. Blood was collected for serum preparation three weeks after the first tick infestation and every week after the second tick infestation for ELISA verification of antibody response against each antigen. The effect(s) of immunization against tick feeding parameters were determined as noted above.

ELISA and western blotting analysis

ELISA and western blot analyses were used to verify the animal antibody response to each individual rTSP. An ELISA standardization assay was first performed to determine the optimal conditions to coat 0.2 μg affinity purified rTSP into the 96 well plates overnight in coating buffer (0.1 M sodium carbonate pH 9.5). Various serum dilutions (1:50, 1:200, 1:400 and 1:600) were tested in combinations with different amounts of coated antigens (50, 100, 200 and 500 ng/ well) followed by 1:2000 or 1:5000 dilutions of the secondary antibody at which the ELISA A_{450nm} read out was recorded. Coated wells were blocked with 300 μL of 5% skim milk in 1x PBS-Tween20 (0.05%) pH 7.4 for 1 h at room temperature (RT). Antibodies, pre-immune or immune sera at a 1:400 dilution were applied to the wells for 1h at RT and washed with 1x PBS-Tween20. Subsequently, a secondary goat anti-bovine IgG horseradish peroxidase (HRP) conjugated at 1:5000 dilution in 5% skim milk in 1x PBS-Tween20 was applied to each well for 1h at RT. To detect antibody binding signals, after sufficient washing (6x) using an ELx405 Microplate Washer

(BioTek Instruments Inc.) with 1x PBS-Tween20, wells were incubated with 1-Step Ultra TMB ELISA substrate (Thermo Fisher Scientific) at RT for 10 min. An equal volume of 2 M sulfuric acid was added to stop the reaction and the A_{450nm} was detected using the Synergy H1 Hybrid Multi-Mode Microplate Reader (BioTek Instruments Inc.).

To determine if antibodies produced in cattle specifically bound to the administered antigens, individual purified recombinant tick saliva proteins were resolved on 10-20% SDS-PAGE and transferred to PVDF membrane for western blot analysis. Membranes were blocked overnight at 4ºC in 5% skim milk in 1x PBS-Tween20. Pre-immune or immune sera (1:1,000) was exposed to the membrane for 1 h at RT. After appropriate washing with 1x PBS-Tween20, a secondary goat anti-bovine IgG HRP conjugated at 1:2000 dilution in 5% skim milk in 1x PBS-Tween20 was exposed for 1 h at RT and then washed again prior to exposing to Amersham ECL Prime Western Blotting Detection Reagent for 5 min and visualized using the Chemidoc™ XRS+ Imaging System (Bio-rad, Hercules, CA, USA).

Statistical analysis

One Way ANOVA and Tukey's honestly significant difference (HSD) test, and Fisher exact test analyses were used to determine if tick-feeding performance on control and immunized cattle were significantly different using the Prism 6 software (GraphPad Software, La Jolla, CA, USA). Data were reported as Mean ± SEM.

Results

Recombinant tick antigens are immunogenic in cattle

Antigens that were used for immunization were selected on the basis that they are

upregulated in *A. americanum* ticks that were stimulated to start feeding on cattle (Mulenga et al., 2007), are present in tick saliva from chapter II (Fig. 1), and are potentially immunogenic (Fig. 2). Thirteen TSPs (Ach, CRT, AAS4, AAS6, AAS19, AAS27, AAS41, AAS46, AV422, IGFBP-rP1, HRF, TCI, and EMPRIN) served as candidate anti-tick vaccine antigens for this study. Of the 13 antigens, two (HRF and EMPRIN) were not found in the *A. americanum* tick saliva proteome (Chapter II of this dissertation). For HRF, it was confirmed as secreted in both *Dermancetor variabilis* (Mulenga et al., 2003) and *A. americanum* in previous studies (Mulenga and Azad, 2005). EMPRIN, a putative extracellular metalloprotease secretion inducing protein, was identified from *A. americanum* ticks that were stimulated to start feeding on cattle, and was upregulated in salivary glands of partially fed ticks (Mulenga et al., 2007).

Recombinant proteins were expressed in *Pichia pastoris* (Chapter III: AAS19- Kim et al., 2015, AAS41 and AAS46- Kim et al., *in preparation*) and previously in the lab (AV422-Mulenga et al., 2013a, AAS6- Mulenga et al., 2013b, Ach- Kim et al., 2014, CRT- Kim et al., 2014, IGFBP-rP1- Radulovic et al., 2015, AAS27- Tirloni et al., *in submission,* AAS4- Porter et al., *in preparation*, and EMPRIN, HRF, and TCI- *unpublished*). Figure 3 summarizes the validation of affinity purified recombinant antigens purity by western blot analysis using anti-hexahistidine tag and silver staining. Table 1 shows the total amount of purified protein recovered using the BCA quantification assay. As shown in Figure 3, all antigens were of high purity. The immunization and bleeding schedule that was accomplished is summarized in Figure 4 and Table 2; this timeline is provided for clarity of data presented below.

Immunizing antigens were subjected to western blot analysis using cattle immune sera (1:1000 dilution) that were collected at day 21 after the booster injection (Fig. 5). As shown in Figure 5, antibody response was confirmed for 11 of the 13 antigens in five of the six immunized

heads of cattle. It is notable that three cattle that were immunized with the low dose antigen (100 μg/antigen for the cocktail mix) had a consistent response, while one of the animals that was immunized with high dose (300 μg/antigen for the cocktail mix) had a poor response. The lack of binding on pre-immune and adjuvant inoculated sera confirmed that the observed binding in Figures 5B1, 5B2, 5B3 and 5C1, 5C2, 5C3 was specific.

Figure 6 summarizes the ELISA analysis to profile the antibody response to immunization and tick feeding. Given that antibody binding was not observed for all antigens when coating 100 ng per well at 1:1000 – 1:5000 dilution of immune sera followed by 1:2000 and 1:5000 secondary antibodies, an ELISA standardization assay was performed to establish an optimal antibody titer to antigen amount to keep all 13 antigen conditions consistent for comparison. The optimal conditions to detect a response from all 13 antigens was at 1:400 serum dilution to 200 ng of antigen/well, followed by 1:5000 secondary antibody and used in ELISA analysis as summarized in Figure 6. Based on observed $A_{450nm,}$ ELISA read outs were classified as high (Fig. 6A for AAS46, AAS41, IGFBP-rP1, AA27, and Ach), moderate (Fig. 6B for AAS6, AAS4, AAS19, CRT, and AV422), and low immunogenic (Fig. 6C for HRF, TCI, and EMPRIN) antigens.

There are two principal data points from Figure 6: (i) highest titer was observed at 14 days after the first booster, and (ii) high dose antigens induced higher antibody titer for all antigens except for AAS46 and EMPRIN. It is also notable that 14 days after the second booster, antibody levels were comparable between low and high dose immunized cattle for all antigens except for AAS46, AAS4, AAS19, and CRT for which low antigen antibody titers were apparently higher than high antigen dose.

Immunization of cattle bolsters acquired immunity against nymph tick feeding

To assess the effects of immunization, cattle were challenge infested with nymph and adult *A. americanum* twice as summarized in Figure 7. The first and second tick challenge infestations were done at day 14 after the second booster (blue arrow head in Fig. 6) and day 32 after the first challenge infestation (maroon arrow head in Fig. 6 and Table 2), respectively. Ticks were allowed to feed to repletion and feeding parameters were documented as summarized in Figure 7. Data presented in Figure 7 is an average of observations of three animals that were immunized for control (PBS, phosphate buffered saline with adjuvant), low and high dose antigen with adjuvant immunized animals.

Figure 7A1 documents the time to completion of feeding for nymphs during first (solid lines) and second (dashed lines) challenge infestation. *A. americanum* nymphs feeding on tick naïve animals are expected to complete feeding after 4-7 days of feeding (Barnard et al., 1985). Data summarized in Figure 7A1 show that immunization against tick feeding did not affect the feeding efficiency of nymph ticks during the first infestation as ticks on both control and immunized cattle completed feeding by day 7.

However, there was apparent slowdown of tick feeding during the second challenge infestation as nymph tick feeding extended beyond. During the second infestation (dashed lines) an average 78%, 61%, and 69% of nymphs completed feeding on adjuvant, low, and high antigen immunized cattle grouped per treatment, respectively. However, tick feeding was significantly slowed during the second infestation on both control and immunized animals. Whereas, tick feeding was completed within 7 days during the first challenge infestation, it took up to 10 days for nymphs in all treatment groups to complete feeding during the second infestation (Fig. 7A1).

Overall, immunization did not protect against primary nymph tick infestation but enhanced acquired immunity against nymph tick feeding (Fig. 7A, and Tables 3A and 3B). Figure 7A2 shows that immunization had no effect during the first challenge infestation but the number of nymph ticks that completed feeding on both low and high dose antigen immunized cattle was lower than those that fed on controls during the second challenge infestation. Whereas in the first infestation 93, 95, and 92% of nymph ticks completed feeding on the three control cattle, 79, 83 and 94% of nymph ticks completed feeding in the second infestation. When comparing the three low antigen dose immunized cattle, 98, 92, and 100% nymph ticks completed feeding in the first infestation compared to the second infestation where 57, 77, and 67% nymph ticks completed feeding. Nymph ticks that fed on the three high antigen dose immunized cattle had 88, 90, and 99% completed feeding in the first infestation, in contrast to the second infestation where 62, 98, and 68% completed feeding. These data indicate that repeated infestation induced tick immunity against nymph tick infestation resulting in 15, 13 and 0% fewer number of nymph ticks feeding to repletion on control cattle in the second infestation, and 41, 16, and 33% and 29, 0, and 31% fewer nymph ticks completed feeding on low and high antigen dose immunized cattle, respectively (Table 3A and 3B).

Next, we assessed the effects of immunization on amounts of blood (measured by engorgement mass, EM) that nymphs ingested. This analysis revealed that although immunization had no significant effect on blood meal feeding first or second infestations, there was an apparent impact on the second infestation of nymphs that fed on the low dose antigen immunized cattle (Fig. 7A3). The EM of second infestation nymphs for PBS control, low and high antigen injected yielded average nymph weights of 9.46, 9.01, and 9.64 mg, respectively, (Fig. 7A3, and Table 3A and 3B). As shown in Figure 7A3, EM of nymphs that fed on two of the three low dose antigen

immunized animals were apparently smaller than the EM of ticks that fed on control cattle showing average percent changes per animal when comparing to all three controls were 0, 0.5, and 3.7% when comparing within control cattle and 0, 12.6, and 13.2% when comparing controls with low antigen injected cattle. It was interesting to note that immunization had no impact on blood meal feeding for nymphs that fed on high dose antigen immunized cattle as the EM for nymphs that fed on two of three immunized animals had no significant differences in EM when comparing to each individual control cattle, with the exception of one high animal that had a reduction of 12.6% in EM when compared to the controls (Table 3).

Similar to EM, immunization had no effect on molting during the first infestation, and there was moderate to no effect during the second infestation (Fig. 7A4, and Table 3A and 3B). The sex ratio (male to female) of molted of ticks showed that, while ticks that fed on control animals had 40 to 60 (male to female), it was reversed to 60 to 40 (male to female) for ticks that fed on immunized cattle (Table 3A and 3B).

Effect of immunization of cattle against adult tick feeding was inconclusive

The effect of immunization adult tick feeding was not completed due to two principal limitations that arose during the study. During the first infestation, the experiment was suspended before ticks completed feeding due to an error in the Animal Use Protocol (AUP). The AUP stipulated that the experiment was going to last for 20 days, however this period did not account for time to prepare animals for tick infestation, the actual time to complete the experiment was 24-28 days. During the second infestation, the error in the AUP was corrected, however the animals were too large for the stanchions, and most the ticks were crushed during feeding, and this might have affected the analysis. That said, the limited data that were collected showed that immunization

did not apparently affect feeding of adult ticks during both first and second challenge infestations as there was no difference in EM of ticks that fed to repletion (Fig. 7B1), egg laying (Fig. 7B2), and ability of ticks to convert the blood meal to eggs (Fig. 7B3).

Discussion

Since the observation that repeatedly infested animals acquires host immunity against tick feeding (Trager et al., 1939a 1939b), there have been efforts to develop vaccines against tick feeding (Allen and Humphreys, 1979, Mulenga et al., 1999, 2001, Willadsen, 2004, 2006). However, efforts to immunize against tick infestation using single vaccine antigens have produced mixed results (reviewed in Merino et al., 2013), however when immunizing with tick salivary gland extracts protection against tick feeding levels increase (Wikel, 1981, Brown et al., 1984, Manohar and Banerjee, 1992, Astigarraga et al., 1995, Jittapalapong et al., 2008, Nikpay and Nabian, 2016), therefore it was thought that a protective vaccine antigen would likely be multi-antigen. Recently, studies have attempted to mimic host immunity that is induced in repeatedly tick-infested animals with partial success that led to commercialization of the Bm86 vaccine (Willadsen et al., 1995) that has in recent years been withdrawn from the Australian market. Given that immune sera of repeatedly tick-infested animals that acquire immunity against tick feeding binds to multiple protein bands on western blots of tick salivary gland, it is thought that a protective vaccine antigen is going to be multi-antigen (Brown et al., 1984, Brown, 1988, Barriga et al., 1991, Mulenga et al., 1999, Narasimhan et al., 2007, Nikpay et al., 2012). This study was initiated against this background and as a logical continuation of studies that were conducted in Chapters II and III of this dissertation. Previous anti-tick immunization studies used under five antigens and produced mixed results (Imamura et al., 2008, Almazan et al., 2012, Parizi, et al., 2012, Moreno-Cid et al.,

2013, Contreras and de la Fuente, 2016, Maruyama et al., 2017). Here for the first time a cocktail of more than 10 antigens was successfully formulated. The finding that each of the 13 recombinant antigens in this study provoked an antibody response demonstrated that immunization of animals with such a huge number of antigens is feasible. Findings in the second chapter of this dissertation that ticks secreted hundreds of proteins every 24 h encouraged formulation of this cocktail tick vaccine.

Host immunity against tick feeding in repeatedly infested animals is directed against TSPs (Wikel 1981, 1982, Nuttall and Labuda, 2004), and from this perspective, this study targeted TSPs. The advantage of targeting TSPs is that the act of tick feeding could serve as booster immunization. On this basis, the goal of this study was two-fold: (i) to evaluate protective vaccine efficacy of the cocktail vaccine against primary tick infestation and (ii) to determine if repeated infestation of animals that were first immunized with tick saliva antigens can bolster immunity resulting from tick feeding. The observation that there was no protection against primary tick infestations is being interpreted with caution. It is potentially possible that the lack of protection against primary infestation might be due to the fact that the appropriate window to infest cattle was missed. From the immunogenicity study, it was observed that the highest antibody titer for all antigens was at 14 days at the first booster. However, primary infestations were done at 14 days after the second booster when titers were lower for all antigens. It is also possible that the TiterMax Gold adjuvant that was used in this study might not be appropriate for cattle. We were encouraged to use the TiterMax Gold adjuvant due to findings in rabbits when immunization with rAAS19 and this adjuvant reduced tick feeding efficiency (Kim et al., 2016).

Although it was not established for adult ticks, nymph ticks that fed on immunized cattle previously infested with ticks showed reduced performance when compared to the controls. This

demonstrates that immunization of cattle using the 13 recombinant tick saliva proteins bolsters the capacity of these cattle to acquire immunity when repeatedly infested. This might not be the most desirable finding for vaccine that will be utilized to immunize cattle against tick feeding. However, it is attractive in the case of immunizing wildlife against tick feeding. Since wildlife serves as the principal blood meal source to maintain tick populations in nature, the cocktail vaccine in this study might be effective over time. The expectation is that after receiving a dose of the vaccine, the acquired tick immunity resulting from repeated infestations will be superior for the immunized wildlife population compared to the general population. Wildlife such as white-tailed deer serve important roles on the impact of ticks and tick-borne diseases in veterinary and public health. In public health, white-tailed deer are the primary blood meal source for both *A. americanum* and *Ixodes scapularis* ticks: the two medically important tick species that transmit majority of human tick-borne disease agents in the US according to the Center for Disease Control (CDC). There is evidence that prevalence of Lyme disease, which is vectored by *I. scapularis* was correlated to deer populations in a geographic location (Kilpatrick et al., 2014). Therefore, it is conceivable that immunization of deer against tick feeding might have broader impacts toward prevention of Lyme disease and other tick-borne diseases. Likewise, the role of deer in preventing re-introduction of *Rhipicephalus* (formerly *Boophilus*) *microplus* to the U.S. has emerged. Since its eradication more than 75 years ago (Graham and Hourrigan, 1977), the U.S. government has prevented *R. microplus*, the primary vector for transmitting *Babesia* parasites in cattle, from re-establishing in the U.S. through mandatory acaricide treatment of all cattle imports from Mexico where these parasites are prevalent (Fernandez-Salas et al., 2012, Rodriguez-Vivas et al., 2014). In recent years, this prevention mechanism has been threatened due to the spread of acaricide resistant ticks being prevalent in Mexico, and most importantly, deer infested with acaricide resistant ticks

crossing into the U.S. from Mexico (Pound et al, 2010, Lohmeyer et al, 2011, Busch et al., 2014). On this basis, finding that the cocktail vaccine in this study bolstered the ability of the immunized hosts to acquired tick resistance following repeated infestation is attractive, and has potential application to immunization of ticks against tick feeding.

In conclusion, this study established a cocktail vaccine against tick feeding, and most importantly has contributed results that will be used to improve the effect of this vaccine in future studies. Based on findings in this study, it might best to limit to one boost immunization, and challenge immunized animals two weeks after booster. It would also be instructive to evaluate other adjuvants, especially those that are approved for use in cattle. The findings in this study warrant that further investigation is needed to improve the formulation of this vaccine to control tick feeding on cattle.

References

Allen, J.R., Humphreys, S.J., 1979. Immunisation of guinea pigs and cattle against ticks. Nature 280, 491-493.

Almazan, C., Moreno-Cantu, O., Moreno-Cid, J.A., Galindo, R.C., Canales, M., Villar, M., de la Fuente, J., 2012. Control of tick infestations in cattle vaccinated with bacterial membranes containing surface-exposed tick protective antigens. Vaccine 30, 265-272.

Astigarraga, A., Oleaga-Perez, A., Perez-Sanchez, R., Encinas-Grandes, A., 1995. A study of the vaccinal value of various extracts of concealed antigens and salivary gland extracts against *Ornithodoros erraticus* and *Ornithodoros moubata*. Vet. Parasitol. 60, 133-147.

Barnard, D.R., Morrison, R.D., Popham, T.W., 1985. Light and temperature sensitivity of feeding-related and reproductive processes in *Amblyomma americanum* (Acari: Ixodidae) on cattle. ee 14, 479-485.

Barriga, O.O., Andujar, F., Sahibi, H., Andrzejewski, W.J., 1991. Antigens of *Amblyomma americanum* ticks recognized by repeatedly infested sheep. J. Parasitol. 77, 710-716.

Bowessidjaou, J., Brossard, M., Aeschlimann, A., 1977. Effects and duration of resistance acquired by rabbits on feeding and egg laying in *Ixodes ricinus* L. Experientia 33, 528-530.

Brossard, M., Papatheodorou, V., 1990. Immunity against female *Ixodes ricinus* L.: effect on feeding and haemoglobin digestion. Ann. Parasitol. Hum. Comp. 65, 32-36.

Brown, S.J., Knapp, F.W., 1981. Response of hypersensitized guinea pigs to the feeding of *Amblyomma americanum* ticks. Parasitology 83, 213-223.

Brown, S.J., Barker, R.W., Askenase, P.W., 1984. Bovine resistance to *Amblyomma americanum* ticks: an acquired immune response characterized by cutaneous basophil infiltrates. Vet. Parasitol. 16, 147-165.

Brown, S.J., 1988. Characterization of tick antigens inducing host immune resistance. II. Description of rabbit-acquired immunity to *Amblyomma americanum* ticks and identification of potential tick antigens by Western blot analysis. Vet. Parasitol. 28, 245-259.

Busch, J.D., Stone, N.E., Nottingham, R., Araya-Anchetta, A., Lewis, J., Hochhalter, C., Giles, J.R., Gruendike, J., Freeman, J., Buckmeier, G., Bodine, D., Duhaime, R., Miller, R.J., Davey, R.B., Olafson, P.U., Scoles, G.A., Wagner, D.M., 2014. Widespread movement of invasive cattle fever ticks (*Rhipicephalus microplus*) in southern Texas leads to shared local infestations on cattle and deer. Parasit. Vectors 7, 188.

Chalaire, K.C., Kim, T.K., Garcia-Rodriguez, H., Mulenga, A., 2011. *Amblyomma americanum* (L.) (Acari: Ixodidae) tick salivary gland serine protease inhibitor (serpin) 6 is secreted into tick saliva during tick feeding. J. Exp. Biol. 214, 665-673.

Contreras, M., de la Fuente, J., 2016. Control of *Ixodes ricinus* and *Dermacentor reticulatus* tick infestations in rabbits vaccinated with the Q38 Subolesin/Akirin chimera. Vaccine 34, 3010-3013.

Fernandez-Salas, A., Rodriguez-Vivas, R.I., Alonso-Diaz, M.A., 2012. First report of a *Rhipicephalus microplus* tick population multi-resistant to acaricides and ivermectin in the Mexican tropics. Vet. Parasitol. 183, 338-342.

Gebbia, J.A., Bosler, E.M., Evans, R.D., Schneider, E.M., 1995. Acquired resistance in dogs to repeated infestation with *Ixodes scapularis* (Acari: Ixodidae) reduces tick viability and reproductive success. Exp. Appl. Acarol. 19, 593-605.

Graham, O.H., Hourrigan, J.L., 1977. Eradication programs for the arthropod parasites of livestock. J. Med. Entomol. 13, 629-658.

Imamura, S., da Silva Vaz, I.,Jr, Konnai, S., Yamada, S., Nakajima, C., Onuma, M., Ohashi, K., 2009. Effect of vaccination with a recombinant metalloprotease from *Haemaphysalis longicornis*. Exp. Appl. Acarol. 48, 345-358.

Jaworski, D.C., Simmen, F.A., Lamoreaux, W., Coons, L.B., Muller, M.T., Needham, G.R., 1995. A secreted calreticulin protein in ixodid tick (*Amblyomma americanum*) saliva. Journal of Insect Physiology 41, 369-375.

Jittapalapong, S., Phichitrasilp, T., Chanphao, H., Rerkamnuychoke, W., Stich, R.W., 2008. Immunization with tick salivary gland extracts. Ann. N. Y. Acad. Sci. 1149, 200-204.

Kilpatrick, H.J., LaBonte, A.M., Stafford, K.C., 2014. The relationship between deer density, tick abundance, and human cases of Lyme disease in a residential community. J. Med. Entomol. 51, 777-784.

Kim, T.K., Curran, J., Mulenga, A., 2014. Dual silencing of long and short *Amblyomma americanum* acidic chitinase forms weakens the tick cement cone stability. J. Exp. Biol. 217, 3493-3503.

Kim, T.K., Ibelli, A.M., Mulenga, A., 2015. *Amblyomma americanu*m tick calreticulin binds C1q but does not inhibit activation of the classical complement cascade. Ticks Tick Borne Dis. 6, 91-101.

Kim, T.K., Tirloni, L., Radulovic, Z., Lewis, L., Bakshi, M., Hill, C., da Silva Vaz, I.,Jr, Logullo, C., Termignoni, C., Mulenga, A., 2015. Conserved *Amblyomma americanum* tick Serpin19, an inhibitor of blood clotting factors Xa and XIa, trypsin and plasmin, has anti-haemostatic functions. Int. J. Parasitol. 45, 613-627.

Kim, T.K., Radulovic, Z., Mulenga, A., 2016. Target validation of highly conserved *Amblyomma americanum* tick saliva serine protease inhibitor 19. Ticks Tick Borne Dis. 7, 405-414.

Larsen, J.E., Lund, O., and Nielsen, M. Improved method for predicting linear B-cell epitopes. Immunome Res. 2006; 2: 2.

Latif, A.A., Newson, R.M., Dhadialla, T.S., 1988. Feeding performance of *Amblyomma variegatum* (Acarina: Ixodidae) fed repeatedly on rabbits. Exp. Appl. Acarol. 5, 83-92.

Lohmeyer, K.H., Pound, J.M., May, M.A., Kammlah, D.M., Davey, R.B., 2011. Distribution of Rhipicephalus (Boophilus) microplus and *Rhipicephalus* (*Boophilus*) *annulatus* (Acari: Ixodidae) infestations detected in the United States along the Texas/Mexico border. J. Med. Entomol. 48, 770-774.

Manohar, G.S., Banerjee, D.P., 1992. Effects of immunization of rabbits on establishment, survival, and reproductive biology of the tick *Hyalomma anatolicum anatolicum*. J. Parasitol. 78, 77-81.

Maruyama, S.R., Garcia, G.R., Teixeira, F.R., Brandao, L.G., Anderson, J.M., Ribeiro, J.M.C., Valenzuela, J.G., Horackova, J., Verissimo, C.J., Katiki, L.M., Banin, T.M., Zangirolamo, A.F., Gardinassi, L.G., Ferreira, B.R., de Miranda-Santos, I. K. F., 2017. Mining a differential sialotranscriptome of *Rhipicephalus microplus* guides antigen discovery to formulate a vaccine that reduces tick infestations. Parasit. Vectors 10, 2.

Merino, O., Alberdi, P., Perez de la Lastra, J M, de la Fuente, J., 2013. Tick vaccines and the control of tick-borne pathogens. Front. Cell. Infect. Microbiol. 3, 30.

Moreno-Cid, J.A., Perez de la Lastra, J M, Villar, M., Jimenez, M., Pinal, R., Estrada-Pena, A., Molina, R., Lucientes, J., Gortazar, C., de la Fuente, J., SUB/AKR Vaccine Study Group, 2013. Control of multiple arthropod vector infestations with subolesin/akirin vaccines. Vaccine 31, 1187-1196.

Mulenga, A., Sugimoto, C., Sako, Y., Ohashi, K., Musoke, A., Shubash, M., Onuma, M., 1999. Molecular characterization of a *Haemaphysalis longicornis* tick salivary gland-associated 29-kilodalton protein and its effect as a vaccine against tick infestation in rabbits. Infect. Immun. 67, 1652-1658.

Mulenga, A., Sugino, M., Nakajim, M., Sugimoto, C., Onuma, M., 2001. Tick-Encoded serine proteinase inhibitors (serpins); potential target antigens for tick vaccine development. J. Vet. Med. Sci. 63, 1063-1069.

Mulenga, A., Macaluso, K.R., Simser, J.A., Azad, A.F., 2003. The American dog tick, *Dermacentor variabilis*, encodes a functional histamine release factor homolog. Insect Biochem. Mol. Biol. 33, 911-919.

Mulenga, A., Azad, A.F., 2005. The molecular and biological analysis of ixodid ticks histamine release factors. Exp. Appl. Acarol. 37, 215-229.

Mulenga, A., Blandon, M., Khumthong, R., 2007. The molecular basis of the *Amblyomma americanum* tick attachment phase. Exp. Appl. Acarol. 41, 267-287.

Mulenga, A., Kim, T.K., Ibelli, A.M., 2013a. Deorphanization and target validation of cross-tick species conserved novel *Amblyomma americanum* tick saliva protein. Int. J. Parasitol. 43, 439-451.

Mulenga, A., Kim, T., Ibelli, A.M., 2013b. *Amblyomma americanum* tick saliva serine protease inhibitor 6 is a cross-class inhibitor of serine proteases and papain-like cysteine proteases that delays plasma clotting and inhibits platelet aggregation. Insect Mol. Biol. 22, 306-319.

Narasimhan, S., Deponte, K., Marcantonio, N., Liang, X., Royce, T.E., Nelson, K.F., Booth, C.J., Koski, B., Anderson, J.F., Kantor, F., Fikrig, E., 2007. Immunity against *Ixodes scapularis* salivary proteins expressed within 24 hours of attachment thwarts tick feeding and impairs *Borrelia* transmission. PLoS One 2, e451.

Nikpay, A., Nabian, S., Taheri, M., 2012. Analysis of immunogenic relevant proteins in *Rhipicephalus* (*Boophilus*) *annulatus* tick. J. Arthropod Borne Dis. 6, 36-44.

Nikpay, A., Nabian, S., 2016. Immunization of cattle with tick salivary gland extracts. J. Arthropod Borne Dis. 10, 281-290.

Nuttall, P.A., Labuda, M., 2004. Tick-host interactions: saliva-activated transmission. Parasitology 129 Suppl, 177.

Parizi, L.F., Githaka, N.W., Logullo, C., Konnai, S., Masuda, A., Ohashi, K., da Silva Vaz, Jr., I., 2012. The quest for a universal vaccine against ticks: cross-immunity insights. Vet. J. 194, 158-165.

Porter, L., Kim, T.K., Radulovic, Z., Mulenga, A., *Amblyomma americanum* serpin 8 (AAS8) inhibits inflammatory proteases and silencing reduces tick engorgement. (*In preparation*).

Pound, J.M., George, J.E., Kammlah, D.M., Lohmeyer, K.H., Davey, R.B., 2010. Evidence for role of white-tailed deer (Artiodactyla: Cervidae) in epizootiology of cattle ticks and southern cattle ticks (Acari: Ixodidae) in reinfestations along the Texas/Mexico border in south Texas: a review and update. J. Econ. Entomol. 103, 211-218.

Radulovic, Z.M., Kim, T.K., Porter, L.M., Sze, S.H., Lewis, L., Mulenga, A., 2014. A 24-48 h fed *Amblyomma americanum* tick saliva immuno-proteome. BMC Genomics 15, 518.

Radulovic, Z.M., Porter, L.M., Kim, T.K., Bakshi, M., Mulenga, A., 2015. *Amblyomma americanum* tick saliva insulin-like growth factor binding protein-related protein 1 binds insulin but not insulin-like growth factors. Insect Mol. Biol.

Rodriguez-Vivas, R.I., Perez-Cogollo, L.C., Rosado-Aguilar, J.A., Ojeda-Chi, M.M., Trinidad-Martinez, I., Miller, R.J., Li, A.Y., de Leon, A.P., Guerrero, F., Klafke, G., 2014. *Rhipicephalus* (*Boophilus*) *microplus* resistant to acaricides and ivermectin in cattle farms of Mexico. Rev. Bras. Parasitol. Vet. 23, 113-122.

Tirloni, L., Kim, T.K., Berger, M., Termignoni, C., da Silva Vaz Jr., I., Mulenga, A., *Amblyomma americanum* serpin 27 AAS27) is a tick salivary anti-inflammatory protein secreted into the host during feeding. (*Submitted to PLoS Negl Trop Dis.- Under review- April 3, 2019*).

Trager, W., 1939a. Acquired Immunity to Ticks. J. Parasitol 25, 57-81.

Trager, W., 1939b. Further observations on acquired immunity to the tick *Dermacentor variabilis* Say. J. Parasitol. 25, 137-139.

Wikel, S., 1982. Immune responses to arthropods and their hosts. Annual Review of Entomology, 21-48.

Wikel, S.K., 1981. The induction of host resistance to tick infestation with a salivary gland antigen. Am. J. Trop. Med. Hyg. 30, 284-288.

Willadsen, P., 2006. Vaccination against ectoparasites. Parasitology 133 Suppl, S25.

Willadsen, P., 2004. Anti-tick vaccines. Parasitology 129 Suppl, 367.

Willadsen, P., Bird, P., Cobon, G.S., Hungerford, J., 1995. Commercialisation of a recombinant vaccine against *Boophilus microplus*. Parasitology 110 Suppl, 43.

CHAPTER V

CONCLUSION: CONTRIBUTIONS FROM THIS DISSERTATION TOWAR UNDERSTANDING THE MOLECULAR BASIS OF TICK FEEDING PHYSIOLOGY

Summary

It has been nearly 120 years since Sabbatani (1899) made the first observation that ticks contain components that interfere or regulate host defenses such as blood clotting. Over 80 years ago, observations by Trager (1939a, b) that animals repeatedly infested with ticks elicit a strong protective immune response have influenced many studies to identify these molecular targets in tick salivary gland and saliva to develop an effective anti-tick vaccine. However, a protective anti-tick vaccine that is effective in controlling multiple tick species remains elusive. This dissertation research contributes in understanding the molecular basis of tick feeding physiology using two ticks, *Amblyomma americanum and Ixodes scapularis*, that are distantly related yet have a growing impact on human and animal health in the U.S. The hypothesis is that these ticks utilize a conserved system to successfully evade host defenses for blood meal feeding and transmitting tick-borne disease agents and defining these conserved pathways will provide knowledge to strengthen the efforts to develop novel tick controls methods. This dissertation touched on three main areas of tick research. **First**: the discovery of potential vaccine targets using LC-MS/MS proteomics (Chapter II), **Second:** functionally define the role(s) of these targets in tick feeding physiology (Chapter III), and **Third**: downstream applications to test the effectiveness of tick saliva proteins as targets for tick vaccine development (Chapter IV). The availability of these data will allow for systematic design of antigens for effective anti-tick vaccines.

Prior to the advent of LC-MS/MS sequencing application to identification of proteins in tick saliva, very little was known on proteins that ticks injected into the host during feeding. Prior to the LC-MS/MS sequencing technology, the majority of putatively annotated TSPs were identified based on presence of a signal peptide. At the start of this dissertation, LC-MS/MS sequencing had been used to identify proteins in tick saliva from single tick feeding time point, most often after five days of tick feeding, presumably because ticks were larger and were easier to handle. The limitation of identifying tick saliva proteins from single feeding time point is that the dynamics of protein profile changes during feeding were not captured. In Chapter II of this dissertation, I successfully utilized the LC-MS/MS sequencing for the first-time, to identify hundreds of TSPs that are sequentially secreted every 24 h during feeding by two medically important ticks species in the U.S., *I. scapularis* and *A. americanum*. Data from these studies suggest that tick saliva is complex and dynamic and probably changes in response to host defenses. The profile of tick saliva changes every 24 h, which we hypothesize is a mechanism of host evasion by the tick through saliva responses. Of significance for pathogen transmission studies, as most tick-borne disease agents are transmitted within the first 48 h of tick feeding, this study focuses on proteins that are injected into the host prior to start of pathogen transmission.

The next phase is to define the functional role(s) of these tick saliva proteins in tick feeding physiology. In Chapter III of my dissertation, I have characterized three saliva serine protease inhibitors (serpins), AAS19, AAS41, and AAS46 from *A. americanum* that were identified from Chapter II. The majority of host defenses such as blood clotting and inflammation is serine protease mediated that are controlled by serpins. Of significance, all three serpins were present within the first 24 h of blood meal feeding at the transcript and protein levels. Biochemical characterization studies showed that AAS19 is an anti-coagulant protein that inhibits trypsin, plasmin, and blood

clotting factors. Studies on AAS41 and AAS46 provided insights into how the tick might evade host defense. Although AAS41 and AAS46 are 97% identical at the nucleotide and protein levels, they do not have the same functions. Biochemical analysis shows that AAS41 is a strong anti-inflammatory protein that inhibits chymase and alpha chymotrypsin, while AAS46 does not inhibit any of the proteases we tested (at above 70% inhibition). Both AAS41 and AAS46 appear to be immunogenic as they bound antibodies to TSPs from rabbits that had acquired tick feeding resistance after repeated infestation. It is notable that AAS46 has a unique B-cell epitope that is absent in AAS41. This could this be a strategy of ticks to evade host defense by secreting a less potent decoy (AAS46), while secreting the potent anti-inflammatory AAS41. Given that the three saliva serpins are secreted within the first 24 h of feeding, are functional at the feeding site, and are immunogenic, these characteristics make them attractive targets for an anti-tick vaccine.

There is evidence that acquired immunity against tick feeding in repeatedly infested animals is provoked by multiple tick saliva proteins (Brown et al., 1984, Brown, 1988, Barriga et al., 1991, Mulenga et al., 1999, Narasimhan et al., 2007, Nikpay et al., 2012). This coupled with the fact that, ticks secrete multiple TSPs during feeding (Chapter II), prompted the investigation in Chapter IV of my dissertation; to evaluate the effects of *A. americanum* tick feeding on cattle that were immunized with 13 different recombinant tick saliva proteins. Although immunization did not protect cattle against primary tick infestations, it enhanced acquired immunity against second round of tick feeding. Of interest, this study captures the dynamics of the host response to the immunizing antigens based on IgG levels in serum, which is informative of when to conduct tick challenge infestation on immunized cattle. Several other limitations and future perspectives are discussed in Chapter IV. This study contributes new strategies towards designing effective anti-tick vaccine cocktails.

As summarized in Figure 1, TSPs identified in this dissertation can be mapped to three broad phases of the tick feeding process: (i) the start of feeding phase: to initiate feeding, suppress tissue repair host defenses, and transmits tick-borne disease agents, (ii) the middle of feeding: to maintain the feeding site and to control host immune defenses, and (iii) the end of feeding: to complete the feeding process and detach from the host skin with minimal damage to the host. With exception of viruses such as Powassan virus and tick-borne encephalitis that are transmitted within minutes of tick attachment, transmission of majority of tick-borne disease agents including *Anaplasma phagocytophilum* and *Borrelia burgdorferi* occur at the earliest timepoints after a respective 24 and 48 h of tick attachment, and the protozoan pathogen, *Babesia microti* transmission occurs after 54 h of attachment (reviewed in Hermance and Thangamani, 2018). Therefore, the proteins identified in the start of feeding from this dissertation, within the first 72 h of feeding, could serve as potential targets for anti-tick vaccines to prevent tick feeding and pathogen transmission. Knowing the saliva proteins that ticks secrete into the host during feeding in the early stages and defining its interacting host molecular mediators at the feeding site could improve on designing effective anti-tick vaccines centered at blocking the functions of tick saliva proteins that are essential to counter host defenses at the tick feeding site.

As the tick continues to feed (middle of feeding) during the slow-feeding phase, it maintains the feeding site while also ingesting low amounts of blood. During this time, the tick must constantly battle with the host defenses to prepare itself for the rapid feeding phase (end of feeding). Given that a majority of these host defenses are involved with the inflammation process and in restricting the blood flow to the feeding site, there is an added benefit to translate the use of tick saliva proteins as therapeutics to treat human diseases. It has been reported that mast cells are present at the tick bite site within 3 hours post-infestation (Hermance and Thangamani, 2018).

Upon degranulation, mast cells release pro-inflammatory proteases such as chymase and tryptase and other compounds like histamine. Given that AAS41, from this dissertation, was highly abundant during the start to middle of tick feeding phases and has anti-inflammatory functions directed towards chymase inhibition, this protein might be one of the tick saliva proteins used to control inflammation at the feeding site. Mast cells have been implicated in the pathogenesis of hypertension, atherosclerosis and aortic aneruysm in humans that have shown to be chymase-dependent in conversion of angiotensin I to angiotensin II (reviewed in Doggrell and Wanstall, 2004). Therefore, blocking chymase with inhibitors such as AAS41, could have applications towards therapy of vascular diseases.

Finally, towards the end of feeding, the tick ingests a blood meal over hundred times its original body weight (Sonenshine, 1993). Upon ingesting a complete blood meal, the tick detaches from its host in which the feeding site is sealed, where blood is not leaking out. It is hypothesized that the tick is secreting both tick and host proteins towards the end of feeding to aid in the wound healing process. Although it is uncertain which tick proteins may contribute to this function, from this study we have identified host proteins involved in wound healing such as fibrinogen and neutrophil gelantinase-associated lipocalin that are secreted towards the end of feeding (Abdollahi et al., 2017, Thorsvik et al., 2019, Laurens et al., 2006). It has been reported in *Opisthorchis viverrini*, the human liver fluke, that they secrete proteins in the granulin family that accelerate wound healing (Smout et al., 2015).

In conclusion, an important aspect to tick research is to apply the knowledge that is generated by understanding tick feeding physiology towards the discovery of molecular components that can be targeted to develop anti-tick vaccines. Accordingly, evidence that tick saliva contains many pharmacological components provides the potential to discover novel

therapeutics for human diseases. This dissertation provides the foundation for the design of effective tick-antigen based vaccines to prevent transmission of tick-borne disease agents.

References

Abdollahi, M., Ng, T.S., Rezaeizadeh, A., Aamidor, S., Twigg, S.M., Min, D., McLennan, S.V., 2017. Insulin treatment prevents wounding associated changes in tissue and circulating neutrophil MMP-9 and NGAL in diabetic rats. PLoS One 12, e0170951.

Barriga, O.O., Andujar, F., Sahibi, H., Andrzejewski, W.J., 1991. Antigens of *Amblyomma americanum* ticks recognized by repeatedly infested sheep. J. Parasitol. 77, 710-716.

Brown, S.J., Barker, R.W., Askenase, P.W., 1984. Bovine resistance to *Amblyomma americanum* ticks: an acquired immune response characterized by cutaneous basophil infiltrates. Vet. Parasitol. 16, 147-165.

Brown, S.J., 1988. Characterization of tick antigens inducing host immune resistance. II. Description of rabbit-acquired immunity to *Amblyomma americanum* ticks and identification of potential tick antigens by Western blot analysis. Vet. Parasitol. 28, 245-259.

Doggrell, S.A., Wanstall, J.C., 2004. Vascular chymase: pathophysiological role and therapeutic potential of inhibition. Cardiovasc. Res. 61, 653-662.

Hermance, M.E., Thangamani, S., 2018. Tick-virus-host interactions at the cutaneous interface: the nidus of flavivirus transmission. Viruses 10, 10.3390/v10070362.

Laurens, N., Koolwijk, P., de Maat, M.P., 2006. Fibrin structure and wound healing. J. Thromb. Haemost. 4, 932-939.

Mulenga, A., Sugimoto, C., Sako, Y., Ohashi, K., Musoke, A., Shubash, M., Onuma, M., 1999. Molecular characterization of a *Haemaphysalis longicornis* tick salivary gland-associated 29-kilodalton protein and its effect as a vaccine against tick infestation in rabbits. Infect. Immun. 67, 1652-1658.

Narasimhan, S., Deponte, K., Marcantonio, N., Liang, X., Royce, T.E., Nelson, K.F., Booth, C.J., Koski, B., Anderson, J.F., Kantor, F., Fikrig, E., 2007. Immunity against *Ixodes scapularis* salivary proteins expressed within 24 hours of attachment thwarts tick feeding and impairs *Borrelia* transmission. PLoS One 2, e451.

Nikpay, A., Nabian, S., 2016. Immunization of cattle with tick salivary gland extracts. J. Arthropod Borne Dis. 10, 281-290.

Sabbatani L. (1899). Fermento anticoagulante de l' "*Ixodes ricinus*." *Arch. Ital. Biol.* 31 37–53.

Smout, M.J., Sotillo, J., Laha, T., Papatpremsiri, A., Rinaldi, G., Pimenta, R.N., Chan, L.Y., Johnson, M.S., Turnbull, L., Whitchurch, C.B., Giacomin, P.R., Moran, C.S., Golledge, J., Daly, N., Sripa, B., Mulvenna, J.P., Brindley, P.J., Loukas, A., 2015. Carcinogenic parasite secretes growth factor that accelerates wound healing and potentially promotes neoplasia. PLoS Pathog. 11, e1005209.

Sonenshine, D.E., 1993. Biology of Ticks. Oxford University Press, Oxford.

Thorsvik, S., van Beelen Granlund, A., Svendsen, T.D., Bakke, I., Royset, E.S., Flo, T.H., Damas, J.K., Ostvik, A.E., Bruland, T., Sandvik, A.K., 2019. Ulcer-associated cell lineage expresses genes involved in regeneration and is hallmarked by high neutrophil gelatinase-associated lipocalin (NGAL) levels. J. Pathol.

Trager, W., 1939a. Acquired immunity to ticks. J. Parasitol 25, 57-81.

Trager, W., 1939b. Further observations on acquired immunity to the tick *Dermacentor variabilis* Say. J. Parasitol. 25, 137-139.

APPENDIX I

CHAPTER II FIGURES AND TABLES

Figure 1. Relative abundance of tick protein classes in *I. scapularis* tick saliva during and after feeding (Kim, et al., 2016). Total normalized spectral abundance factor (NSAF) for each protein class is expressed as a percent of total NSAF per time point. A key is provided listing the 24 classes of proteins identified in tick saliva as tick-derived proteins.

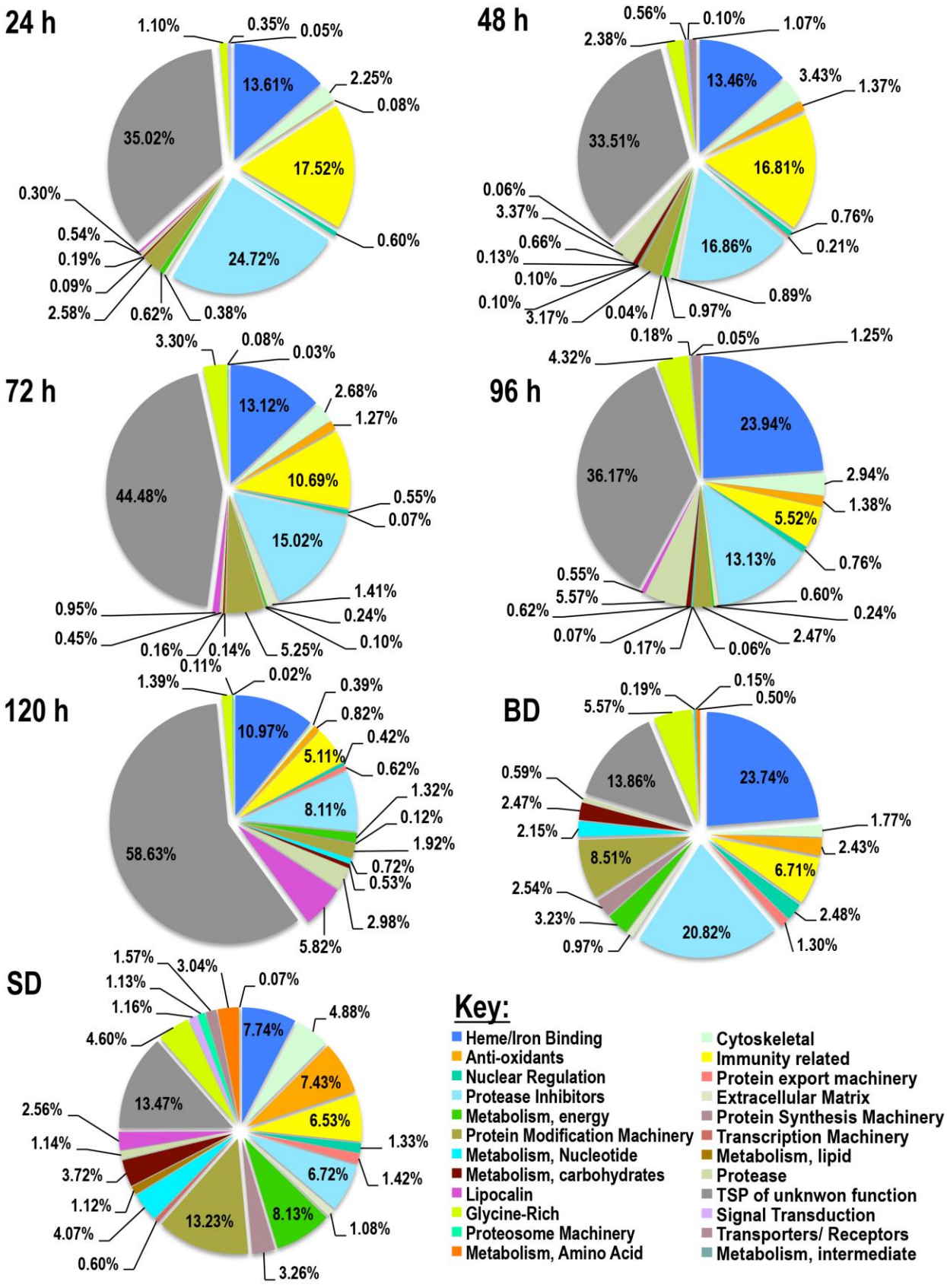
24 h
1.10%
0.35%
0.05%
13.61%
2.25%
0.08%
35.02%
17.52%
0.30%
0.60%
0.54%
24.72%
0.19%
0.09%
2.58%
0.62%
0.38%
48 h
0.56%
0.10%
1.07%
2.38%
13.46%
3.43%
1.37%
33.51%
16.81%
0.06%
3.37%
0.76%
0.66%
0.21%
0.13%
16.86%
0.10%
0.89%
0.10%
3.17%
0.04%
0.97%
72 h
3.30%
0.08%
0.03%
13.12%
2.68%
1.27%
10.69%
44.48%
0.55%
0.07%
15.02%
1.41%
0.95%
0.24%
0.45%
0.10%
0.16%
0.14%
5.25%
0.11%
96 h
0.18%
0.05%
1.25%
4.32%
23.94%
2.94%
36.17%
1.38%
5.52%
0.76%
13.13%
0.55%
0.60%
5.57%
0.62%
0.24%
0.07%
2.47%
0.17%
0.06%
120 h
1.39%
0.02%
0.39%
10.97%
0.82%
0.42%
5.11%
0.62%
1.32%
8.11%
0.12%
58.63%
1.92%
0.72%
0.53%
2.98%
5.82%
BD
0.19%
0.15%
0.50%
5.57%
23.74%
0.59%
13.86%
2.47%
1.77%
2.15%
2.43%
8.51%
6.71%
2.54%
2.48%
3.23%
20.82%
0.97%
1.30%
SD
1.57%
3.04%
0.07%
1.13%
4.88%
1.16%
7.74%
4.60%
7.43%
2.56%
13.47%
6.53%
1.33%
1.14%
6.72%
1.42%
3.72%
1.12%
8.13%
1.08%
13.23%
4.07%
0.60%
3.26%
Key:
Heme/Iron Binding
Anti-oxidants
Nuclear Regulation
Protease Inhibitors
Metabolism, energy
Protein Modification Machinery
Metabolism, Nucleotide
Metabolism, carbohydrates
Lipocalin
Glycine-Rich
Proteosome Machinery
Metabolism, Amino Acid
Cytoskeletal
Immunity related
Protein export machinery
Extracellular Matrix
Protein Synthesis Machinery
Transcription Machinery
Metabolism, lipid
Protease
TSP of unknwon function
Signal Transduction
Transporters/ Receptors
Metabolism, intermediate

Figure 2. Relative abundance of host (rabbit) protein classes in *I. scapularis* tick saliva during and after feeding (Kim, et al., 2016). Total normalized spectral abundance factor (NSAF) for each protein class is expressed as a percent of total NSAF per time point. A key is provided listing the 18 classes of proteins identified in tick saliva as host-derived proteins.

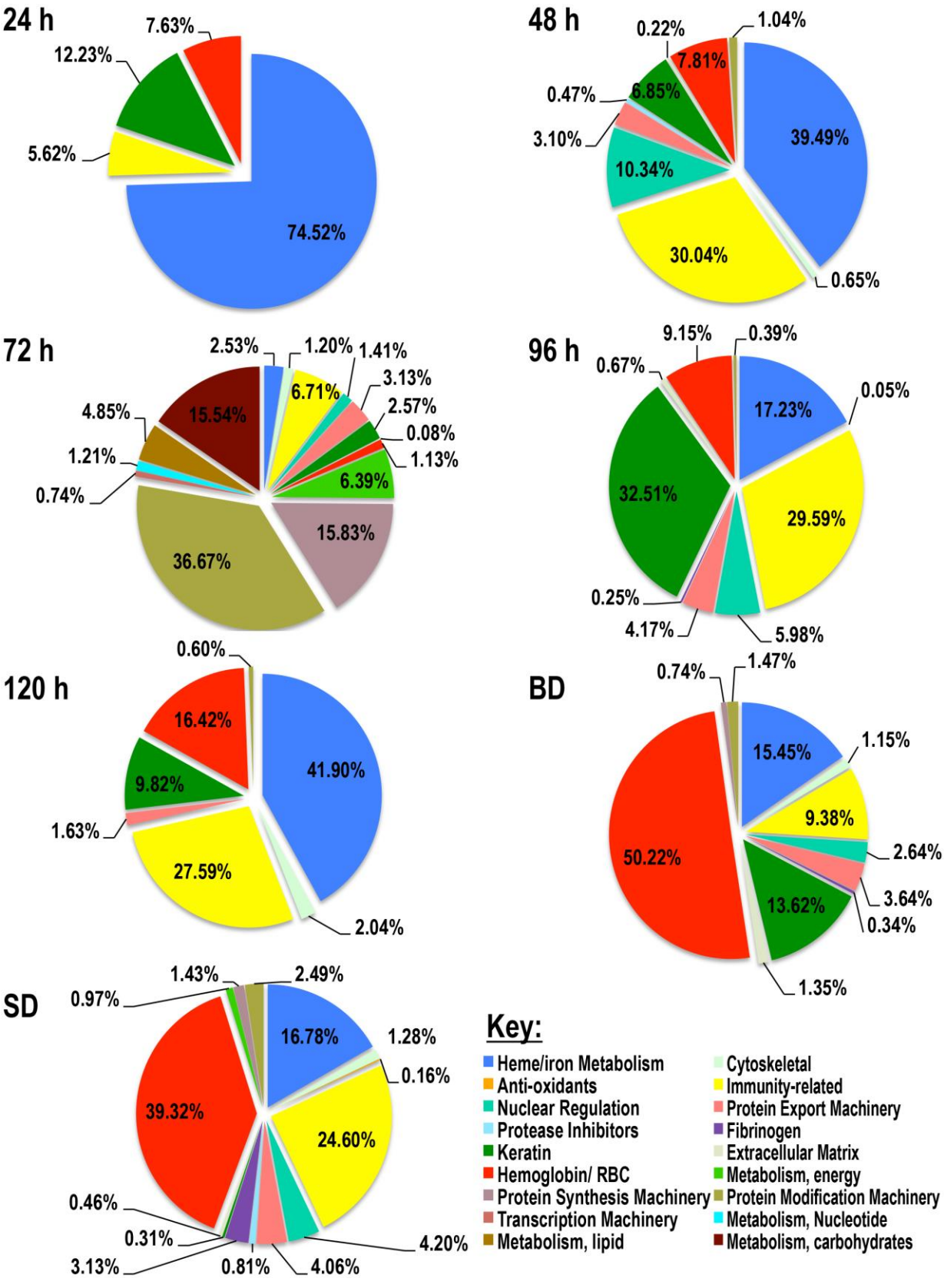
24 h
7.63%
12.23%
5.62%
74.52%
48 h
0.22%
1.04%
7.81%
0.47%
6.85%
3.10%
39.49%
10.34%
30.04%
0.65%
72 h
2.53%
1.20%
1.41%
6.71%
3.13%
2.57%
4.85%
15.54%
0.08%
1.21%
1.13%
0.74%
6.39%
15.83%
36.67%
96 h
9.15%
0.39%
0.67%
0.05%
17.23%
32.51%
29.59%
0.25%
4.17%
5.98%
120 h
0.60%
16.42%
41.90%
9.82%
1.63%
27.59%
2.04%
BD
0.74%
1.47%
15.45%
1.15%
9.38%
50.22%
2.64%
3.64%
13.62%
0.34%
1.35%
SD
1.43%
2.49%
0.97%
16.78%
1.28%
0.16%
39.32%
24.60%
0.46%
0.31%
4.20%
3.13%
0.81%
4.06%
Key:
Heme/iron Metabolism
Anti-oxidants
Nuclear Regulation
Protease Inhibitors
Keratin
Hemoglobin/ RBC
Protein Synthesis Machinery
Transcription Machinery
Metabolism, lipid
Cytoskeletal
Immunity-related
Protein Export Machinery
Fibrinogen
Extracellular Matrix
Metabolism, energy
Protein Modification Machinery
Metabolism, Nucleotide
Metabolism, carbohydrates

Figure 1. Secretion dynamics of proteases and protease inhibitors in *I. scapularis* tick saliva during feeding (Kim, et al., 2016). Normalized spectral abundance factor (NSAF) for each protein as a proxy for relative abundance is expressed as a percent of total NSAF per time point within each class. Z-scores were calculated and used to generate heat maps as described in materials and methods section. Red color indicates proteins of high abundance and blue color indicates proteins of low abundance, both increasing/decreasing in abundance with color intensity. Dendrograms show protein clustering (C) according to secretion patterns. Branches are labeled starting with the letter of the protein class. Fig 3A (metalloproteases), and Fig 3B (protease inhibitors, B1 = Serpins, B2 = TIL domain protease inhibitors, B3 = α-2-macroglobulin, and B4 = Cystatins) are grouped by functional classes.

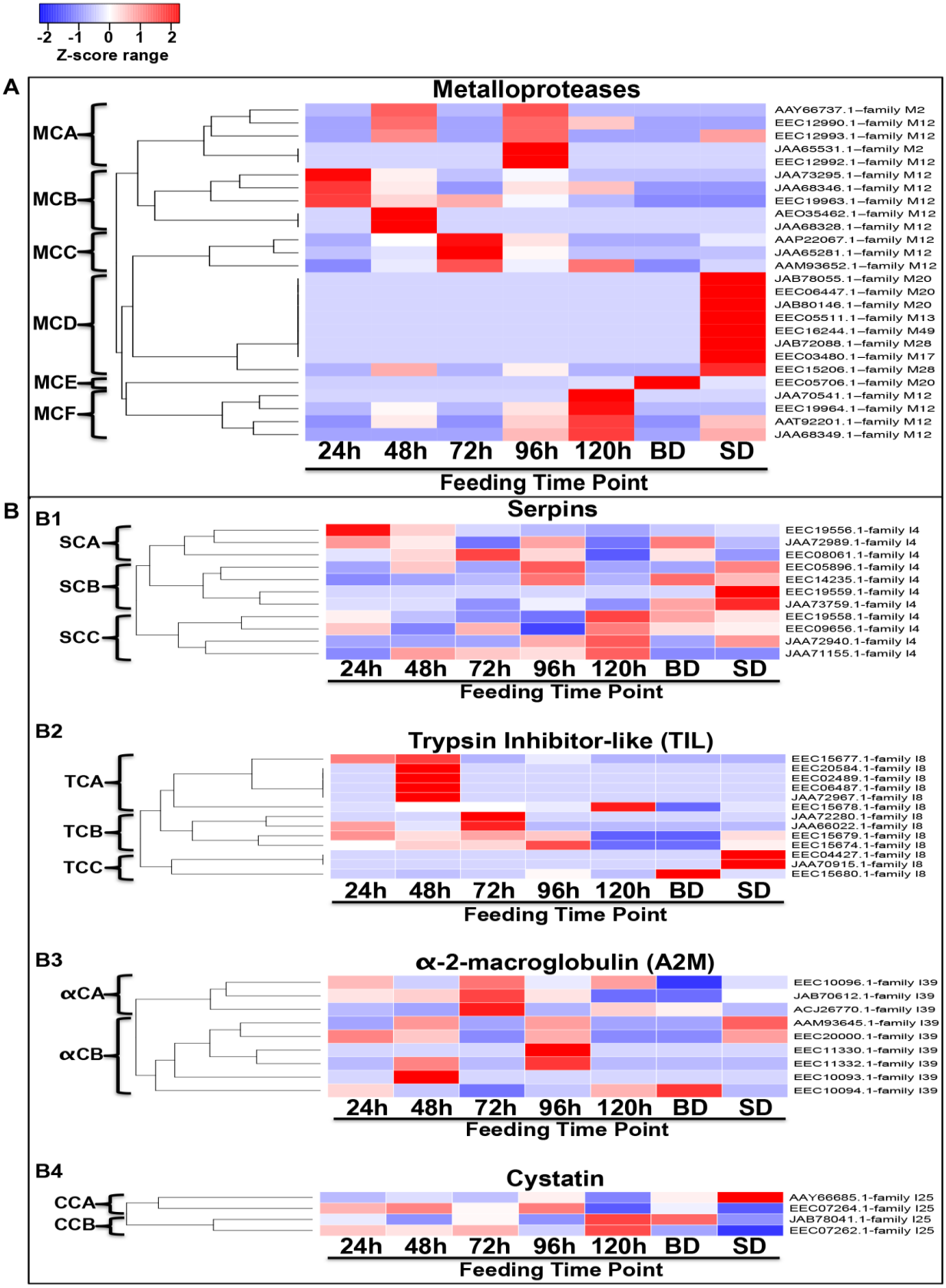
-2 -1 0 1 2
Z-score range
A
Metalloproteases
MCA
MCB
MCC
MCD
MCE
MCF
AAY66737.1–family M2
EEC12990.1–family M12
EEC12993.1–family M12
JAA65531.1–family M2
EEC12992.1–family M12
JAA73295.1–family M12
JAA68346.1–family M12
EEC19963.1–family M12
AEO35462.1–family M12
JAA68328.1–family M12
AAP22067.1–family M12
JAA65281.1–family M12
AAM93652.1–family M12
JAB78055.1–family M20
EEC06447.1–family M20
JAB80146.1–family M20
EEC05511.1–family M13
EEC16244.1–family M49
JAB72088.1–family M28
EEC03480.1–family M17
EEC15206.1–family M28
EEC05706.1–family M20
JAA70541.1–family M12
EEC19964.1–family M12
AAT92201.1–family M12
JAA68349.1–family M12
24h 48h 72h 96h 120h BD SD
Feeding Time Point
B
B1
Serpins
SCA
SCB
SCC
EEC19556.1-family I4
JAA72989.1-family I4
EEC08061.1-family I4
EEC05896.1-family I4
EEC14235.1-family I4
EEC19559.1-family I4
JAA73759.1-family I4
EEC19558.1-family I4
EEC09656.1-family I4
JAA72940.1-family I4
JAA71155.1-family I4
24h 48h 72h 96h 120h BD SD
Feeding Time Point
B2
Trypsin Inhibitor-like (TIL)
TCA
TCB
TCC
EEC15677.1-family I8
EEC20584.1-family I8
EEC02489.1-family I8
EEC06487.1-family I8
JAA72967.1-family I8
EEC15678.1-family I8
JAA72280.1-family I8
JAA66022.1-family I8
EEC15679.1-family I8
EEC15674.1-family I8
EEC04427.1-family I8
JAA70915.1-family I8
EEC15680.1-family I8
24h 48h 72h 96h 120h BD SD
Feeding Time Point
B3
α-2-macroglobulin (A2M)
αCA
αCB
EEC10096.1-family I39
JAB70612.1-family I39
ACJ26770.1-family I39
AAM93645.1-family I39
EEC20000.1-family I39
EEC11330.1-family I39
EEC11332.1-family I39
EEC10093.1-family I39
EEC10094.1-family I39
24h 48h 72h 96h 120h BD SD
Feeding Time Point
B4
Cystatin
CCA
CCB
AAY66685.1-family I25
EEC07264.1-family I25
JAB78041.1-family I25
EEC07262.1-family I25
24h 48h 72h 96h 120h BD SD
Feeding Time Point

Figure 2. Secretion dynamics of *I. scapularis* tick saliva proteins associated with anti-inflammatory (lipocalins), anti-microbial, heme binding, and anti-oxidant functions (Kim, et al., 2016). Normalized spectral abundance factor (NSAF) for each protein as a proxy for relative abundance is expressed as a percent of total NSAF per time point within each class. Z-scores were calculated and used to generate heat maps as described in materials and methods section. Red color indicates proteins of high abundance and blue color indicates proteins of low abundance, both increasing/decreasing in abundance with color intensity. Dendrograms show protein clustering (C) according to secretion patterns. Branches are labeled starting with the letter of the protein class. Fig 4A (Lipocalins), Fig 4B (Anti-microbial), Fig 4C (Heme binding), and Fig 4D (Anti-oxidants) are grouped by functional classes.

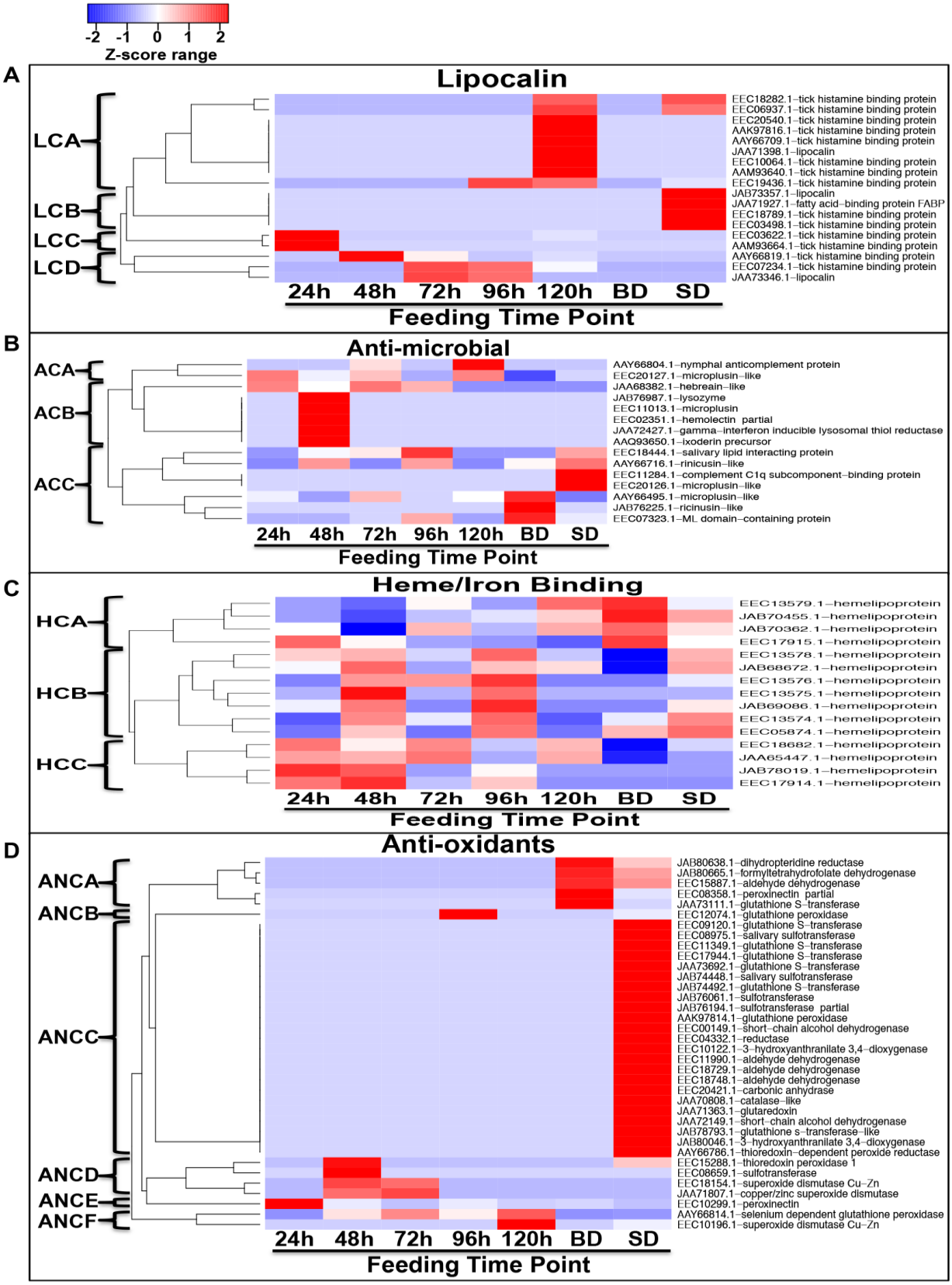
-2 -1 0 1 2
Z-score range
A
Lipocalin
LCA
LCB
LCC
LCD
EEC18282.1–tick histamine binding protein
EEC06937.1–tick histamine binding protein
EEC20540.1–tick histamine binding protein
AAK97816.1–tick histamine binding protein
AAY66709.1–tick histamine binding protein
JAA71398.1–lipocalin
EEC10064.1–tick histamine binding protein
AAM93640.1–tick histamine binding protein
EEC19436.1–tick histamine binding protein
JAB73357.1–lipocalin
JAA71927.1–fatty acid–binding protein FABP
EEC18789.1–tick histamine binding protein
EEC03498.1–tick histamine binding protein
EEC03622.1–tick histamine binding protein
AAM93664.1–tick histamine binding protein
AAY66819.1–tick histamine binding protein
EEC07234.1–tick histamine binding protein
JAA73346.1–lipocalin
24h 48h 72h 96h 120h BD SD
Feeding Time Point
B
Anti-microbial
ACA
ACB
ACC
AAY66804.1–nymphal anticomplement protein
EEC20127.1–microplusin–like
JAA68382.1–hebrein–like
JAB76987.1–lysozyme
EEC11013.1–microplusin
EEC02351.1–hemolectin partial
JAA72427.1–gamma–interferon inducible lysosomal thiol reductase
AAQ93650.1–ixoderin precursor
EEC18444.1–salivary lipid interacting protein
AAY66716.1–rinicusin–like
EEC11284.1–complement C1q subcomponent–binding protein
EEC20126.1–microplusin–like
AAY66495.1–microplusin–like
JAB76225.1–ricinusin–like
EEC07323.1–ML domain–containing protein
24h 48h 72h 96h 120h BD SD
Feeding Time Point
C
Heme/Iron Binding
HCA
HCB
HCC
EEC13579.1–hemelipoprotein
JAB70455.1–hemelipoprotein
JAB70362.1–hemelipoprotein
EEC17915.1–hemelipoprotein
EEC13578.1–hemelipoprotein
JAB68672.1–hemelipoprotein
EEC13576.1–hemelipoprotein
EEC13575.1–hemelipoprotein
JAB69086.1–hemelipoprotein
EEC13574.1–hemelipoprotein
EEC05874.1–hemelipoprotein
EEC18682.1–hemelipoprotein
JAA65447.1–hemelipoprotein
JAB78019.1–hemelipoprotein
EEC17914.1–hemelipoprotein
24h 48h 72h 96h 120h BD SD
Feeding Time Point
D
Anti-oxidants
ANCA
ANCB
ANCC
ANCD
ANCE
ANCF
JAB80638.1–dihydropteridine reductase
JAB80665.1–formyltetrahydrofolate dehydrogenase
EEC15887.1–aldehyde dehydrogenase
EEC08358.1–peroxinectin partial
JAA73111.1–glutathione S–transferase
EEC12074.1–glutathione peroxidase
EEC09120.1–glutathione S–transferase
EEC08975.1–salivary sulfotransferase
EEC11349.1–glutathione S–transferase
EEC17944.1–glutathione S–transferase
JAA73692.1–glutathione S–transferase
JAB74448.1–salivary sulfotransferase
JAB74492.1–glutathione S–transferase
JAB76061.1–sulfotransferase
JAB76194.1–sulfotransferase partial
AAK97814.1–glutathione peroxidase
EEC00149.1–short–chain alcohol dehydrogenase
EEC04332.1–reductase
EEC10122.1–3–hydroxyanthranilate 3,4–dioxygenase
EEC11990.1–aldehyde dehydrogenase
EEC18729.1–aldehyde dehydrogenase
EEC18748.1–aldehyde dehydrogenase
EEC20421.1–carbonic anhydrase
JAA70808.1–catalase–like
JAA71363.1–glutaredoxin
JAA72149.1–short–chain alcohol dehydrogenase
JAB78793.1–glutathione s–transferase–like
JAB80046.1–3–hydroxyanthranilate 3,4–dioxygenase
AAY66786.1–thioredoxin–dependent peroxide reductase
EEC15288.1–thioredoxin peroxidase 1
EEC08659.1–sulfotransferase
EEC18154.1–superoxide dismutase Cu–Zn
JAA71807.1–copper/zinc superoxide dismutase
EEC10299.1–peroxinectin
AAY66814.1–selenium dependent glutathione peroxidase
EEC10196.1–superoxide dismutase Cu–Zn
24h 48h 72h 96h 120h BD SD
Feeding Time Point

Figure 3. Secretion dynamics of *I. scapularis* tick saliva proteins of unknown function(s), glycine rich and proteins associated with the extracellular matrix (Kim, et al., 2016). Normalized spectral abundance factor (NSAF) for each protein as a proxy for relative abundance is expressed as a percent of total NSAF per time point within each class. Z-scores were calculated and used to generate heat maps as described in materials and methods section. Red color indicates proteins of high abundance and blue color indicates proteins of low abundance, both increasing/decreasing in abundance with color intensity. Dendrograms show protein clustering (C) according to secretion patterns. Branches are labeled starting with the letter of the protein class. Fig 5A (Tick saliva proteins of unknown function), Fig 5B (Glycine-rich), and Fig 5C (Extracellular matrix) are grouped by functional classes.

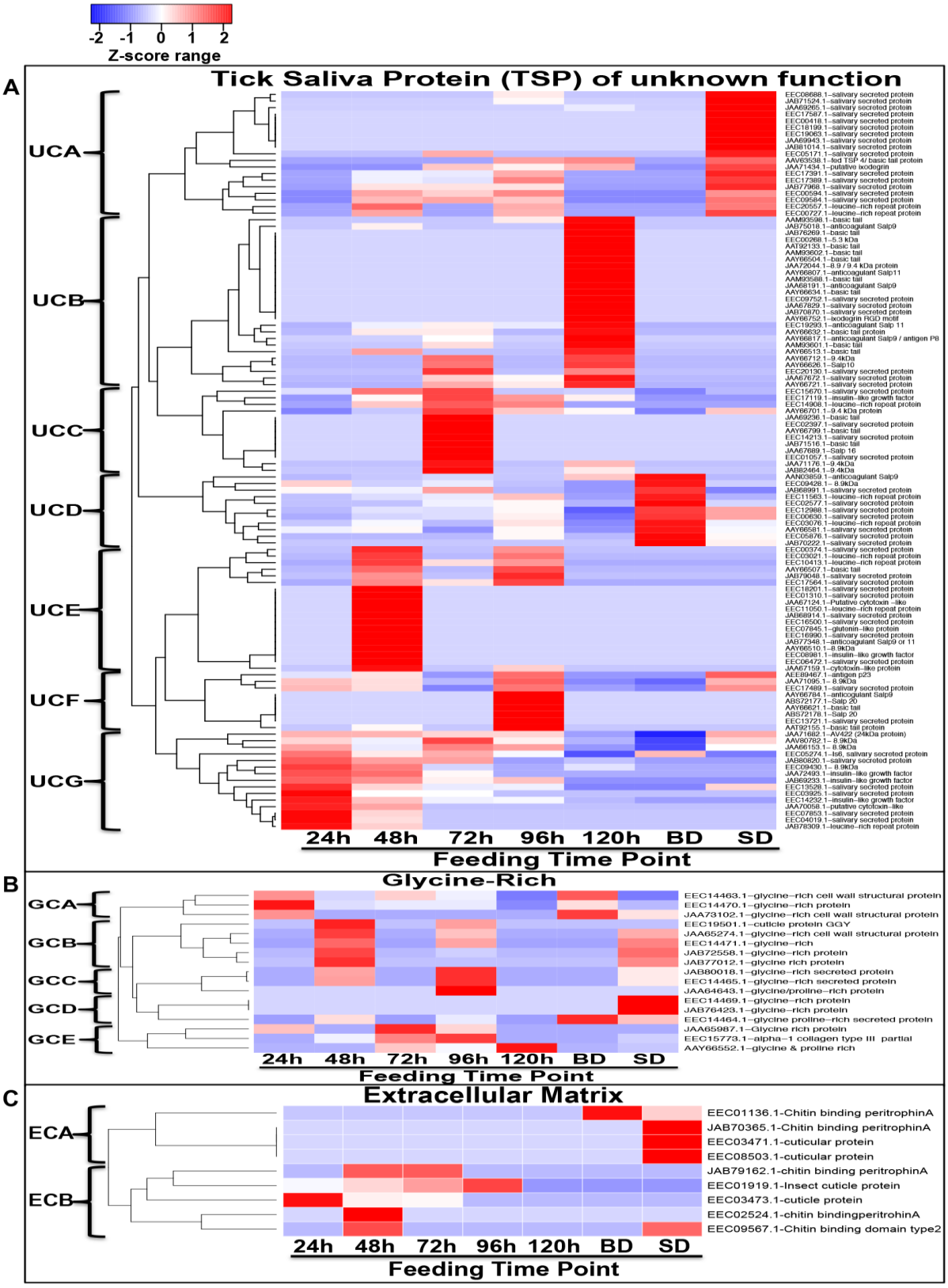
-2 -1 0 1 2
Z-score range
A
Tick Saliva Protein (TSP) of unknown function
UCA
UCB
UCC
UCD
UCE
UCF
UCG
24h 48h 72h 96h 120h BD SD
Feeding Time Point
B
Glycine-Rich
GCA
GCB
GCC
GCD
GCE
24h 48h 72h 96h 120h BD SD
Feeding Time Point
C
Extracellular Matrix
ECA
ECB
EEC01136.1-Chitin binding peritrophinA
JAB70365.1-Chitin binding peritrophinA
EEC03471.1-cuticular protein
EEC08503.1-cuticular protein
JAB79162.1-chitin binding peritrophinA
EEC01919.1-Insect cuticle protein
EEC03473.1-cuticle protein
EEC02524.1-chitin bindingperitrohinA
EEC09567.1-Chitin binding domain type2
24h 48h 72h 96h 120h BD SD
Feeding Time Point

Figure 6. Phylogeny analysis of tick saliva protein of unknown function identified in *I. scapularis* saliva during and after feeding (Kim, et al., 2016). A guide phylogeny tree of tick saliva proteins (TSPs) of unknown function sequences was constructed using the Neighbor Joining method with bootstrap replicates set to 1000. Number at each node represents bootstrap values that signify the level of confidence in the branch. Five main groups cluster as: (CA) basic tail or tailless proteins, (CB) GPIIb/IIIa antagonist, (CC) insulin binding-like proteins (CD) 7-9kDa proteins and (CE) leucine rich proteins.

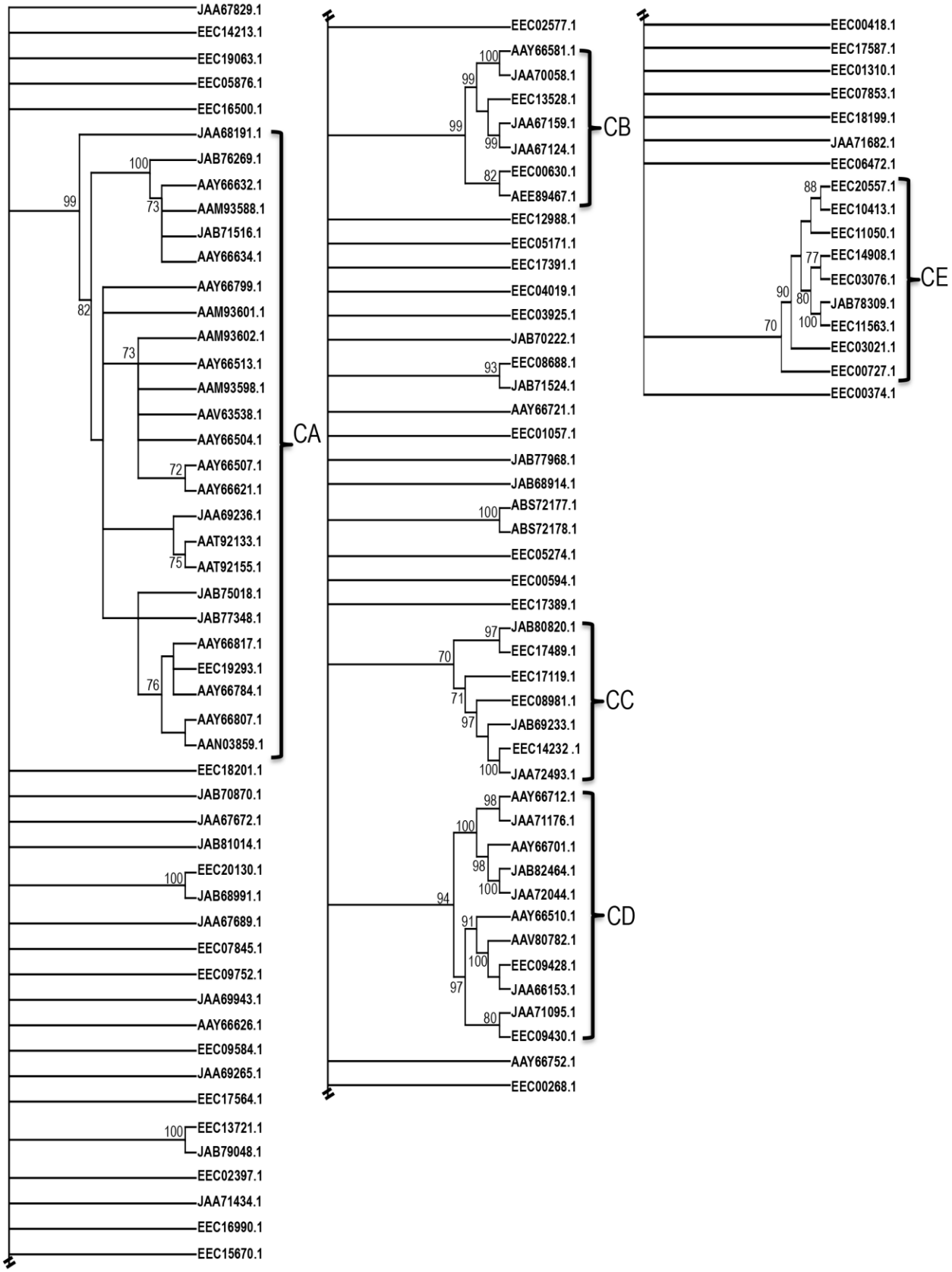
JAA67829.1
EEC14213.1
EEC19063.1
EEC05876.1
EEC16500.1
JAA68191.1
JAB76269.1
AAY66632.1
AAM93588.1
JAB71516.1
AAY66634.1
AAY66799.1
AAM93601.1
AAM93602.1
AAY66513.1
AAM93598.1
AAV63538.1
AAY66504.1
AAY66507.1
AAY66621.1
JAA69236.1
AAT92133.1
AAT92155.1
JAB75018.1
JAB77348.1
AAY66817.1
EEC19293.1
AAY66784.1
AAY66807.1
AAN03859.1
CA
EEC18201.1
JAB70870.1
JAA67672.1
JAB81014.1
EEC20130.1
JAB68991.1
JAA67689.1
EEC07845.1
EEC09752.1
JAA69943.1
AAY66626.1
EEC09584.1
JAA69265.1
EEC17564.1
EEC13721.1
JAB79048.1
EEC02397.1
JAA71434.1
EEC16990.1
EEC15670.1
EEC02577.1
AAY66581.1
JAA70058.1
EEC13528.1
JAA67159.1
JAA67124.1
EEC00630.1
AEE89467.1
CB
EEC12988.1
EEC05171.1
EEC17391.1
EEC04019.1
EEC03925.1
JAB70222.1
EEC08688.1
JAB71524.1
AAY66721.1
EEC01057.1
JAB77968.1
JAB68914.1
ABS72177.1
ABS72178.1
EEC05274.1
EEC00594.1
EEC17389.1
JAB80820.1
EEC17489.1
EEC17119.1
EEC08981.1
JAB69233.1
EEC14232 .1
JAA72493.1
CC
AAY66712.1
JAA71176.1
AAY66701.1
JAB82464.1
JAA72044.1
AAY66510.1
AAV80782.1
EEC09428.1
JAA66153.1
JAA71095.1
EEC09430.1
CD
AAY66752.1
EEC00268.1
EEC00418.1
EEC17587.1
EEC01310.1
EEC07853.1
EEC18199.1
JAA71682.1
EEC06472.1
EEC20557.1
EEC10413.1
EEC11050.1
EEC14908.1
EEC03076.1
JAB78309.1
EEC11563.1
EEC03021.1
EEC00727.1
CE
EEC00374.1

Figure 7. Relative abundance of tick saliva proteins (TSP) of unknown function during and after feeding (Kim, et al., 2016). Normalized spectral abundance factor (NSAF) for TSP that segregated together in Fig 6 was subjected to Z-score statistic analysis and used to generate heat maps as described in materials and methods section "Relative abundance and graphical visualization". Red color indicates proteins of high abundance and blue color indicates proteins of low abundance, both increasing/decreasing in abundance with color intensity. Clustering patterns of dendrograms were based on similarity in secretion patterns. A= basic tail or tailless proteins, B= GPIIb/IIIa antagonist, C= insulin-like growth factor binding proteins, D= 7-9kDa proteins, and E= Leucine-rich proteins.

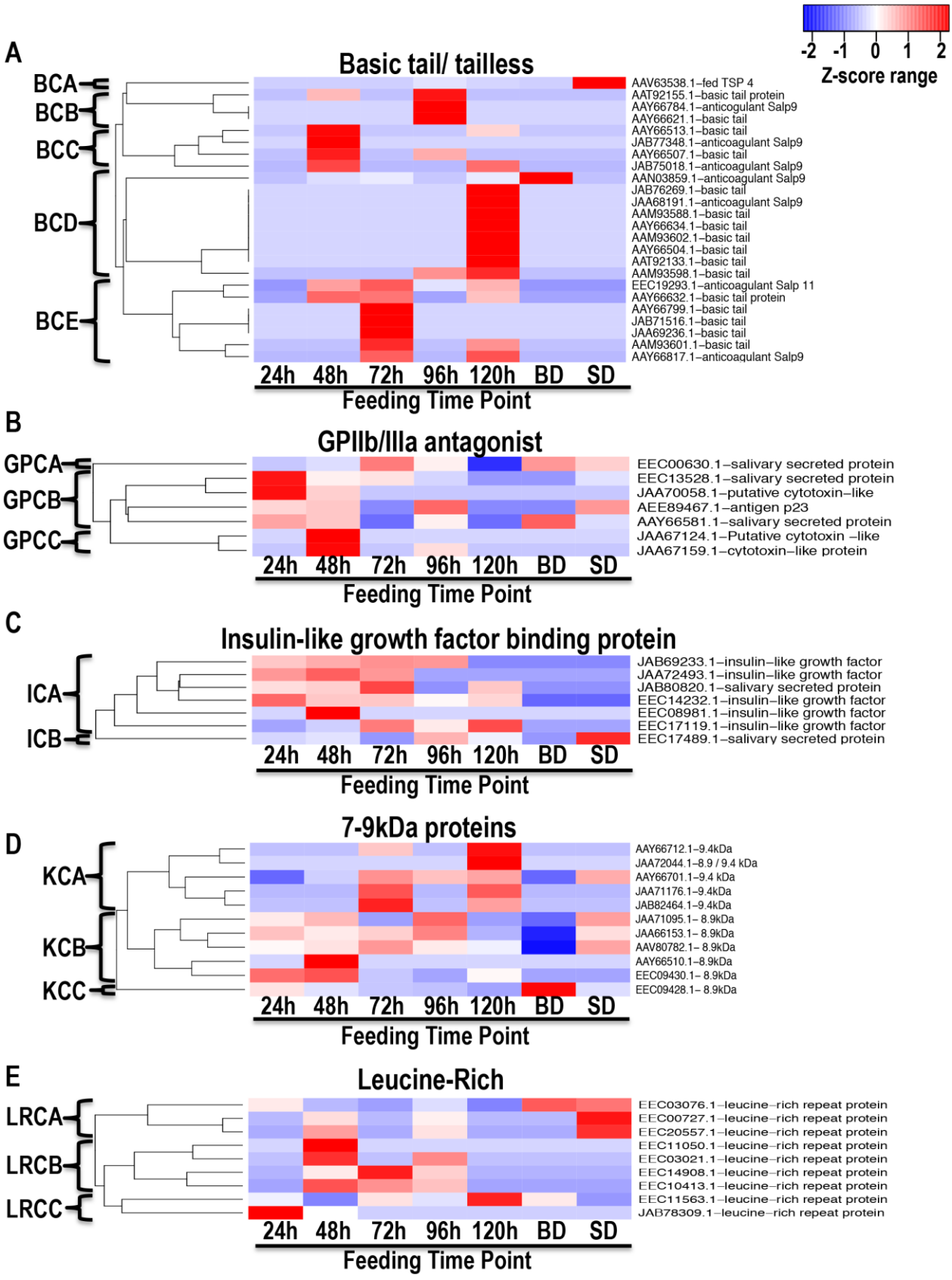
A
Basic tail/ tailless
BCA
BCB
BCC
BCD
BCE
AAV63538.1–fed TSP 4
AAT92155.1–basic tail protein
AAY66784.1–anticogulant Salp9
AAY66621.1–basic tail
AAY66513.1–basic tail
JAB77348.1–anticoagulant Salp9
AAY66507.1–basic tail
JAB75018.1–anticoagulant Salp9
AAN03859.1–anticoagulant Salp9
JAB76269.1–basic tail
JAA68191.1–anticoagulant Salp9
AAM93588.1–basic tail
AAY66634.1–basic tail
AAM93602.1–basic tail
AAY66504.1–basic tail
AAT92133.1–basic tail
AAM93598.1–basic tail
EEC19293.1–anticoagulant Salp 11
AAY66632.1–basic tail protein
AAY66799.1–basic tail
JAB71516.1–basic tail
JAA69236.1–basic tail
AAM93601.1–basic tail
AAY66817.1–anticoagulant Salp9
24h 48h 72h 96h 120h BD SD
Feeding Time Point
-2 -1 0 1 2
Z-score range
B
GPIIb/IIIa antagonist
GPCA
GPCB
GPCC
EEC00630.1–salivary secreted protein
EEC13528.1–salivary secreted protein
JAA70058.1–putative cytotoxin–like
AEE89467.1–antigen p23
AAY66581.1–salivary secreted protein
JAA67124.1–Putative cytotoxin –like
JAA67159.1–cytotoxin–like protein
24h 48h 72h 96h 120h BD SD
Feeding Time Point
C
Insulin-like growth factor binding protein
ICA
ICB
JAB69233.1–insulin–like growth factor
JAA72493.1–insulin–like growth factor
JAB80820.1–salivary secreted protein
EEC14232.1–insulin–like growth factor
EEC08981.1–insulin–like growth factor
EEC17119.1–insulin–like growth factor
EEC17489.1–salivary secreted protein
24h 48h 72h 96h 120h BD SD
Feeding Time Point
D
7-9kDa proteins
KCA
KCB
KCC
AAY66712.1–9.4kDa
JAA72044.1–8.9 / 9.4 kDa
AAY66701.1–9.4 kDa
JAA71176.1–9.4kDa
JAB82464.1–9.4kDa
JAA71095.1– 8.9kDa
JAA66153.1– 8.9kDa
AAV80782.1– 8.9kDa
AAY66510.1–8.9kDa
EEC09430.1– 8.9kDa
EEC09428.1– 8.9kDa
24h 48h 72h 96h 120h BD SD
Feeding Time Point
E
Leucine-Rich
LRCA
LRCB
LRCC
EEC03076.1–leucine–rich repeat protein
EEC00727.1–leucine–rich repeat protein
EEC20557.1–leucine–rich repeat protein
EEC11050.1–leucine–rich repeat protein
EEC03021.1–leucine–rich repeat protein
EEC14908.1–leucine–rich repeat protein
EEC10413.1–leucine–rich repeat protein
EEC11563.1–leucine–rich repeat protein
JAB78309.1–leucine–rich repeat protein
24h 48h 72h 96h 120h BD SD
Feeding Time Point

Table 1 Numbers and cumulative relative abundance of tick protein classes in *I. scapularis* saliva (Kim, et al., 2016).

	Feeding Time Point													
	24		48		72		96		120		BD		SD	
Functional Class	Protein	NSAF (%)*	Protein	NSAF (%)*	Protein	NSAF (%)*	Protein	NSAF (%)*	Protein	NSAF (%)*	Protein	NSAF (%)*	Protein	NSAF (%)*
Anti-oxidant	1	0.08	6	1.37	3	1.27	3	1.38	3	0.82	6	2.43	32	7.43
Anti-microbial/ Pathogen recognition domain	4	17.5	11	16.8	6	10.7	6	5.52	4	5.11	5	6.71	7	6.53
Cytoskeletal	6	2.25	16	3.43	9	2.68	10	2.94	1	0.39	6	1.77	27	4.88
Extracellular matrix/cell adhesion	2	0.38	5	0.89	3	1.41	1	0.6	0	0	1	0.97	5	1.08
Glycine-rich protein	4	1.1	11	2.38	5	3.3	13	4.32	2	1.39	4	5.57	14	4.6
Heme/iron metabolism	11	13.6	15	13.5	11	13.1	15	23.9	8	11	7	23.7	12	7.74
Lipocalin	2	0.3	1	0.06	3	0.95	3	0.55	12	5.82	0	0	7	2.56
Metabolism, amino acid	0	0	0	0	0	0	0	0	0	0	1	0.5	20	3.04
Metabolism, carbohydrate	2	0.19	4	0.66	1	0.16	4	0.62	4	0.53	5	2.47	20	3.72
Metabolism, energy	2	0.62	8	0.97	2	0.24	2	0.24	5	1.32	5	3.23	40	8.13
Metabolism, intermediate	0	0	0	0	0	0	0	0	0	0	0	0	1	0.07
Metabolism, lipid	1	0.09	2	0.13	1	0.14	1	0.07	0	0	0	0	14	1.12
Metabolism, nucleotide	0	0	2	0.1	0	0	1	0.17	1	0.72	3	2.15	14	4.07
Nuclear regulation	1	0.6	2	0.76	1	0.55	1	0.76	1	0.42	1	2.48	7	1.33
Proteinase	3	0.54	18	3.37	4	0.45	17	5.57	10	2.98	1	0.59	15	1.14
Proteinase inhibitor	25	24.7	35	16.9	22	15	28	13.1	15	8.11	16	20.8	25	6.72
Protein export machinery	0	0	3	0.21	1	0.07	0	0	1	0.62	2	1.3	9	1.42
Protein modification machinery	5	2.58	10	3.17	4	5.25	10	2.47	8	1.92	14	8.51	46	13.2
Protein synthesis machinery	0	0	1	0.04	1	0.1	0	0	1	0.12	5	2.54	24	3.26
Proteasome machinery	1	0.05	2	0.1	1	0.08	1	0.05	1	0.11	1	0.19	10	1.13
Signal transduction	1	0.35	3	0.56	0	0	2	0.18	0	0	0	0	8	1.16
Transcription machinery	0	0	1	0.1	0	0	1	0.06	0	0	0	0	7	0.6
Transporters/receptors	0	0	8	1.07	1	0.03	7	1.25	1	0.02	2	0.15	15	1.57
TSP of unknown function	27	35	62	33.5	51	44.5	52	36.2	50	58.6	12	13.9	39	13.5
Total	98	100	226	100	130	100	178	100	128	100	96	100	418	100

Table 2 Numbers and cumulative relative abundance of host (rabbit) protein classes in *I. scapularis* saliva (Kim, et al., 2016).

	Feeding Time Point													
	24		48		72		96		120		BD		SD	
Functional Class	Protein	NSAF (%)*	Protein	NSAF (%)*	Protein	NSAF (%)*	Protein	NSAF (%)*	Protein	NSAF (%)*	Protein	NSAF (%)*	Protein	NSAF (%)*
Cytoskeletal	0	0	1	0.65	3	1.2	1	0.05	2	2.04	1	1.15	1	1.28
Oxidant metabolism/ detoxification	0	0	0	0	0	0	0	0	0	0	0	0	1	0.16
Extracellular matrix/cell adhesion	0	0	1	0.22	1	0.08	2	0.67	0	0	2	1.35	1	0.46
Fibrinogen	0	0	0	0	0	0	1	0.25	0	0	1	0.34	3	3.13
Heme/iron metabolism	2	74.5	5	39.5	2	2.53	4	17.2	4	41.9	3	15.5	6	16.8
Hemoglobin/RBC products	1	7.63	2	7.81	1	1.13	2	9.15	2	16.4	3	50.2	3	39.3
Immunity	1	5.62	6	30	5	6.71	9	29.6	8	27.6	2	9.38	10	24.6
Keratin	5	12.2	5	6.85	6	2.57	7	32.5	5	9.82	5	13.6	1	0.31
Metabolism, carbohydrate	0	0	0	0	5	15.5	0	0	0	0	0	0	0	0
Metabolism, energy	0	0	0	0	3	6.39	0	0	0	0	0	0	1	0.97
Metabolism, lipid	0	0	0	0	1	4.85	0	0	0	0	0	0	0	0
Metabolism, nucleotide	0	0	0	0	1	1.21	0	0	0	0	0	0	0	0
Nuclear regulation	0	0	2	10.3	2	1.41	1	5.98	0	0	1	2.64	1	4.2
Proteinase inhibitor	0	0	1	0.47	0	0	0	0	0	0	0	0	2	0.81
Protein export machinery	0	0	2	3.1	4	3.13	1	4.17	2	1.63	2	3.64	2	4.06
Protein modification machinery	0	0	1	1.04	10	36.7	1	0.39	1	0.6	1	1.47	3	2.49
Protein synthesis machinery	0	0	0	0	4	15.8	0	0	0	0	1	0.74	2	1.43
Transcription machinery	0	0	0	0	2	0.74	0	0	0	0	0	0	0	0
Total	9	100	26	100	50	100	29	100	24	100	22	100	37	100

References

Kim, T.K., Tirloni, L., Pinto, A.F., Moresco, J., Yates, J.R.,3rd, da Silva Vaz, I.,Jr, Mulenga, A., 2016. *Ixodes scapularis* tick saliva proteins sequentially secreted every 24 h during blood feeding. PLoS Negl Trop. Dis. 10, e0004323.

APPENDIX II

CHAPTER II Part II FIGURES AND TABLES

Figure 1: Identification of *Amblyomma americanum* tick saliva proteins. Adult *A. americanum* ticks that were partially fed for 24, 72, 120, and 168 h were stimulated to salivate by injecting 2% pilocarpine into hemolymph. Saliva was electrophoresed on a 12.5% acrylamide gel and Coommassie blue stained. Protein bands were excised and then gel slices (C1-C29, D1-D43, E1-E46, and F1-F39) were subjected to LC-MS/MS sequencing protein identification using the "In-Gel" digestion method as described. Please note that proteins that were identified from gel slices are summarized in Tables 1A (≥250 kDa to 150-100 kDa proteins), 1B (100-75 kDa to 50-37 kDa proteins), and 1C (37-25 kDa to 15-10 kDa).

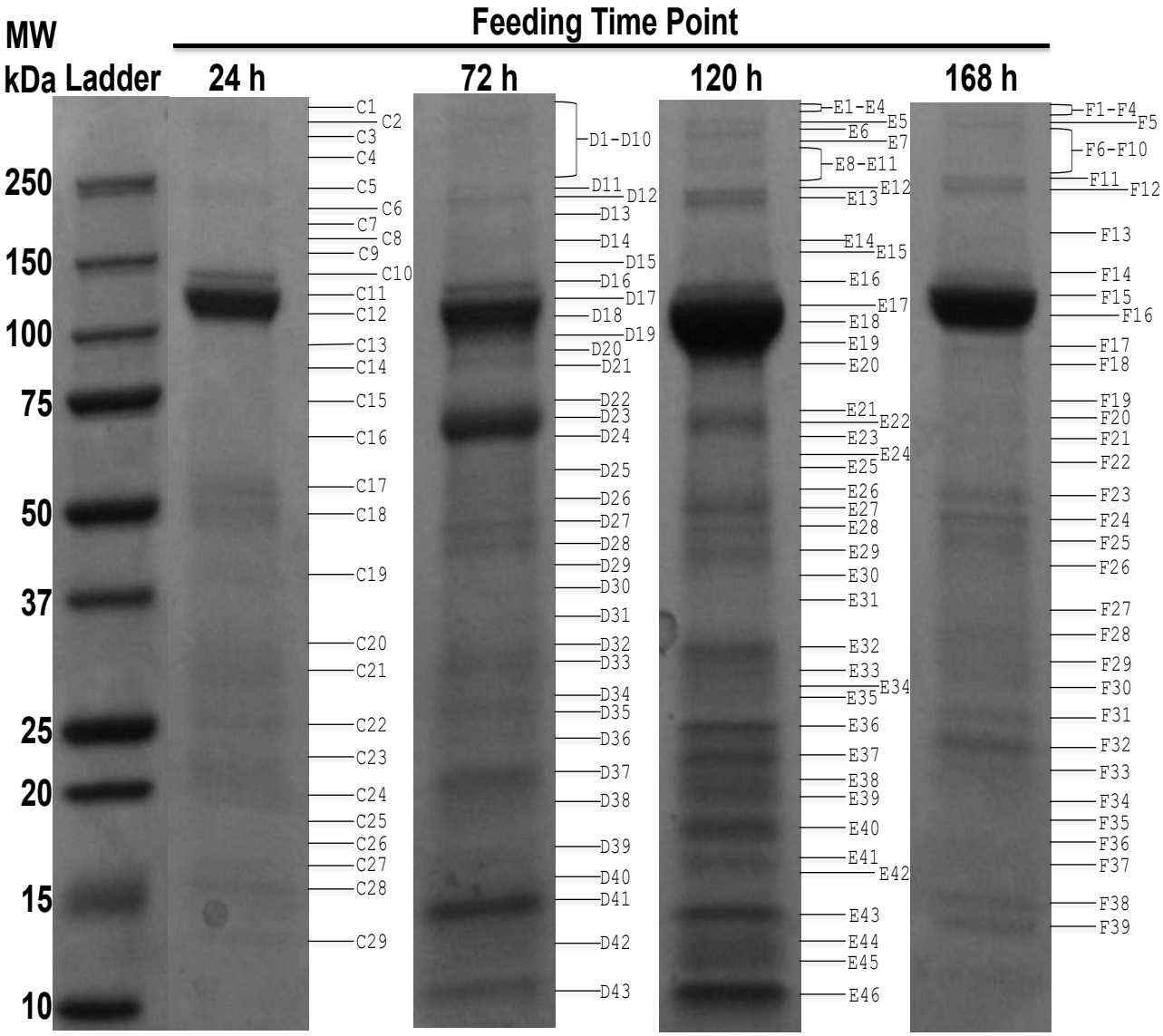
MW
kDa Ladder
Feeding Time Point
24 h
72 h
120 h
168 h
250
150
100
75
50
37
25
20
15
10
C1
C2
C3
C4
C5
C6
C7
C8
C9
C10
C11
C12
C13
C14
C15
C16
C17
C18
C19
C20
C21
C22
C23
C24
C25
C26
C27
C28
C29
D1-D10
D11
D12
D13
D14
D15
D16
D17
D18
D19
D20
D21
D22
D23
D24
D25
D26
D27
D28
D29
D30
D31
D32
D33
D34
D35
D36
D37
D38
D39
D40
D41
D42
D43
E1-E4
E5
E6
E7
E8-E11
E12
E13
E14
E15
E16
E17
E18
E19
E20
E21
E22
E23
E24
E25
E26
E27
E28
E29
E30
E31
E32
E33
E34
E35
E36
E37
E38
E39
E40
E41
E42
E43
E44
E45
E46
F1-F4
F5
F6-F10
F11
F12
F13
F14
F15
F16
F17
F18
F19
F20
F21
F22
F23
F24
F25
F26
F27
F28
F29
F30
F31
F32
F33
F34
F35
F36
F37
F38
F39

Figure 2: Protein (Figure 2A = tick saliva proteins, Figure 2B = rabbit host proteins) composition in *Amblyomma americanum* tick saliva every 24 h during feeding: Pilocarpine induced *A. americanum* tick saliva was subjected to LC-MS/MS sequencing using the "In-Solution" digestion approach as described in materials and methods. Cumulative normalized spectral abundance factors (NSAF) values as index for relative abundance of detected proteins are presented for each functional class. Please note the labels are oriented horizontally and read left to right starting from cytoskeletal proteins (red), antioxidant/detoxification (green), extracellular matrix (orange), then back to glycine rich proteins (light-tan), immune related (pink) and continues this pattern.

A

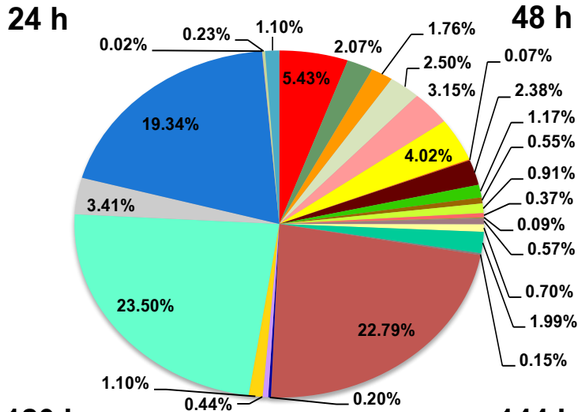

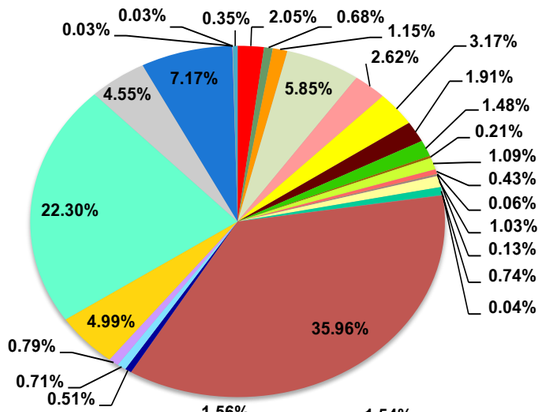

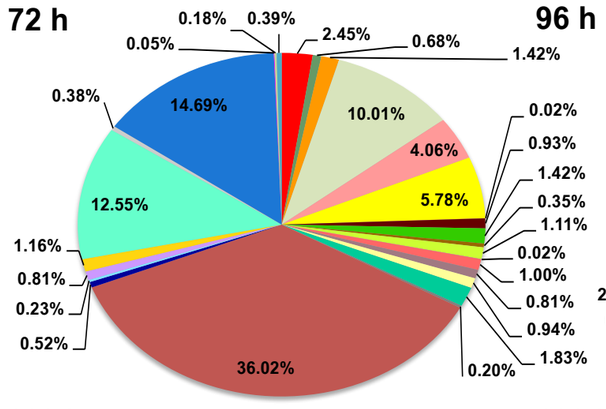

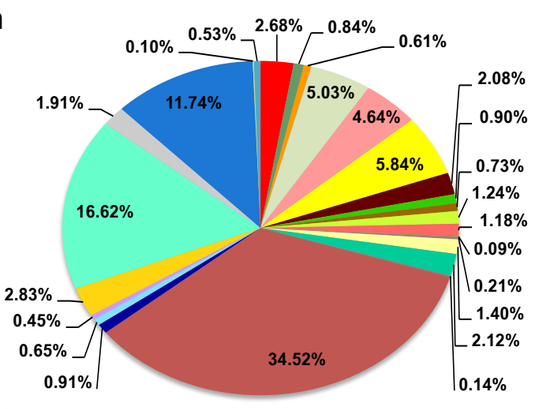

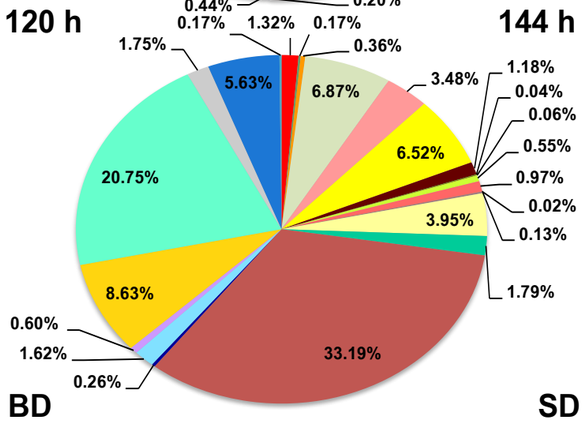

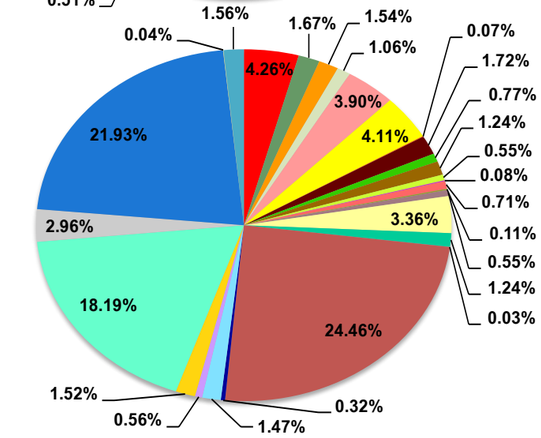

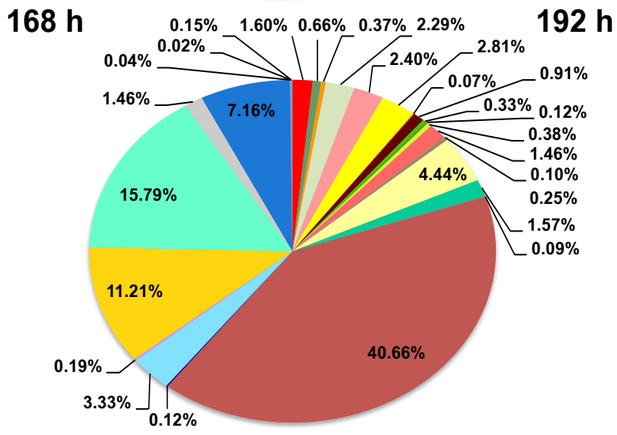

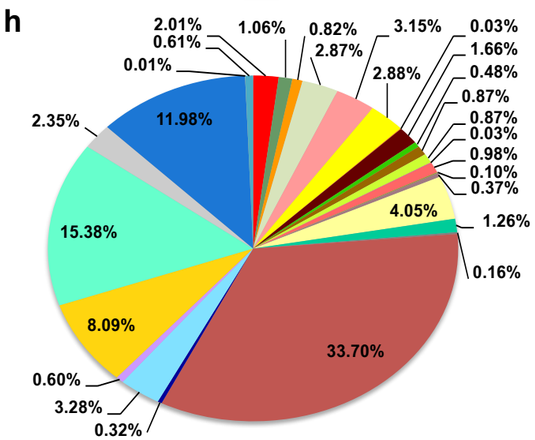

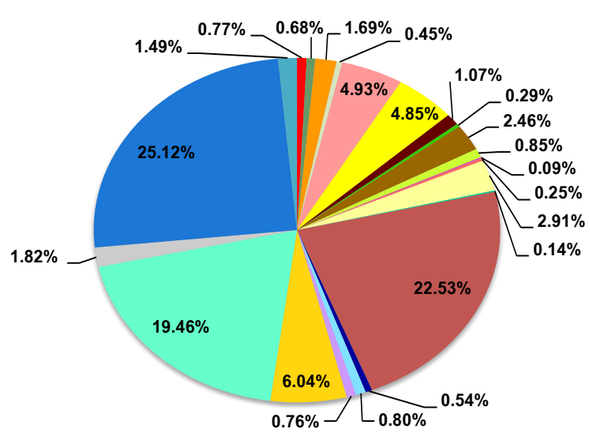

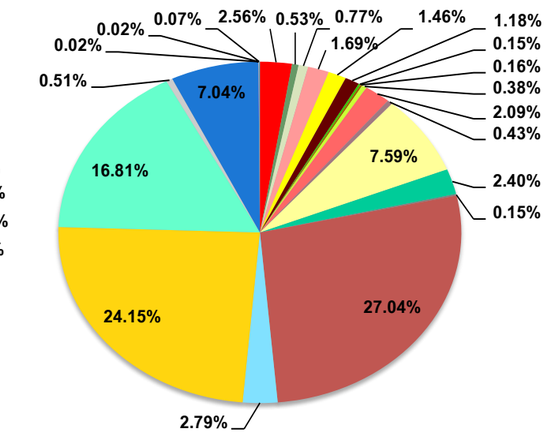

Key:

- Cytoskeletal
- Glycine rich
- Metabolism,amino acid
- Metabolism,carbohydrates
- Nuclear regulation
- Protease
- TSP of unknown function
- Ixodegrin
- Signal transduction
- Transcription machinery
- Antioxidant/ Detoxification
- Immune related
- Metabolism,nucleic acid
- Metabolism,lipid
- Protein export
- Proteosome machinery
- Mucin
- Histamine binding protein/ Lipocalin
- Heme/ Iron binding
- Transporter/ Receptor
- Extracellular matrix
- Antimicrobial
- Metabolism,energy
- Metabolism,intermediates
- Protein modification
- Protein synthesis
- Evasin
- Protease inhibitor
- Transposon element

B

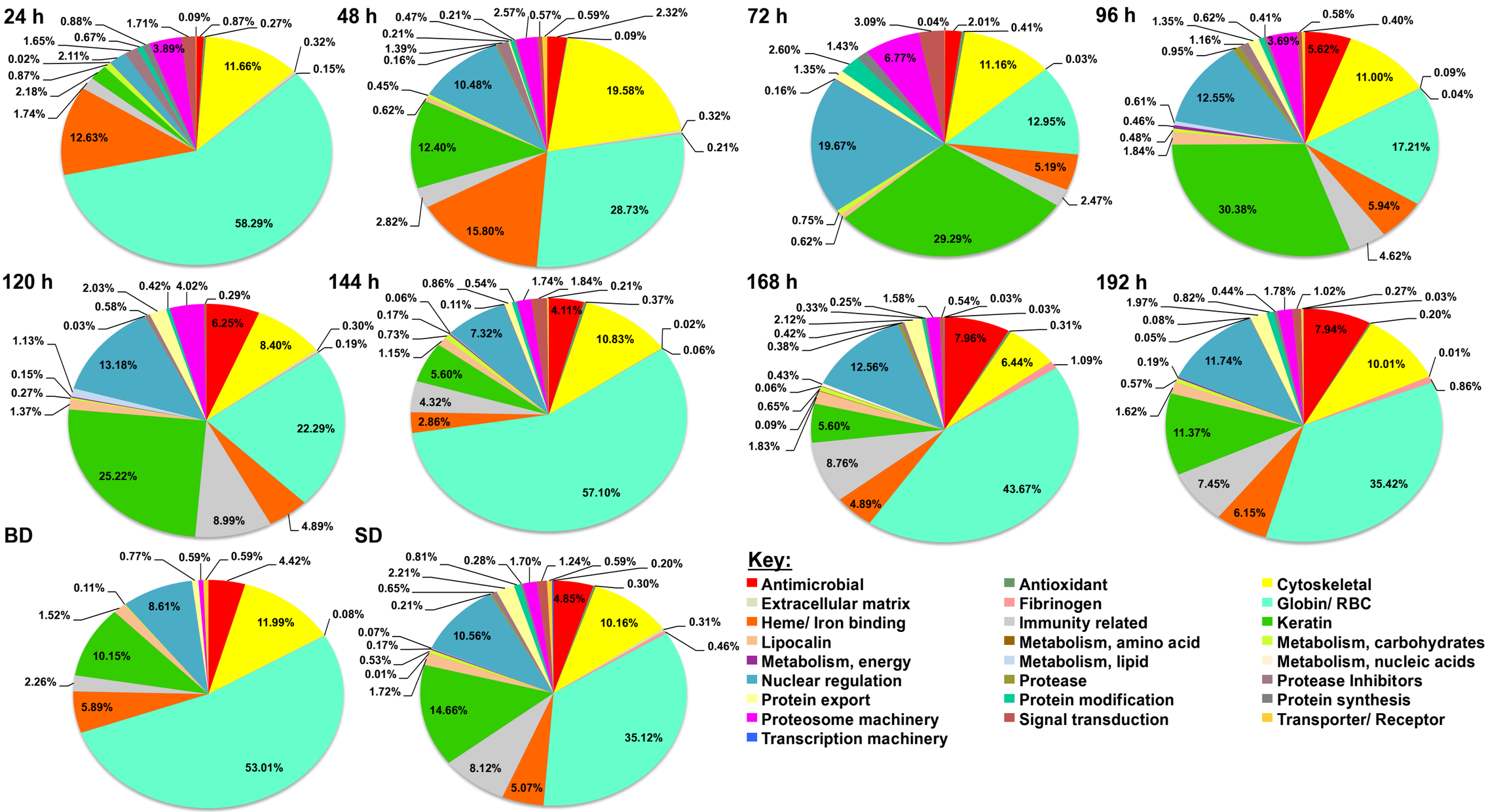
24 h
0.88%
1.71%
0.09%
0.87%
0.27%
1.65%
0.67%
3.89%
0.32%
0.02%
2.11%
11.66%
0.15%
0.87%
2.18%
1.74%
12.63%
58.29%
48 h
0.47%
0.21%
2.57%
0.57%
0.59%
2.32%
0.21%
0.09%
1.39%
0.16%
19.58%
0.45%
10.48%
0.32%
0.62%
0.21%
12.40%
2.82%
15.80%
28.73%
72 h
3.09%
0.04%
2.01%
0.41%
2.60%
1.43%
6.77%
11.16%
0.03%
1.35%
0.16%
12.95%
19.67%
5.19%
2.47%
0.75%
0.62%
29.29%
96 h
1.35%
0.62%
0.41%
0.58%
0.40%
1.16%
0.95%
3.69%
5.62%
11.00%
0.09%
0.61%
12.55%
0.04%
0.46%
17.21%
0.48%
1.84%
30.38%
5.94%
4.62%
120 h
2.03%
0.42%
4.02%
0.29%
0.58%
6.25%
0.03%
8.40%
0.30%
1.13%
13.18%
0.19%
0.15%
22.29%
0.27%
1.37%
25.22%
8.99%
4.89%
144 h
0.86%
0.54%
1.74%
1.84%
0.21%
0.06%
0.11%
4.11%
0.37%
0.17%
0.73%
7.32%
10.83%
0.02%
1.15%
0.06%
5.60%
4.32%
2.86%
57.10%
168 h
0.33%
0.25%
1.58%
0.54%
0.03%
2.12%
0.03%
0.42%
7.96%
0.31%
0.38%
12.56%
6.44%
1.09%
0.43%
0.06%
0.65%
5.60%
0.09%
1.83%
8.76%
4.89%
43.67%
192 h
1.97%
0.82%
0.44%
1.78%
1.02%
0.27%
0.03%
0.08%
0.20%
0.05%
7.94%
10.01%
0.01%
0.19%
11.74%
0.86%
0.57%
1.62%
11.37%
7.45%
6.15%
35.42%
BD
0.77%
0.59%
0.59%
4.42%
0.11%
8.61%
1.52%
11.99%
0.08%
10.15%
2.26%
5.89%
53.01%
SD
0.81%
0.28%
1.70%
1.24%
0.59%
0.20%
2.21%
0.30%
0.65%
4.85%
0.21%
10.16%
0.31%
0.07%
10.56%
0.46%
0.17%
0.53%
0.01%
1.72%
14.66%
35.12%
8.12%
5.07%
Key:
Antimicrobial
Extracellular matrix
Heme/ Iron binding
Lipocalin
Metabolism, energy
Nuclear regulation
Protein export
Proteosome machinery
Transcription machinery
Antioxidant
Fibrinogen
Immunity related
Metabolism, amino acid
Metabolism, lipid
Protease
Protein modification
Signal transduction
Cytoskeletal
Globin/ RBC
Keratin
Metabolism, carbohydrates
Metabolism, nucleic acids
Protease Inhibitors
Protein synthesis
Transporter/ Receptor

Figure 3: Overall secretion dynamics of protein classes in *Amblyomma americanum* tick saliva. Normalized spectral abundance factors (NSAF) values of tick (Figure 3A) and rabbit host (Figure 3B) were normalized using the z-score statistics and then used to generate heat maps using heatmap2 function in gplots library using R as described in materials and methods.

A

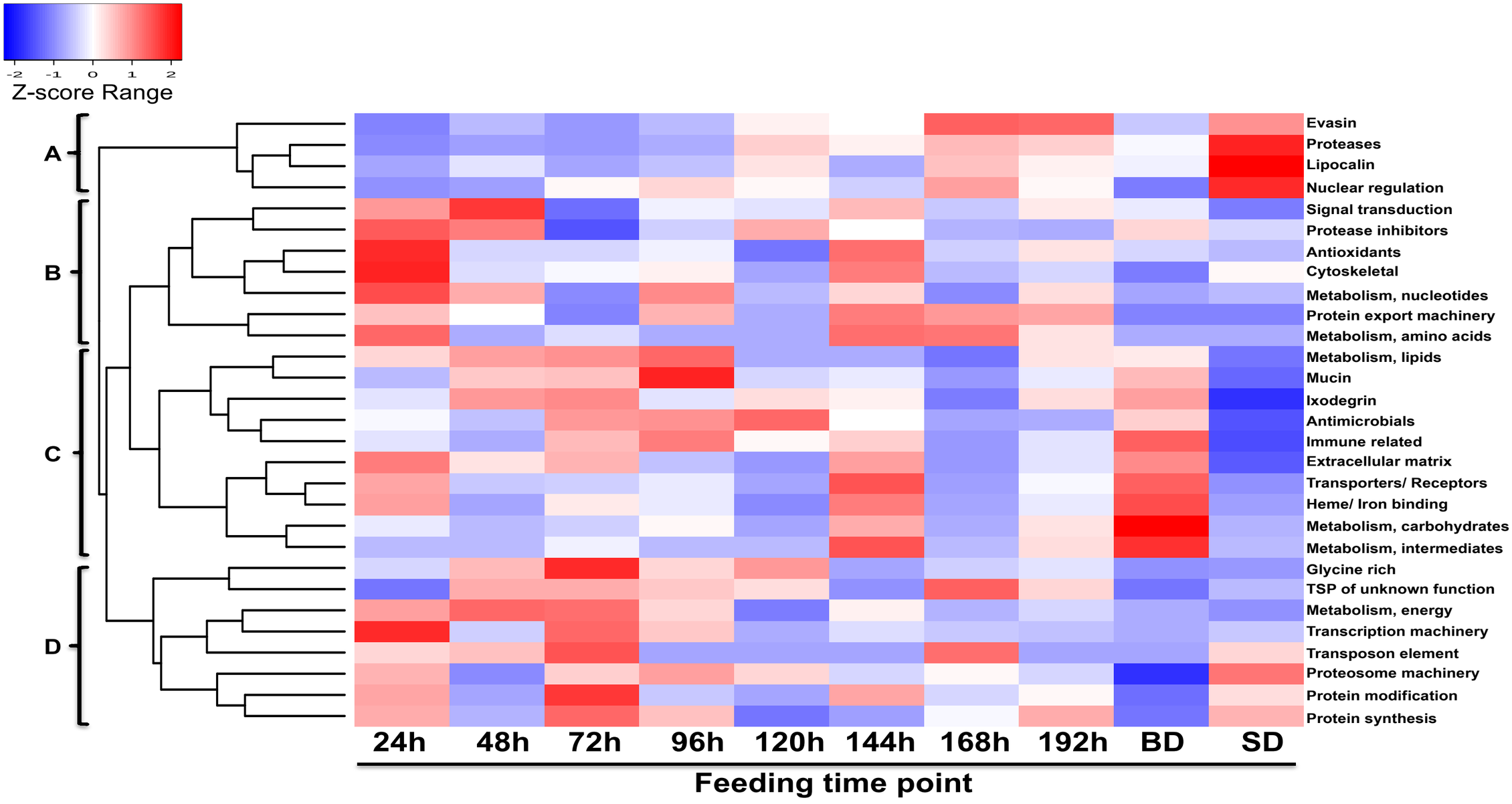
-2
-1
0
1
2
Z-score Range
A
B
C
D
Evasin
Proteases
Lipocalin
Nuclear regulation
Signal transduction
Protease inhibitors
Antioxidants
Cytoskeletal
Metabolism, nucleotides
Protein export machinery
Metabolism, amino acids
Metabolism, lipids
Mucin
Ixodegrin
Antimicrobials
Immune related
Extracellular matrix
Transporters/ Receptors
Heme/ Iron binding
Metabolism, carbohydrates
Metabolism, intermediates
Glycine rich
TSP of unknown function
Metabolism, energy
Transcription machinery
Transposon element
Proteosome machinery
Protein modification
Protein synthesis
24h
48h
72h
96h
120h
144h
168h
192h
BD
SD
Feeding time point

B

-2 -1 0 1 2

Z-score Range

A

B

C

D

Transporters/ Receptors
Transcription machinery
Globin/ RBC
Heme/ Iron binding
Cytoskeletal
Protease inhibitors
Extracellular matrix
Antioxidants
Metabolism, carbohydrates
Protein synthesis
Protein modification
Signal transduction
Proteosome machinery
Fibrinogen
Metabolism, nucleotides
Metabolism, amino acids
Antimicrobials
Lipocalin
Protein export machinery
Immune related
Nuclear regulation
Keratin
Metabolism, lipids
Metabolism, energy
Proteases

24h 48h 72h 96h 120h 144h 168h 192h BD SD

Feeding time point

Figure 4: Secretion dynamics of non-housekeeping tick saliva protein families in *Amblyomma americanum* tick saliva. Normalized spectral abundance factors (NSAF) values of tick saliva proteins that did not show similarity to housekeeping proteins were normalized using the z-score statistics and then used to generate heat maps using heatmap2 function in gplots library using R as described in materials and methods. (Protease Inhibitors are labeled as A- Serpins, B- Cystatins, C- α2-macroglobulin, D-Kunitz type, E- trypsin inhibitor like; Protease are labeled as F- cysteine, G- metalloprotease, H- serine; and other protein classes as I- Lipocalin, J- heme/iron binding, K- antioxidants, L- glycine rich, M- extracellular matrix, N- antimicrobial, O- Mucin/ mucin-like, P- Evasin ,Q- Ixodegrin, R- Immune related, and S- tick saliva proteins of unknown function).

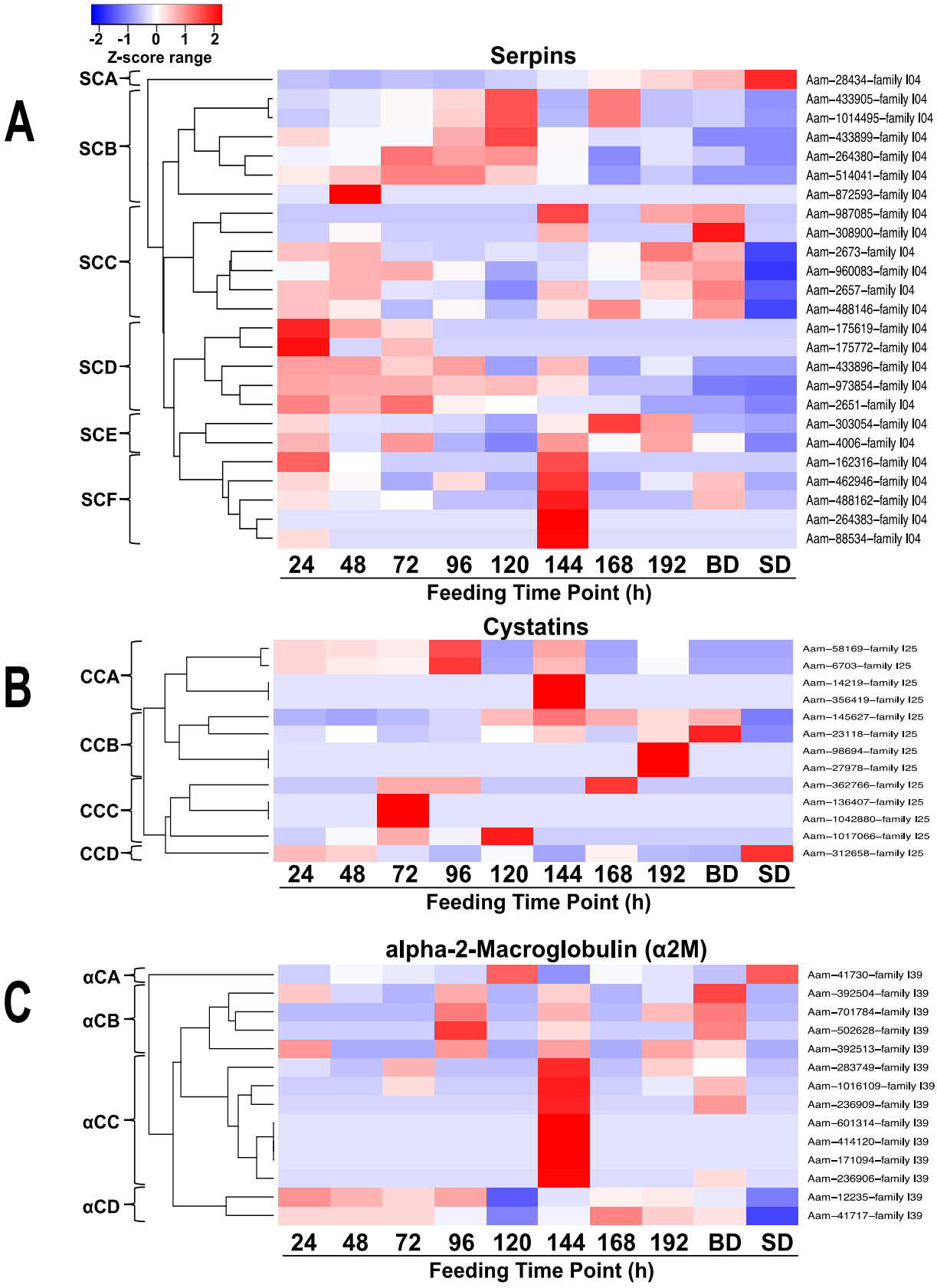
A
Z-score range
-2 -1 0 1 2
Serpins
SCA
SCB
SCC
SCD
SCE
SCF
Aam-28434-family I04
Aam-433905-family I04
Aam-1014495-family I04
Aam-433899-family I04
Aam-264380-family I04
Aam-514041-family I04
Aam-872593-family I04
Aam-987085-family I04
Aam-308900-family I04
Aam-2673-family I04
Aam-960083-family I04
Aam-2657-family I04
Aam-488146-family I04
Aam-175619-family I04
Aam-175772-family I04
Aam-433896-family I04
Aam-973854-family I04
Aam-2651-family I04
Aam-303054-family I04
Aam-4006-family I04
Aam-162316-family I04
Aam-462946-family I04
Aam-488162-family I04
Aam-264383-family I04
Aam-88534-family I04
24 48 72 96 120 144 168 192 BD SD
Feeding Time Point (h)
B
Cystatins
CCA
CCB
CCC
CCD
Aam-58169-family I25
Aam-6703-family I25
Aam-14219-family I25
Aam-356419-family I25
Aam-145627-family I25
Aam-23118-family I25
Aam-98694-family I25
Aam-27978-family I25
Aam-362766-family I25
Aam-136407-family I25
Aam-1042880-family I25
Aam-1017066-family I25
Aam-312658-family I25
24 48 72 96 120 144 168 192 BD SD
Feeding Time Point (h)
C
alpha-2-Macroglobulin (α2M)
αCA
αCB
αCC
αCD
Aam-41730-family I39
Aam-392504-family I39
Aam-701784-family I39
Aam-502628-family I39
Aam-392513-family I39
Aam-283749-family I39
Aam-1016109-family I39
Aam-236909-family I39
Aam-601314-family I39
Aam-414120-family I39
Aam-171094-family I39
Aam-236906-family I39
Aam-12235-family I39
Aam-41717-family I39
24 48 72 96 120 144 168 192 BD SD
Feeding Time Point (h)

D

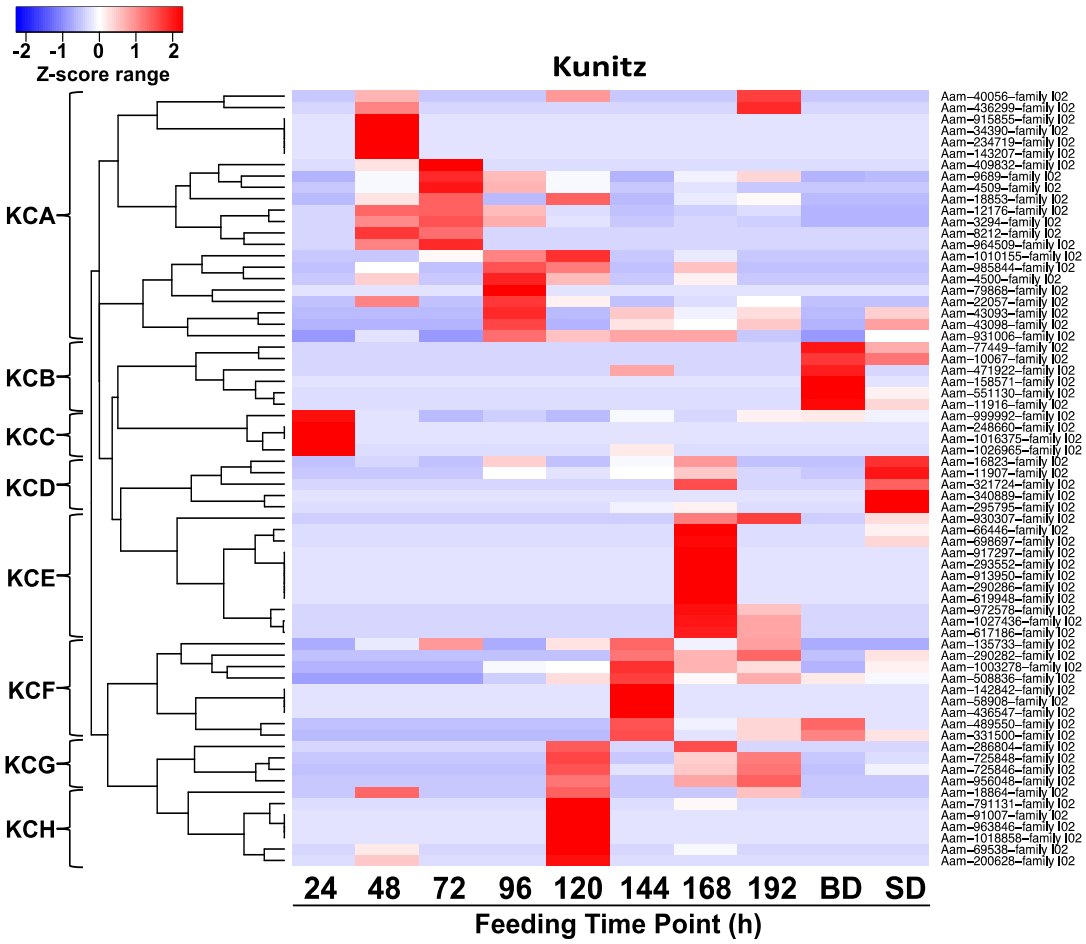
-2 -1 0 1 2
Z-score range
Kunitz
KCA
KCB
KCC
KCD
KCE
KCF
KCG
KCH
Aam–40056–family I02
Aam–436299–family I02
Aam–915855–family I02
Aam–34390–family I02
Aam–234719–family I02
Aam–143207–family I02
Aam–409832–family I02
Aam–9689–family I02
Aam–4509–family I02
Aam–18853–family I02
Aam–12176–family I02
Aam–3294–family I02
Aam–8212–family I02
Aam–964509–family I02
Aam–1010155–family I02
Aam–985844–family I02
Aam–4500–family I02
Aam–79868–family I02
Aam–22057–family I02
Aam–43093–family I02
Aam–43098–family I02
Aam–931006–family I02
Aam–77449–family I02
Aam–10067–family I02
Aam–471922–family I02
Aam–158571–family I02
Aam–551130–family I02
Aam–11916–family I02
Aam–999992–family I02
Aam–248660–family I02
Aam–1016375–family I02
Aam–1026965–family I02
Aam–16823–family I02
Aam–11907–family I02
Aam–321724–family I02
Aam–340889–family I02
Aam–295795–family I02
Aam–930307–family I02
Aam–66446–family I02
Aam–698697–family I02
Aam–917297–family I02
Aam–293552–family I02
Aam–913950–family I02
Aam–290286–family I02
Aam–619948–family I02
Aam–972578–family I02
Aam–1027436–family I02
Aam–617186–family I02
Aam–135733–family I02
Aam–290282–family I02
Aam–1003278–family I02
Aam–508836–family I02
Aam–142842–family I02
Aam–58908–family I02
Aam–436547–family I02
Aam–489550–family I02
Aam–331500–family I02
Aam–286804–family I02
Aam–725848–family I02
Aam–725846–family I02
Aam–956048–family I02
Aam–18864–family I02
Aam–791131–family I02
Aam–91007–family I02
Aam–963846–family I02
Aam–1018858–family I02
Aam–69538–family I02
Aam–200628–family I02
24 48 72 96 120 144 168 192 BD SD
Feeding Time Point (h)

E

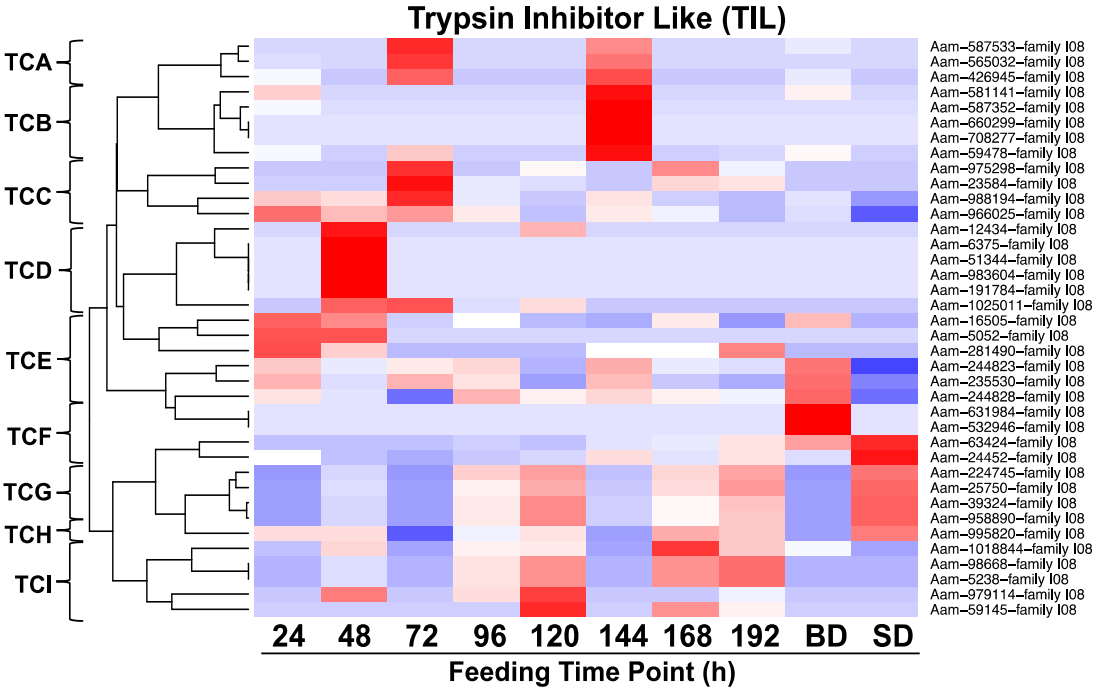
Trypsin Inhibitor Like (TIL)
TCA
TCB
TCC
TCD
TCE
TCF
TCG
TCH
TCI
Aam–587533–family I08
Aam–565032–family I08
Aam–426945–family I08
Aam–581141–family I08
Aam–587352–family I08
Aam–660299–family I08
Aam–708277–family I08
Aam–59478–family I08
Aam–975298–family I08
Aam–23584–family I08
Aam–988194–family I08
Aam–966025–family I08
Aam–12434–family I08
Aam–6375–family I08
Aam–51344–family I08
Aam–983604–family I08
Aam–191784–family I08
Aam–1025011–family I08
Aam–16505–family I08
Aam–5052–family I08
Aam–281490–family I08
Aam–244823–family I08
Aam–235530–family I08
Aam–244828–family I08
Aam–631984–family I08
Aam–532946–family I08
Aam–63424–family I08
Aam–24452–family I08
Aam–224745–family I08
Aam–25750–family I08
Aam–39324–family I08
Aam–958890–family I08
Aam–995820–family I08
Aam–1018844–family I08
Aam–98668–family I08
Aam–5238–family I08
Aam–979114–family I08
Aam–59145–family I08
24 48 72 96 120 144 168 192 BD SD
Feeding Time Point (h)

F

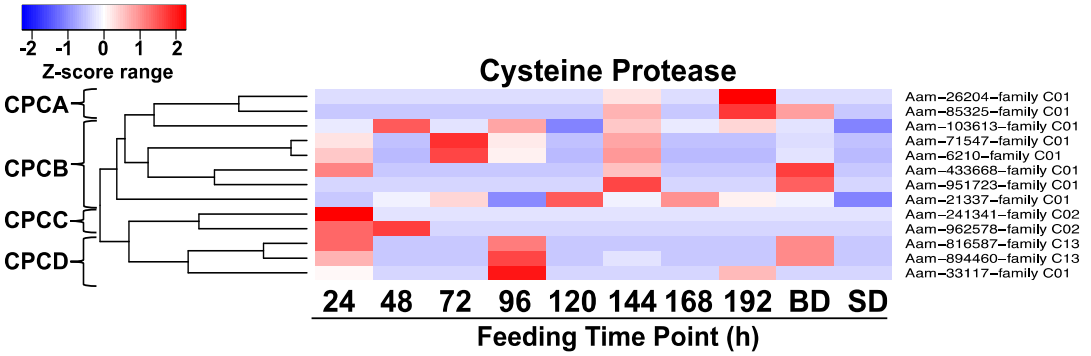
-2 -1 0 1 2
Z-score range
Cysteine Protease
CPCA
CPCB
CPCC
CPCD
Aam-26204-family C01
Aam-85325-family C01
Aam-103613-family C01
Aam-71547-family C01
Aam-6210-family C01
Aam-433668-family C01
Aam-951723-family C01
Aam-21337-family C01
Aam-241341-family C02
Aam-962578-family C02
Aam-816587-family C13
Aam-894460-family C13
Aam-33117-family C01
24 48 72 96 120 144 168 192 BD SD
Feeding Time Point (h)

G

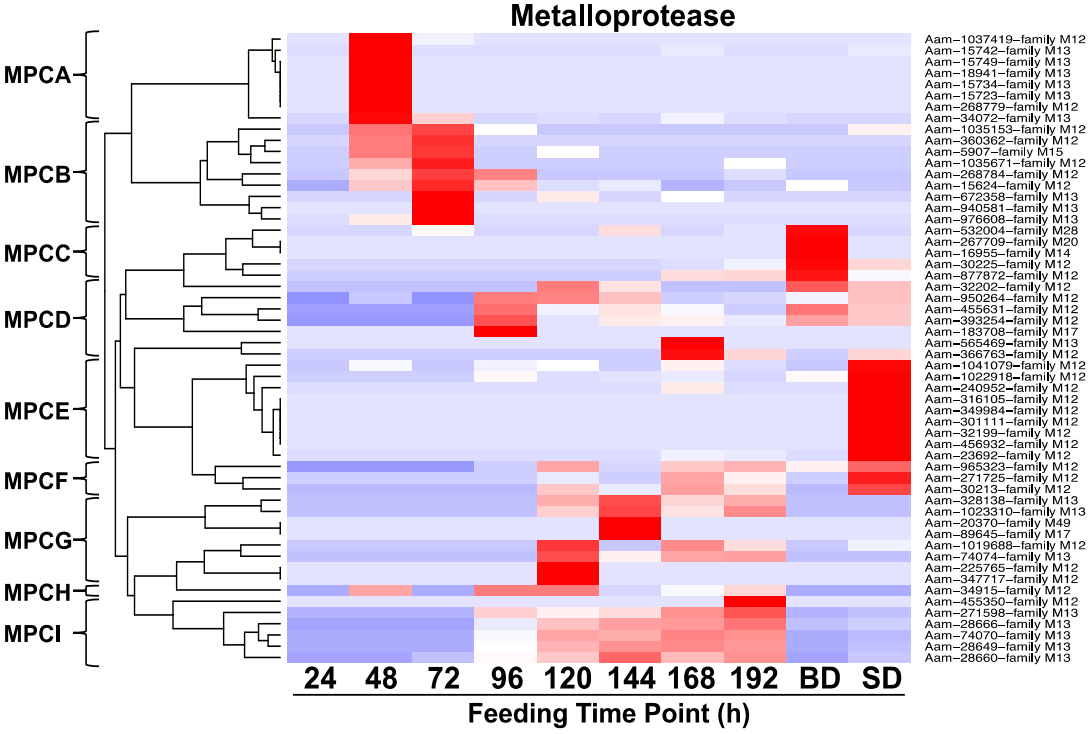
Metalloprotease
MPCA
MPCB
MPCC
MPCD
MPCE
MPCF
MPCG
MPCH
MPCI
Aam-1037419-family M12
Aam-15742-family M13
Aam-15749-family M13
Aam-18941-family M13
Aam-15734-family M13
Aam-15723-family M13
Aam-268779-family M12
Aam-34072-family M13
Aam-1035153-family M12
Aam-360362-family M12
Aam-5907-family M15
Aam-1035671-family M12
Aam-268784-family M12
Aam-15624-family M12
Aam-672358-family M13
Aam-940581-family M13
Aam-976608-family M13
Aam-532004-family M28
Aam-267709-family M20
Aam-16955-family M14
Aam-30225-family M12
Aam-877872-family M12
Aam-32202-family M12
Aam-950264-family M12
Aam-455631-family M12
Aam-393254-family M12
Aam-183708-family M17
Aam-565469-family M13
Aam-366763-family M12
Aam-1041079-family M12
Aam-1022918-family M12
Aam-240952-family M12
Aam-316105-family M12
Aam-349984-family M12
Aam-301111-family M12
Aam-32199-family M12
Aam-456932-family M12
Aam-23692-family M12
Aam-965323-family M12
Aam-271725-family M12
Aam-30213-family M12
Aam-328138-family M13
Aam-1023310-family M13
Aam-20370-family M49
Aam-89645-family M17
Aam-1019688-family M12
Aam-74074-family M13
Aam-225765-family M12
Aam-347717-family M12
Aam-34915-family M12
Aam-455350-family M12
Aam-271598-family M13
Aam-28666-family M13
Aam-74070-family M13
Aam-28649-family M13
Aam-28660-family M13
24 48 72 96 120 144 168 192 BD SD
Feeding Time Point (h)

H

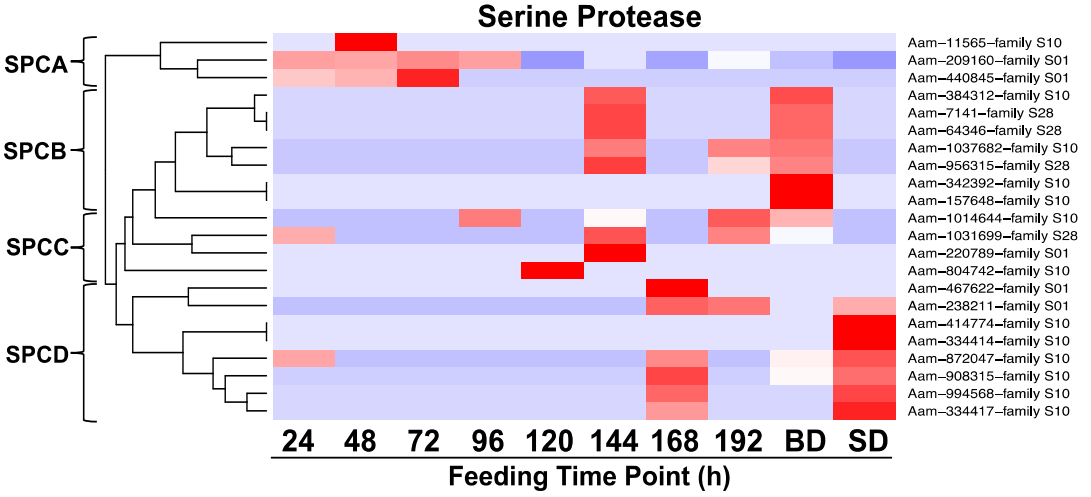
Serine Protease
SPCA
SPCB
SPCC
SPCD
Aam-11565-family S10
Aam-209160-family S01
Aam-440845-family S01
Aam-384312-family S10
Aam-7141-family S28
Aam-64346-family S28
Aam-1037682-family S10
Aam-956315-family S28
Aam-342392-family S10
Aam-157648-family S10
Aam-1014644-family S10
Aam-1031699-family S28
Aam-220789-family S01
Aam-804742-family S10
Aam-467622-family S01
Aam-238211-family S01
Aam-414774-family S10
Aam-334414-family S10
Aam-872047-family S10
Aam-908315-family S10
Aam-994568-family S10
Aam-334417-family S10
24 48 72 96 120 144 168 192 BD SD
Feeding Time Point (h)

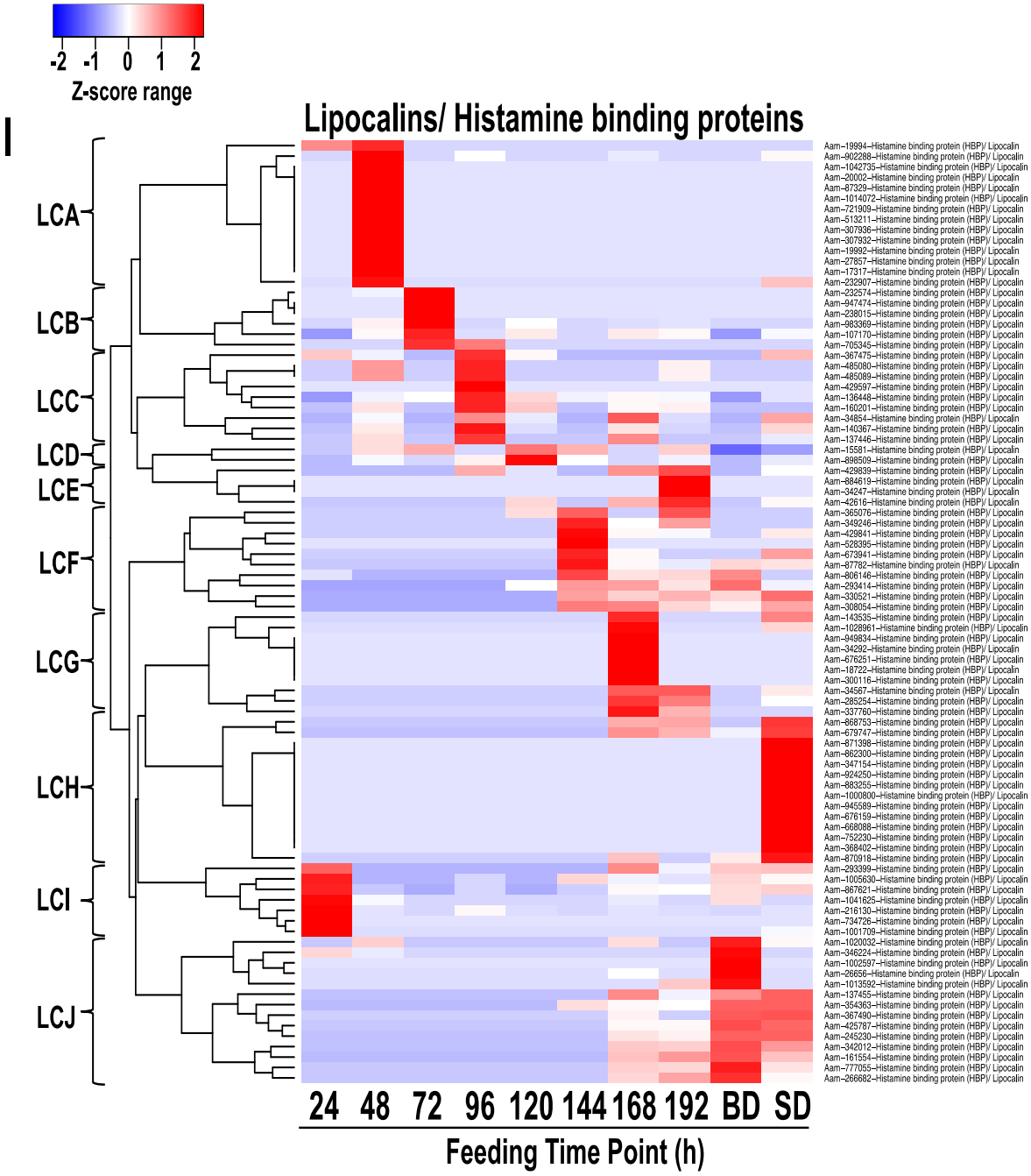
-2 -1 0 1 2
Z-score range
Lipocalins/ Histamine binding proteins
LCA
LCB
LCC
LCD
LCE
LCF
LCG
LCH
LCI
LCJ
Aam−19994−Histamine binding protein (HBP)/ Lipocalin
Aam−902288−Histamine binding protein (HBP)/ Lipocalin
Aam−1042735−Histamine binding protein (HBP)/ Lipocalin
Aam−20002−Histamine binding protein (HBP)/ Lipocalin
Aam−87329−Histamine binding protein (HBP)/ Lipocalin
Aam−1014072−Histamine binding protein (HBP)/ Lipocalin
Aam−721909−Histamine binding protein (HBP)/ Lipocalin
Aam−513211−Histamine binding protein (HBP)/ Lipocalin
Aam−307936−Histamine binding protein (HBP)/ Lipocalin
Aam−307932−Histamine binding protein (HBP)/ Lipocalin
Aam−19992−Histamine binding protein (HBP)/ Lipocalin
Aam−27857−Histamine binding protein (HBP)/ Lipocalin
Aam−17317−Histamine binding protein (HBP)/ Lipocalin
Aam−232907−Histamine binding protein (HBP)/ Lipocalin
Aam−232574−Histamine binding protein (HBP)/ Lipocalin
Aam−947474−Histamine binding protein (HBP)/ Lipocalin
Aam−238015−Histamine binding protein (HBP)/ Lipocalin
Aam−983369−Histamine binding protein (HBP)/ Lipocalin
Aam−107170−Histamine binding protein (HBP)/ Lipocalin
Aam−705345−Histamine binding protein (HBP)/ Lipocalin
Aam−987475−Histamine binding protein (HBP)/ Lipocalin
Aam−485080−Histamine binding protein (HBP)/ Lipocalin
Aam−485089−Histamine binding protein (HBP)/ Lipocalin
Aam−429597−Histamine binding protein (HBP)/ Lipocalin
Aam−136448−Histamine binding protein (HBP)/ Lipocalin
Aam−160201−Histamine binding protein (HBP)/ Lipocalin
Aam−34854−Histamine binding protein (HBP)/ Lipocalin
Aam−140367−Histamine binding protein (HBP)/ Lipocalin
Aam−137446−Histamine binding protein (HBP)/ Lipocalin
Aam−15581−Histamine binding protein (HBP)/ Lipocalin
Aam−898509−Histamine binding protein (HBP)/ Lipocalin
Aam−429839−Histamine binding protein (HBP)/ Lipocalin
Aam−884619−Histamine binding protein (HBP)/ Lipocalin
Aam−34247−Histamine binding protein (HBP)/ Lipocalin
Aam−42616−Histamine binding protein (HBP)/ Lipocalin
Aam−365076−Histamine binding protein (HBP)/ Lipocalin
Aam−349246−Histamine binding protein (HBP)/ Lipocalin
Aam−429841−Histamine binding protein (HBP)/ Lipocalin
Aam−528395−Histamine binding protein (HBP)/ Lipocalin
Aam−673941−Histamine binding protein (HBP)/ Lipocalin
Aam−87782−Histamine binding protein (HBP)/ Lipocalin
Aam−806146−Histamine binding protein (HBP)/ Lipocalin
Aam−293414−Histamine binding protein (HBP)/ Lipocalin
Aam−330521−Histamine binding protein (HBP)/ Lipocalin
Aam−308054−Histamine binding protein (HBP)/ Lipocalin
Aam−143535−Histamine binding protein (HBP)/ Lipocalin
Aam−1028961−Histamine binding protein (HBP)/ Lipocalin
Aam−949834−Histamine binding protein (HBP)/ Lipocalin
Aam−34292−Histamine binding protein (HBP)/ Lipocalin
Aam−676251−Histamine binding protein (HBP)/ Lipocalin
Aam−18722−Histamine binding protein (HBP)/ Lipocalin
Aam−300116−Histamine binding protein (HBP)/ Lipocalin
Aam−34567−Histamine binding protein (HBP)/ Lipocalin
Aam−285254−Histamine binding protein (HBP)/ Lipocalin
Aam−337760−Histamine binding protein (HBP)/ Lipocalin
Aam−868753−Histamine binding protein (HBP)/ Lipocalin
Aam−679747−Histamine binding protein (HBP)/ Lipocalin
Aam−871398−Histamine binding protein (HBP)/ Lipocalin
Aam−862300−Histamine binding protein (HBP)/ Lipocalin
Aam−347154−Histamine binding protein (HBP)/ Lipocalin
Aam−924250−Histamine binding protein (HBP)/ Lipocalin
Aam−883255−Histamine binding protein (HBP)/ Lipocalin
Aam−1000800−Histamine binding protein (HBP)/ Lipocalin
Aam−945589−Histamine binding protein (HBP)/ Lipocalin
Aam−676159−Histamine binding protein (HBP)/ Lipocalin
Aam−668088−Histamine binding protein (HBP)/ Lipocalin
Aam−752230−Histamine binding protein (HBP)/ Lipocalin
Aam−368402−Histamine binding protein (HBP)/ Lipocalin
Aam−870918−Histamine binding protein (HBP)/ Lipocalin
Aam−293399−Histamine binding protein (HBP)/ Lipocalin
Aam−1005630−Histamine binding protein (HBP)/ Lipocalin
Aam−867621−Histamine binding protein (HBP)/ Lipocalin
Aam−1041625−Histamine binding protein (HBP)/ Lipocalin
Aam−216130−Histamine binding protein (HBP)/ Lipocalin
Aam−734726−Histamine binding protein (HBP)/ Lipocalin
Aam−1001709−Histamine binding protein (HBP)/ Lipocalin
Aam−1020032−Histamine binding protein (HBP)/ Lipocalin
Aam−346224−Histamine binding protein (HBP)/ Lipocalin
Aam−1002597−Histamine binding protein (HBP)/ Lipocalin
Aam−26656−Histamine binding protein (HBP)/ Lipocalin
Aam−1013592−Histamine binding protein (HBP)/ Lipocalin
Aam−137455−Histamine binding protein (HBP)/ Lipocalin
Aam−354363−Histamine binding protein (HBP)/ Lipocalin
Aam−367490−Histamine binding protein (HBP)/ Lipocalin
Aam−425787−Histamine binding protein (HBP)/ Lipocalin
Aam−245230−Histamine binding protein (HBP)/ Lipocalin
Aam−342012−Histamine binding protein (HBP)/ Lipocalin
Aam−161554−Histamine binding protein (HBP)/ Lipocalin
Aam−777055−Histamine binding protein (HBP)/ Lipocalin
Aam−266682−Histamine binding protein (HBP)/ Lipocalin
24 48 72 96 120 144 168 192 BD SD
Feeding Time Point (h)

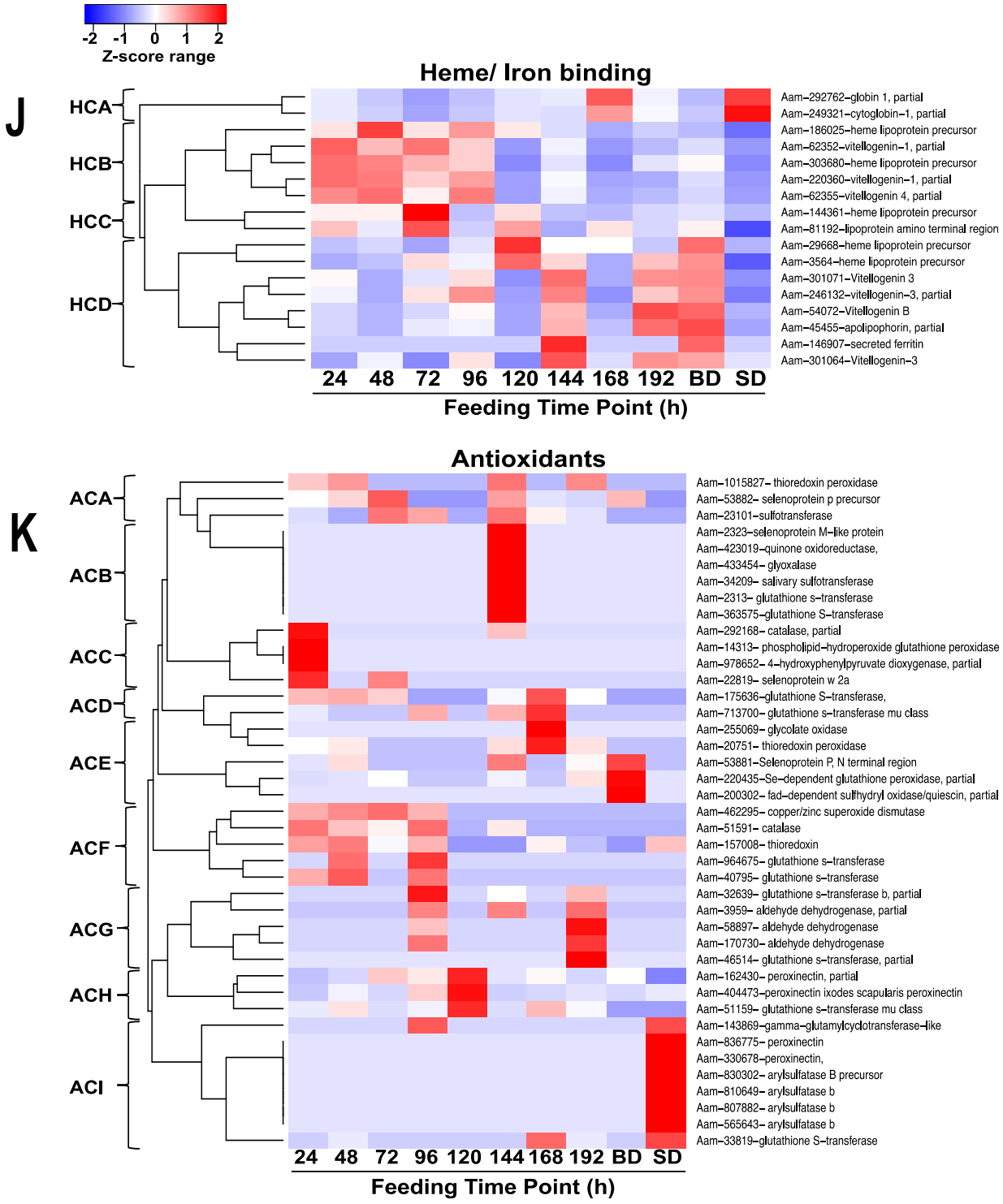
J
-2 -1 0 1 2
Z-score range
Heme/ Iron binding
HCA
HCB
HCC
HCD
Aam–292762–globin 1, partial
Aam–249321–cytoglobin–1, partial
Aam–186025–heme lipoprotein precursor
Aam–62352–vitellogenin–1, partial
Aam–303680–heme lipoprotein precursor
Aam–220360–vitellogenin–1, partial
Aam–62355–vitellogenin 4, partial
Aam–144361–heme lipoprotein precursor
Aam–81192–lipoprotein amino terminal region
Aam–29668–heme lipoprotein precursor
Aam–3564–heme lipoprotein precursor
Aam–301071–Vitellogenin 3
Aam–246132–vitellogenin–3, partial
Aam–54072–Vitellogenin B
Aam–45455–apolipophorin, partial
Aam–146907–secreted ferritin
Aam–301064–Vitellogenin–3
24 48 72 96 120 144 168 192 BD SD
Feeding Time Point (h)
K
Antioxidants
ACA
ACB
ACC
ACD
ACE
ACF
ACG
ACH
ACI
Aam–1015827– thioredoxin peroxidase
Aam–53882– selenoprotein p precursor
Aam–23101–sulfotransferase
Aam–2323–selenoprotein M–like protein
Aam–423019–quinone oxidoreductase,
Aam–433454– glyoxalase
Aam–34209– salivary sulfotransferase
Aam–2313– glutathione s–transferase
Aam–363575–glutathione S–transferase
Aam–292168– catalase, partial
Aam–14313– phospholipid–hydroperoxide glutathione peroxidase
Aam–978652– 4–hydroxyphenylpyruvate dioxygenase, partial
Aam–22819– selenoprotein w 2a
Aam–175636–glutathione S–transferase,
Aam–713700– glutathione s–transferase mu class
Aam–255069– glycolate oxidase
Aam–20751– thioredoxin peroxidase
Aam–53881–Selenoprotein P, N terminal region
Aam–220435–Se–dependent glutathione peroxidase, partial
Aam–200302– fad–dependent sulfhydryl oxidase/quiescin, partial
Aam–462295– copper/zinc superoxide dismutase
Aam–51591– catalase
Aam–157008– thioredoxin
Aam–964675– glutathione s–transferase
Aam–40795– glutathione s–transferase
Aam–32639– glutathione s–transferase b, partial
Aam–3959– aldehyde dehydrogenase, partial
Aam–58897– aldehyde dehydrogenase
Aam–170730– aldehyde dehydrogenase
Aam–46514– glutathione s–transferase, partial
Aam–162430– peroxinectin, partial
Aam–404473–peroxinectin ixodes scapularis peroxinectin
Aam–51159– glutathione s–transferase mu class
Aam–143869–gamma–glutamylcyclotransferase–like
Aam–836775– peroxinectin
Aam–330678–peroxinectin,
Aam–830302– arylsulfatase B precursor
Aam–810649– arylsulfatase b
Aam–807882– arylsulfatase b
Aam–565643– arylsulfatase b
Aam–33819–glutathione S–transferase
24 48 72 96 120 144 168 192 BD SD
Feeding Time Point (h)

L

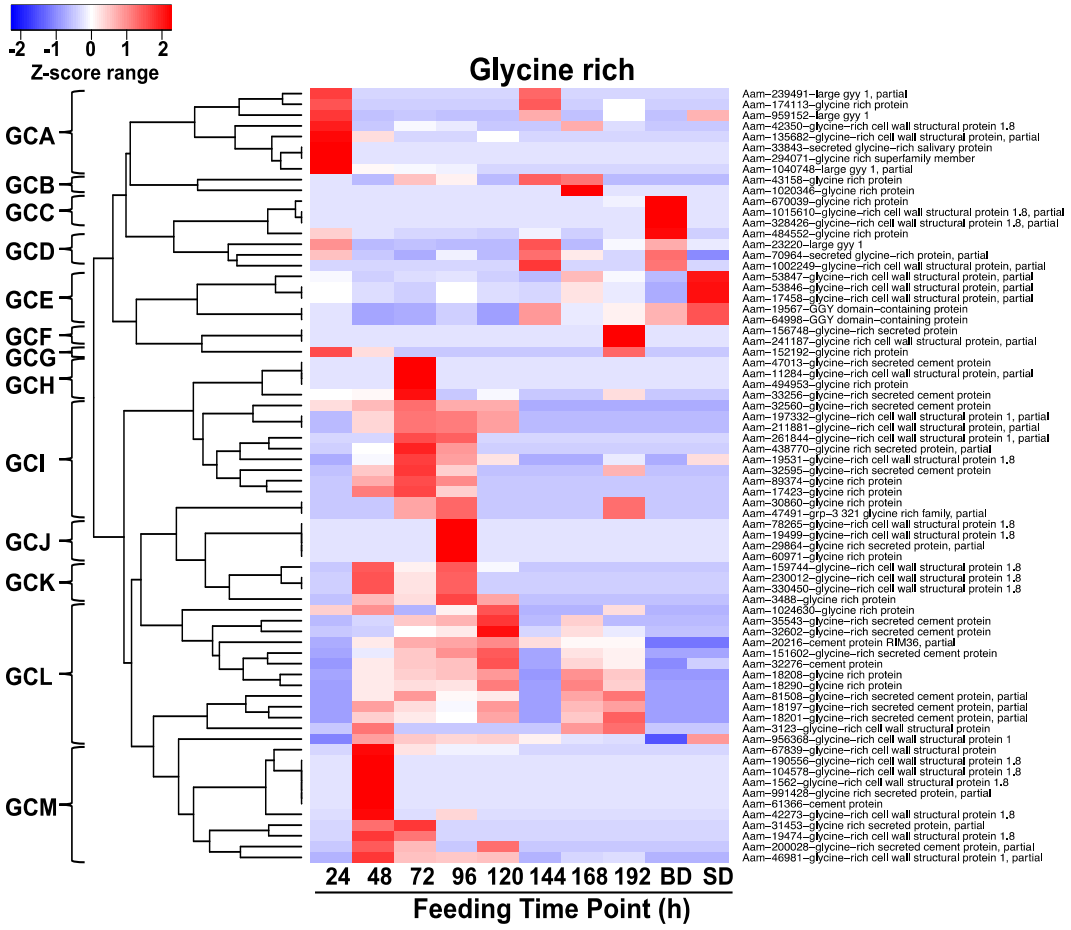
-2 -1 0 1 2
Z-score range
Glycine rich
GCA
GCB
GCC
GCD
GCE
GCF
GCG
GCH
GCI
GCJ
GCK
GCL
GCM
Aam–239491–large gyy 1, partial
Aam–174113–glycine rich protein
Aam–959152–large gyy 1
Aam–42350–glycine–rich cell wall structural protein 1.8
Aam–135682–glycine–rich cell wall structural protein, partial
Aam–33843–secreted glycine–rich salivary protein
Aam–294071–glycine rich superfamily member
Aam–1040748–large gyy 1, partial
Aam–43158–glycine rich protein
Aam–1020346–glycine rich protein
Aam–670039–glycine rich protein
Aam–1015610–glycine–rich cell wall structural protein 1.8, partial
Aam–328426–glycine–rich cell wall structural protein 1.8, partial
Aam–484552–glycine rich protein
Aam–23220–large gyy 1
Aam–70964–secreted glycine–rich protein, partial
Aam–1002249–glycine–rich cell wall structural protein, partial
Aam–53847–glycine–rich cell wall structural protein, partial
Aam–53846–glycine–rich cell wall structural protein, partial
Aam–17458–glycine–rich cell wall structural protein, partial
Aam–19567–GGY domain–containing protein
Aam–64998–GGY domain–containing protein
Aam–156748–glycine–rich secreted protein
Aam–241187–glycine rich cell wall structural protein, partial
Aam–152192–glycine rich protein
Aam–47013–glycine–rich secreted cement protein
Aam–11284–glycine–rich cell wall structural protein, partial
Aam–494953–glycine rich protein
Aam–33256–glycine–rich secreted cement protein
Aam–32560–glycine–rich secreted cement protein
Aam–197332–glycine–rich cell wall structural protein 1, partial
Aam–211881–glycine–rich cell wall structural protein, partial
Aam–261844–glycine–rich cell wall structural protein 1, partial
Aam–438770–glycine rich secreted protein, partial
Aam–19531–glycine–rich cell wall structural protein 1.8
Aam–32595–glycine–rich secreted cement protein
Aam–89374–glycine rich protein
Aam–17423–glycine rich protein
Aam–30860–glycine rich protein
Aam–47491–grp–3 321 glycine rich family, partial
Aam–78265–glycine–rich cell wall structural protein 1.8
Aam–19499–glycine–rich cell wall structural protein 1.8
Aam–29864–glycine rich secreted protein, partial
Aam–60971–glycine rich protein
Aam–159744–glycine–rich cell wall structural protein 1.8
Aam–230012–glycine–rich cell wall structural protein 1.8
Aam–330450–glycine–rich cell wall structural protein 1.8
Aam–3488–glycine rich protein
Aam–1024630–glycine rich protein
Aam–35543–glycine–rich secreted cement protein
Aam–32602–glycine–rich secreted cement protein
Aam–20216–cement protein RIM36, partial
Aam–151602–glycine–rich secreted cement protein
Aam–32276–cement protein
Aam–18208–glycine rich protein
Aam–18290–glycine rich protein
Aam–81508–glycine–rich secreted cement protein, partial
Aam–18197–glycine–rich secreted cement protein, partial
Aam–18201–glycine–rich secreted cement protein, partial
Aam–3123–glycine–rich cell wall structural protein
Aam–956368–glycine–rich cell wall structural protein 1
Aam–67839–glycine–rich cell wall structural protein
Aam–190556–glycine–rich cell wall structural protein 1.8
Aam–104578–glycine–rich cell wall structural protein 1.8
Aam–1562–glycine–rich cell wall structural protein 1.8
Aam–991428–glycine rich secreted protein, partial
Aam–61366–cement protein
Aam–42273–glycine–rich cell wall structural protein 1.8
Aam–31453–glycine rich secreted protein, partial
Aam–19474–glycine–rich cell wall structural protein 1.8
Aam–200028–glycine–rich secreted cement protein, partial
Aam–46981–glycine–rich cell wall structural protein 1, partial
24 48 72 96 120 144 168 192 BD SD
Feeding Time Point (h)

M

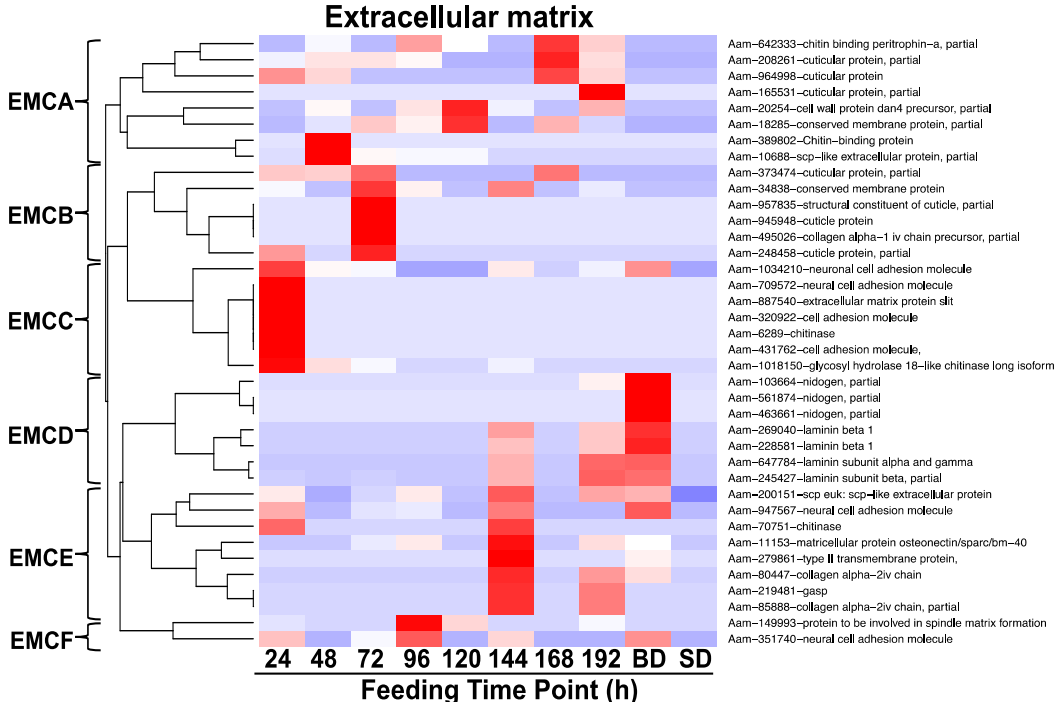
Extracellular matrix
EMCA
EMCB
EMCC
EMCD
EMCE
EMCF
Aam–642333–chitin binding peritrophin–a, partial
Aam–208261–cuticular protein, partial
Aam–964998–cuticular protein
Aam–165531–cuticular protein, partial
Aam–20254–cell wall protein dan4 precursor, partial
Aam–18285–conserved membrane protein, partial
Aam–389802–Chitin–binding protein
Aam–10688–scp–like extracellular protein, partial
Aam–373474–cuticular protein, partial
Aam–34838–conserved membrane protein
Aam–957835–structural constituent of cuticle, partial
Aam–945948–cuticle protein
Aam–495026–collagen alpha–1 iv chain precursor, partial
Aam–248458–cuticle protein, partial
Aam–1034210–neuronal cell adhesion molecule
Aam–709572–neural cell adhesion molecule
Aam–887540–extracellular matrix protein slit
Aam–320922–cell adhesion molecule
Aam–6289–chitinase
Aam–431762–cell adhesion molecule,
Aam–1018150–glycosyl hydrolase 18–like chitinase long isoform
Aam–103664–nidogen, partial
Aam–561874–nidogen, partial
Aam–463661–nidogen, partial
Aam–269040–laminin beta 1
Aam–228581–laminin beta 1
Aam–647784–laminin subunit alpha and gamma
Aam–245427–laminin subunit beta, partial
Aam–200151–scp euk: scp–like extracellular protein
Aam–947567–neural cell adhesion molecule
Aam–70751–chitinase
Aam–11153–matricellular protein osteonectin/sparc/bm–40
Aam–279861–type II transmembrane protein,
Aam–80447–collagen alpha–2iv chain
Aam–219481–gasp
Aam–85888–collagen alpha–2iv chain, partial
Aam–149993–protein to be involved in spindle matrix formation
Aam–351740–neural cell adhesion molecule
24 48 72 96 120 144 168 192 BD SD
Feeding Time Point (h)

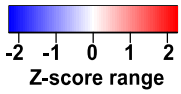
-2 -1 0 1 2
Z-score range

N

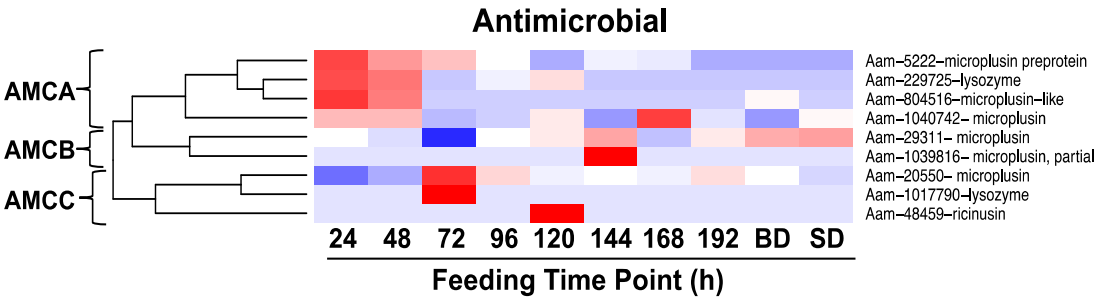
Antimicrobial
AMCA
AMCB
AMCC
Aam–5222–microplusin preprotein
Aam–229725–lysozyme
Aam–804516–microplusin–like
Aam–1040742– microplusin
Aam–29311– microplusin
Aam–1039816– microplusin, partial
Aam–20550– microplusin
Aam–1017790–lysozyme
Aam–48459–ricinusin
24 48 72 96 120 144 168 192 BD SD
Feeding Time Point (h)

O

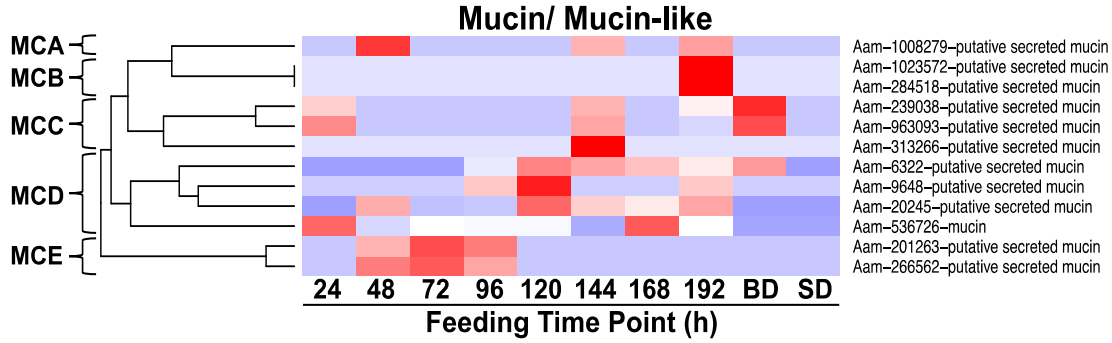
Mucin/ Mucin-like
MCA
MCB
MCC
MCD
MCE
Aam–1008279–putative secreted mucin
Aam–1023572–putative secreted mucin
Aam–284518–putative secreted mucin
Aam–239038–putative secreted mucin
Aam–963093–putative secreted mucin
Aam–313266–putative secreted mucin
Aam–6322–putative secreted mucin
Aam–9648–putative secreted mucin
Aam–20245–putative secreted mucin
Aam–536726–mucin
Aam–201263–putative secreted mucin
Aam–266562–putative secreted mucin
24 48 72 96 120 144 168 192 BD SD
Feeding Time Point (h)

P

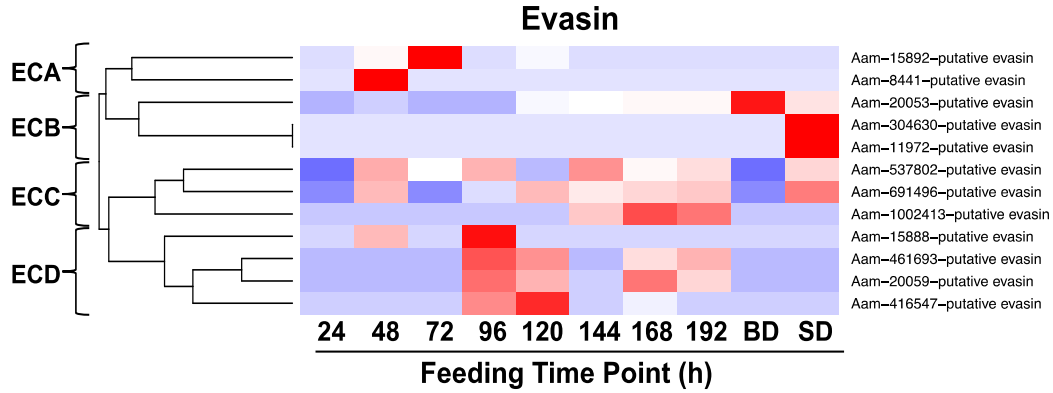
Evasin
ECA
ECB
ECC
ECD
Aam–15892–putative evasin
Aam–8441–putative evasin
Aam–20053–putative evasin
Aam–304630–putative evasin
Aam–11972–putative evasin
Aam–537802–putative evasin
Aam–691496–putative evasin
Aam–1002413–putative evasin
Aam–15888–putative evasin
Aam–461693–putative evasin
Aam–20059–putative evasin
Aam–416547–putative evasin
24 48 72 96 120 144 168 192 BD SD
Feeding Time Point (h)

Q

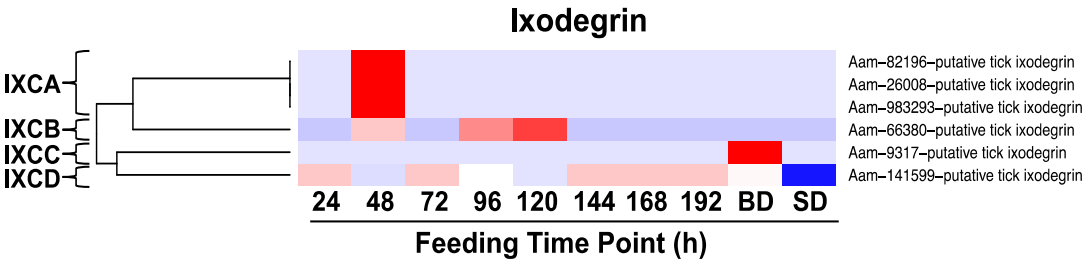
Ixodegrin
IXCA
IXCB
IXCC
IXCD
Aam–82196–putative tick ixodegrin
Aam–26008–putative tick ixodegrin
Aam–983293–putative tick ixodegrin
Aam–66380–putative tick ixodegrin
Aam–9317–putative tick ixodegrin
Aam–141599–putative tick ixodegrin
24 48 72 96 120 144 168 192 BD SD
Feeding Time Point (h)

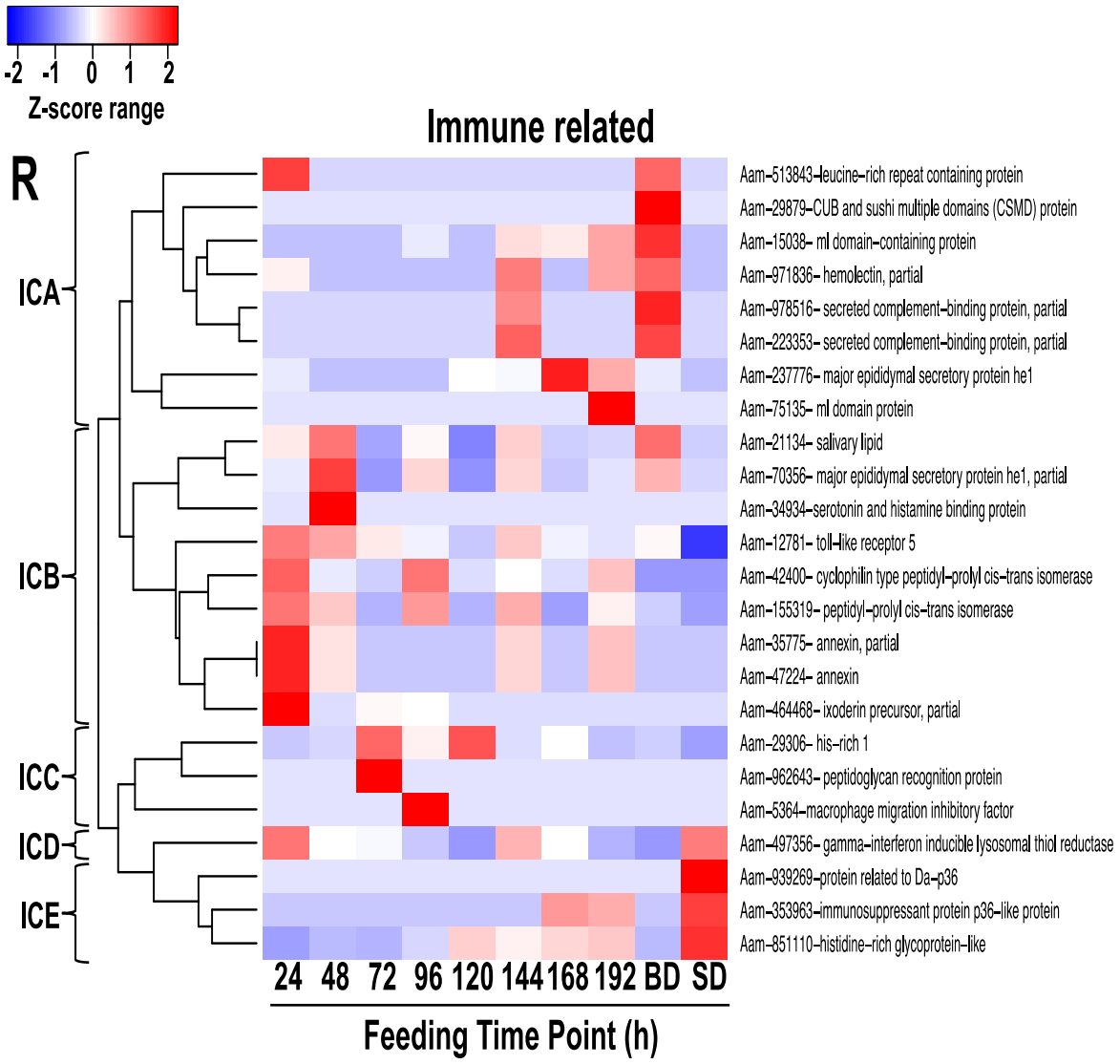
-2 -1 0 1 2
Z-score range
Immune related
R
ICA
ICB
ICC
ICD
ICE
Aam-513843-leucine-rich repeat containing protein
Aam-29879-CUB and sushi multiple domains (CSMD) protein
Aam-15038- ml domain-containing protein
Aam-971836- hemolectin, partial
Aam-978516- secreted complement-binding protein, partial
Aam-223353- secreted complement-binding protein, partial
Aam-237776- major epididymal secretory protein he1
Aam-75135- ml domain protein
Aam-21134- salivary lipid
Aam-70356- major epididymal secretory protein he1, partial
Aam-34934-serotonin and histamine binding protein
Aam-12781- toll-like receptor 5
Aam-42400- cyclophilin type peptidyl-prolyl cis-trans isomerase
Aam-155319- peptidyl-prolyl cis-trans isomerase
Aam-35775- annexin, partial
Aam-47224- annexin
Aam-464468- ixoderin precursor, partial
Aam-29306- his-rich 1
Aam-962643- peptidoglycan recognition protein
Aam-5364-macrophage migration inhibitory factor
Aam-497356- gamma-interferon inducible lysosomal thiol reductase
Aam-939269-protein related to Da-p36
Aam-353963-immunosuppressant protein p36-like protein
Aam-851110-histidine-rich glycoprotein-like
24 48 72 96 120 144 168 192 BD SD
Feeding Time Point (h)

S

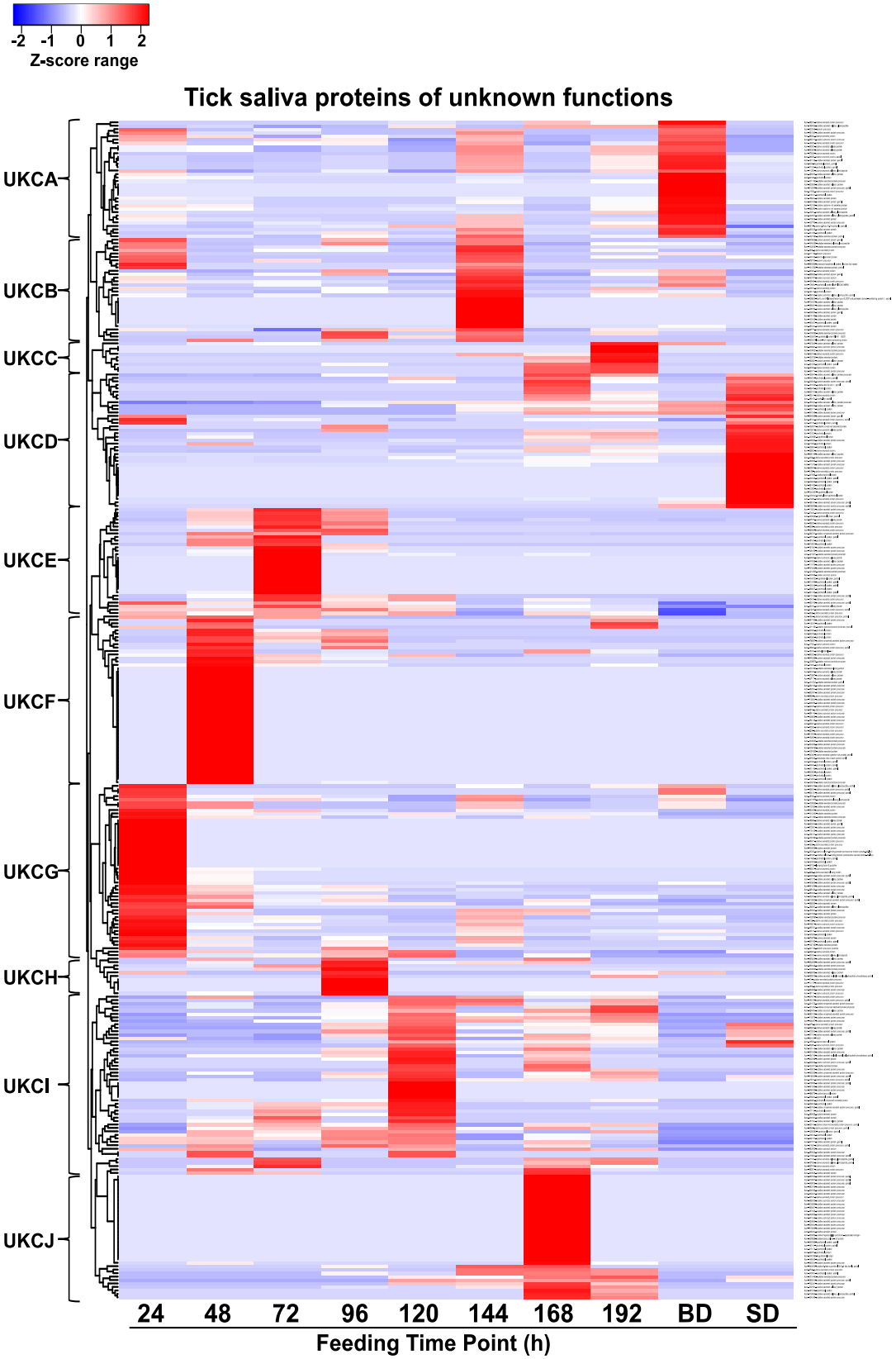
-2 -1 0 1 2
Z-score range
Tick saliva proteins of unknown functions
UKCA
UKCB
UKCC
UKCD
UKCE
UKCF
UKCG
UKCH
UKCI
UKCJ
24 48 72 96 120 144 168 192 BD SD
Feeding Time Point (h)

Table 1A. *Amblyomma americanum* saliva proteins (250-100 kDa) identified from in-gel digestion and LC-MS/MS during feeding

	Feeding Time Points (h)											
	24 h			72 h			120 h			168 h		
Molecular weight	Gel Band	Contig	Description	Gel Band	Contig	Description	Gel Band	Contig	Description	Gel Band	Contig	Description
≥ 250 kDa	C1-C4	N/A	N/A	D1	N/A	N/A	E1-E4	N/A	N/A	F1-F2	N/A	N/A
				D2	XP_002711050.1	keratin 6A-like	E5	Aam-426945	TIL domain containing protein, partial	F3	Aam-28660	putative neutral endopeptidase-like protein, partial
				D3-D8	N/A	N/A		Aam-59478	TIL domain containing protein, partial	F4	Aam-28660	putative neutral endopeptidase-like protein, partial
	C5	Aam-3564	heme lipoprotein precursor	D9	Aam-3564	heme lipoprotein precursor		Aam-587352	TIL domain containing protein, partial	F5-F10	N/A	N/A
							E6-E7	N/A	N/A	F11	Aam-54072	Vitellogenin B
				D10	XP_002719410.1	keratin 10	E8	Aam-3564	heme lipoprotein precursor		Aam-3564	heme lipoprotein precursor
				D11-D12	N/A	N/A	E9-E11	N/A	N/A			
250 - 150 kDa	C6-C7	N/A	N/A	D13	N/A	N/A	E12	Aam-3564	heme lipoprotein precursor	F12	N/A	N/A
	C8	Aam-3564	heme lipoprotein precursor	D14	XP_017197646.1	keratin 6A-like		XP_002711050.1	keratin 6A-like			
							E13	Aam-54072	Vitellogenin B	F13	N/A	N/A
	C9	Aam-3564	heme lipoprotein precursor	D15	XP_017197646.1	keratin 6A-like	E14	N/A	N/A			
		Aam-220360	putative vitellogenin-1, partial				E15	Aam-3564	heme lipoprotein precursor			
	C10	Aam-3564	heme lipoprotein precursor		Aam-220360	putative vitellogenin-1, partial	E17	Aam-186025	heme lipoprotein precursor		Aam-392504	putative alpha-2-macroglobulin-like protein
		Aam-220360	putative vitellogenin-1, partial	D16	Aam-62355	vitellogenin 4, partial		Aam-954297	glucose dehydrogenase, putative			
								Aam-144361	heme lipoprotein precursor			
		Aam-392504	putative alpha-2-macroglobulin-like protein		Aam-62352	putative vitellogenin-1, partial	E18	Aam-3564	heme lipoprotein precursor	F14	Aam-220360	putative vitellogenin-1, partial
		Aam-62355	vitellogenin 4, partial					Aam-186025	heme lipoprotein precursor			
	C11	Aam-3564	heme lipoprotein precursor	D17	Aam-3564	heme lipoprotein precursor		Aam-50363	hypothetical protein		Aam-3564	heme lipoprotein precursor
		Aam-186025	heme lipoprotein precursor					Aam-220360	putative vitellogenin-1, partial			
		Aam-392513	putative alpha-2-macroglobulin-like protein, partial	D18	Aam-3564	heme lipoprotein precursor		Aam-954297	glucose dehydrogenase, putative			
	C12	Aam-220360	putative vitellogenin-1, partial				E19	Aam-3564	heme lipoprotein precursor	F15	Aam-3564	heme lipoprotein precursor
					Aam-186025	heme lipoprotein precursor		Aam-54072	Vitellogenin B			
		Aam-3564	heme lipoprotein precursor					Aam-252303	glucose dehydrogenase, putative	F16	Aam-3564	heme lipoprotein precursor
				D19	Aam-3564	heme lipoprotein precursor		Aam-279098	glucose dehydrogenase, putative			
		Aam-186025	heme lipoprotein precursor					Aam-80557	glucose dehydrogenase, putative		Aam-186025	heme lipoprotein precursor
		Aam-50363	hypothetical protein					Aam-220360	putative vitellogenin-1, partial			

Table 1B. *Amblyomma americanum* saliva proteins (100-37 kDa) identified from in-gel digestion and LC-MS/MS during feeding

Molecular weight	Feeding Time Points (h)											
	24 h			72 h			120 h			168 h		
	Gel Band	Contig	Description	Gel Band	Contig	Description	Gel Band	Contig	Description	Gel Band	Contig	Description
100 - 75 kDa	C13	Aam-3564	heme lipoprotein precursor	D20	N/A		E20	Aam-75534	metabotropic glutamate receptor 2/3	F17	Aam-3564	heme lipoprotein precursor
				D21	CAA41424.1	liver transferrin		Aam-3564	heme lipoprotein precursor		Aam-54072	Vitellogenin B
	C14	AAB58347.2	serum albumin precursor					XP_002711050.1	keratin 6A-like	F18	Aam-3564	heme lipoprotein precursor
				D22	NP_001075813.1	serum albumin precursor	E21	4F5V_A	Chain A, Crystal Structure Of Leporine Serum Albumin		Aam-75534	metabotropic glutamate receptor 2/3
		Aam-3564	heme lipoprotein precursor					Aam-3564	heme lipoprotein precursor	F19	4F5V_A	Chain A, Crystal Structure Of Leporine Serum Albumin
	C15	N/A	N/A		XP_017197646.1	keratin 6A-like		Aam-949183	Basic tail secreted protein		Aam-3564	heme lipoprotein precursor
											XP_002711050.1	keratin 6A-like
75 - 50 kDa	C16	Aam-28434	Serine protease inhibitor	D23	4F5V_A	Chain A, Crystal Structure Of Leporine Serum Albumin	E22	Aam-3564	heme lipoprotein precursor	F20	Aam-3564	heme lipoprotein precursor
							E23	XP_002719410.1	keratin 10			
		Aam-24638	Putative lysosomal & prostatic acid phosphatase	D24	4F5V_A	Chain A, Crystal Structure Of Leporine Serum Albumin		Aam-3564	heme lipoprotein precursor	F21	N/A	N/A
							E25	Aam-271199	putative lysosomal & prostatic acid phosphatase			
		Aam-271199	putative lysosomal & prostatic acid phosphatase	D25	XP_002719410.1	keratin 10		Aam-24638	Putative lysosomal & prostatic acid phosphatase	F22	Aam-3564	heme lipoprotein precursor
								Aam-28434	Serine protease inhibitor			
		Aam-28434	Serine protease inhibitor					XP_002711050.1	keratin 6A-like	F23	Aam-28434	Serine protease inhibitor
	C17	Aam-2651	Serine protease inhibitor		AAB58347.2	serum albumin precursor	E26	Aam-28434	Serine protease inhibitor			
								Aam-488146	serine protease inhibitor		Aam-488146	serine protease inhibitor
		Aam-20799	actin		XP_002711050.1	keratin 6A-like		Aam-271199	putative lysosomal & prostatic acid phosphatase			
								Aam-24638	Putative lysosomal & prostatic acid phosphatase	F24	Aam-20799	actin
		Aam-973854	serine protease inhibitor				E27	Aam-20799	actin			
								XP_017200220.1	beta actin		CAA43139.1	alpha-smooth muscle actin
				D26	AAA31288.1	Ig gamma heavy chain constant region, partial		Aam-2651	Serine protease inhibitor			
	C18	N/A	N/A				E28	Aam-1027384	putative secreted protein, partial		XP_017200220.1	beta actin
								AAB58347.2	serum albumin precursor			
50 - 37 kDa	C19	Aam-30101	AV422	D27	Aam-28434	Serine protease inhibitor	E29	Aam-12781	putative toll-like receptor 5	F25	Aam-1027384	putative secreted protein, partial
								Aam-1027384	putative secreted protein, partial			
		Aam-16505	putative inducible metalloproteinase	D28	N/A	N/A		AAC78495.1	annexin I		XP_002711050.1	keratin 6A-like
					Aam-20799	actin		Aam-20216	putative cement protein RIM36, partial			
		Aam-235530	putative tick til 20	D29	XP_017200220.1	beta actin	E30	Aam-3564	heme lipoprotein precursor	F26	Aam-12781	putative toll-like receptor 5
					Aam-2651	Serine protease inhibitor		Aam-34094	putative glyceraldehyde 3-phosphate dehydrogenase			
		Aam-328185	putative secreted protein precursor	D30	XP_002716936.1	fibrinogen, beta chain		Aam-17458	putative glycine-rich cell wall structural protein, partial	F27	N/A	N/A
					NP_001075579.1	haptoglobin	E31	N/A	N/A			

Table 1C. *Amblyomma americanum* saliva proteins (37-10 kDa) identified from in-gel digestion and LC-MS/MS during feeding

Molecular weight	Feeding Time Points (h)											
	24 h			72 h			120 h			168 h		
	Gel Band	Contig	Description	Gel Band	Contig	Description	Gel Band	Contig	Description	Gel Band	Contig	Description
100 - 75 kDa	C13	Aam-3564	heme lipoprotein precursor	D20	N/A		E20	Aam-75534	metabotropic glutamate receptor 2/3	F17	Aam-3564	heme lipoprotein precursor
				D21	CAA41424.1	liver transferrin		Aam-3564	heme lipoprotein precursor		Aam-54072	Vitellogenin B
	C14	AAB58347.2	serum albumin precursor					XP_002711050.1	keratin 6A-like	F18	Aam-3564	heme lipoprotein precursor
				D22	NP_001075813.1	serum albumin precursor	E21	4F5V_A	Chain A, Crystal Structure Of Leporine Serum Albumin		Aam-75534	metabotropic glutamate receptor 2/3
		Aam-3564	heme lipoprotein precursor					Aam-3564	heme lipoprotein precursor	F19	4F5V_A	Chain A, Crystal Structure Of Leporine Serum Albumin
	C15	N/A	N/A		XP_017197646.1	keratin 6A-like		Aam-949183	Basic tail secreted protein		Aam-3564	heme lipoprotein precursor
							E22	Aam-3564	heme lipoprotein precursor		XP_002711050.1	keratin 6A-like
75 - 50 kDa	C16	Aam-28434	Serine protease inhibitor	D23	4F5V_A	Chain A, Crystal Structure Of Leporine Serum Albumin	E23	XP_002719410.1	keratin 10	F20	Aam-3564	heme lipoprotein precursor
		Aam-24638	Putative lysosomal & prostatic acid phosphatase	D24	4F5V_A	Chain A, Crystal Structure Of Leporine Serum Albumin		Aam-3564	heme lipoprotein precursor	F21	N/A	N/A
		Aam-271199	putative lysosomal & prostatic acid phosphatase				E25	Aam-271199	putative lysosomal & prostatic acid phosphatase			
				D25	XP_002719410.1	keratin 10		Aam-24638	Putative lysosomal & prostatic acid phosphatase	F22	Aam-3564	heme lipoprotein precursor
		Aam-28434	Serine protease inhibitor					Aam-28434	Serine protease inhibitor			
	C17	Aam-2651	Serine protease inhibitor		AAB58347.2	serum albumin precursor	E26	XP_002711050.1	keratin 6A-like	F23	Aam-28434	Serine protease inhibitor
								Aam-28434	Serine protease inhibitor			
		Aam-20799	actin		XP_002711050.1	keratin 6A-like		Aam-488146	serine protease inhibitor		Aam-488146	serine protease inhibitor
								Aam-271199	putative lysosomal & prostatic acid phosphatase			
		Aam-973854	serine protease inhibitor				E27	Aam-24638	Putative lysosomal & prostatic acid phosphatase	F24	Aam-20799	actin
				D26	AAA31288.1	Ig gamma heavy chain constant region, partial		Aam-20799	actin			
	C18	N/A	N/A					XP_017200220.1	beta actin		CAA43139.1	alpha-smooth muscle actin
								Aam-2651	Serine protease inhibitor			
							E28	Aam-1027384	putative secreted protein, partial		XP_017200220.1	beta actin
								AAB58347.2	serum albumin precursor			
50 - 37 kDa	C19	Aam-30101	AV422	D27	Aam-28434	Serine protease inhibitor	E29	Aam-12781	putative toll-like receptor 5	F25	Aam-1027384	putative secreted protein, partial
				D28	N/A	N/A		Aam-1027384	putative secreted protein, partial		XP_002711050.1	keratin 6A-like
		Aam-16505	putative inducible metalloproteinase					AAC78495.1	annexin I			
					Aam-20799	actin		Aam-20216	putative cement protein RIM36, partial			
		Aam-235530	putative tick til 20	D29	XP_017200220.1	beta actin	E30	Aam-3564	heme lipoprotein precursor	F26	Aam-12781	putative toll-like receptor 5
					Aam-2651	Serine protease inhibitor		Aam-34094	putative glyceraldehyde 3-phosphate dehydrogenase			
		Aam-328185	putative secreted protein precursor	D30	XP_002716936.1	fibrinogen, beta chain		Aam-17458	putative glycine-rich cell wall structural protein, partial	F27	N/A	N/A
					NP_001075579.1	haptoglobin	E31	N/A	N/A			

Table 2A. Numbers and cumulative relative abundance of tick protein classes in *Amblyomma americanum* saliva during 24-120h of feeding

	Feeding Time Point									
	24 h		48 h		72 h		96 h		120 h	
Classification	Protein Count	NSAF (%)	Protein Count	NSAF (%)	Protein Count	NSAF (%)	Protein Count	NSAF (%)	Protein Count	NSAF (%)
cytoskeletal	44	5.42605084	18	2.04831341	27	2.44512553	16	2.68188319	8	1.320143
antioxidant/detoxification	19	2.07005164	15	0.67599552	11	0.6756392	15	0.84292185	3	0.17210248
extracellular matrix	21	1.75925515	11	1.15412314	17	1.42291373	11	0.60885623	6	0.36116727
glycine rich	26	2.50210089	47	5.85211069	47	10.0099223	44	5.03151197	29	6.8748816
antimicrobial	6	3.14944265	6	2.62382314	5	4.05517976	5	4.64296164	5	3.47602683
immune related	13	4.02155086	11	3.16672117	10	5.78302191	11	5.84230359	8	6.51887898
metabolism-amino acid	3	0.07295858	0	0	1	0.01670156	0	0	0	0
metabolism-nucleic acid	7	2.37691856	18	1.90753634	9	0.93411625	9	2.08301483	13	1.17843463
metabolism-energy	18	1.17104098	17	1.47774007	13	1.4191621	10	0.89509331	2	0.03934355
metabolism-carbohydrates	11	0.546138	7	0.2130726	8	0.34794144	9	0.73122564	3	0.05556129
metabolism-lipid	12	0.90938486	18	1.08760145	16	1.11244881	12	1.23831428	8	0.54872965
metabolism-intermediates	0	0	0	0	1	0.01668221	0	0	0	0
nuclear regulation	7	0.37109935	7	0.43104507	8	0.9987874	7	1.18105188	7	0.97356269
protein export	1	0.0850697	1	0.05559611	0	0	1	0.08909444	1	0.01817576
protein modification	16	0.56569301	6	0.13387869	16	0.8115158	7	0.21048658	5	0.12672984
protease	17	0.70041492	25	1.02764173	20	0.94019608	26	1.40390342	27	3.95412851
proteasome machinery	10	1.9861461	8	0.73509424	8	1.83461303	8	2.117754	8	1.78587615
protein synthesis	6	0.15424728	2	0.04370454	5	0.20339802	3	0.14007568	0	0
TSP	112	22.7908915	174	35.9564371	112	36.0226724	129	34.5162985	97	33.1873387
mucin	3	0.20422887	5	0.51112529	4	0.51678033	6	0.90899489	4	0.26194085
evasin	0	0	6	0.70577064	2	0.2275009	6	0.65058522	7	1.61850351
ixodegrin	1	0.44425286	5	0.78564437	1	0.81072139	2	0.44603407	2	0.60481047
histamine binding protein/lipocalin	12	1.09763673	33	4.98784055	9	1.15787004	18	2.83391671	14	8.63089518
protease inhibitor	60	23.4959258	84	22.2971215	57	12.5495838	70	16.6217162	70	20.7480351
signal transduction	13	3.40707235	11	4.54547722	3	0.37849404	7	1.90692379	8	1.74636622
storage	16	19.3405061	16	7.16668135	15	14.6942121	16	11.7444496	9	5.63226155
transposon element	1	0.02379926	2	0.02669351	1	0.04632694	0	0	0	0
transcription machinery	4	0.22699884	1	0.02914687	3	0.17668301	3	0.10338157	0	0
transporter/ receptor	11	1.1011243	6	0.3540637	6	0.39178992	8	0.52724684	2	0.16610624
Total	470	100	560	100	435	100	459	100	346	100

Table 2B. Numbers and cumulative relative abundance of tick protein classes in *Amblyomma americanum* saliva during 144 h to completion of feeding

	Feeding Time Point									
	144 h		168 h		192 h		BD		SD	
Classification	Protein Count	NSAF (%)	Protein Count	NSAF (%)	Protein Count	NSAF (%)	Protein Count	NSAF (%)	Protein Count	NSAF (%)
cytoskeletal	40	4.25721562	13	1.60107859	18	2.00757386	5	0.77082462	16	2.560331
antioxidant/detoxification	21	1.66703577	11	0.65946156	17	1.06298334	6	0.67931641	12	0.534176
extracellular matrix	18	1.53830431	7	0.37315341	19	0.82214413	14	1.68756314	0	0
glycine rich	16	1.064742	22	2.29286194	33	2.86605231	9	0.44939919	10	0.766337
antimicrobial	4	3.8989751	4	2.40427204	3	3.14833104	3	4.93007411	3	1.690492
immune related	15	4.11387049	10	2.80737655	15	2.88455792	13	4.8521471	8	1.455037
metabolism-amino acid	4	0.07080056	2	0.06813028	1	0.03471437	0	0	0	0
metabolism-nucleic acid	14	1.72060419	10	0.90789488	16	1.66323649	3	1.07090873	8	1.177294
metabolism-energy	13	0.76892736	9	0.33182615	10	0.4825252	2	0.29120271	6	0.146919
metabolism-carbohydrates	22	1.24172915	4	0.11728364	14	0.86962849	14	2.46372253	5	0.162773
metabolism-lipid	14	0.55451717	5	0.38238891	14	0.87233815	10	0.85112078	3	0.383523
metabolism-intermediates	1	0.07593915	0	0	1	0.03178415	1	0.0855524	0	0
nuclear regulation	10	0.70663889	8	1.45911132	8	0.98455184	1	0.25227988	11	2.090831
protein export	1	0.11442347	1	0.10229207	1	0.09752031	0	0	0	0
protein modification	18	0.55453113	10	0.25289012	13	0.36709669	0	0	11	0.430365
protease	41	3.36365726	37	4.442869	41	4.04716207	37	2.90988682	37	7.593923
proteasome machinery	9	1.24480358	8	1.57329669	8	1.25827778	5	0.14336434	8	2.396472
protein synthesis	2	0.02871444	3	0.09029027	6	0.15692606	0	0	3	0.149096
TSP	124	24.4632794	152	40.6619591	141	33.7016695	76	22.5319016	77	27.0417
mucin	7	0.31763118	3	0.1229915	9	0.32417685	3	0.54184075	0	0
evasin	5	1.47038307	7	3.32616207	6	3.284717	1	0.80011384	5	2.787864
ixodegrin	1	0.55751786	1	0.19282328	1	0.60254858	2	0.75545352	0	0
histamine binding protein/ lipocalin	17	1.51995289	49	11.2079815	40	8.09117812	26	6.03767584	52	24.15436
protease inhibitor	91	18.192251	84	15.7941316	84	15.3798634	61	19.4620361	41	16.80505
signal transduction	13	2.95873629	10	1.45723547	9	2.35219606	7	1.82374777	5	0.513632
storage	17	21.9342058	14	7.15532332	16	11.9837401	17	25.1201075	10	7.042648
transposon element	0	0	1	0.04208445	0	0	0	0	1	0.023598
transcription machinery	2	0.0366112	1	0.02280705	1	0.01449543	0	0	1	0.021314
transporter/ receptor	11	1.56400161	5	0.15002323	7	0.60801075	8	1.48976031	3	0.072269
Total	551	100	491	100	552	100	324	100	336	100

Table 3A. Numbers and cumulative relative abundance of rabbit protein classes in *Amblyomma americanum* saliva during 24-120h of feeding

	Feeding Time Point									
	24 h		48 h		72 h		96 h		120 h	
Classification	Protein Count	NSAF (%)	Protein Count	NSAF (%)	Protein Count	NSAF (%)	Protein Count	NSAF (%)	Protein Count	NSAF (%)
cytoskeletal	44	5.42605084	18	2.04831341	27	2.44512553	16	2.68188319	8	1.320143
antioxidant/detoxification	19	2.07005164	15	0.67599552	11	0.6756392	15	0.84292185	3	0.17210248
extracellular matrix	21	1.75925515	11	1.15412314	17	1.42291373	11	0.60885623	6	0.36116727
glycine rich	26	2.50210089	47	5.85211069	47	10.0099223	44	5.03151197	29	6.8748816
antimicrobial	6	3.14944265	6	2.62382314	5	4.05517976	5	4.64296164	5	3.47602683
immune related	13	4.02155086	11	3.16672117	10	5.78302191	11	5.84230359	8	6.51887898
metabolism-amino acid	3	0.07295858	0	0	1	0.01670156	0	0	0	0
metabolism-nucleic acid	7	2.37691856	18	1.90753634	9	0.93411625	9	2.08301483	13	1.17843463
metabolism-energy	18	1.17104098	17	1.47774007	13	1.4191621	10	0.89509331	2	0.03934355
metabolism-carbohydrates	11	0.546138	7	0.2130726	8	0.34794144	9	0.73122564	3	0.05556129
metabolism-lipid	12	0.90938486	18	1.08760145	16	1.11244881	12	1.23831428	8	0.54872965
metabolism-intermediates	0	0	0	0	1	0.01668221	0	0	0	0
nuclear regulation	7	0.37109935	7	0.43104507	8	0.9987874	7	1.18105188	7	0.97356269
protein export	1	0.0850697	1	0.05559611	0	0	1	0.08909444	1	0.01817576
protein modification	16	0.56569301	6	0.13387869	16	0.8115158	7	0.21048658	5	0.12672984
protease	17	0.70041492	25	1.02764173	20	0.94019608	26	1.40390342	27	3.95412851
proteasome machinery	10	1.9861461	8	0.73509424	8	1.83461303	8	2.117754	8	1.78587615
protein synthesis	6	0.15424728	2	0.04370454	5	0.20339802	3	0.14007568	0	0
TSP	112	22.7908915	174	35.9564371	112	36.0226724	129	34.5162985	97	33.1873387
mucin	3	0.20422887	5	0.51112529	4	0.51678033	6	0.90899489	4	0.26194085
evasin	0	0	6	0.70577064	2	0.2275009	6	0.65058522	7	1.61850351
ixodegrin	1	0.44425286	5	0.78564437	1	0.81072139	2	0.44603407	2	0.60481047
histamine binding protein/lipocalin	12	1.09763673	33	4.98784055	9	1.15787004	18	2.83391671	14	8.63089518
protease inhibitor	60	23.4959258	84	22.2971215	57	12.5495838	70	16.6217162	70	20.7480351
signal transduction	13	3.40707235	11	4.54547722	3	0.37849404	7	1.90692379	8	1.74636622
storage	16	19.3405061	16	7.16668135	15	14.6942121	16	11.7444496	9	5.63226155
transposon element	1	0.02379926	2	0.02669351	1	0.04632694	0	0	0	0
transcription machinery	4	0.22699884	1	0.02914687	3	0.17668301	3	0.10338157	0	0
transporter/ receptor	11	1.1011243	6	0.3540637	6	0.39178992	8	0.52724684	2	0.16610624
Total	470	100	560	100	435	100	459	100	346	100

Table 3B. Numbers and cumulative relative abundance of rabbit protein classes in *Amblyomma americanum* saliva during 144 h to completion of feeding

	Feeding Time Point									
	144 h		168 h		192 h		BD		SD	
Classification	Protein Count	NSAF (%)	Protein Count	NSAF (%)	Protein Count	NSAF (%)	Protein Count	NSAF (%)	Protein Count	NSAF (%)
cytoskeletal	40	4.25721562	13	1.60107859	18	2.00757386	5	0.77082462	16	2.560331
antioxidant/detoxification	21	1.66703577	11	0.65946156	17	1.06298334	6	0.67931641	12	0.534176
extracellular matrix	18	1.53830431	7	0.37315341	19	0.82214413	14	1.68756314	0	0
glycine rich	16	1.064742	22	2.29286194	33	2.86605231	9	0.44939919	10	0.766337
antimicrobial	4	3.8989751	4	2.40427204	3	3.14833104	3	4.93007411	3	1.690492
immune related	15	4.11387049	10	2.80737655	15	2.88455792	13	4.8521471	8	1.455037
metabolism-amino acid	4	0.07080056	2	0.06813028	1	0.03471437	0	0	0	0
metabolism-nucleic acid	14	1.72060419	10	0.90789488	16	1.66323649	3	1.07090873	8	1.177294
metabolism-energy	13	0.76892736	9	0.33182615	10	0.4825252	2	0.29120271	6	0.146919
metabolism-carbohydrates	22	1.24172915	4	0.11728364	14	0.86962849	14	2.46372253	5	0.162773
metabolism-lipid	14	0.55451717	5	0.38238891	14	0.87233815	10	0.85112078	3	0.383523
metabolism-intermediates	1	0.07593915	0	0	1	0.03178415	1	0.0855524	0	0
nuclear regulation	10	0.70663889	8	1.45911132	8	0.98455184	1	0.25227988	11	2.090831
protein export	1	0.11442347	1	0.10229207	1	0.09752031	0	0	0	0
protein modification	18	0.55453113	10	0.25289012	13	0.36709669	0	0	11	0.430365
protease	41	3.36365726	37	4.442869	41	4.04716207	37	2.90988682	37	7.593923
proteasome machinery	9	1.24480358	8	1.57329669	8	1.25827778	5	0.14336434	8	2.396472
protein synthesis	2	0.02871444	3	0.09029027	6	0.15692606	0	0	3	0.149096
TSP	124	24.4632794	152	40.6619591	141	33.7016695	76	22.5319016	77	27.0417
mucin	7	0.31763118	3	0.1229915	9	0.32417685	3	0.54184075	0	0
evasin	5	1.47038307	7	3.32616207	6	3.284717	1	0.80011384	5	2.787864
ixodegrin	1	0.55751786	1	0.19282328	1	0.60254858	2	0.75545352	0	0
histamine binding protein/ lipocalin	17	1.51995289	49	11.2079815	40	8.09117812	26	6.03767584	52	24.15436
protease inhibitor	91	18.192251	84	15.7941316	84	15.3798634	61	19.4620361	41	16.80505
signal transduction	13	2.95873629	10	1.45723547	9	2.35219606	7	1.82374777	5	0.513632
storage	17	21.9342058	14	7.15532332	16	11.9837401	17	25.1201075	10	7.042648
transposon element	0	0	1	0.04208445	0	0	0	0	1	0.023598
transcription machinery	2	0.0366112	1	0.02280705	1	0.01449543	0	0	1	0.021314
transporter/ receptor	11	1.56400161	5	0.15002323	7	0.60801075	8	1.48976031	3	0.072269
Total	551	100	491	100	552	100	324	100	336	100

Table 4. *Amblyomma americanum* tick saliva protein classes that are conserved in other tick saliva proteomes at 70% identity.

Classification	*I. scapularis*	*H. longicornis*	*D. andersoni*	*R. microplus*	*O. moubata*	*R. sanguinues*
Cytoskeletal	38	29	19	14	5	0
Detoxification	13	9	9	5	0	2
Extracellular matrix	3	6	9	3	0	1
Glycine rich	5	4	4	4	0	0
Immune related	4	3	3	4	1	1
Metabolism, amino acids	4	1	0	0	0	0
Metaolism, carbohydrates	4	3	6	1	1	0
Metabolim, energy	20	11	12	0	4	0
Metabolism, lipids	2	1	3	4	0	0
Metabolism, nucleic acids	11	9	1	0	2	0
Nuclear regulation	6	5	6	4	0	0
Protein export	1	0	0	0	0	0
Protein modification	16	14	8	9	7	0
Protease	6	6	8	3	0	0
Proteosome machinery	9	8	5	0	0	8
Protein synthesis	4	2	3	2	0	0
Secreted saliva proteins	4	6	23	15	0	0
Lipocalin	0	0	0	4	0	0
Protease Inhibitors	6	14	10	12	1	1
Signal transduction	6	3	6	1	1	0
Heme/Iron binding	1	7	2	9	2	0
Transcription machinery	2	0	1	1	0	0
Transporters/ receptors	3	1	0	1	0	0
Total Protein Matches	**168**	**142**	**138**	**96**	**24**	**13**

(> 70% identical)

APPENDIX III

CHAPTER III Part IA FIGURES AND TABLES

Figure 1. Structure-based sequence alignment (Kim, et al., 2015). AAS19 (GAYW01000076) protein sequence was aligned with its homologs in other tick species: *Rhipicephalus pulchellus* (L7LRY7), *Ixodes ricinus* (V5IHU3), *Amblyomma maculatum* (G3ML49 and G3ML50), *Rhipicephalus microplus* (V9VP22), *Ixodes scapularis* (B7QJF1), *Amblyomma triste* (A0A023GPF9) and *Amblyomma cajenense* (A0A023FM57). Secondary structures assigned based on AAS19 comparative tertiary structure, are labeled as ‘‘H’’ for α-helix and ‘‘E’’ for β-strand. Helices are labeled from ‘‘hA’’ to ‘‘hI’’ and β-strands that constitute β-sheet A–C are labeled as ‘‘s1-6A’’, ‘‘s1-5B’’ and ‘‘s1-4C’’, respectively. The “RGD” motif and two putative N-glycosylation sites are boxed by solid and broken lines, respectively. The residues that correspond to the basic patches are indicated by an asterisk (*). The high and low conserved residues are highlighted in black and gray, respectively. The 100% conserved reactive center loop (RCL) region is denoted with broken lines (---).

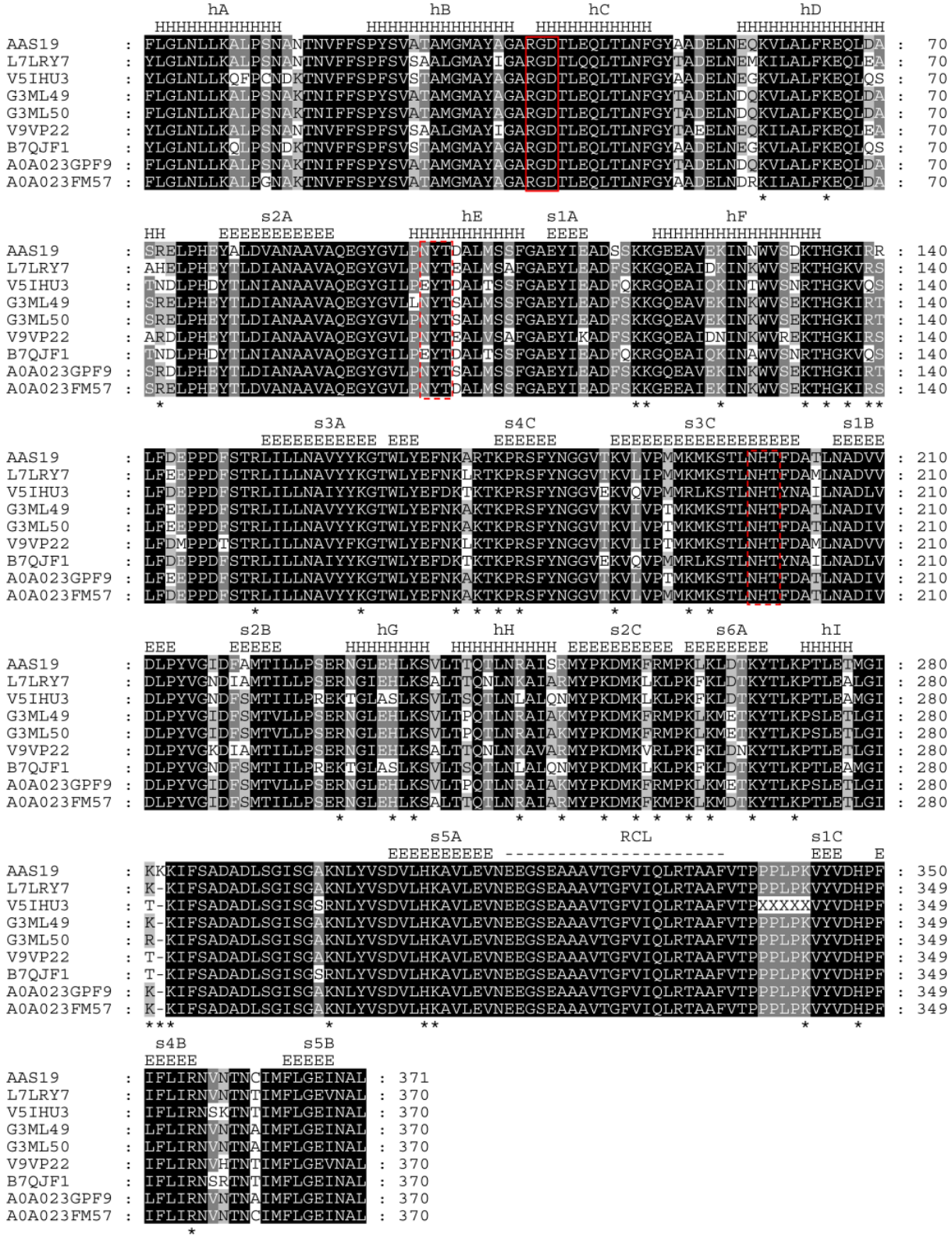
hA hB hC hD
s2A hE s1A hF
s3A s4C s3C s1B
s2B hG hH s2C s6A hI
s5A RCL s1C
s4B s5B
AAS19 : FLGLNLLKALPSNANTNVFFSPYSVATAMGMAYAGARGDTLEQLTLNFGYAADELNEQKVLALFREQLDA : 70
L7LRY7 : YLGLNLLKALPSNANTNVFFSPFSVSAALGMAYIGARGDTLQQLTLNFGYTADELNEMKILALFKEQLEA : 70
V5IHU3 : YLGLNLLKQFPCNDKTNVFFSPFSVSTAMGMAYAGARGDTLEQLTLNFGYAADELNEGKVLALFKEQLQS : 70
G3ML49 : FLGLNLLKALPSNAKTNIFFSPYSVATAMGMAYAGARGDTLEQLTLNFGYTADELNDQKVLALFKEQLDA : 70
G3ML50 : FLGLNLLKALPSNAKTNIFFSPYSVATAMGMAYAGARGDTLEQLTLNFGYTADELNDQKVLALFKEQLDA : 70
V9VP22 : YLGLNLLKALPSNANTNVFFSPFSVSAALGMAYIGARGDTLEQLTLNFGYTAEELNEQKILALFKEQLEA : 70
B7QJF1 : YLGLNLLKQLPSNDKTNVFFSPFSVSTAMGMAYAGARGDTLEQLTLNFGYAADELNEGKVLALFKEQLQS : 70
A0A023GPF9 : FLGLNLLKALPSNAKTNIFFSPYSVATAMGMAYAGARGDTLEQLTLNFGYTADELNDQKVLALFKEQLDA : 70
A0A023FM57 : FLGLNLLKALPGNAKTNVFFSPYSVATAMGMAYAGARGDTLEQLTLNFGYAADELNDRKILALFKEQLDA : 70
AAS19 : SRELPHEYALDVANAAVAQEGYGVLPNYTDALMSSFGAEYIEADSSKKGEEAVEKINNWVSDKTHGKIRR : 140
L7LRY7 : AHELPHEYTLDIANAAVAQEGYGVLPNYTEALMSAFGAEYLEADFSKKGQEAIDKINKWVSEKTHGKVRS : 140
V5IHU3 : TNDLPHDYTLNIANAAVAQEGYGILPEYTDALTSSFGAEYIEADFQKRGQEAIQKINTWVSNRTHGKVQS : 140
G3ML49 : SRELPHEYTLDIANAAVAQEGYGVLLNYTSALMSSFGAEYLEADFSKKGQEAVEKINKWVSEKTHGKIRT : 140
G3ML50 : SRELPHEYTLDIANAAVAQEGYGVLPNYTSALMSSFGAEYLEADFSKKGQEAVEKINKWVSEKTHGKIRT : 140
V9VP22 : ARDLPHEYTLDIANAAVAQEGYGVLPNYTEALVSAFGAEYLKADFSKKGQEAIDNINKWVREKTHGKIRS : 140
B7QJF1 : TNDLPHDYTLNIANAAVAQEGYGILPEYTDALTSSFGAEYIEADFQKRGQEAIQKINAWVSNRTHGKVQS : 140
A0A023GPF9 : SRDLPHEYTLDIANAAVAQEGYGVLPNYTSALMSSFGAEYLEADFSKKGQEAVEKINKWVSEKTHGKIRT : 140
A0A023FM57 : SRELPHEYTLDVANAAVAQEGYGVLPNYTDALMSSFGAEYIEADFSKKGEEAIEKINKWVSEKTHGKIRS : 140
AAS19 : LFDEPPDFSTRLILLNAVYYKGTWLYEFNKARTKPRSFYNGGVTKVLVPMMKMKSTLNHTFDATLNADVV : 210
L7LRY7 : LFEEPPDFSTRLILLNAVYYKGTWLYEFNKLRTKPRSFYNGGVTKVLIPMMKMKSTLNHTFDAMLNADVV : 210
V5IHU3 : LFDEPPDFSTRLILLNAIYYKGTWLYEFDKTKTKPRSFYNGGVEKVQVPMMRLKSTLNHTYNAILNADLV : 210
G3ML49 : LFEEPPDFSTRLILLNAVYYKGTWLYEFNKAKTKPRSFYNGGVTKVIVPTMKMKSTLNHTFDATLNADIV : 210
G3ML50 : LFEEPPDFSTRLILLNAVYYKGTWLYEFNKAKTKPRSFYNGGVTKVLVPTMKMKSTLNHTFDATLNADIV : 210
V9VP22 : LFDMPPDTSTRLILLNAVYFKGTWLYEFNKLKTKPRSFYNGGVTKVLIPTMKMKSTLNHTFDAMLNADVV : 210
B7QJF1 : LFDEPPDFSTRLILLNAIYYKGTWLYEFDKTKTKPRSFYNGGVEKVQVPMMRLKSTLNHTYNAILNADLV : 210
A0A023GPF9 : LFEEPPDFSTRLILLNAVYYKGTWLYEFNKAKTKPRSFYNGGVTKVLVPTMKMKSTLNHTFDATLNADIV : 210
A0A023FM57 : LFDEPPDFSTRLILLNAVYYKGTWLYEFNKAKTKPRSFYNGGVTKVLVPMMKMKSTLNHTFDATLNADIV : 210
AAS19 : DLPYVGIDFAMTILLPSERNGLEHLKSVLTTQTLNRAISRMYPKDMKFRMPKLKLDIKYTLKPTLETMGI : 280
L7LRY7 : DLPYVGNDIAMTILLPSERNGIEHLKSALTTQNLNKAIARMYPKDMKLKLPKFKLDTKYTLKPTLEALGI : 280
V5IHU3 : DLPYVGNDFSMTIILPREKTGLASLKSVLTSQTLNLALQNMYPKDMKLKLPKFKLDTKYTLKPTLEAMGI : 280
G3ML49 : DLPYVGIDFSMTVLLPSERNGLEHLKSVLTPQTLNRAIAKMYPKDMKFRMPKLKMETKYTLKPSLETLGI : 280
G3ML50 : DLPYVGIDFSMTVLLPSERNGLEHLKSVLTPQTLNRAIAKMYPKDMKFRMPKLKMETKYTLKPSLETLGI : 280
V9VP22 : DLPYVGKDIAMTILLPSERNGIEHLKSALTTQNLNKAVARMYPKDMKVRLPKFKLDNKYTLKPTLETLGI : 280
B7QJF1 : DLPYVGNDFSMTIILPREKTGLASLKSVLTSQTLNLALQNMYPKDMKLKLPKFKLDTKYTLKPTLEAMGI : 280
A0A023GPF9 : DLPYVGIDFSMTVLLPSERNGLEHLKSVLTPQTLNRAIAKMYPKDMKFRMPKLKMETKYTLKPSLETLGI : 280
A0A023FM57 : DLPYVGIDFSMTILLPSERNGLEHLKSALTTQTLNRAIARMYPKDMKFKMPKLKMDIKYTLKPTLETLGI : 280
AAS19 : KKKIFSADADLSGISGAKNLYVSDVLHKAVLEVNEEGSEAAAVTGFVIQLRTAAFVTPPPLPKVYVDHPF : 350
L7LRY7 : K-KIFSADADLSGISGAKNLYVSDVLHKAVLEVNEEGSEAAAVTGFVIQLRTAAFVTPPPLPKVYVDHPF : 349
V5IHU3 : T-KIFSADADLSGISGSRNLYVSDVLHKAVLEVNEEGSEAAAVTGFVIQLRTAAFVTPXXXXXVYVDHPF : 349
G3ML49 : K-KIFSADADLSGISGAKNLYVSDVLHKAVLEVNEEGSEAAAVTGFVIQLRTAAFVTPPPLPKVYVDHPF : 349
G3ML50 : R-KIFSADADLSGISGAKNLYVSDVLHKAVLEVNEEGSEAAAVTGFVIQLRTAAFVTPPPLPKVYVDHPF : 349
V9VP22 : T-KIFSADADLSGISGAKNLYVSDVLHKAVLEVNEEGSEAAAVTGFVIQLRTAAFVTPPPLPKVYVDHPF : 349
B7QJF1 : T-KIFSADADLSGISGSRNLYVSDVLHKAVLEVNEEGSEAAAVTGFVIQLRTAAFVTPPPLPKVYVDHPF : 349
A0A023GPF9 : K-KIFSADADLSGISGAKNLYVSDVLHKAVLEVNEEGSEAAAVTGFVIQLRTAAFVTPPPLPKVYVDHPF : 349
A0A023FM57 : K-KIFSADADLSGISGAKNLYVSDVLHKAVLEVNEEGSEAAAVTGFVIQLRTAAFVTPPPLPKVYVDHPF : 349
AAS19 : IFLIRNVNTNCIMFLGEINAL : 371
L7LRY7 : IFLIRNVNTNTIMFLGEVNAL : 370
V5IHU3 : IFLIRNSKTNTIMFLGEINAL : 370
G3ML49 : LFLIRNVNTNAIMFLGEINAL : 370
G3ML50 : LFLIRNVNTNAIMFLGEINAL : 370
V9VP22 : IFLIRNVHTNTIMFLGEVNAL : 370
B7QJF1 : IFLIRNSRTNTIMFLGEINAL : 370
A0A023GPF9 : LFLIRNVNTNAIMFLGEINAL : 370
A0A023FM57 : IFLIRNVNTNCIMFLGEINAL : 370

Figure 2. Structure and putative glycosaminoglycan-binding sites of AAS19 (Kim, et al., 2015). AAS19 model was constructed using the coordinates generated with Modeler 9v14 program and protein C inhibitor as template (PDB 2OL2). Calculation of electrostatic potential surface map was generated using APBS tool in VMD program. (A) Electrostatic surface potential (blue and red for positive and negative charge, respectively) and ribbon diagram of the native protein C inhibitor (PCI template) showing the GAG-binding along the helix H. Residues responsible by GAG-binding activity are shown as sticks and labeled (Li and Huntington, 2008). (B) Electrostatic surface potential and ribbon diagram of AAS19 model showing putative GAG-binding sites (GAGBS 1-4). Clusters of basic amino acid residues potentially involved in formation of GAGBS 1-4 [K^{137}-R^{139}-R^{140}-K^{161}-K^{264}-K^{268}-K^{308}], [K^{8}-K^{236}-R^{246}-R^{250}], [R^{172}-K^{174}-R^{176}-K^{185}-K^{192}-K^{194}-K^{343}], and [K^{117}-K^{118}-R^{151}-K^{272}-K^{298}] are shown as sticks and labeled.

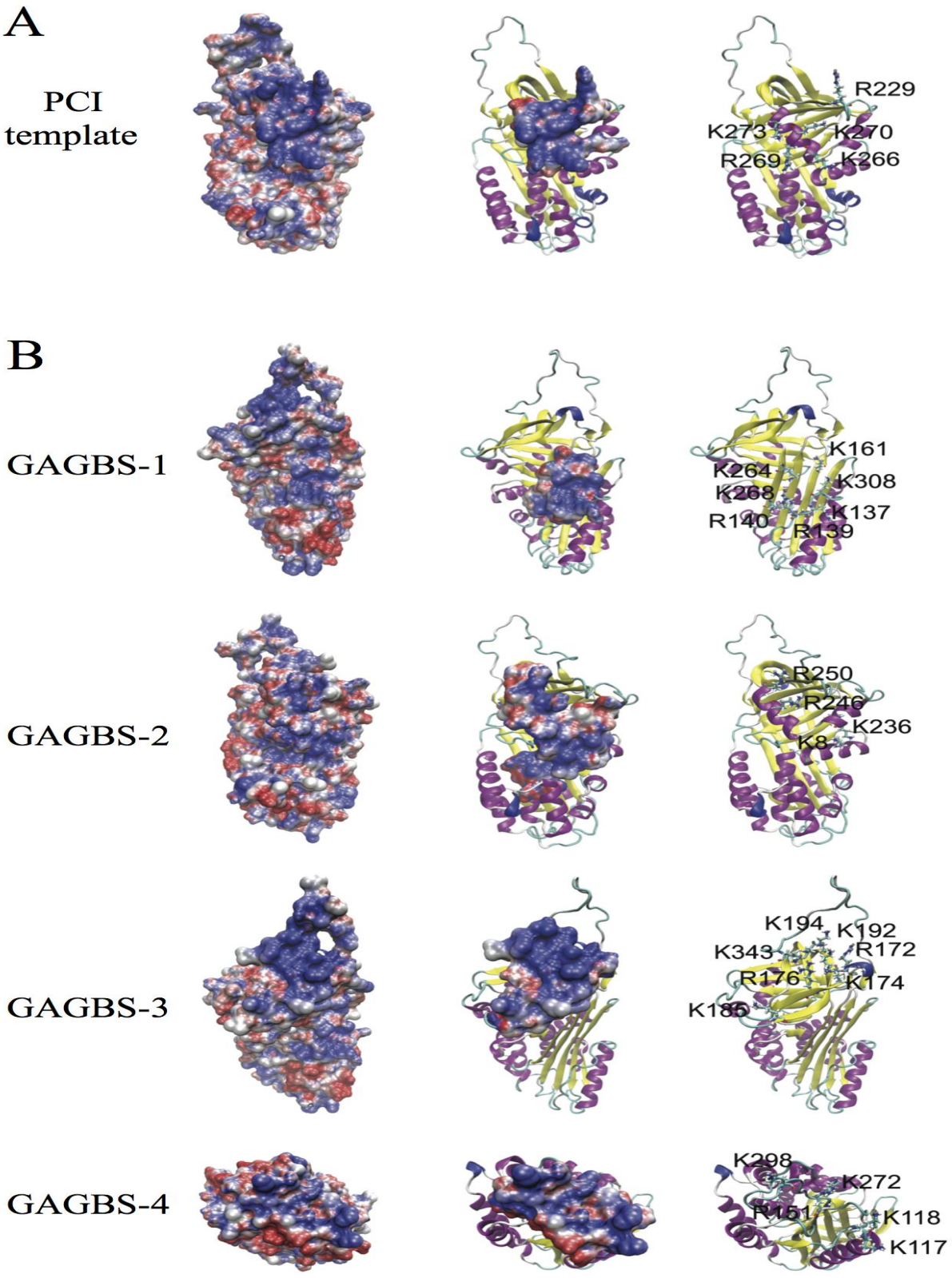
A
PCI template
R229
K273
K270
R269
K266
B
GAGBS-1
K161
K264
K308
K268
K137
R140
R139
GAGBS-2
R250
R246
K236
K8
GAGBS-3
K194
K192
K343
R172
R176
K174
K185
GAGBS-4
K298
K272
R151
K118
K117

Figure 3. Temporal and spatial expression analysis of AAS19 mRNA through 120h post attachment (Kim, et al., 2015). AAS19 mRNA relative expression analysis in unfed (UF), 24, 48, 72, 96, and 120h fed tick dissected tissues: (A) salivary gland, (B) midgut and (C) carcass analyzed by quantitative RT-PCR. To determine the AAS19 mRNA relative expression (y-axis), data were analyzed using the $2^{-\Delta\Delta Ct}$ method comparing to RPS4 in three biological replicates of different tissues in relation to time of feeding (x-axis). The lowest expressed time point was used as calibrator for each tissue.

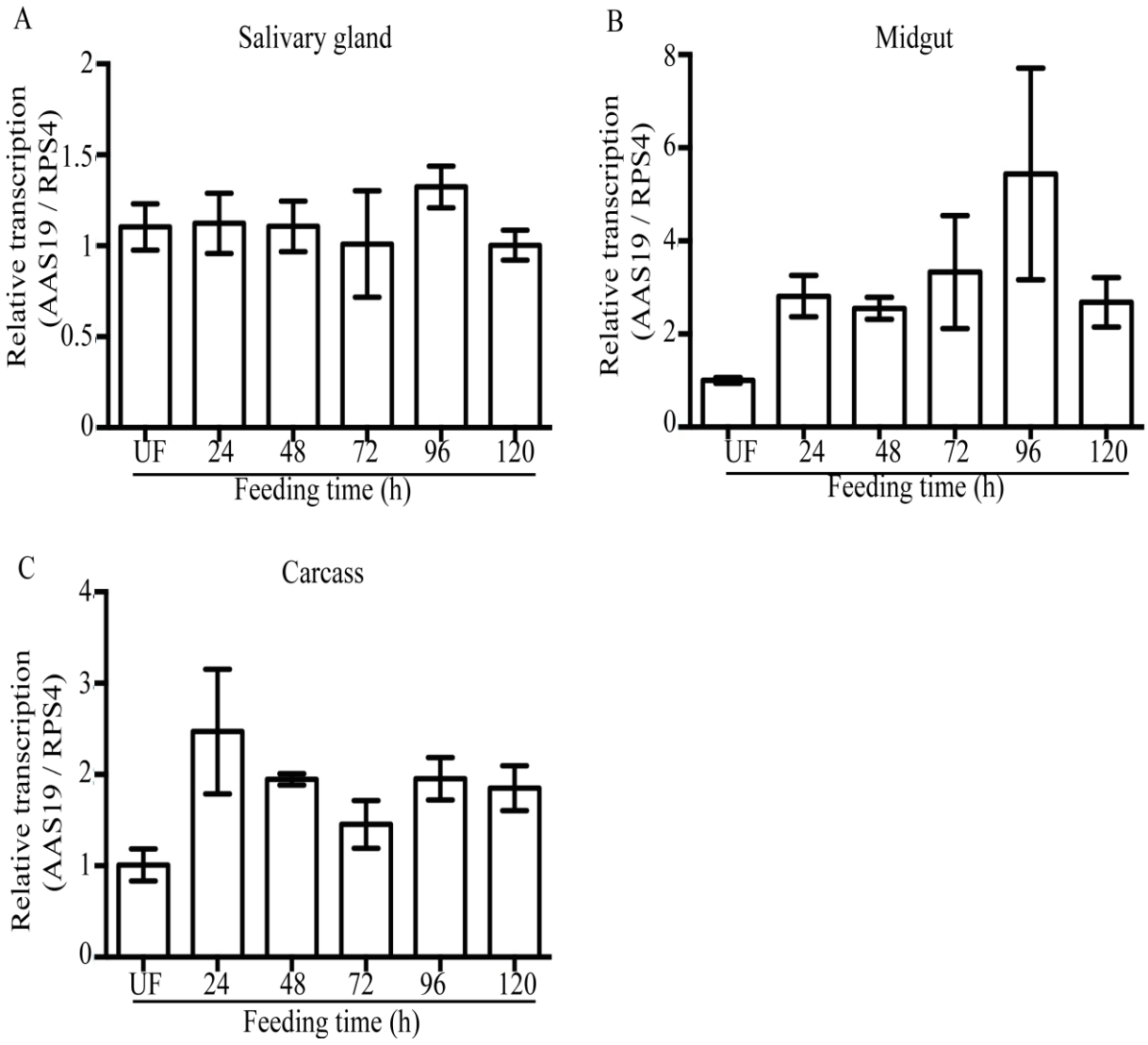
A
Salivary gland
Relative transcription (AAS19 / RPS4)
2
1.5
1
0.5
0
UF
24
48
72
96
120
Feeding time (h)
B
Midgut
Relative transcription (AAS19 / RPS4)
8
6
4
2
0
UF
24
48
72
96
120
Feeding time (h)
C
Carcass
Relative transcription (AAS19 / RPS4)
4
3
2
1
0
UF
24
48
72
96
120
Feeding time (h)

Figure 4. Expression and affinity purification of recombinant (r) *Amblyomma americanum* AAS19 in *Pichia pastoris* (Kim, et al., 2015). Construction of expression plasmid, induction and validation of expression levels using the antibody to the C-terminus hexahistidine tag and affinity purification of rAAS19 were performed as described in Materials and Methods. (A) Daily expression levels of rAAS19 through 5 days, (B) Affinity purified rAAS19 resolved on a 10% SDS-PAGE and silver staining (L = molecular weight ladder, T = total protein loaded onto column, R = column run through, B = binding buffer wash, W1 and W2 = wash buffers, E1-E4 = eluted rAAS19). Purified rAAS19 fractions used for assays in Fig. 5-9 are noted with asterisks (*). Western blotting analysis with (C) 1:50 dilution pre-immune sera, (D) 1:250 dilution immune sera to replete-fed *A. americanum* tick saliva proteins, and (E) antibody to C-terminus hexahistidine tag. Lanes L, 1 and 2 in C, D and E = molecular weight ladder, glycosylated and de-glycosylated rAAS19.

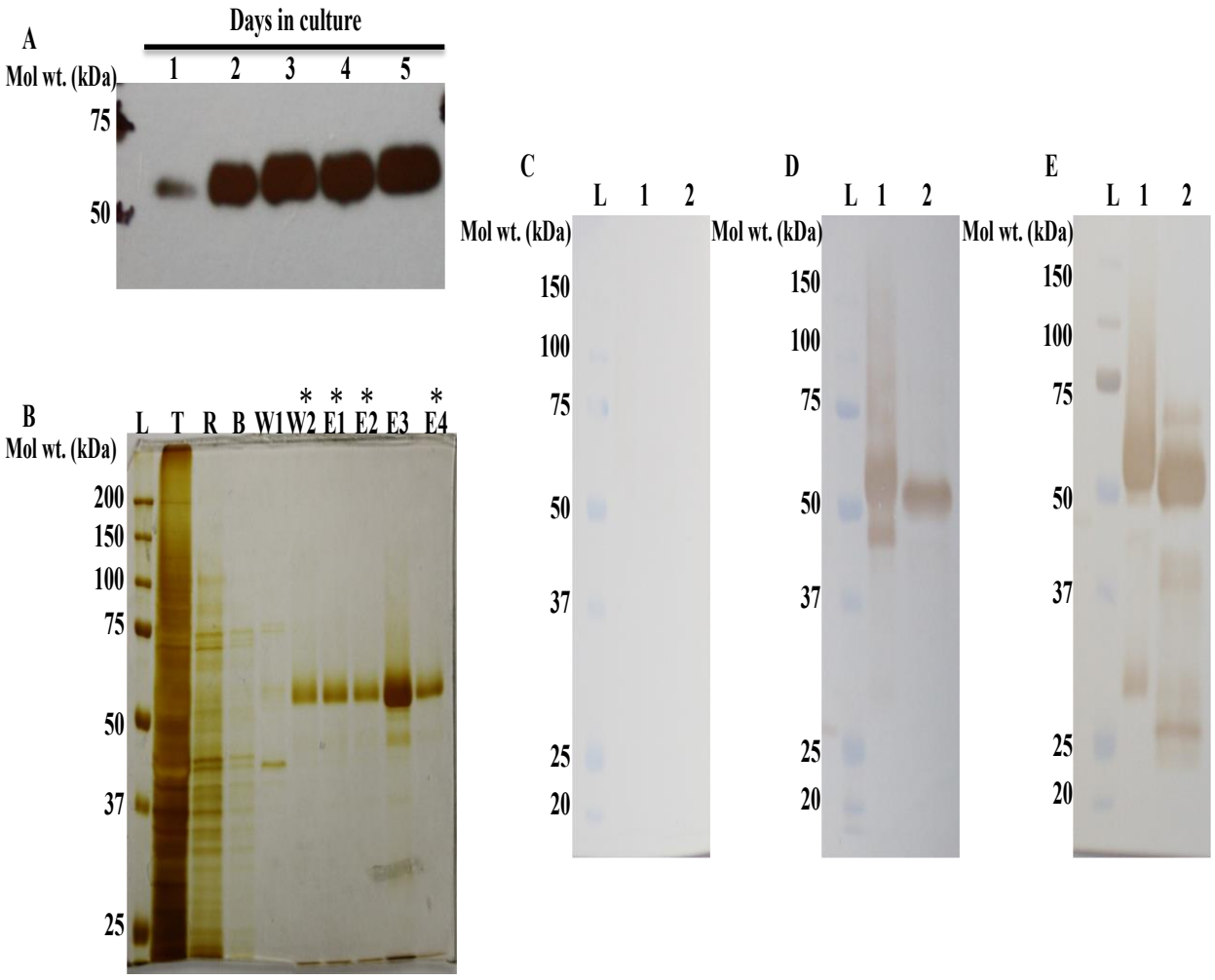
A
Days in culture
1 2 3 4 5
Mol wt. (kDa)
75
50
B
L T R B W1 W2 E1 E2 E3 E4
Mol wt. (kDa)
200
150
100
75
50
37
25
C
L 1 2
Mol wt. (kDa)
150
100
75
50
37
25
20
D
L 1 2
Mol wt. (kDa)
150
100
75
50
37
25
20
E
L 1 2
Mol wt. (kDa)
150
100
75
50
37
25
20

Figure 5. Protease inhibitor function profiling (Kim, et al., 2015). Enzymes at indicated concentrations in material and methods were pre-incubated with rAAS19 (1 µM) at 37°C for 15 min. Subsequently specific colorimetric substrate were added and hydrolysis monitored at A_{450nm} over 30min at 30°C. The percent enzyme activity inhibition level was determined using the formula: 100 - $V_{max}(V_i)/V_{max}$ (V_0) X 100 where V_{max} (V_i) = activity in presence of, and V_{max} (V_0) = activity in absence of rAAS19. Data are presented as mean ± SEM of triplicate readings.

A

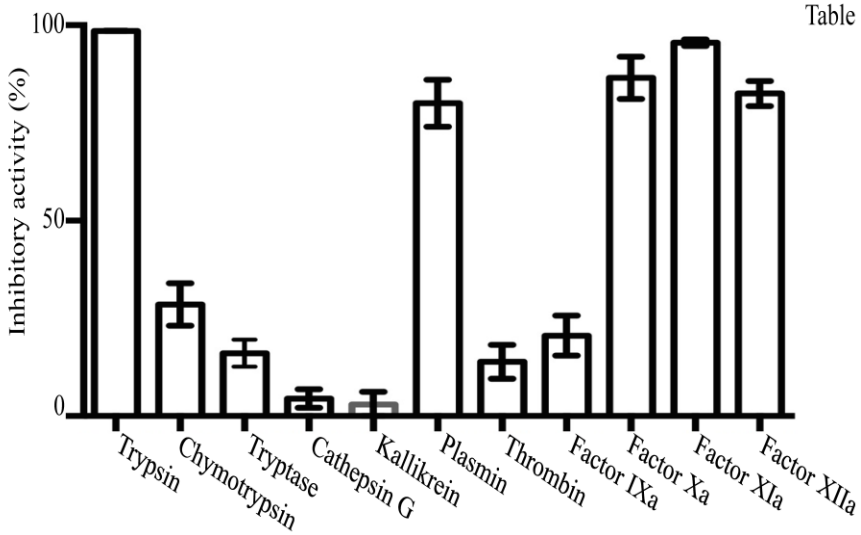

B

Table insert: r*Aam*S19 (1μM) inhibitory activity

Protease (μM)	Inhibitory activity (%)
Trypsin	98.58 ± 0.0316
Chymotrypsin	28.52 ± 5.399
Tryptase	16.08 ± 3.441
Cathepsin G	4.50 ± 2.362
Kallikrein	2.947 ± 1.145
Plasmin	80.04 ± 2.465
Thrombin	13.91 ± 2.168
Factor IXa	20.56 ± 2.557
Factor Xa	86.53 ± 1.910
Factor Xia	95.55 ± 0.292
Factor XIIa	82.51 ± 1.135

Figure 6. Stoichiometry inhibition (SI) assay for AAS19 (Kim, et al., 2015). Residual enzyme activity without (a) and with presence of increasing (b-g) rAAS19 amounts were pre-incubated for 1 h at 37°C with constant concentration of trypsin (A&B: 10 nM), plasmin (C&D: 10 nM), factor Xa (E&F: 5 nM), and factor XIa (G&H: 5 nM), resulting in molar ratios varying from 0 to 10 (for plasmin and trypsin) or 0 to 20 (for factor Xa and factor XIa). Residual enzymatic activity was measured using specific colorimetric substrate for each enzyme noted in materials and methods. The data were plotted as enzymatic residual activity (V_i/V_0) versus molar ratio (rAAS19:protease). The stoichiometry of inhibition (SI) was determined by fitting data onto a linear regression line.

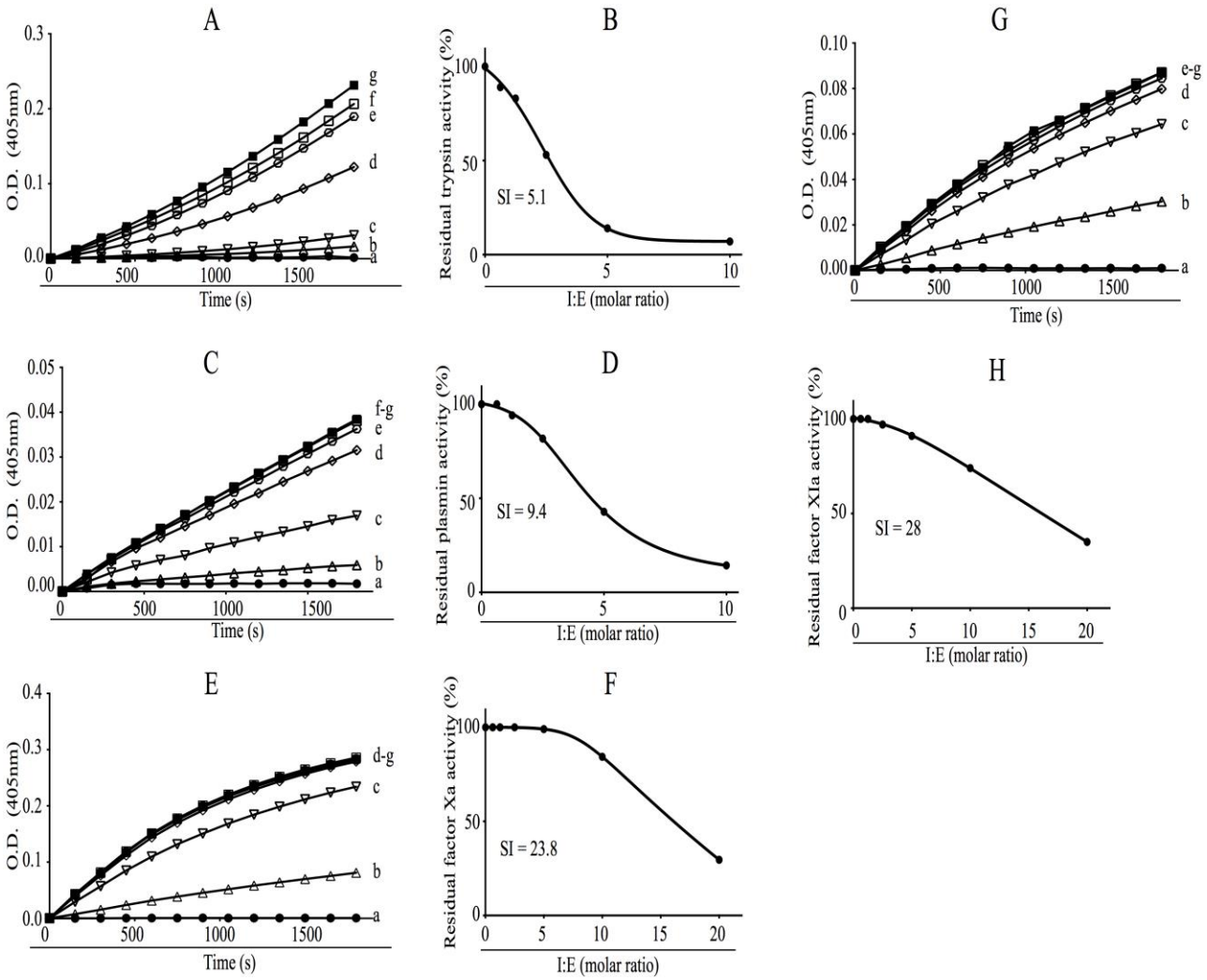
A
O.D. (405nm)
Time (s)
g
f
e
d
c
b
a
B
Residual trypsin activity (%)
SI = 5.1
I:E (molar ratio)
G
O.D. (405nm)
Time (s)
e-g
d
c
b
a
C
O.D. (405nm)
Time (s)
f-g
e
d
c
b
a
D
Residual plasmin activity (%)
SI = 9.4
I:E (molar ratio)
H
Residual factor XIa activity (%)
SI = 28
I:E (molar ratio)
E
O.D. (405nm)
Time (s)
d-g
c
b
a
F
Residual factor Xa activity (%)
SI = 23.8
I:E (molar ratio)

Figure 7. SDS-stable complex formation assay (Kim, et al., 2015). Increasing amounts of rAAS19 were pre-incubated for 1 h at 37°C with constant concentration of trypsin (A), factor Xa (B) and factor XIa (C), resulting in molar ratios varying from 0.625:1 to 10:1 (rAAS19:protease). Samples were resolved on 12.5% SDS-PAGE and Coomassie blue stained to identify SDS-stable complexes.

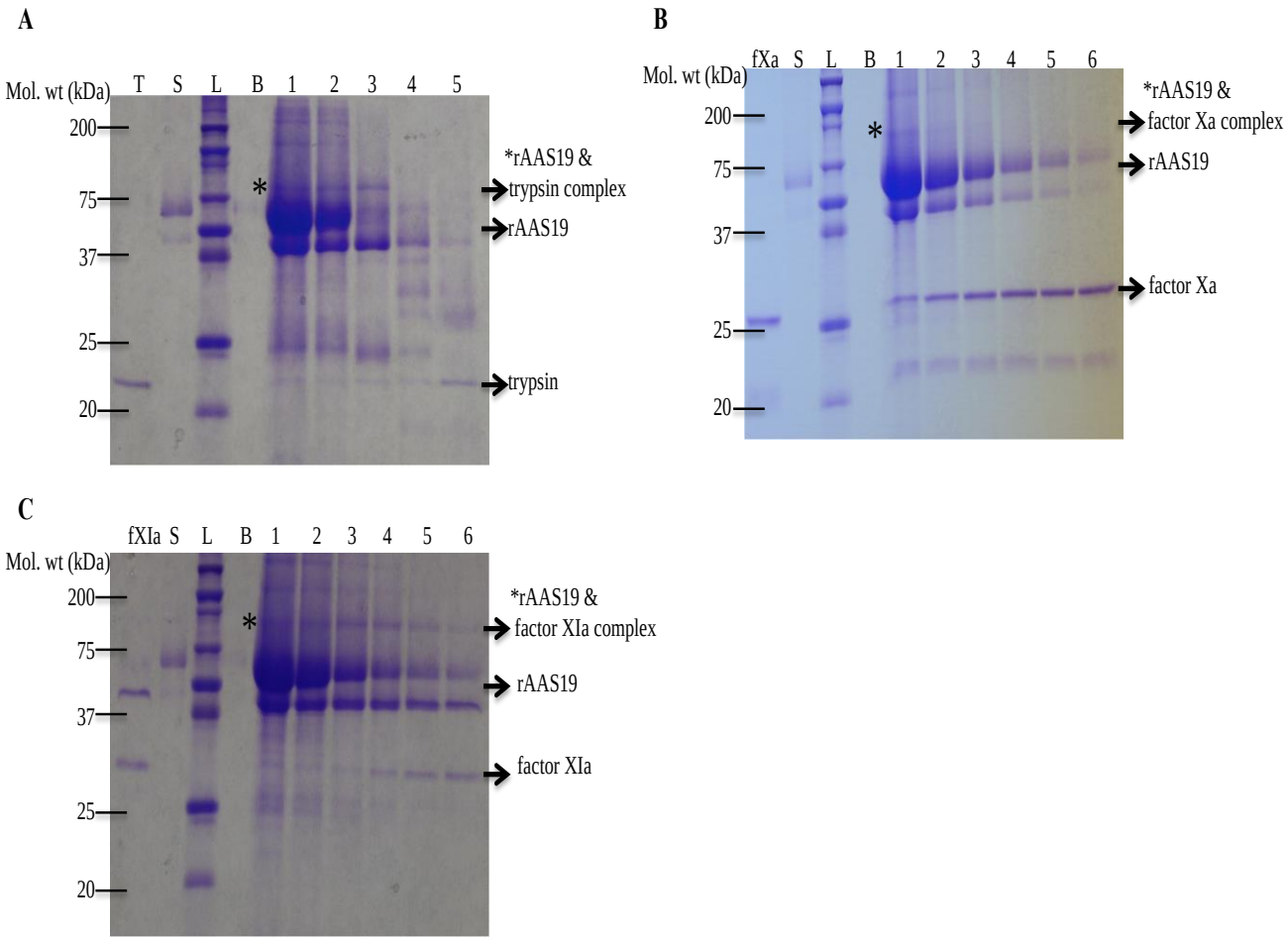
A
Mol. wt (kDa)
T S L B 1 2 3 4 5
200
75
37
25
20
*
*rAAS19 &
trypsin complex
rAAS19
trypsin
B
Mol. wt (kDa)
fXa S L B 1 2 3 4 5 6
200
75
37
25
20
*
*rAAS19 &
factor Xa complex
rAAS19
factor Xa
C
Mol. wt (kDa)
fXIa S L B 1 2 3 4 5 6
200
75
37
25
20
*
*rAAS19 &
factor XIa complex
rAAS19
factor XIa

Figure 8. Effect of rAAS19 on thrombin activated platelet aggregation (Kim, et al., 2015). (A) The platelet aggregation function assay was done using platelet rich plasma (PRP) approach described in materials and methods. Tyrode buffer without thrombin (a), various amounts of rAAS19 with 1 μM (b), 0.5 μM (c), and 0.25 μM (d) rAAS19 and thrombin only (e) were pre-incubated with thrombin (3 U) in a 50 μL reaction for 15 min at 37°C. Platelet aggregation was initiated with addition of 100 μL pre-warmed PRP and monitored at intervals of 20 seconds over 30 min at A_{650nm}. (B) Percent reduction of thrombin-induced platelet aggregation inhibition by rAAS19. In the assay used here, platelet aggregation was directly proportional to reduced optical density (OD, A_{650nm}). Data are presented as M ± SEM of duplicate platelet aggregation assays.

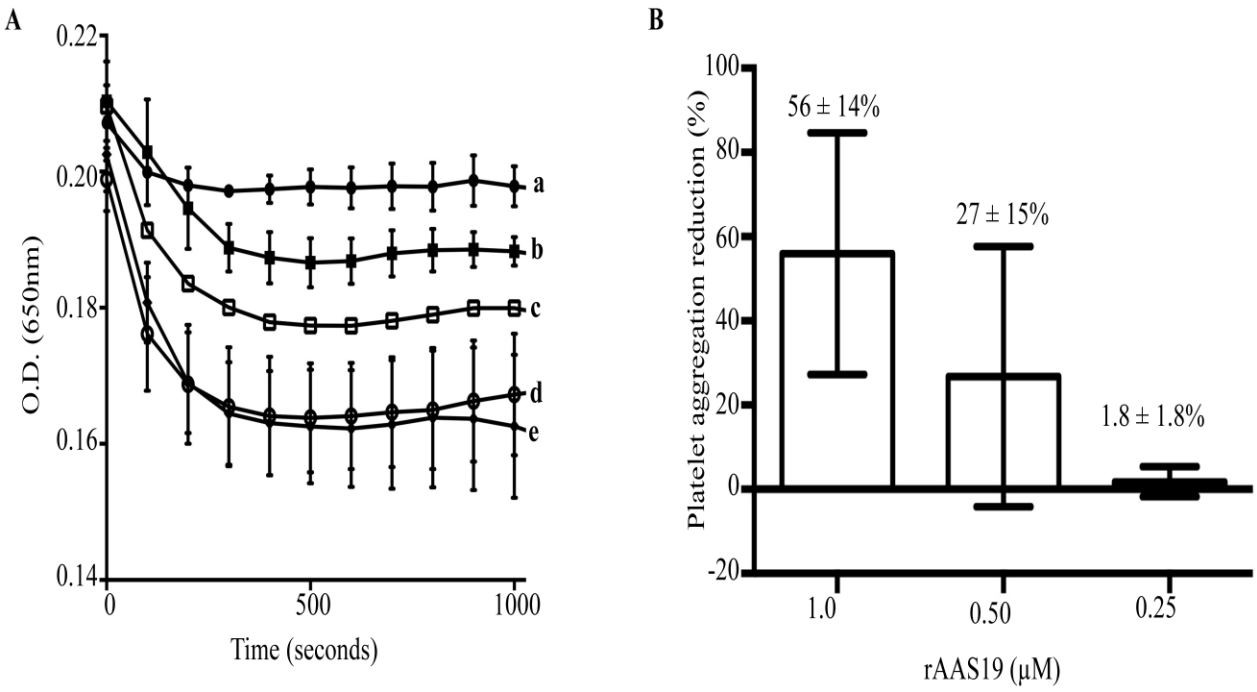
A
0.22
0.20
0.18
0.16
0.14
O.D. (650nm)
0
500
1000
Time (seconds)
a
b
c
d
e
B
100
80
60
40
20
0
-20
Platelet aggregation reduction (%)
56 ± 14%
27 ± 15%
1.8 ± 1.8%
1.0
0.50
0.25
rAAS19 (μM)

Figure 9. The effect of rAA19 on plasma clotting time in the recalcification time (RCT), activated partial thromboplastin time (aPTT), and thrombin time (TT) assays (Kim, et al., 2015). (A) Universal coagulation reference human plasma [UCRP] (50 μL) was incubated with 0 (arrow head R-CT1), 0.625, 1.25 and 5 (arrow head R-CT2), and 10 (arrow head R-CT3) μM rAAS19 in 90 μL Tris-HCl reaction buffer for 15 min at 37°C before the addition of 150 mM $CaCl_2$ (10 μL) with clotting was monitored at every 20 s for 30 min. (B) UCRP (50 μL) was incubated with with 0, 0.625, 1.25 (arrow head A-CT1), 5 (arrow head A-CT2), and 10 (arrow head A-CT3) μM rAAS19 up to 100 μL of Tris-HCl reaction buffer for 15 min at 37°C. Followed by the addition of aPTT reagent and incubation for 5 min at 37°C before the addition of 25 mM $CaCl_2$ (10 μL), clotting time was monitored every 10 s for 5 min. (C) rAAS19 with 0, 0.625 (arrow head T-CT1), 1.25 and 5 (arrow head T-CT2), and 10 (arrow head T-CT3) were incubated with 25 μL of the TT reagent containing $CaCl_2$ for 15 min at 37°C before addition of 50 μL of pre-warmed UCRP with clotting time monitored every 10 s for 5 min. All assays were done in duplicate, with clotting time monitored at A_{650nm}.

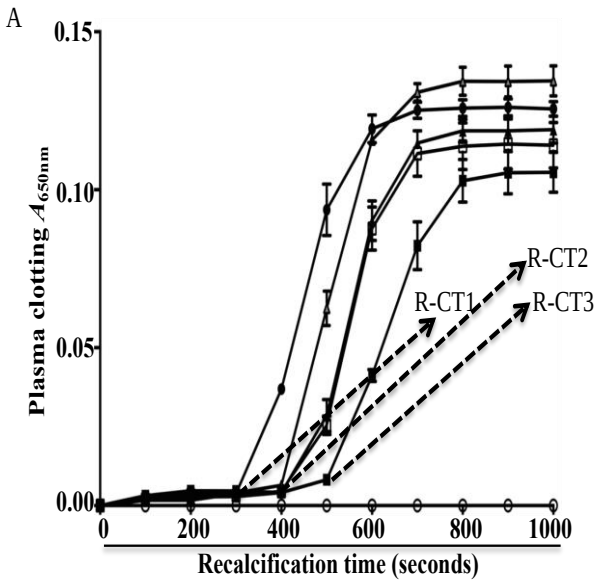
A
0.15
0.10
0.05
0.00
Plasma clotting A_{650nm}
0
200
400
600
800
1000
Recalcification time (seconds)
R-CT1
R-CT2
R-CT3

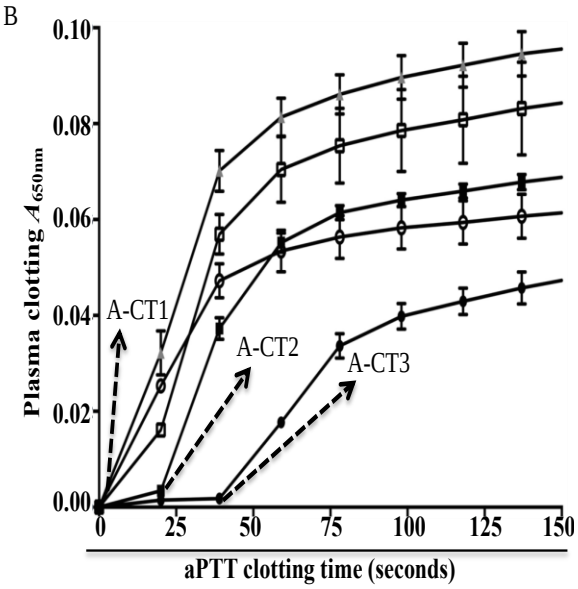
B
0.10
0.08
0.06
0.04
0.02
0.00
Plasma clotting A_{650nm}
0
25
50
75
100
125
150
aPTT clotting time (seconds)
A-CT1
A-CT2
A-CT3

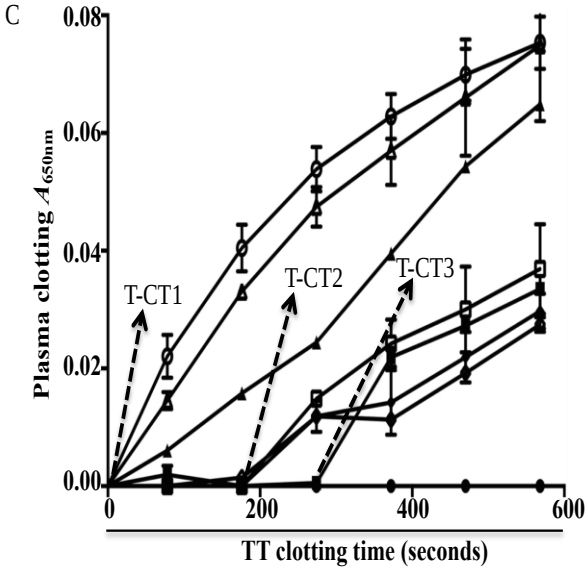
C
0.08
0.06
0.04
0.02
0.00
Plasma clotting A_{650nm}
0
200
400
600
TT clotting time (seconds)
T-CT1
T-CT2
T-CT3

Table 1. Proteases used in rAAS19 protease inhibitor profiling (Kim, et al., 2015).

Proteases	Biological function	References
thrombin	Common, intrinsic and extrinsic coagulation pathways. Fibrinolysis pathway. Platelet activation and aggregation pathways via activation of protease-activated receptors (PARs). Wound healing/Tissue remodeling. Inflammation.	Davie et al., 1991; Gartner et al., 1978; Hoffman, 2003; Olszewska-Pazdrak et al., 2010; Reimers et al., 1976
trypsin	Digestion. Wound healing/Tissue remodeling. Inflammation and pain via activation of PAR2.	Cattaruzza et al., 2014; Walsh et al., 1964; White et al., 2013
cathepsin G	Platelet activation. Wound healing/Tissue remodeling. Inflammation. Antimicrobial properties.	Korkmaz et al., 2008; Mak et al., 2003; Renesto and Chignard, 1993
kallikrein	Wound healing/Tissue remodeling. Inflammation. Intrinsic coagulation pathway	Chao et al., 2010; Li et al., 2007
elastase	Wound healing/Tissue remodeling. Inflammation. Digestion of elastin. Activation of platelets and lymphocytes. Antimicrobial properties	Belaaouaj, 2002; Kessenbrock et al., 2011; Kessenbrock et al., 2008; Korkmaz et al., 2008; Renesto and Chignard, 1993
plasmin	Fibrinolysis pathway. Inflammation	Carmo et al., 2014; Collen, 1999; Li et al., 2012; Mancek-Keber, 2014
factor IXa	Intrinsic coagulation pathway. Platelet Amyloid Precursor Protein Pathway	Davie et al., 1991; Hoffman, 2003
factor Xa	Common, intrinsic and extrinsic coagulation pathways.	Davie et al., 1991; Hoffman, 2003
factor XIa	Intrinsic coagulation pathway. Platelet Amyloid Precursor Protein Pathway	Davie et al., 1991; Hoffman, 2003
factor XIIa	Intrinsic coagulation pathway.	Davie et al., 1991; Hoffman, 2003
tissue-type plasminogen activator (t-PA)	Fibrinolysis pathway. Platelet Amyloid Precursor Protein Pathway.	Angles-Cano, 1994; Angles-Cano et al., 1994; Collen, 1999
urokinase plasminogen activator (u-PA)	Fibrinolysis pathway. Platelet Amyloid Precursor Protein Pathway.	Angles-Cano, 1994; Angles-Cano et al., 1994; Collen, 1999
α-chymotrypsin	Wound healing/Tissue remodeling. Inflammation. Digestion. Regulation of proteases: chymotrypsin, cathepsin G, mast cell chymase.	Algermissen et al., 1999a; Korkmaz et al., 2008; Matsunaga et al., 1994; Matsunaga et al., 2000
chymase	Wound healing/Tissue remodeling. Inflammation.	Algermissen et al., 1999a; Algermissen et al., 1999b; Caughey, 2007
tryptase	Wound healing/Tissue remodeling. Inflammation.	Algermissen et al., 1999a; Caughey, 2007; Hallgren and Pejler, 2006
proteinase-3	Wound healing/Tissue remodeling. Inflammation. Platelet Activation. Antimicrobial properties	Algermissen et al., 1999a; Kessenbrock et al., 2008; Korkmaz et al., 2008; Renesto et al., 1994

References

Kim, T.K., Tirloni, L., Radulovic, Z., Lewis, L., Bakshi, M., Hill, C., da Silva Vaz, I.,Jr, Logullo, C., Termignoni, C., Mulenga, A., 2015. Conserved *Amblyomma americanum* tick Serpin19, an inhibitor of blood clotting factors Xa and XIa, trypsin and plasmin, has anti-haemostatic functions. Int. J. Parasitol. 45, 613-627.

APPENDIX IV

CHAPTER III Part IB FIGURES AND TABLES

Figure 1. Validating the disruption of AAS19 mRNA in AAS19 double stranded (ds) RNA injected ticks (Kim, et al., 2016). Fifteen ticks were microinjected with 0.5–1 μL (~3 μg/μL) of AAS19- or EGFP- (control) dsRNA in nuclease free water. At 48 h post-attachment, three ticks per treatment of EGFP-dsRNA injected control and AAS19-dsRNA injected ticks, were manually detached. Tick organs including salivary glands (SG), midguts (MG), synganglion (SYN), Malpighian tubules (MT), ovaries (OV) and carcass (CA, tick remnants after removal of SG, MG, OV, and MT) were dissected and individually processed for mRNA extraction and then subjected to two-step quantitative (q) reverse transcriptase (RT)-PCR using AAS19 primers described in materials and methods section 2.4. Relative expression (RQ) of AAS19 mRNA was determined using the Comparative C_T Method ($\Delta\Delta C_T$). Relative suppression of AAS19 mRNA was determined using the following formula, $S = 100-(RQ^T/RQ^C \text{ X } 100)$ where S = mRNA suppression, RQ^T and RQ^C = RQ of tissues of AAS19-dsRNA and EGFP-dsRNA injected ticks respectively.

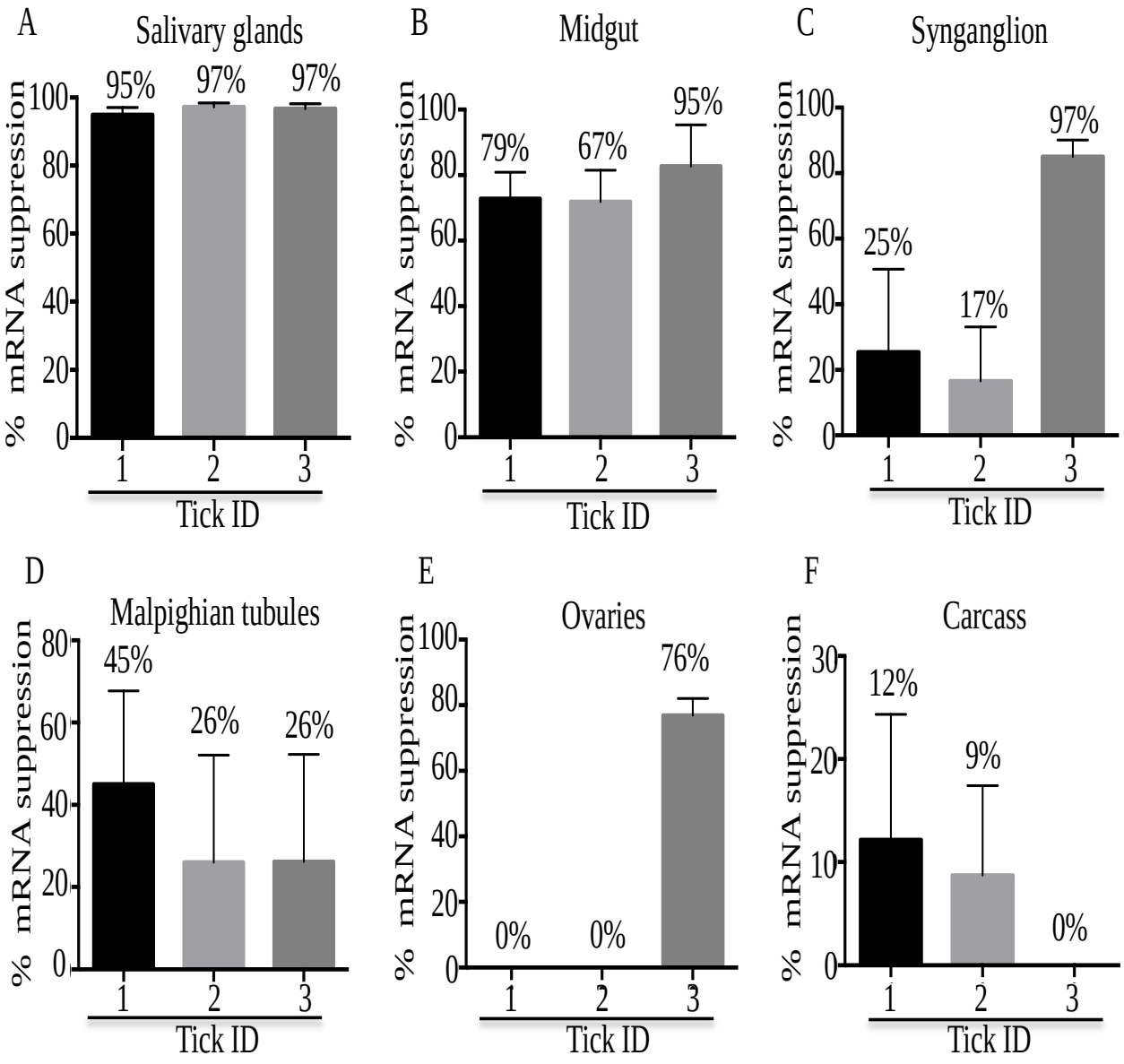
A
Salivary glands
95%
97%
97%
% mRNA suppression
100
80
60
40
20
0
1
2
3
Tick ID
B
Midgut
79%
67%
95%
% mRNA suppression
100
80
60
40
20
0
1
2
3
Tick ID
C
Synganglion
25%
17%
97%
% mRNA suppression
100
80
60
40
20
0
1
2
3
Tick ID
D
Malpighian tubules
45%
26%
26%
% mRNA suppression
80
60
40
20
0
1
2
3
Tick ID
E
Ovaries
0%
0%
76%
% mRNA suppression
100
80
60
40
20
0
1
2
3
Tick ID
F
Carcass
12%
9%
0%
% mRNA suppression
30
20
10
0
1
2
3
Tick ID

Fig. 2. Phenotype and engorgement weights of AAS19 dsRNA injected ticks (Kim, et al., 2016). (A) Spontaneously detached ticks were photographed to document phenotypic changes of AAS19-dsRNA injected ticks compared to control EGFP-dsRNA injected ticks. Deformed ticks are asterisks marked (*). (B) After spontaneously detaching from the host, ticks were individually weighed to determine engorgement weights (EWs) as indices for amounts of blood imbibed by ticks. EWs were subjected to unpaired student t-test and Mann-Whitney analysis to determine statistical significance. Data is reported as mean (M) EWs (M ± SEM).

A


EGFP dsRNA injected
AAS19 dsRNA injected
* * * * * *

B

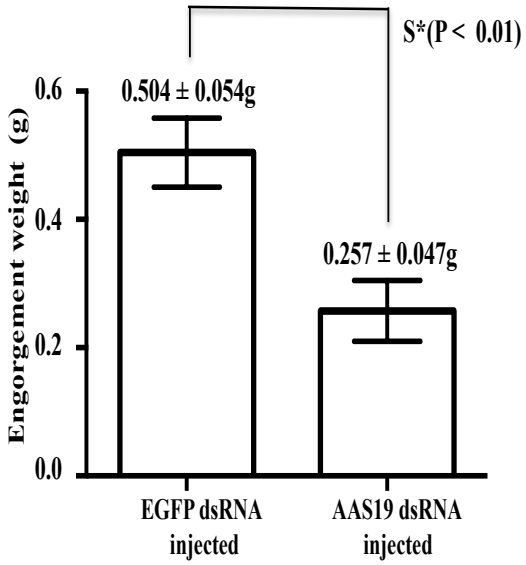
S*(P < 0.01)
0.504 ± 0.054g
0.257 ± 0.047g
Engorgement weight (g)
0.6
0.4
0.2
0.0
EGFP dsRNA injected
AAS19 dsRNA injected

Figure 3. Western blotting analyses (Kim, et al., 2016). Yeast and bacteria expressed rAAS19 (Fig. 3A) and crude tick saliva protein (Figs. 3B, C, and D) extracts were subjected to western blotting analysis using the rabbit antibody to yeast expressed rAAS19 as described in materials and methods section 2.6. Figure 3A, rB = *E. coli* expressed rAA19, rY+ and rY- = deglycosylated and glycosylated, respectively, *Pichia pastoris* expressed rAAS19. Crude protein extracts of dissected salivary glands (SG), midgut (MG), synganglion (SYN), Malpighian tubules (MT), ovaries (OVR) and the remnants as carcass (CA) were subjected to western blotting analyses using antibodies to yeast expressed rAAS19 (Fig. 3B), control PBS and adjuvant injected antibody (Fig. 3C), and rabbit pre-immune serum (Fig. 3D). Lanes 1, 2, 3, and 4 = Protein extracts of unfed, 24, 72, and 120 h fed ticks respectively. L = molecular weight ladder, Asterisks marked (*) indicate potential glycosylated native AAS19 form.

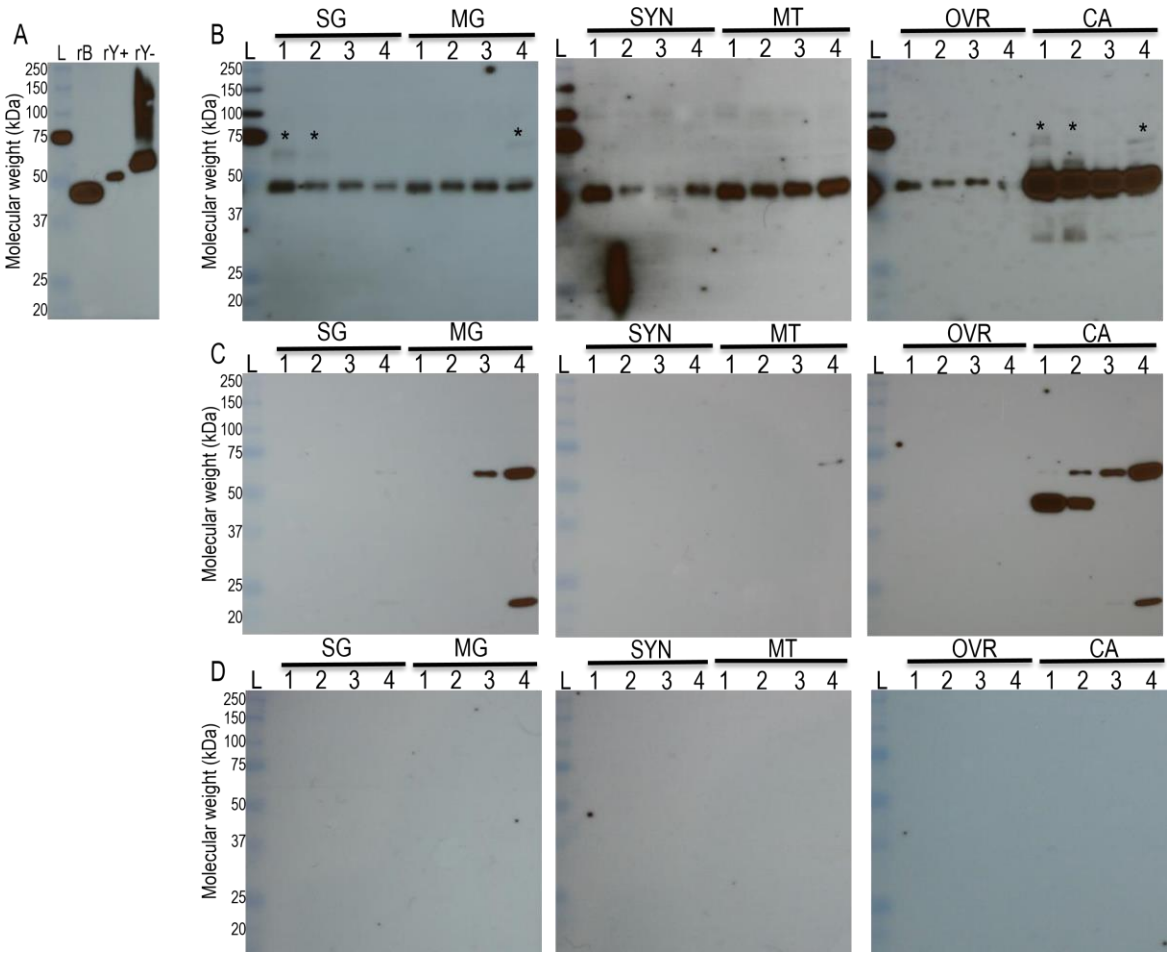
A
L rB rY+ rY-
Molecular weight (kDa)
250
150
100
75
50
37
25
20
B
SG MG SYN MT OVR CA
L 1 2 3 4 1 2 3 4 L 1 2 3 4 1 2 3 4 L 1 2 3 4 1 2 3 4
C
D

Figure 4. Effect of repeated tick infestation on antibody levels in immunized rabbits (Kim, et al., 2016). Affinity purified recombinant (r) AAS19 was subjected to routine ELISA as described in section 2.6. Data points are represented by (1) pre-immune (2) immune sera collected at two weeks after the booster, (3) two and (4) four weeks post-first tick infestation, and (5) two weeks after second tick infestation. Filled circle (●) = control rabbit inoculated with TiterMax Gold in PBS, filled triangle (▲) and square (■) = immunized rabbits one and two.

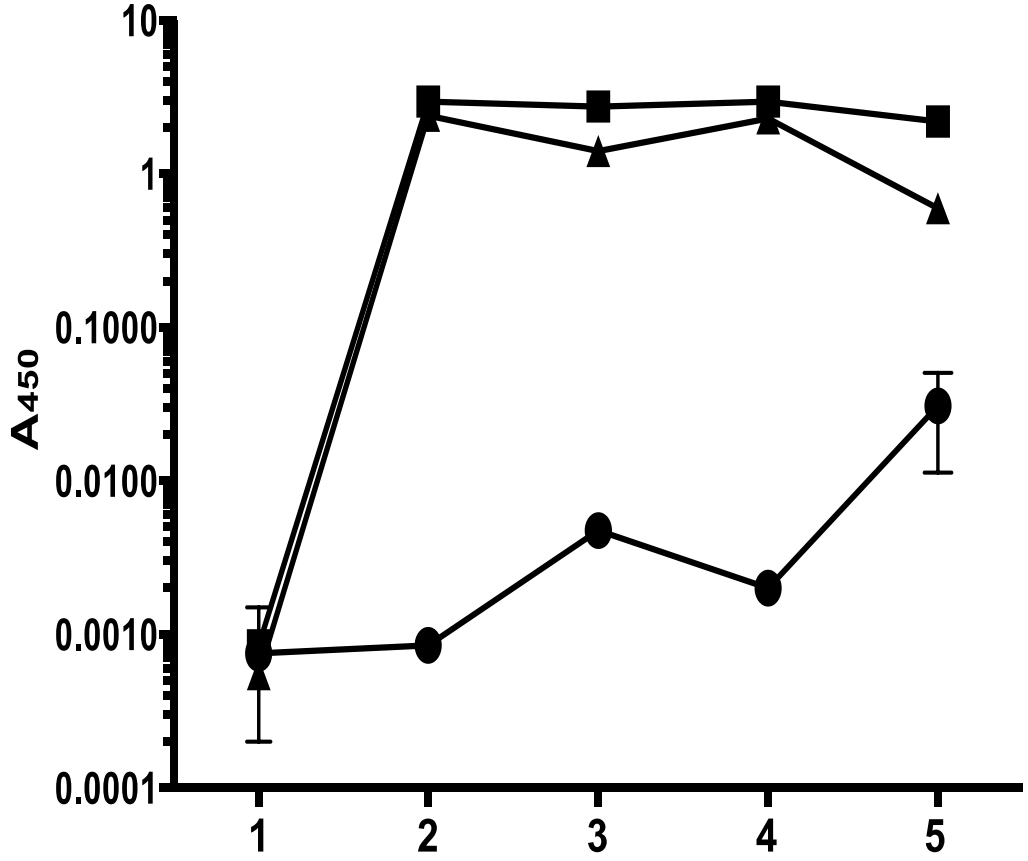
10
1
0.1000
0.0100
0.0010
0.0001
A450
1
2
3
4
5

Figure 5. Effect of rAAS19 immunization on completion of feeding (Kim, et al., 2016). Ticks challenged on rAAS19 rabbits were observed through 3 weeks of feeding until detachment. (A) Detached ticks were recorded every 24 hours for 20 days for the first tick challenge infestation on control rabbit (broken lines) and rabbit (R)1 (solid lines) and R2 (dotted lines) that were immunized with rAAS19. (B) Detached ticks from second tick challenge infestation on control, R1, and R2 for 22 days. Each node represents the number of detached ticks. Data is reported as mean of number of detached ticks (M ± SEM).

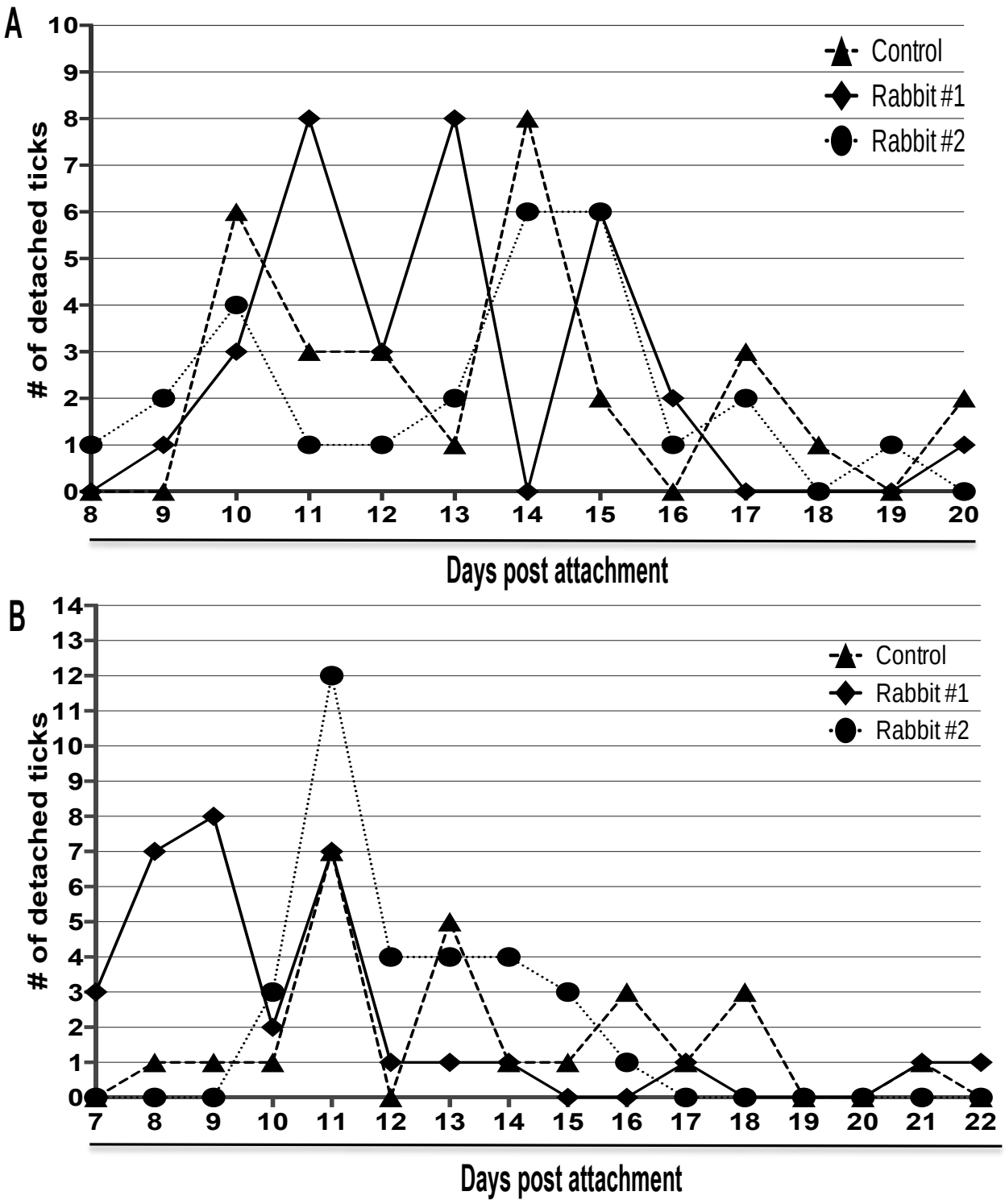
A
# of detached ticks
Days post attachment
Control
Rabbit #1
Rabbit #2
B
# of detached ticks
Days post attachment
Control
Rabbit #1
Rabbit #2

Figure 6. Effect of rAAS19 immunization on blood meal size and egg laying (Kim, et al., 2016). Ticks were allowed to feed on control and immunized rabbits (R)1 and 2 to repletion. Engorgement weights (EW) of detached ticks that fed on control and immunized rabbit groups were recorded from first (A) and second (B) infestations as indices for amounts of blood imbibed by ticks. Engorged ticks were incubated at 25°C at 85-90% relative humidity until oviposition. Eggs were collected and weighed from the first (C) and second (D) infestations. To determine the egg mass conversion ratio (EMCR), as a measure of the tick's ability to utilize the blood meal to produce eggs, from first (E) and second (F) infestations, weights of egg masses were divided by engorgement mass. EW, egg weights and EMCRs were subjected to One-Way ANOVA and Tukey's analysis to determine statistical significance. Data is reported as mean of EW, egg weights or EMCR (M ± SEM).

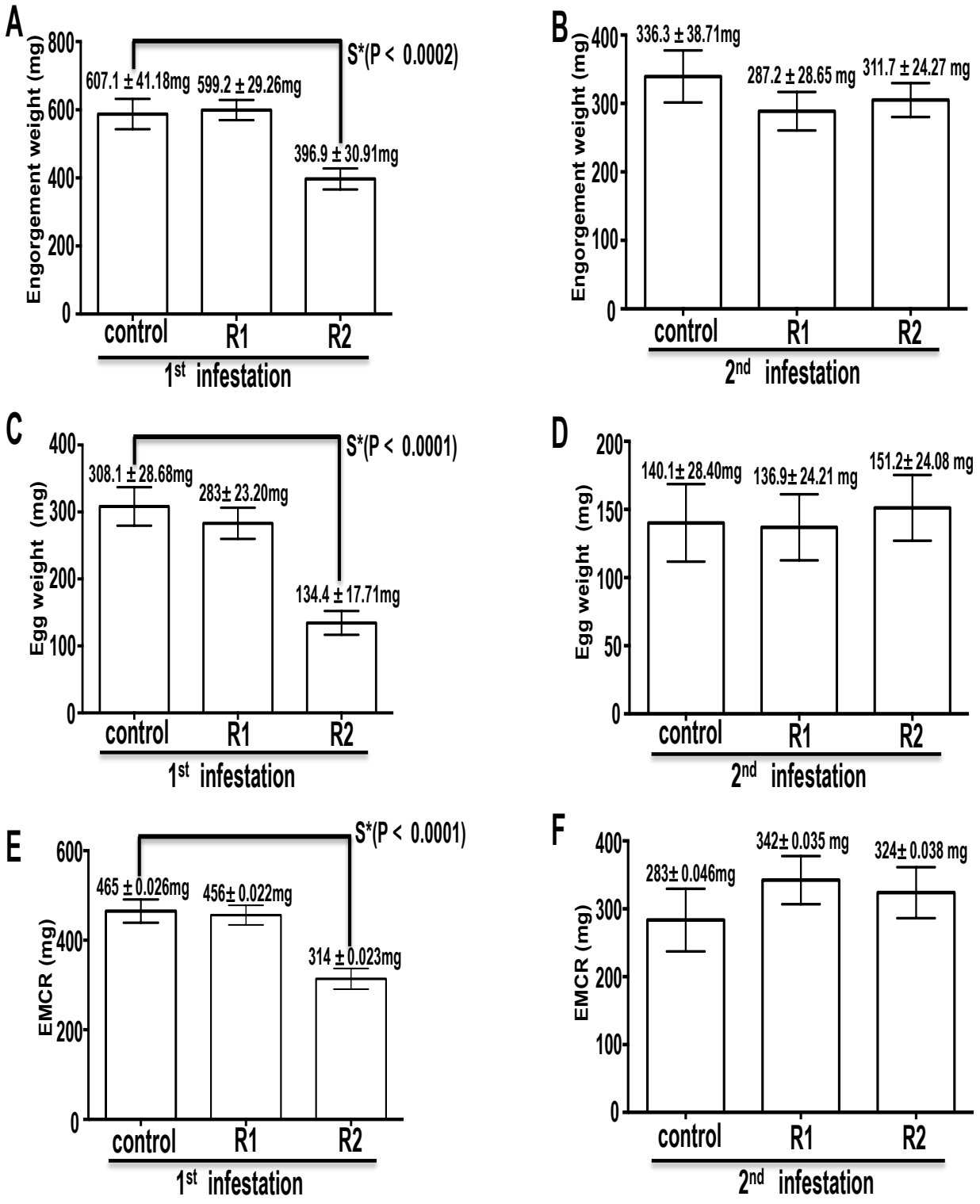
A
Engorgement weight (mg)
800
600
400
200
0
607.1 ± 41.18mg
599.2 ± 29.26mg
396.9 ± 30.91mg
S*(P < 0.0002)
control
R1
R2
1st infestation
B
Engorgement weight (mg)
400
300
200
100
0
336.3 ± 38.71mg
287.2 ± 28.65 mg
311.7 ± 24.27 mg
control
R1
R2
2nd infestation
C
Egg weight (mg)
400
300
200
100
0
308.1 ± 28.68mg
283± 23.20mg
134.4 ± 17.71mg
S*(P < 0.0001)
control
R1
R2
1st infestation
D
Egg weight (mg)
200
150
100
50
0
140.1± 28.40mg
136.9± 24.21 mg
151.2± 24.08 mg
control
R1
R2
2nd infestation
E
EMCR (mg)
600
400
200
0
465 ± 0.026mg
456± 0.022mg
314 ± 0.023mg
S*(P < 0.0001)
control
R1
R2
1st infestation
F
EMCR (mg)
400
300
200
100
0
283± 0.046mg
342± 0.035 mg
324± 0.038 mg
control
R1
R2
2nd infestation

Table 1. Effect of rAAS19 immunization on *Amblyomma americanum* egg laying (Kim, et al., 2016).

	1st infestation			2nd infestation		
Parameters	Control rabbit	Rabbit 1	Rabbit 2	Control rabbit	Rabbit 1	Rabbit 2
Egg Weight (mg)	308.18	283	134.40	140.14	136.9	151.16
Egg Mass Conversion Ratio (mg)	0.465	0.456	0.313	0.283	0.342	0.32
% Ticks failed to lay eggs	6.9 (2/29)	6.25 (2/32)	3.71 (1/26)	48 (12/25)	60.6 (20/33)	67.74 (21/31)

References

Kim, T.K., Radulovic, Z., Mulenga, A., 2016. Target validation of highly conserved *Amblyomma americanum* tick saliva serine protease inhibitor 19. Ticks Tick Borne Dis. 7, 405-414.

APPENDIX V

CHAPTER III Part II FIGURES AND TABLES

Figure 1. *Amblyomma americanum* serpin (AAS) 41 and 46 are nearly identical. Mature protein coding regions of AAS41 and 46 nucleotide (A) and amino acid (B) sequences were subjected multiple sequence alignment using ClustalW on MacVector. The reactive center loop (RCL) is boxed in blue; the P1 active site of the RCL is indicated with an asterisks (*) showing AAS41 has a leucine “L” and AAS46 has threonine “T” at the P1 site.

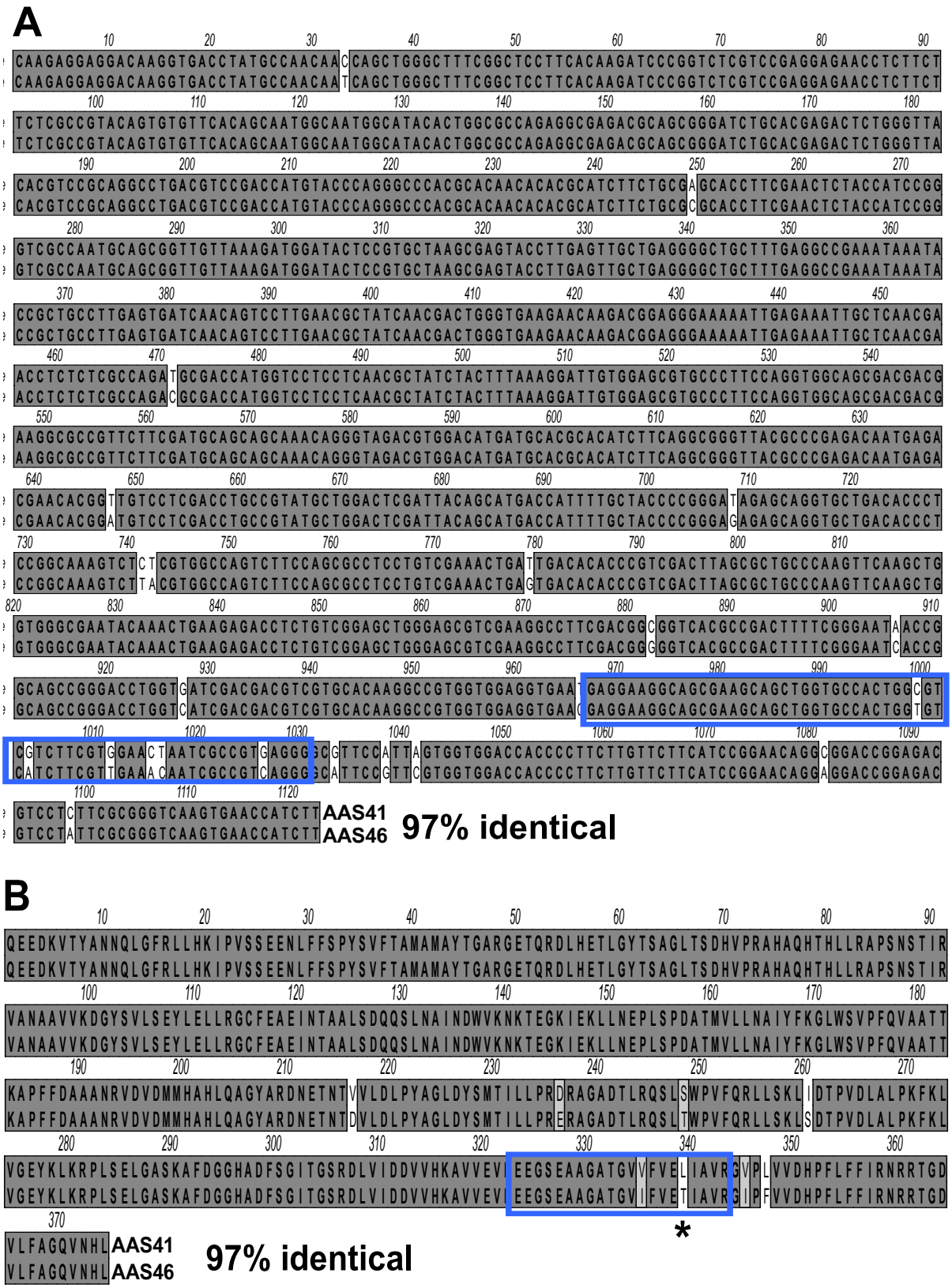
A
AAS41
AAS46
97% identical
B
AAS41
AAS46
97% identical
*

Figure 2. *Amblyomma americanum* AAS41/46 transcript and protein are expressed in major tick organs and secreted saliva. Temporal and spatial expression analysis of AAS41/46 mRNA was determine in unfed, 24, 48, 72, 96, and 120 h fed tick dissected tissues: salivary glands (A1), midguts (A2) and remnants as carcass (A3), analyzed by qRT-PCR. (B) The secretion dynamics of AAS41/46 from unfed to fed tick saliva. AAS41/46 protein abundance in tick saliva is presented by the normalized spectral abundance factor (NSAF) (y-axis) for unfed non-exposed and host exposed (dog-, human-, rabbit- exposed) and feeding time points (x-axis). Towards the end of tick feeding, ticks that noted as apparently fully engorged but not detached (BD), and fully engorged spontaneously detached (SD).

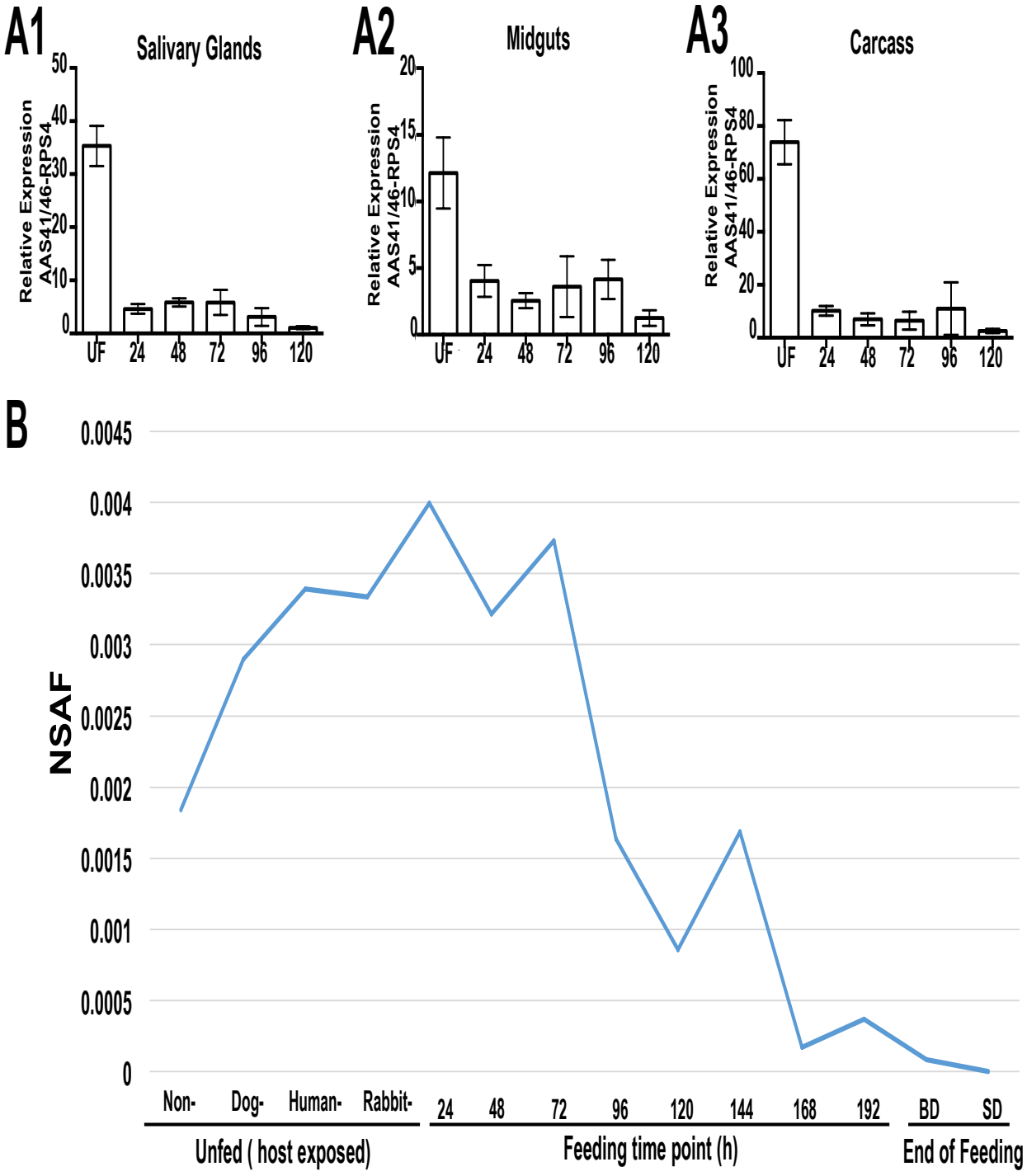
A1
Salivary Glands
Relative Expression AAS41/46-RPS4
50
40
30
20
10
0
UF
24
48
72
96
120
A2
Midguts
Relative Expression AAS41/46-RPS4
20
15
10
5
0
UF
24
48
72
96
120
A3
Carcass
Relative Expression AAS41/46-RPS4
100
80
60
40
20
0
UF
24
48
72
96
120
B
NSAF
0.0045
0.004
0.0035
0.003
0.0025
0.002
0.0015
0.001
0.0005
0
Non-
Dog-
Human-
Rabbit-
24
48
72
96
120
144
168
192
BD
SD
Unfed (host exposed)
Feeding time point (h)
End of Feeding

Figure 3. *Amblyomma americanum* native AAS41/46 protein are present in major tick organs and in all life stages. *Pichia pastoris* transformed with AAS41 (A) and AAS46 (B) recombinant plasmids was cultured at 28°C and recombinant protein expression was induced by inoculating 5% methanol daily through five days (1-5). Verification of protein expression was performed by western blot analysis using antibody to the hexa-histidine tag. (C) Affinity purified rAAS41 and rAAS46 that were treated with deglycosylation enzyme mix (+) or without treatment (-) were resolved by 10% SDS-PAGE for western blot analysis using antibody to the hexa-histidine tag. Monospecific IgG antibodies to AAS41/46 were purified from serum of repeatedly infested rabbits with *A. americanum* ticks and the quality confirmed by western blot analysis against deglycosylated (+) and glycosylated (-) rAAS41/46 (D) at 1:2000 dilution (0.5 mg/mg). This monospecific IgG antibody (0.5 mg/mg, 1:500 dilution) was then used to screen for native AAS41/46 in various female adult tick tissues: salivary glands (E), midguts (F) and remnants as carcass (G) from different time points, and all life stages: egg, larvae, nymphs, and male and female adults (H). Purified IgG (0.6 mg/mg, 1:2000 or 1:500 dilution) from pre-immune serum were included as controls for respective western blots above (I-M).

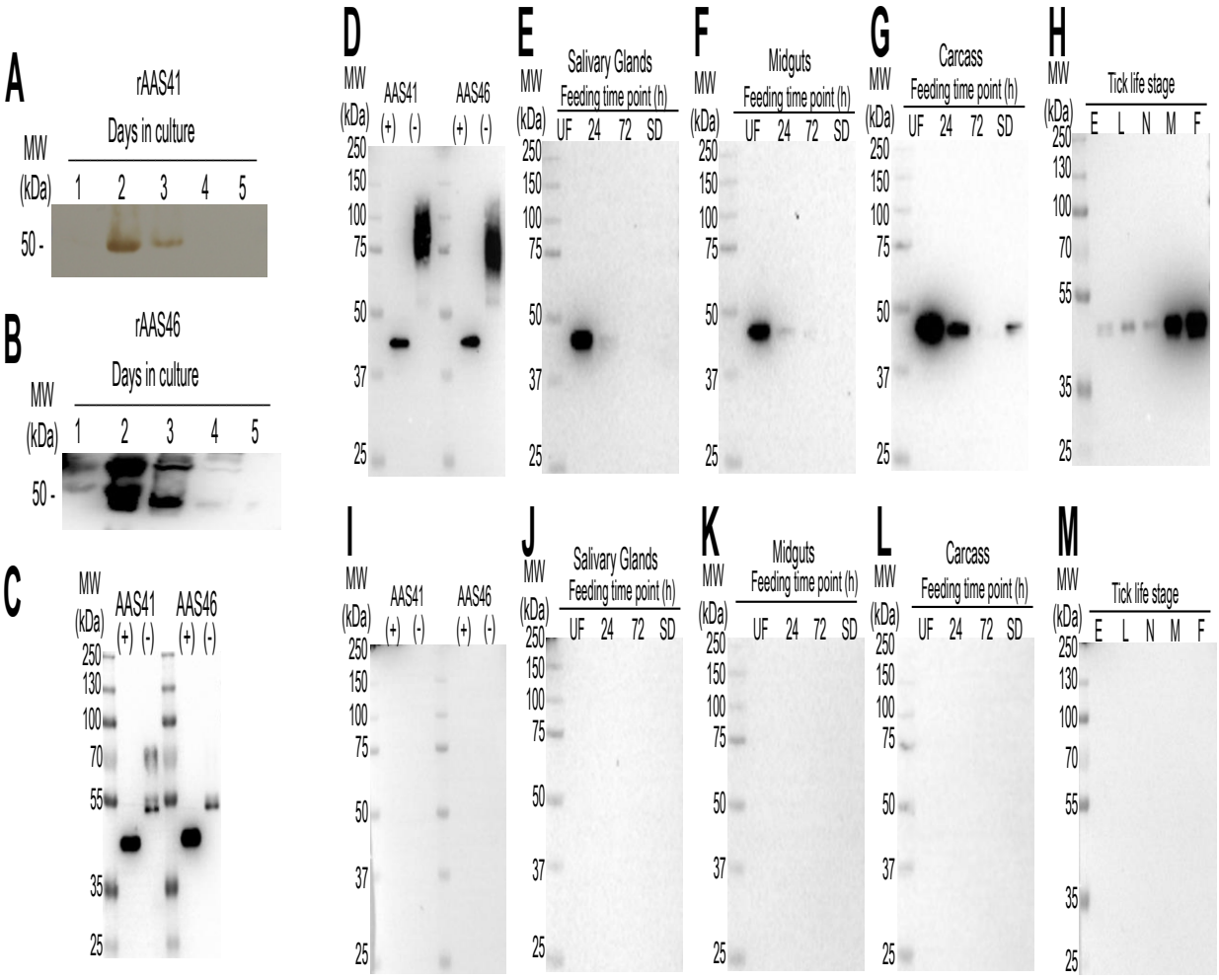
A
rAAS41
Days in culture
MW
(kDa)
1 2 3 4 5
50 -
B
rAAS46
Days in culture
MW
(kDa)
1 2 3 4 5
50 -
C
MW
(kDa)
AAS41
(+) (-)
AAS46
(+) (-)
250
130
100
70
55
35
25
D
MW
(kDa)
AAS41
(+) (-)
AAS46
(+) (-)
250
150
100
75
50
37
25
E
MW
(kDa)
Salivary Glands
Feeding time point (h)
UF 24 72 SD
250
150
100
75
50
37
25
F
MW
(kDa)
Midguts
Feeding time point (h)
UF 24 72 SD
250
150
100
75
50
37
25
G
MW
(kDa)
Carcass
Feeding time point (h)
UF 24 72 SD
250
150
100
75
50
37
25
H
MW
(kDa)
Tick life stage
E L N M F
250
130
100
70
55
35
25
I
MW
(kDa)
AAS41
(+) (-)
AAS46
(+) (-)
250
150
100
75
50
37
25
J
MW
(kDa)
Salivary Glands
Feeding time point (h)
UF 24 72 SD
250
150
100
75
50
37
25
K
MW
(kDa)
Midguts
Feeding time point (h)
UF 24 72 SD
250
150
100
75
50
37
25
L
MW
(kDa)
Carcass
Feeding time point (h)
UF 24 72 SD
250
150
100
75
50
37
25
M
MW
(kDa)
Tick life stage
E L N M F
250
130
100
70
55
35
25

Figure 4. *Amblyomma americanum* rAAS41 and rAAS46 are immunogenic proteins and cross-react to rabbit serum from repeatedly infested *Ixodes scapularis*. Affinity purified rAAS41 and rAAS46 that were treated with deglycosylation enzyme mix (+) or without treatment (-) were resolved by 10% SDS-PAGE for western blot analysis using antibodies to tick saliva proteins from serum of rabbits that were repeatedly infested with *A. americanum* ticks for 24 h (A), 48 h (B), replete fed (C), and including the pre-immune serum control (D) at 1:500 dilution. Likewise, rAAS41 and rAAS46 bound by antibodies to tick saliva proteins from serum of rabbits that were repeatedly infested with *I. scapularis* replete fed nymphs infected with *Borrelia burgdorferi* sensu stricto (E), replete fed uninfected nymphs (F), replete fed adults (G), and including the pre-immune serum control (H) at 1:50 dilution.

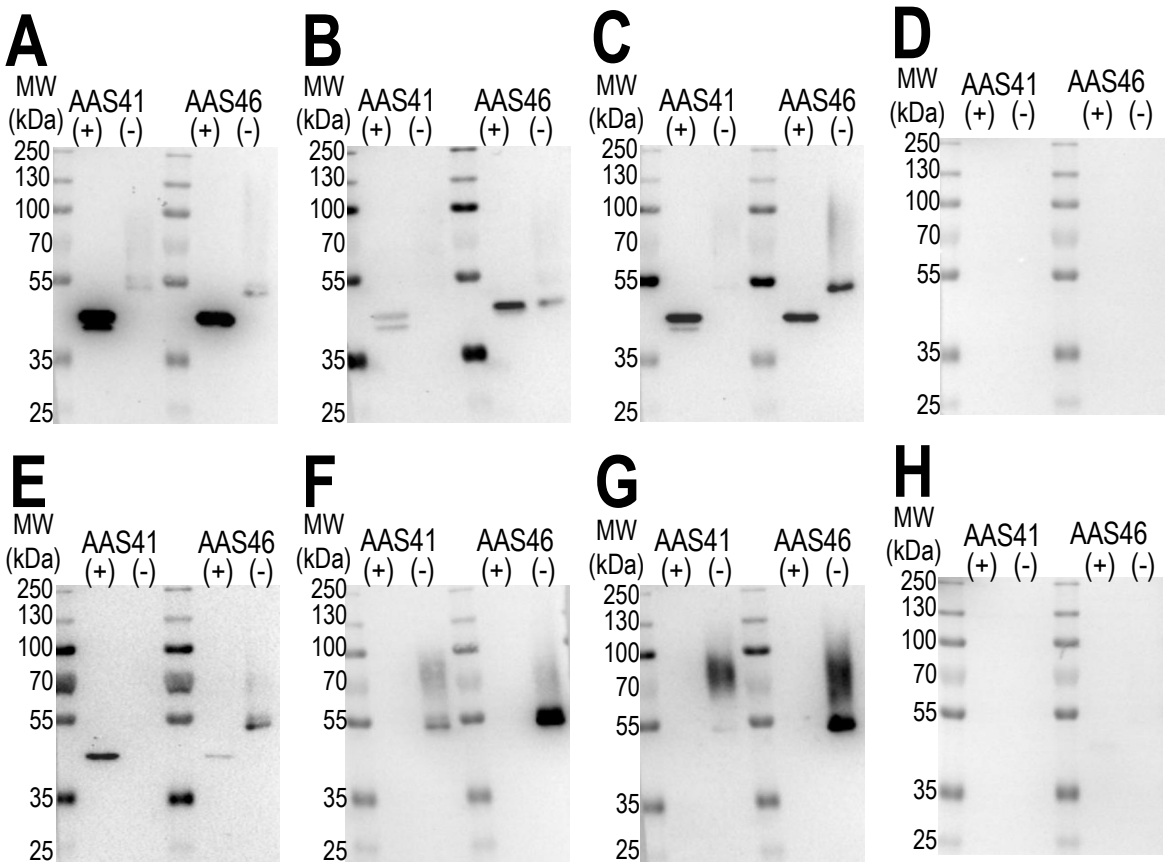
A
B
C
D
E
F
G
H
MW (kDa)
AAS41
AAS46
(+) (-) (+) (-)
250
130
100
70
55
35
25

Figure 5. Protease inhibitor profiling for affinity purified rAAS41 and rAAS46. Indicated proteases were incubated with affinity purified rAAS41 or rAAS46 (1 μM) at 37° C for 15 min followed by addition of appropriate substrate (0.2 mM). Protease kinetics was monitored every 11 s over 15 min in triplicate.

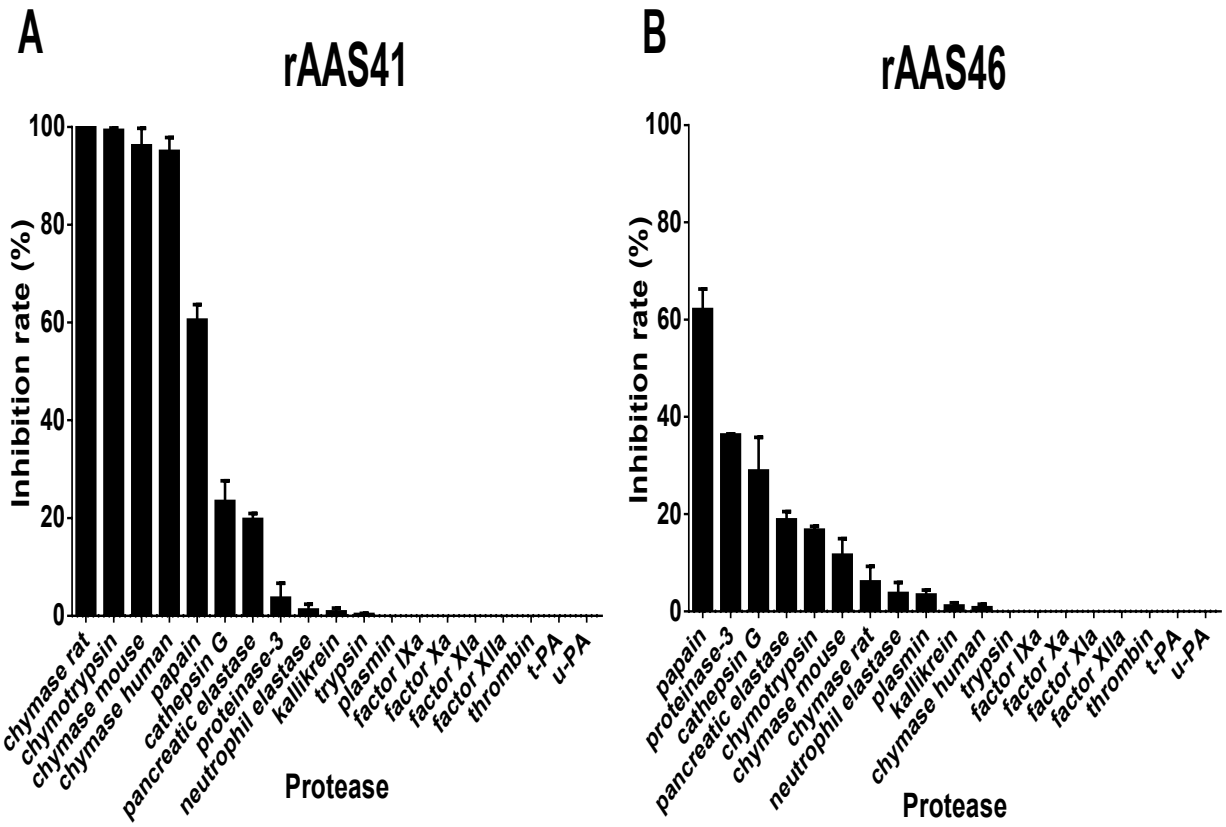
A
rAAS41
Inhibition rate (%)
100
80
60
40
20
0
chymase rat
chymotrypsin
chymase mouse
chymase human
papain
cathepsin G
pancreatic elastase
proteinase-3
neutrophil elastase
kallikrein
trypsin
plasmin
factor IXa
factor Xa
factor XIa
factor XIIa
thrombin
t-PA
u-PA
Protease
B
rAAS46
Inhibition rate (%)
100
80
60
40
20
0
papain
proteinase-3
cathepsin G
pancreatic elastase
chymotrypsin
chymase mouse
chymase rat
neutrophil elastase
plasmin
kallikrein
chymase human
trypsin
factor IXa
factor Xa
factor XIa
factor XIIa
thrombin
t-PA
u-PA
Protease

Figure 6. Stoichiometry of inhibition against chymase and chymotrypsin. Stoichiometry inhibition (SI) was determined by measuring residual enzyme activity of human chymase (13nM) and (B) bovine α-Chymotrypsin (8nM) following incubation rAAS41 at variable molar ratios (rAAS41:Protease) ranging from 0 to 10. The data were plotted as residual protease activity (Vi/V0) versus molar ratio (rAAS41:Protease).

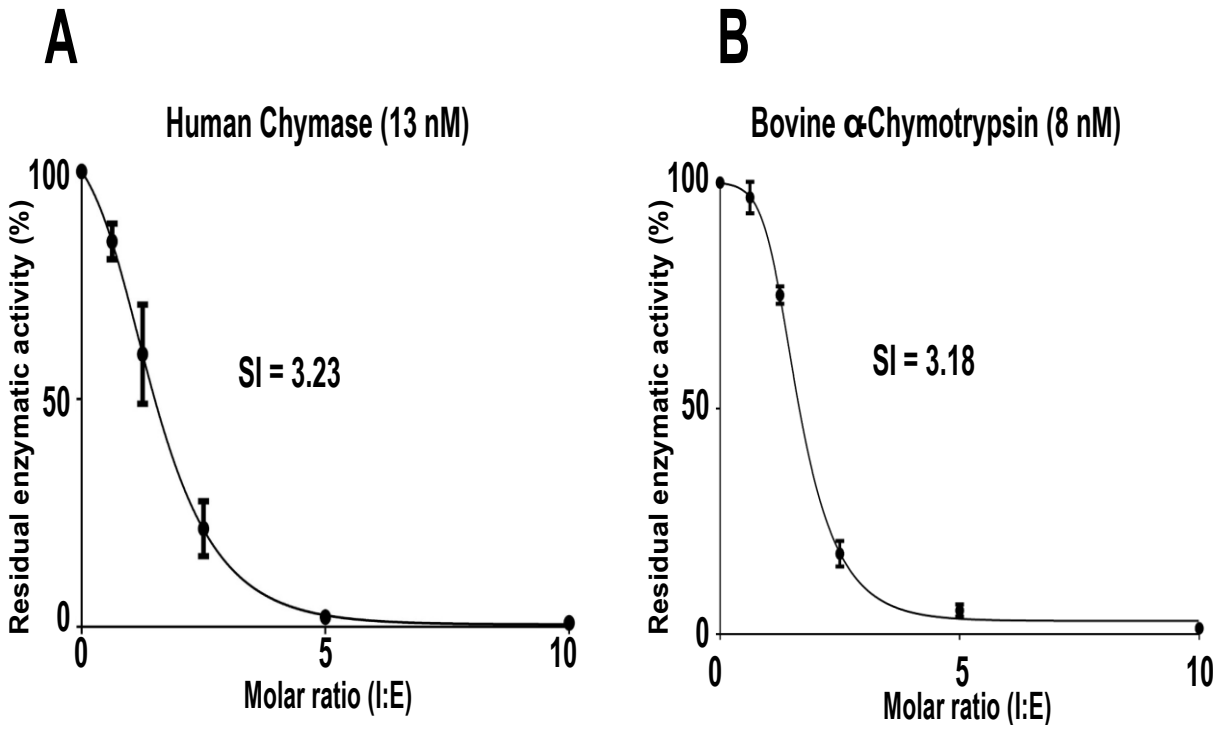
A
Human Chymase (13 nM)
Residual enzymatic activity (%)
100
50
0
SI = 3.23
0
5
10
Molar ratio (I:E)
B
Bovine α-Chymotrypsin (8 nM)
Residual enzymatic activity (%)
100
50
0
SI = 3.18
0
5
10
Molar ratio (I:E)

Figure 7. Affinity purified rAAS41 forms stable heat- and SDS- stable complexes with target proteases. Increasing amounts of rAAS41 were pre-incubated for 1 h at 37°C with 0.1 μg of human chymase (A) or 0.1 μg of bovine α-chymotrypsin (B) in molar ratios varying from 0.625:1 to 10:1 (rAAS41:protease). Samples were treated with a deglycosylation enzyme (DE) mix (to remove glycans that were masking results) and resolved on a 10% SDS-PAGE and silver stained to visualize covalent complexes. The rAAS41:protease complex is denoted by the black arrow (←). A (+) or (-) denotes treatment with without deglycosylation, respectively.

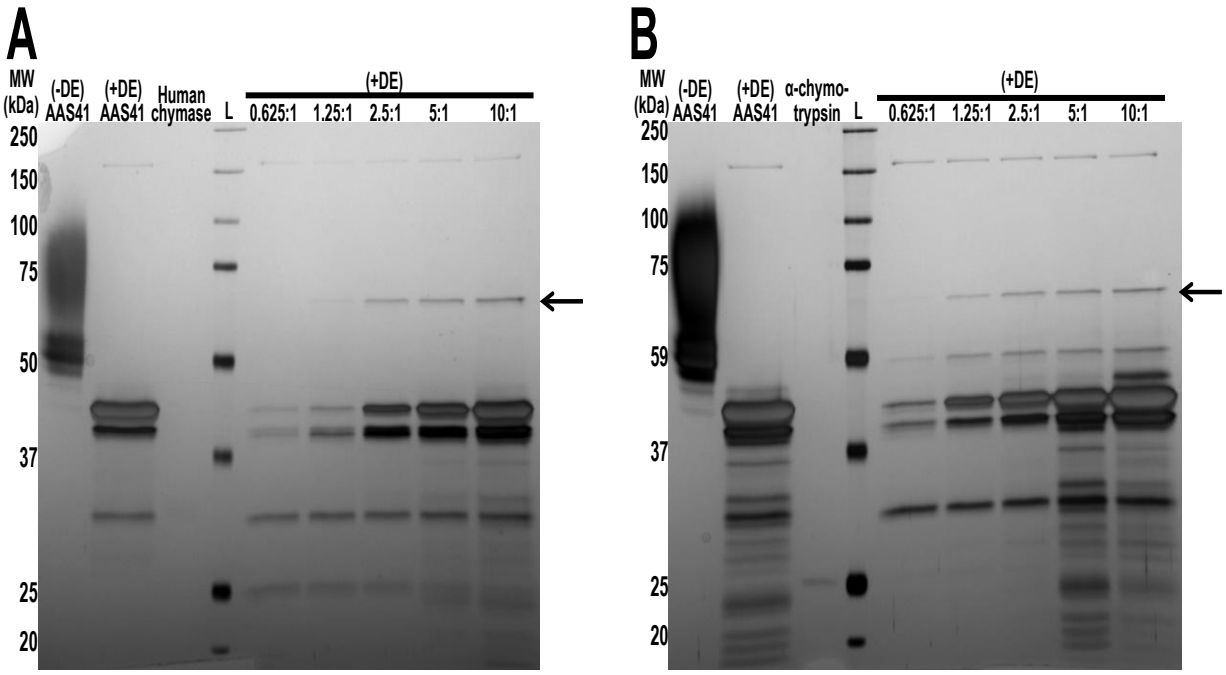
A
MW (kDa)
(-DE) AAS41
(+DE) AAS41
Human chymase
L
(+DE)
0.625:1
1.25:1
2.5:1
5:1
10:1
250
150
100
75
50
37
25
20
B
MW (kDa)
(-DE) AAS41
(+DE) AAS41
α-chymo-trypsin
L
(+DE)
0.625:1
1.25:1
2.5:1
5:1
10:1
250
150
100
75
59
37
25
20

Figure 8. rAAS41 is an effective inhibitor of chymase. Discontinuous method inhibition of chymase by rAAS41 was conducted as described. (A) Semilogarithmic plots of residual enzymatic activity of chymase versus time of incubation for reactions at various concentrations of rAAS41 (33 – 500 nM). (B) Plot of k_{obs} as a function of rAAS41 concentration. Linear regression of the slope represents the second-order rate constant k_a for the inhibition of chymase by rAAS41.

and human chymase was determined as k_a 5.6 ± 0.365 x 10^3 M^{-1} s^{-1}; demonstrating rAAS41 might be a fast and effective inhibitor of human chymase (Fig. 8).

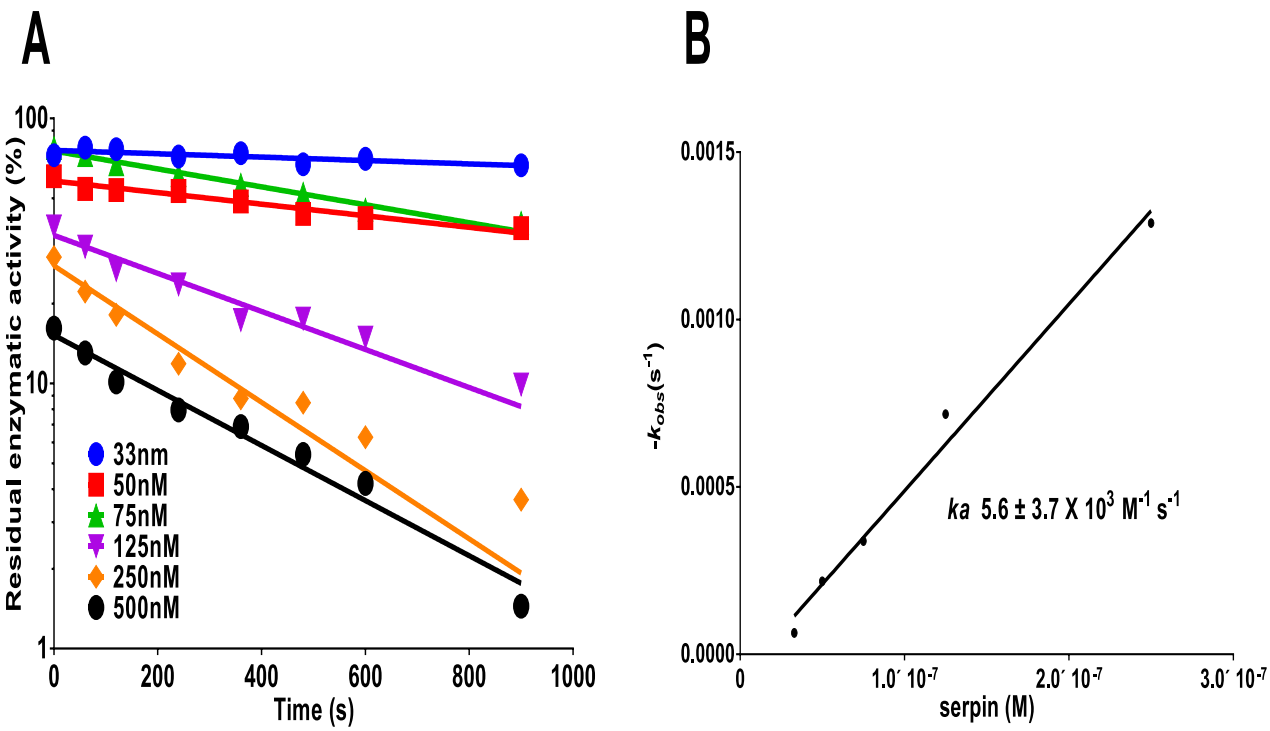
A
B
Residual enzymatic activity (%)
100
10
1
0
200
400
600
800
1000
Time (s)
33nm
50nM
75nM
125nM
250nM
500nM
-kobs(s-1)
0.0015
0.0010
0.0005
0.0000
1.0´ 10-7
2.0´ 10-7
3.0´ 10-7
serpin (M)
ka 5.6 ± 3.7 X 10^3 M-1 s-1

Figure 9. rAAS41 blocks compound 48/80-induced acute inflammation in rats. (A) Rat paw edema induced by intradermal injection of 100 μL of compound 48/80 (1 μg) in saline (circles), or co-injected with 25 μg of rAAS41 (squares), or 100 μL of rAAS41 only (triangles). Edema formation was estimated using a digital plethysmometer at different intervals. Posterior paws from 5 animals were used for each data point. $^{*}P$=0.0142, $^{**}P$=0.009, and $^{***}P$=0.0072 (t-test). (B) Vascular permeability (Miles assay) was performed by intravenous injection of 700 µL Evan's blue dye into the tails of rats. Ten minutes later, 100 µL of (i) saline, (ii) compound 48/80 (1 µg) only, (iii) compound 48/80 (1 µg) co-injected with rAAS41 (25 µg), or (iv) only rAAS41 (25 µg) was injected intradermally on the back right (R) and left (L) sides of the rat. After 60 minutes, animals were sacrificed and skin removed to allow injection sites to be photographed. (C) Evans blue extravasation was estimated after extraction with formamide and reading at 620 nm. Results are the average of experiments obtained with 6 animals. *P=0.0033 (t-test).

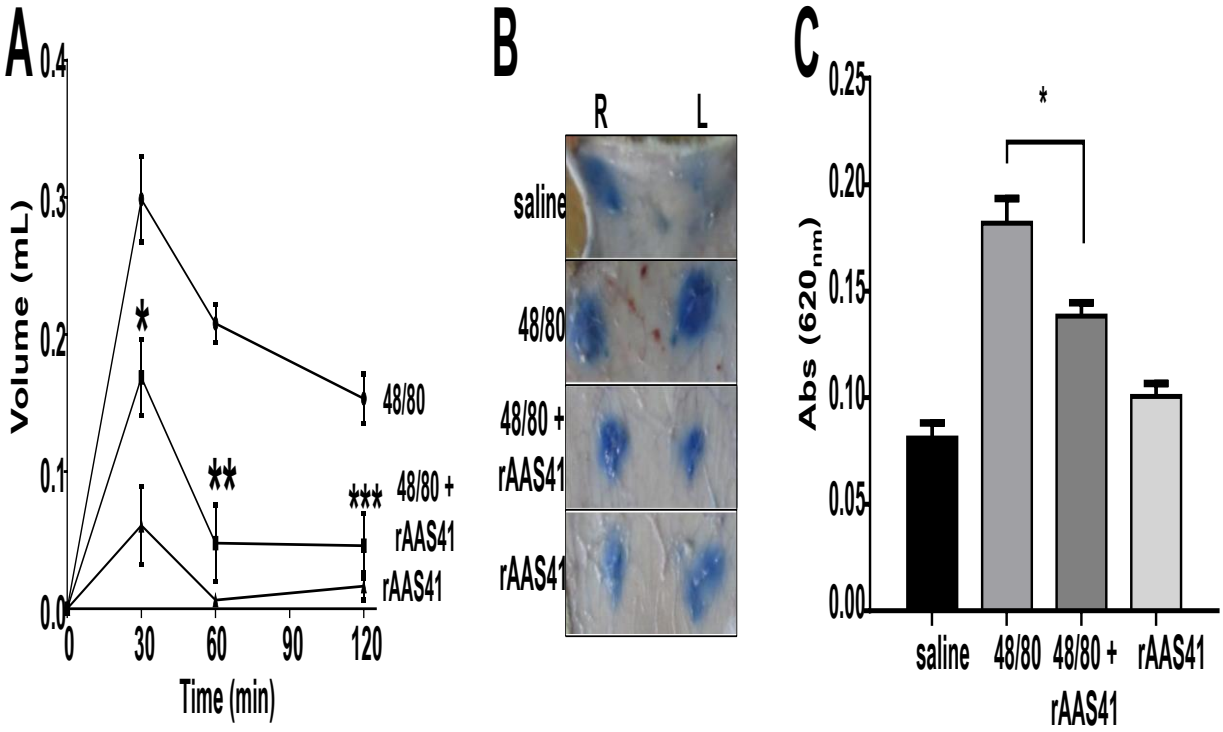
A
Volume (mL)
0.4
0.3
0.2
0.1
0.0
0
30
60
90
120
Time (min)
*
**
***
48/80
48/80 +
rAAS41
rAAS41
B
R
L
saline
48/80
48/80 +
rAAS41
rAAS41
C
Abs (620nm)
0.25
0.20
0.15
0.10
0.05
0.00
*
saline
48/80
48/80 +
rAAS41
rAAS41

Figure 10. RNAi-mediated silencing of AAS41/46 mRNA affects tick feeding. Double stranded (ds) RNA of AAS41/46 and GFP (control) was synthesized *in vitro* and microinjected in ticks to trigger disruption of AAS41/46 mRNA. (A) Prior to assessing effects of RNAi silencing against tick feeding, the timeline to depletion of AAS41/46 mRNA in unfed ticks was determined. Subsequently dsRNA injected unfed ticks were incubated for the time period required to deplete mRNA from unfed ticks before feeding on rabbits. (B) At 48 h post attachment AAS41/46-dsRNA and GFP-dsRNA injected ticks sampled disruption of cognate mRNA was validated by qRT-PCR in tissues that were dissected from individual ticks. (C) Ticks were allowed to feed to repletion and observed and phenotypes were documented upon detachment from the host. (D) Effects of RNAi silencing on: (D1) amount of blood ingested, (D2) egg laying, and (D3) ability to convert blood meal into eggs.

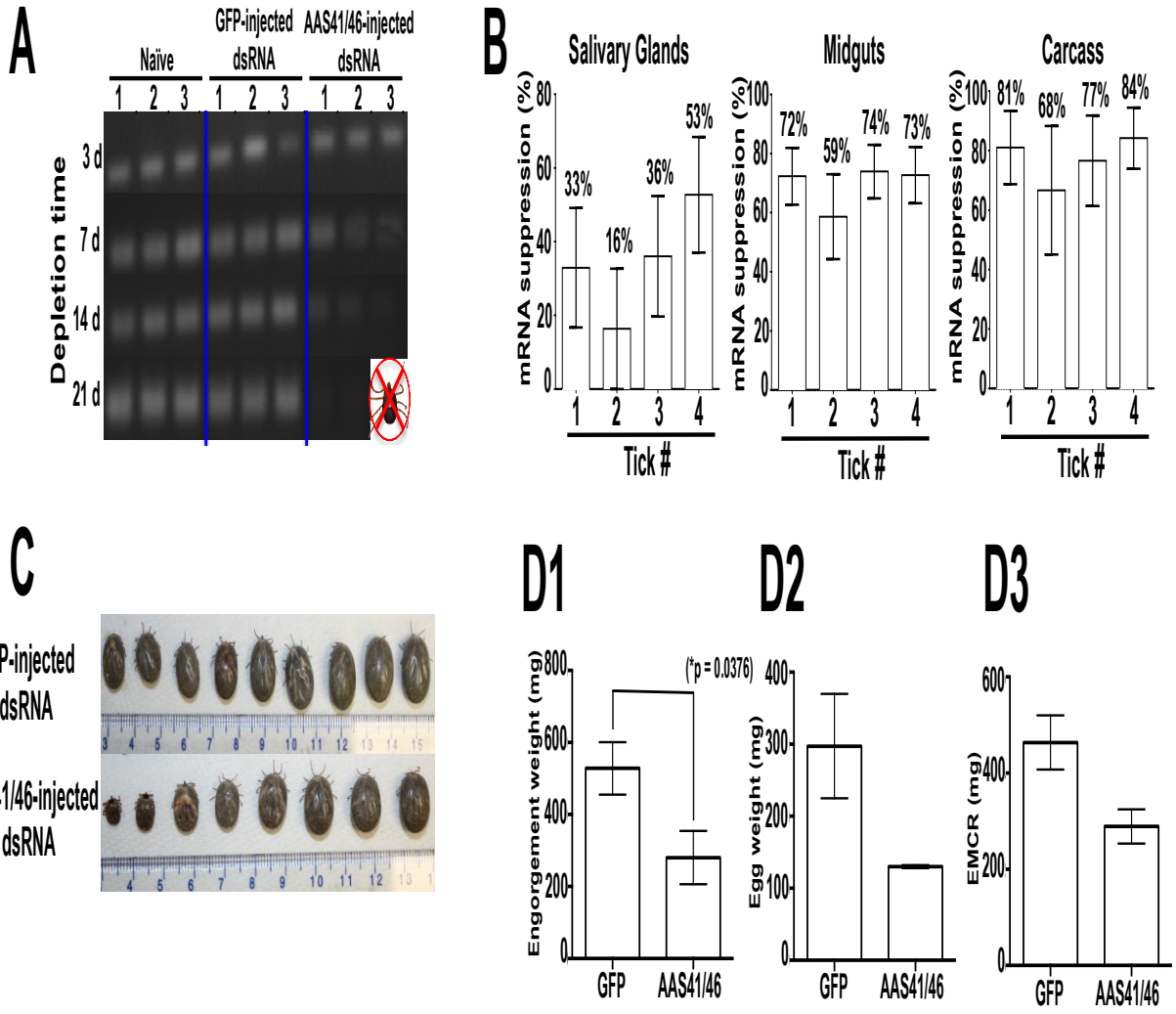
A
Naïve
GFP-injected dsRNA
AAS41/46-injected dsRNA
1 2 3 1 2 3 1 2 3
Depletion time
3 d
7 d
14 d
21 d
B
Salivary Glands
Midguts
Carcass
mRNA suppression (%)
33%
16%
36%
53%
72%
59%
74%
73%
81%
68%
77%
84%
Tick #
C
GFP-injected dsRNA
AAS41/46-injected dsRNA
D1
D2
D3
Engorgement weight (mg)
(*p = 0.0376)
Egg weight (mg)
EMCR (mg)
GFP
AAS41/46

Table 1. Commercially available mammalian proteases and substrates

Protease	Source	Company	molarity (nM)	substrate	Company	substrate (μM)
chymase	human (recombinant)	Sigma-Aldrich, St. Louis, MO, USA	83.33	S-7388	Sigma-Aldrich, St. Louis, MO, USA	200
chymotrypsin	bovine (pancreas)	Sigma-Aldrich, St. Louis, MO, USA	2.72	S-7388	Sigma-Aldrich, St. Louis, MO, USA	200
elastase	human (neutrophil)	Molecular Innovation, Novi, MI, USA	14.86	MeOSuc-AAVP	Sigma-Aldrich, St. Louis, MO, USA	200
elastase	porcine (pancrease)	Sigma-Aldrich, St. Louis, MO, USA	61.78	S-4760	Sigma-Aldrich, St. Louis, MO, USA	200
trypsin	bovine (pancreas)	Sigma-Aldrich, St. Louis, MO, USA	0.25	B7632	Sigma-Aldrich, St. Louis, MO, USA	200
factor XIa	human	Enzyme Research Laboratories, South Bend, IN, USA	3.69	CS 31 (02)	Hyphen BioMed, Neuville-sur-Oise, France	200
factor XIIa	human	Enzyme Research Laboratories, South Bend, IN, USA	15.00	CS 31 (02)	Hyphen BioMed, Neuville-sur-Oise, France	200
kallikrein	porcine (pancreas)	Sigma-Aldrich, St. Louis, MO, USA	10.00	CS 31 (02)	Hyphen BioMed, Neuville-sur-Oise, France	200
proteinase-3	human (neutrophil)	Sigma-Aldrich, St. Louis, MO, USA	280.00	MeOSuc-AAVP	Sigma-Aldrich, St. Louis, MO, USA	200
factor IXa beta	bovine	Enzyme Research Laboratories, South Bend, IN, USA	314.35	Pefachrome FIXa	Pentapharm, Aesch, Switzerland	200
t-PA	human (recombinant)	Molecular Innovations, Inc., Novi, MI, USA	23.57	Pefachrome FIXa	Pentapharm, Aesch, Switzerland	200
u-PA	human (recombinant)	Molecular Innovations, Inc., Novi, MI, USA	29.63	Pefachrome FIXa	Pentapharm, Aesch, Switzerland	200
factor Xa	bovine	New England Biolabs, Ipswich, MA, USA	10.00	S-2222	Diapharma Group Inc., West Chester, OH, USA	200
plasmin	human	Enzyme Research Laboratories, South Bend, IN, USA	5.31	S-2251	Diapharma Group Inc., West Chester, OH, USA	200
cathepsin G	human (neutrophil)	Athens Research & Technology, Athens, GA, USA	425.53	S-7388	Sigma-Aldrich, St. Louis, MO, USA	200
papain	papaya	Spectrum Chemical Manufacturing Corp., New Brunsick, NJ, USA	427.35	P3169	Sigma-Aldrich, St. Louis, MO, USA	200
thrombin	human	Enzyme Research Laboratories	19.24	B-7632	Sigma-Aldrich, St. Louis, MO, USA	200

APPENDIX VI

CHAPTER IV FIGURES AND TABLES

Figure 1. The secretion dynamics of tick saliva protein antigens used in a cocktail tick vaccine. Normalized spectral abundance factor (NSAF) (y-axis) as index for relative abundance for 11 of the 13 antigens (CRT-calreticulin, Ach- acidic chitinase, AAS 4, 6, 19, 27, 41, and 46-*A. americanum* serine protease inhibitors [serpins], AV422-cross-species conserved ticks saliva protein, IGFBP-insulin growth factor binding protein, TCI-tick carboxypeptidase inhibitor) were extracted from chapter II of this dissertation and displayed every 24 h of feeding (x-axis). Ticks towards the end of feeding that were apparently fully engorged but not detached from the host were labeled as BD, and fully engorged and replete fed as SD.

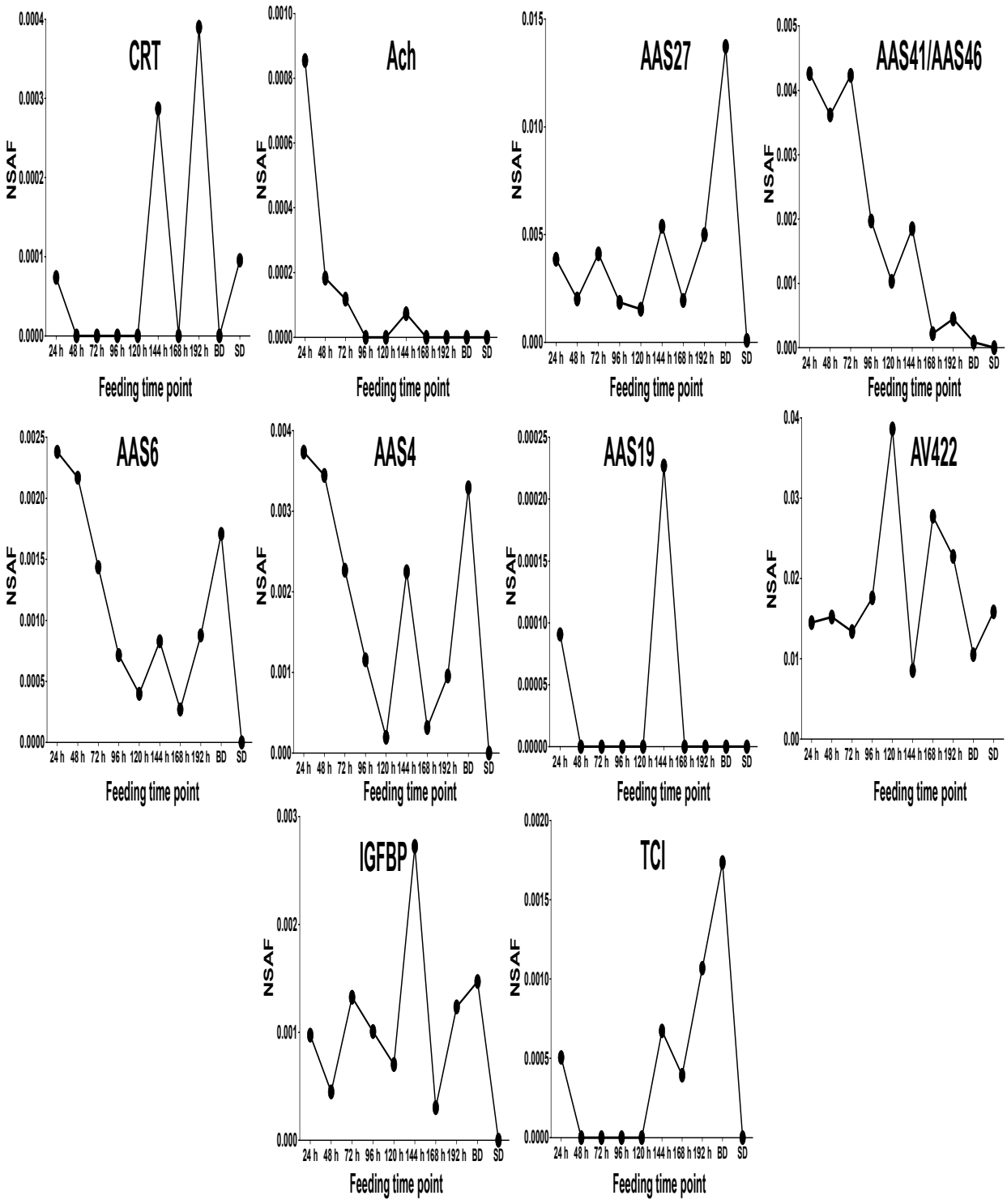
CRT
Ach
AAS27
AAS41/AAS46
AAS6
AAS4
AAS19
AV422
IGFBP
TCI
NSAF
Feeding time point
24 h 48 h 72 h 96 h 120 h 144 h 168 h 192 h BD SD

Figure 2. Prediction of linear B cell epitopes from 13 candidate tick saliva antigens. *In silico* analysis of the mature protein sequences for the 13 candidate antigens were analyzed using the B-cell prediction tool for linear epitopes in the Immune Epitope Database and Analysis Resource (IEDB) server charts for (A) serpins, (B) low to mid molecular weight proteins (<30kDa) and (C) high molecular weight proteins (>40kDa). Predicted peptides above the default threshold value were reported on a graph (highlighted in yellow), while less scoring peptides below the threshold were highlighted in green). Peptide identifications are provided in a table format next to each graph for each protein.

A1 AAS46

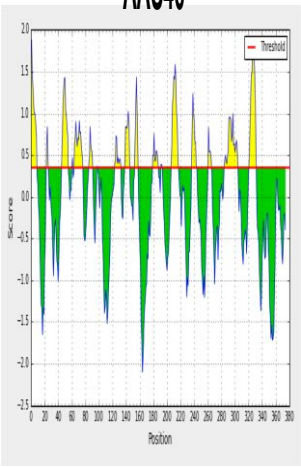

Predicted peptides

No.	Start	End	Peptide	Length
1	1	8	QEEDKVTY	8
2	23	25	VSS	3
3	45	54	TGARGETQRD	10
4	60	61	GY	2
5	64	76	AGLTSDHVPRAHA	13
6	85	90	PSNSTI	6
7	97	97	V	1
8	123	132	AALSDQQSLN	10
9	138	145	VKNKTEGK	8
10	153	157	PLSPD	5
11	179	187	AATTKAPFF	9
12	191	193	ANR	3
13	206	216	GYARDNETNTD	11
14	236	243	ERAGADTL	8
15	261	265	DTPVD	5
16	284	304	SELGASKAFDGGHADFSGITG	21
17	321	331	VNEEGSEAAGA	11

A2 AAS41

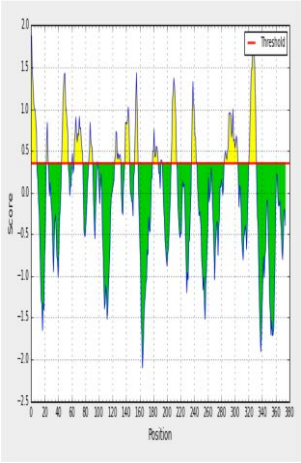

Predicted peptides

No.	Start	End	Peptide	Length
1	1	8	QEEDKVTY	8
2	23	25	VSS	3
3	45	54	TGARGETQRD	10
4	60	61	GY	2
5	64	76	AGLTSDHVPRAHA	13
6	85	90	PSNSTI	6
7	97	97	V	1
8	123	132	AALSDQQSLN	10
9	138	145	VKNKTEGK	8
10	153	157	PLSPD	5
11	179	187	AATTKAPFF	9
12	191	193	ANR	3
13	206	214	GYARDNETN	9
14	236	244	DRAGADTLR	9
15	284	304	SELGASKAFDGGHADFSGITG	21
16	321	331	VNEEGSEAAGA	11

A3 AAS27

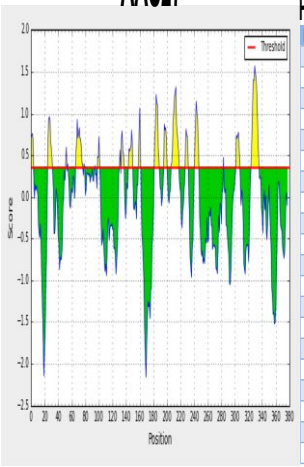

Predicted peptides

No.	Start	End	Peptide	Length
1	1	3	LTE	3
2	25	31	SRPDENV	7
3	51	52	GA	2
4	54	54	L	1
5	66	76	ASLSEGDVREA	11
6	78	79	TH	2
7	94	94	E	1
8	98	101	SAAV	4
9	130	131	QQ	2
10	133	137	QQAID	5
11	144	149	QGATRN	6
12	158	161	PLST	4
13	182	188	KPSETSK	7
14	196	200	IQPVE	5
15	206	217	SRRETPRGFSEE	12
16	227	231	YRDSD	5
17	241	246	QRDGVE	6
18	283	283	P	1
19	302	307	LSGITG	6
20	324	335	VNEEGTEAAAAS	12

A4 AAS19

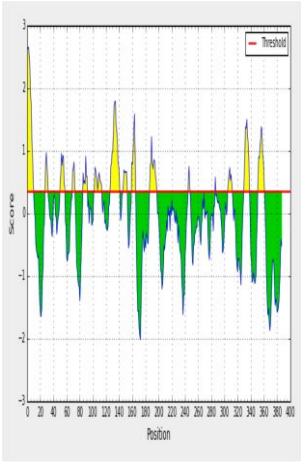

Predicted peptides

No.	Start	End	Peptide	Length
1	1	9	AEPDEDGRW	9
2	27	31	PSNAN	5
3	50	57	AGARGDTL	8
4	69	72	DELN	4
5	85	91	DASRELP	7
6	102	113	AVAQEGYGVLPN	12
7	126	140	YIEADSSKKGEEAVE	15
8	146	152	VSDKTHG	7
9	159	164	DEPPDF	6
10	186	197	KARTKPRSFYNG	12
11	245	247	RNG	3
12	286	286	T	1
13	305	311	ADLSGIS	7
14	330	338	NEEGSEAAA	9
15	351	360	FVTPPPLPKV	10

A5 AAS4

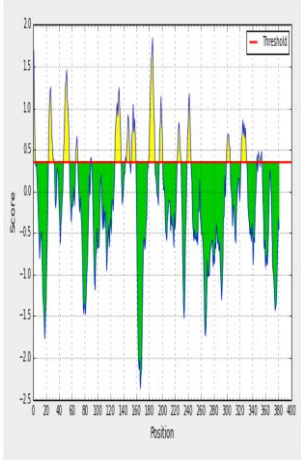

Predicted peptides

No.	Start	End	Peptide	Length
1	1	3	END	3
2	24	32	TQNPSSNVF	9
3	47	56	AGARGSSEAE	10
4	66	69	VGLT	4
5	89	90	NV	2
6	127	136	FANEGPRVAA	10
7	143	149	RGKTRGK	7
8	152	159	GILPEGQP	8
9	179	188	KFDPANTENK	10
10	196	200	TEVSK	5
11	224	229	IPYSGD	6
12	239	244	DSPTGL	6
13	300	305	ANFTGI	6
14	322	331	VEVNEEGTIA	10
15	347	347	A	1
16	349	351	LPP	3
17	353	354	QF	2

A6 AAS6

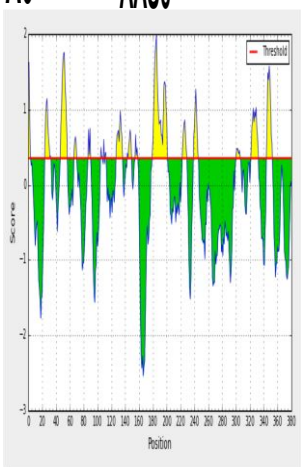

Predicted peptides

No.	Start	End	Peptide	Length
1	1	3	ETD	3
2	24	32	AQNPSSNVF	9
3	47	56	TGAGGSSEAE	10
4	66	69	VGLT	4
5	87	90	SPNV	4
6	105	107	EVA	3
7	109	109	S	1
8	111	112	KQ	2
9	127	136	FANEGSRVAA	10
10	143	149	RGKTRGK	7
11	155	158	PEGQ	4
12	179	201	QFDPSQTKDKPFLNQGTTEVSKP	23
13	223	229	EIPYSGD	7
14	239	245	DSPTGLA	7
15	300	306	ANFSAIS	7
16	322	332	VEVNEEGTVAT	11
17	344	352	LHTPPPPIQ	9

B1

EMP

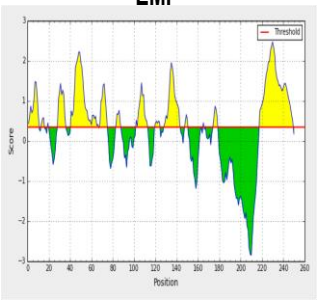

No.	Start	End	Peptide	Length
1	1	10	AIQTSEEIPG	10
2	13	15	VIL	3
3	19	19	S	1
4	29	35	TDYPDKK	7
5	41	66	KDGKDVPREPGDKKYVVNSDKNTLEV	26
6	68	74	DAGYGDA	7
7	83	87	DGENA	5
8	102	112	ISKNQVEGDPL	11
9	120	124	GVPTP	5
10	128	143	WFKDDEPLNSSDPRIT	16
11	148	150	NNV	3
12	163	163	D	1
13	165	165	R	1
14	167	167	Q	1
15	174	178	NGISN	5
16	218	249	RVKPDFEESDTDQNPENKNLSDQKEGQDIRQR	32

B2

IGFBP-rP1

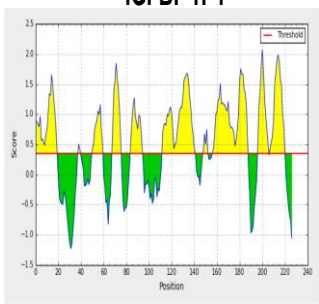

No.	Start	End	Peptide	Length
1	1	18	RKECGPCDLDRCEPPSGQ	18
2	38	39	EG	2
3	50	59	SLVDGPCGED	10
4	68	75	LAPGDPAE	8
5	84	94	EPVCGTDGVTY	11
6	112	141	EAASRGPCYSAPRVVTAPENTRNRTGGRAA	30
7	148	152	GFPVP	5
8	156	187	WRVDRGDGPLKSLPTDSSRINVQSRGGPDSFE	32
9	196	205	DPRPEDTATY	10
10	207	220	CAPANQNAEPSAAA	14

B3

AV422

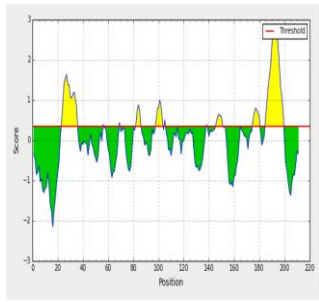

No.	Start	End	Peptide	Length
1	23	35	NPSGVATTDAEVD	13
2	56	56	A	1
3	69	69	E	1
4	82	86	GTDVR	5
5	98	103	QTLPDQ	6
6	105	105	K	1
7	138	138	G	1
8	146	150	SKCGE	5
9	175	180	YGEANA	6
10	185	199	LLPPPGTKPSGKPTS	15

B4

HRF

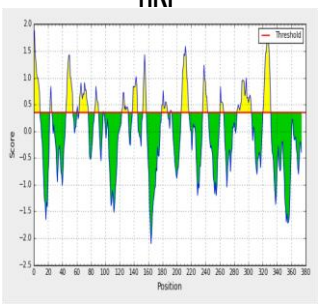

No.	Start	End	Peptide	Length
1	8	16	ISGDEMFTD	9
2	37	37	R	1
3	39	63	QGEIQLDGANPSAEEVDEGTDENVE	25
4	94	94	A	1
5	96	116	QEKWKEEGKSAEEIDDAKGKL	21
6	138	140	CNA	3
7	150	157	REQDGGGE	8

B5

TCI

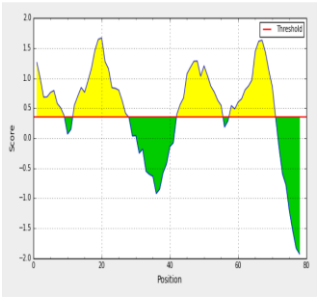

No.	Start	End	Peptide	Length
1	1	9	SQANDCVSN	9
2	12	27	GCLPESDCPEEARVNY	16
3	42	55	GCKSKGGECNPLNR	14
4	58	70	RELQSERGSCPEG	13

C1

CRT

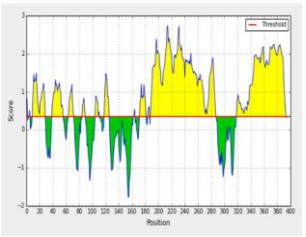

Predicted peptides

No.	Start	End	Peptide	Length
1	1	1	D	1
2	4	5	VY	2
3	9	28	EFNDGDGWKSRWVESTKGDN	20
4	39	55	FYGDAEKSKGLQTSEDA	17
5	64	71	FEPFSNEG	8
6	85	89	NIDCG	5
7	105	110	LHGESP	6
8	112	112	K	1
9	118	125	DICGPGTK	8
10	163	164	NT	2
11	172	181	EVAEKGELES	10
12	184	186	SFL	3
13	188	287	PKKIKDPEAKKPEDWDDRAKIDDPEDKKPEDWDKPEYIPDPDATKPEDWDD DMDGEWEPPQINNPEYKGEWKPKQIDNPAYKGAWVHPEIDNPEYTADPK DEEYARVHGEETWAALKDEEKKMKEKQEEEEDAKSKKEDDAKDEDEFEDE	100
14	318	393	EKEEDKEKEDEETTAAPEDDDHKHEE	76

C2

Ach

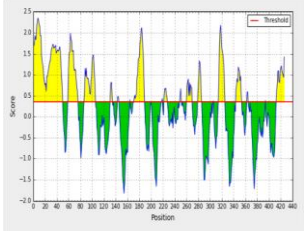

Predicted peptides

No.	Start	End	Peptide	Length
1	1	49	MPQQDGDATTPSTSSTSLSTSAASSVSTSQAPANATSSTTTGAASSGRS	49
2	59	75	ANTRPNPANYGVDDIPG	17
3	86	105	AGVDPQTWELKSEVPEYEGN	20
4	131	134	WQHE	4
5	143	145	ANS	3
6	164	164	L	1
7	171	188	WPFPGVSYRGGSPRDKEN	18
8	218	219	LE	2
9	222	227	YDIPEI	6
10	249	251	TDV	3
11	260	269	IDIGPQKTLN	10
12	279	285	SSGAPKS	7
13	305	306	QH	2
14	314	325	RDVPPRPGPFVR	12
15	344	353	KREFDEEGKC	10
16	363	364	IG	2
17	394	394	D	1

Figure 3. Recombinant expression of 13 tick saliva proteins in *Pichia pastoris*. Each of the 13 candidate tick saliva proteins were expressed using the pPICZα plasmid and *P. pastoris* (X-33 strain) system to as described in materials and methods. Recombinant proteins were affinity purified under native conditions and verified by (A) western blot analyses using the antibody to the hexa-histidine fusion tag and purity of the purified recombinant protein confirmed by (B) silver stain analysis. Protein concentrations are shown in the Table 1 insert in Figure 3.

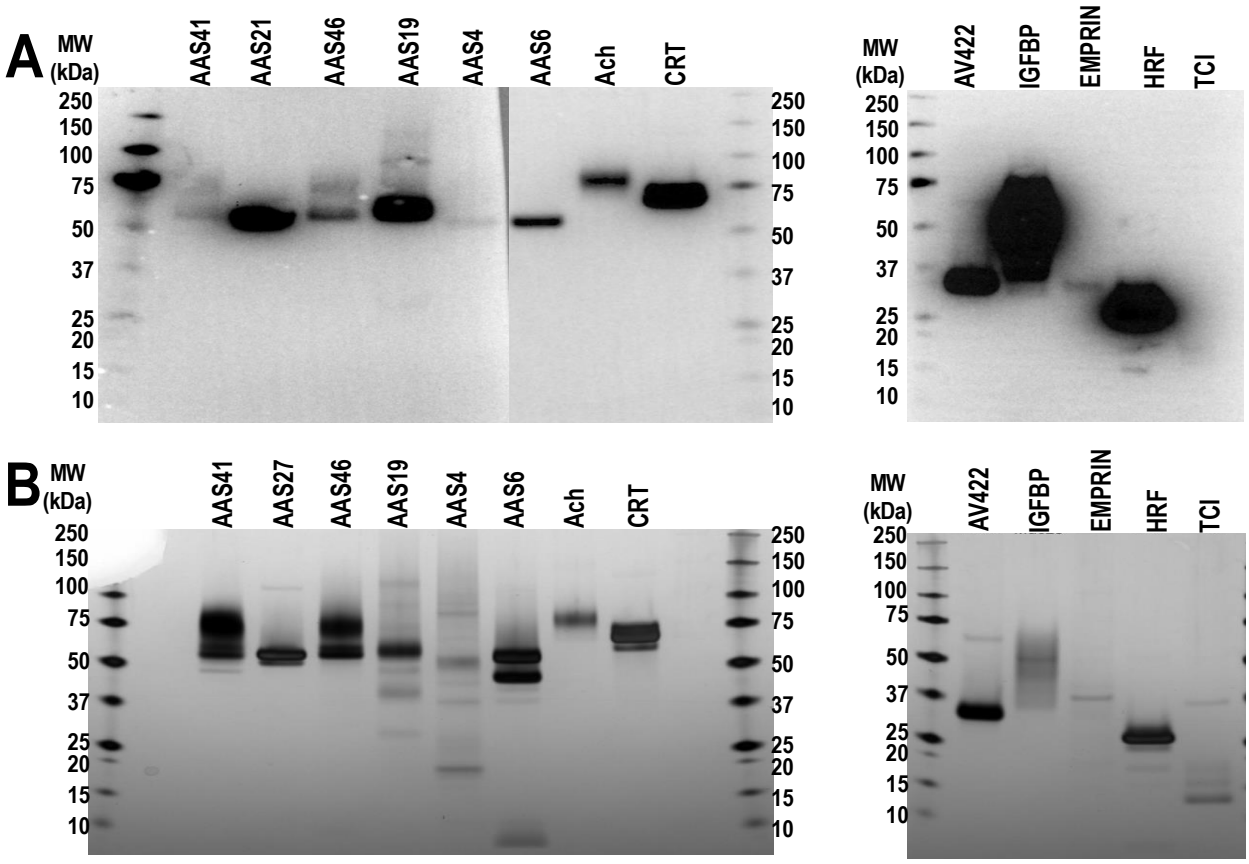
A
MW (kDa)
AAS41
AAS21
AAS46
AAS19
AAS4
AAS6
Ach
CRT
250
150
100
75
50
37
25
20
15
10
MW (kDa)
AV422
IGFBP
EMPRIN
HRF
TCI
B
MW (kDa)
AAS41
AAS27
AAS46
AAS19
AAS4
AAS6
Ach
CRT
MW (kDa)
AV422
IGFBP
EMPRIN
HRF
TCI

Figure 4. Immunization protocol and timeline. The experimental outline for immunization of cattle with 13 tick saliva antigens as a cocktail vaccine is shown in the diagram. A PBS-adjuvant control, and adjuvant with low and high amounts of cocktail vaccine were administered to three cattle per treatment. After two rounds of boosters, ticks were placed on immunized cattle to determine protective efficacy of the cocktail vaccine. Table 2 provides the timeline for blood collections, immunizations, and tick feeding challenge studies.

Experimental Outline

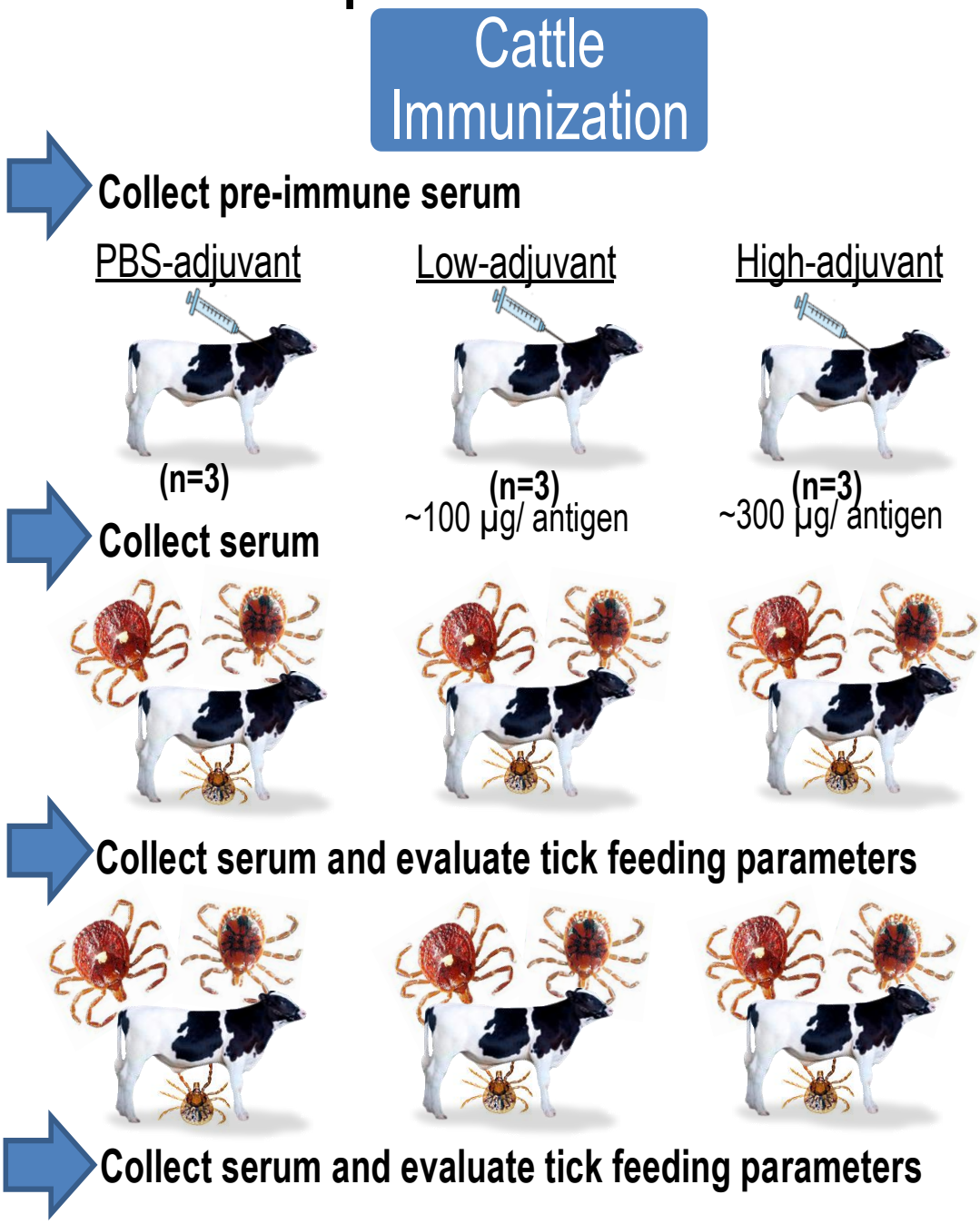

Figure 5. The selected recombinant tick saliva protein antigens are immunogenic in cattle. Affinity purified recombinant tick saliva proteins were resolved on a 10-20% Tris-Glycine SDS-PAGE for western blot analysis using antibodies of (A) PBS-adjuvant immunized, (B) low and (C) high antigen dose immunized, and (D) pre-immune sera at 1:1000 dilutions followed by goat anti-bovine IgG horseradish peroxidase (HRP) conjugated at 1:2000 dilution, and detected using a chemiluminescent substrate.

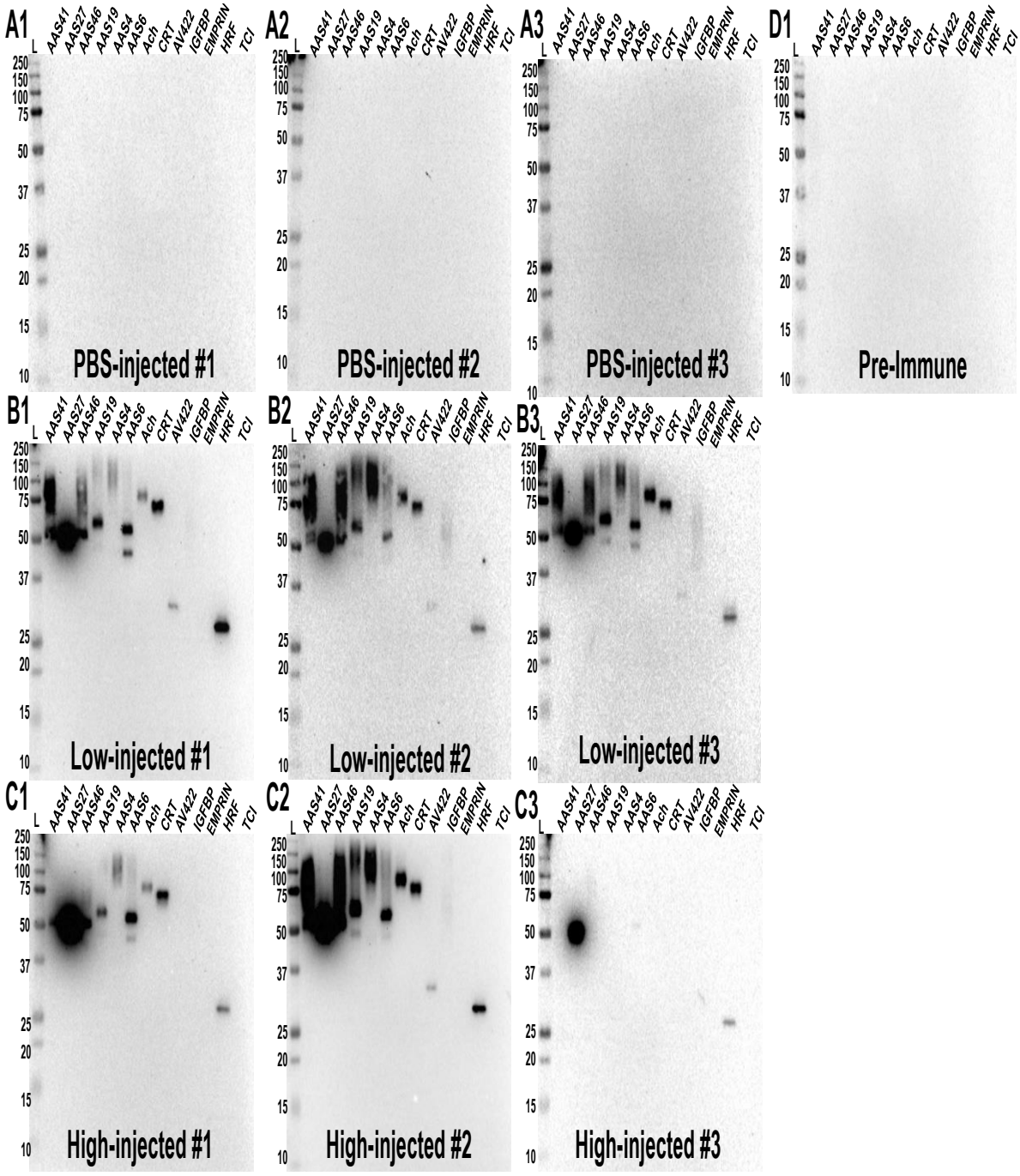
A1
L
AAS41
AAS27
AAS46
AAS19
AAS4
AAS6
Ach
CRT
AV422
IGFBP
EMPRIN
HRF
TCI
250
150
100
75
50
37
25
20
15
10
PBS-injected #1
A2
PBS-injected #2
A3
PBS-injected #3
D1
Pre-Immune
B1
Low-injected #1
B2
Low-injected #2
B3
Low-injected #3
C1
High-injected #1
C2
High-injected #2
C3
High-injected #3

Figure 6. Cattle antibody response to recombinant tick saliva antigens. Thirteen individual affinity purified recombinant tick saliva proteins were subjected to routine ELISA as described in materials and methods. Data points are represented by a total of 13 sera collections in the x-axis starting with the 1 (pre-immune), 2 (7 days after immunization), 3 (14 days after immunization), 4 (21 days after immunization), 5 (7 days after booster), 6 (14 days after booster), 7 (21 days after booster), 8 (7 days after second booster), 9 (14 days after second booster), 10 (21 days after first tick infestation), 11 (48 days after first infestation), 12 (7 days after second infestation), and 13 (14 days after second infestation) and A_{450nm} in the Y-axis. Based on observed A_{450nm}, antigens were group as (A1-5) highly immunogenic, (B1-5) moderately immunogenic, and (C1-3) lowly immunogenic. Filled blue circle and line (●) = PBS controls, filled red squares and line (■) = low antigen immunized, and filled green star and line (★) = high antigen immunized serums. Blue (⬇) and maroon (⬇) arrows indicate timepoints for first and second tick infestations, respectively.

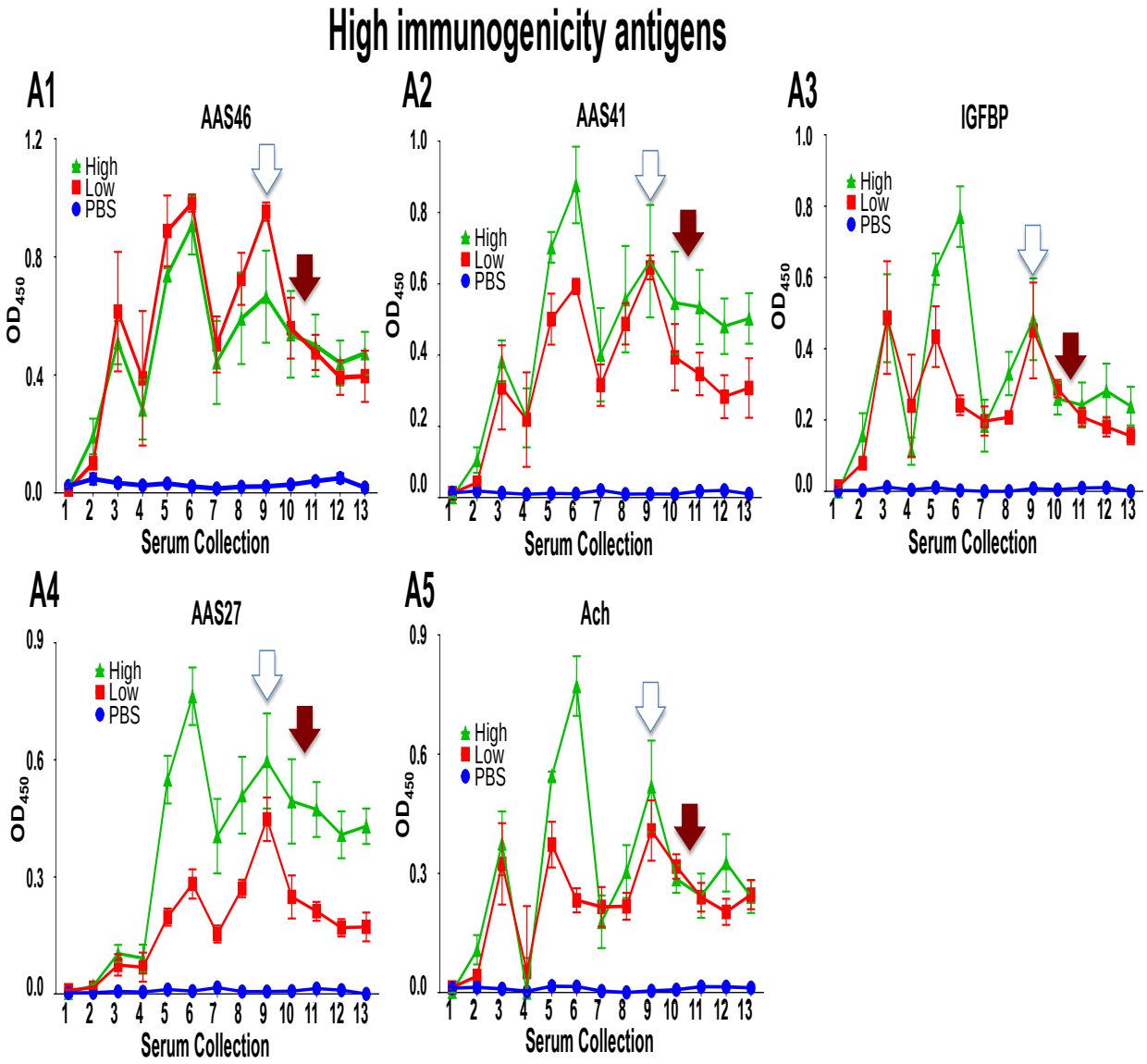
High immunogenicity antigens
A1
AAS46
A2
AAS41
A3
IGFBP
A4
AAS27
A5
Ach
High
Low
PBS
OD450
Serum Collection

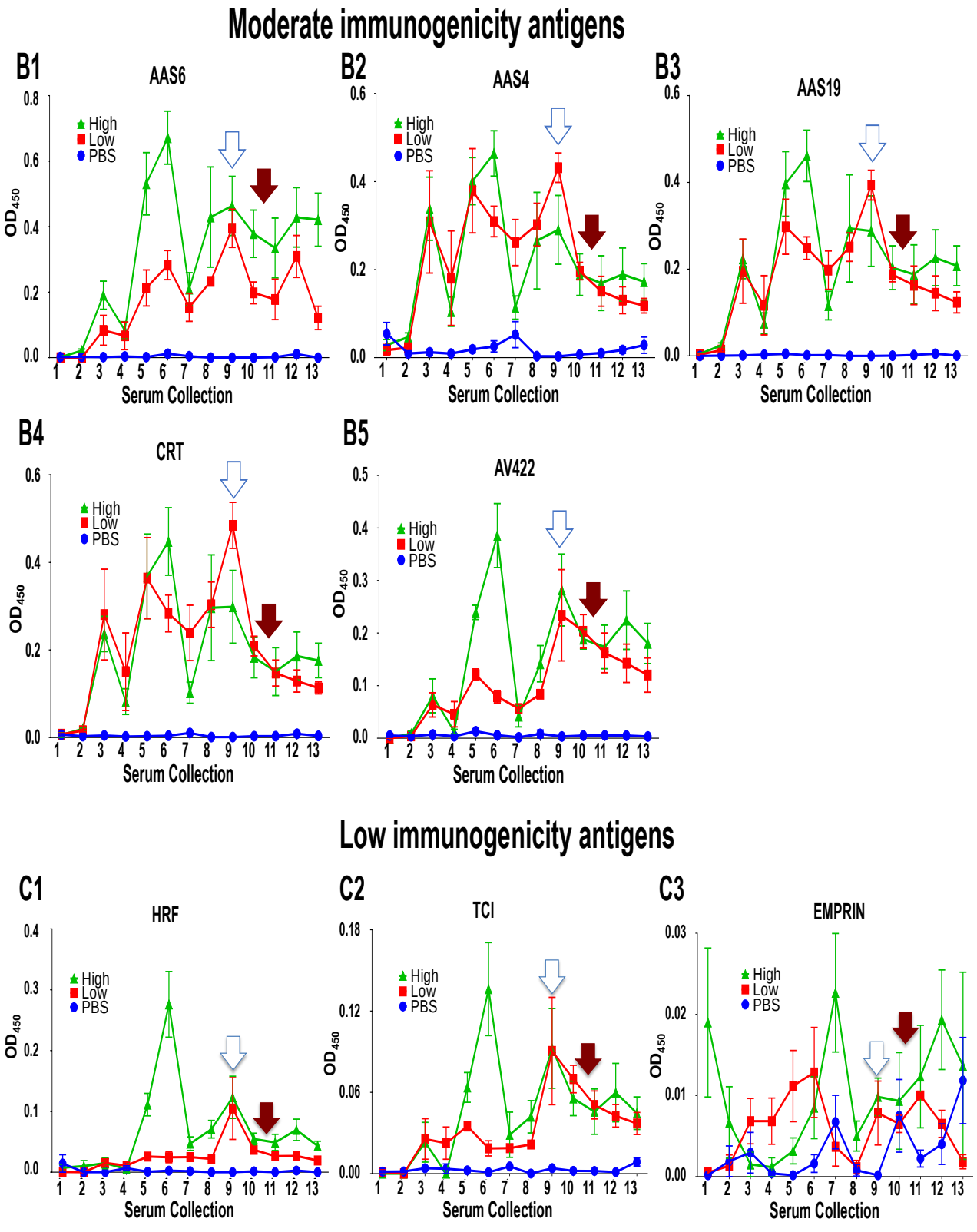
Moderate immunogenicity antigens
B1
AAS6
B2
AAS4
B3
AAS19
B4
CRT
B5
AV422
Low immunogenicity antigens
C1
HRF
C2
TCI
C3
EMPRIN
High
Low
PBS
OD450
Serum Collection

Figure 7. Effects of immunization on nymph (Fig. 7A) and adult (Fig. 7B) *A. americanum* feeding success. Tick feeding parameters for nymph ticks including; feeding dynamics (A1), % engorged (A2), engorgement weight (A3), and % molted (A4) were recorded during the first and second infestations. (B1) Engorgement weights (EW) of detached ticks that fed on control and immunized cattle groups were recorded from first and second infestations as indices for amounts of blood imbibed by ticks. Please note that due to limitations that are noted in the results section, analysis of adult tick feeding parameters was incomplete. Engorged ticks were incubated at 25°C and 85-90% relative humidity until molting (nymph) or egg laying (adult). (B2) Eggs were collected and weighed from the first and second infestations. (B3) To determine the egg mass conversion ratio (EMCR), as a measure of the tick's ability to utilize the blood meal to produce eggs, weights of egg masses were divided by engorgement weights (EW). EW, egg weights and EMCRs were subjected to One-Way ANOVA and Tukey's analysis to determine statistical significance. Data is reported as mean of EW, egg weights or EMCR (M ± SEM).

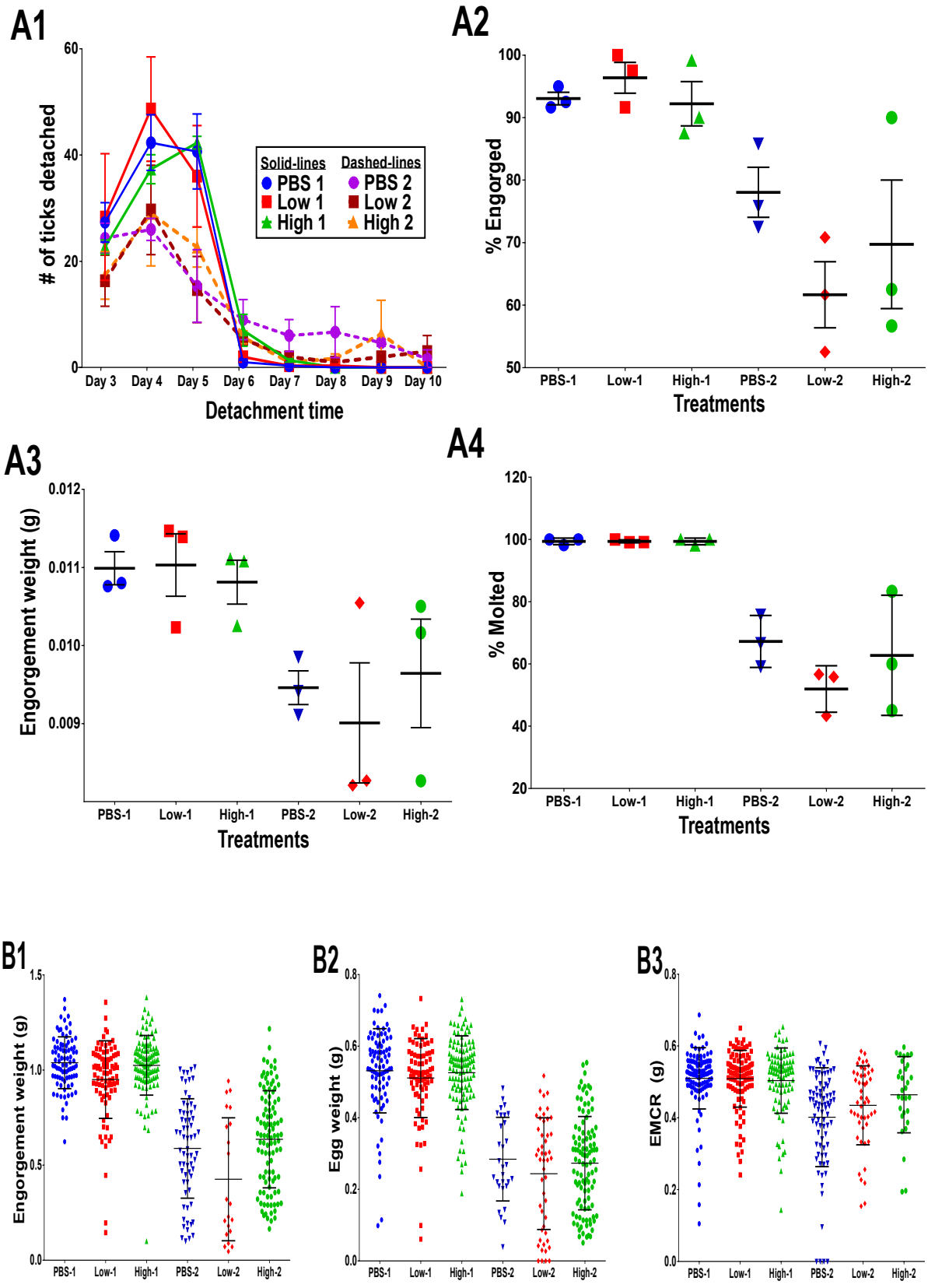
A1
# of ticks detached
Detachment time
Day 3
Day 4
Day 5
Day 6
Day 7
Day 8
Day 9
Day 10
Solid-lines
PBS 1
Low 1
High 1
Dashed-lines
PBS 2
Low 2
High 2
A2
% Engorged
Treatments
PBS-1
Low-1
High-1
PBS-2
Low-2
High-2
A3
Engorgement weight (g)
Treatments
A4
% Molted
Treatments
B1
Engorgement weight (g)
B2
Egg weight (g)
B3
EMCR (g)

Table 1. Purified recombinant antigens concentrations

	Signal peptide	Mature size (AA)	ExpectedMW (kDa)	pI	Glycosylated (based on MW shift)	Final concentration (mg)
Ach	Yes	426	47.11	6.45	Yes	2.52
CRT	Yes	394	45.81	4.36	Yes	5.46
AAS19	Yes	387	43.09	6.74	Yes	3.52
AAS27	Yes	377	41.79	5.19	Yes	4.58
AAS4	Yes	381	41.42	6.16	Yes	3.88
AAS6	Yes	380	41.41	5.75	Yes	3.31
AAS46	Yes	374	41.17	5.59	Yes	3.04
AAS41	Yes	374	41.1	5.71	Yes	4.3
EMPRIN	Yes	250	27.82	5.21	Yes	2.37
IGFBP	Yes	226	24.42	8.73	Yes	4.04
AV422	Yes	211	23	9.32	Yes	6.16
HRF	No	173	19.66	4.58	Yes	8.13
TCI	Yes	78	8.373	8.69	Yes	2.19

Table 2. Immunization timeline

Time	Description
Day 0	Pre-Immune
	Primary injection
Day 7	7 days after primary injection
Day 14	14 days after primary injection
Day 21	21 days after primary injection
	Booster injection
Day 28	7 days after booster injection
Day 35	14 days after booster injection
Day 42	21 days after booster injection
	2nd Booster injection
Day 49	7 days after 2nd booster injection
Day 55	14 days after 2nd booster injection
	1st tick infestation
Day 112	3 weeks after 1st tick infestation
Day 123	2nd tick infestation
Day 139	Right after 2nd tick infestation
Day 146	1 week after 2nd tick infestation
Day 153	2 weeks after 2nd tick infestation

Table 3. First (3A) and second (3B) infestations of *A. americanum* nymph feeding parameters on cattle immunized with PBS control, low, and high tick saliva protein antigens cocktail vaccine

A **1st infestation**

Animal #	average weight (mg)	Engorged out of 120 (%)	Molted (%)	Not Molted (%)	Females (%)	Males (%)
702- control	11.41	111 (92.50)	109 (98.20)	2 (1.67)	61 (55.96)	48 (44.04)
705- control	10.76	114 (95.00)	114 (100)	0 (0.00)	58 (50.88)	56 (49.12)
714- control	10.80	110 (91.67)	110 (100)	0 (0.00)	52 (47.27)	58 (52.73)
711- low	10.23	117 (97.50)	116 (99.15)	1 (0.83)	54 (46.55)	62 (53.45)
715- low	11.39	110 (91.67)	110 (100)	0 (0.00)	68 (61.82)	42 (38.18)
722- low	11.47	120 (100.00)	119 (99.17)	1 (0.83)	72 (60.50)	47 (39.50)
709- high	10.25	105 (87.50)	105 (100)	0 (0.00)	51 (48.57)	54 (51.43)
717- high	11.11	108 (90.00)	106 (98.15)	2 (1.67)	62 (58.49)	44 (41.51)
720- high	11.08	119 (99.17)	119 (100)	0 (0.00)	60 (50.42)	59 (49.58)

B **2nd infestation**

Animal #	average weight (mg)	Engorged out of 110 (%)	Molted (%)	Not Molted (%)	Females (%)	Males (%)
702- control	9.41	87 (79.09)	80 (91.95)	7 (8.05)	39 (48.75)	41 (51.25)
705- control	9.11	91 (82.73)	71 (78.02)	20 (21.98)	37 (52.11)	34 (47.89)
714- control	9.85	103 (93.63)	91 (88.35)	12 (11.65)	54 (59.34)	37 (40.66)
711- low	8.27	63 (57.27)	52 (82.54)	11 (17.46)	26 (50.00)	26 (50.00)
715- low	10.55	85 (77.27)	68 (80.00)	17 (20.00)	27 (39.71)	41 (60.29)
722- low	8.21	74 (67.27)	67 (90.54)	7 (9.46)	28 (41.79)	39 (58.21)
709- high	8.27	68 (61.81)	54 (79.41)	14 (20.59)	20 (37.04)	34 (62.96)
717- high	10.50	108 (98.18)	100 (92.59)	8 (7.41)	55 (55.00)	45 (45.00)
720- high	10.16	75 (68.18)	72 (96.00)	3 (4.00)	38 (52.78	34 (47.22)

APPENDIX VII

CHAPTER V FIGURES

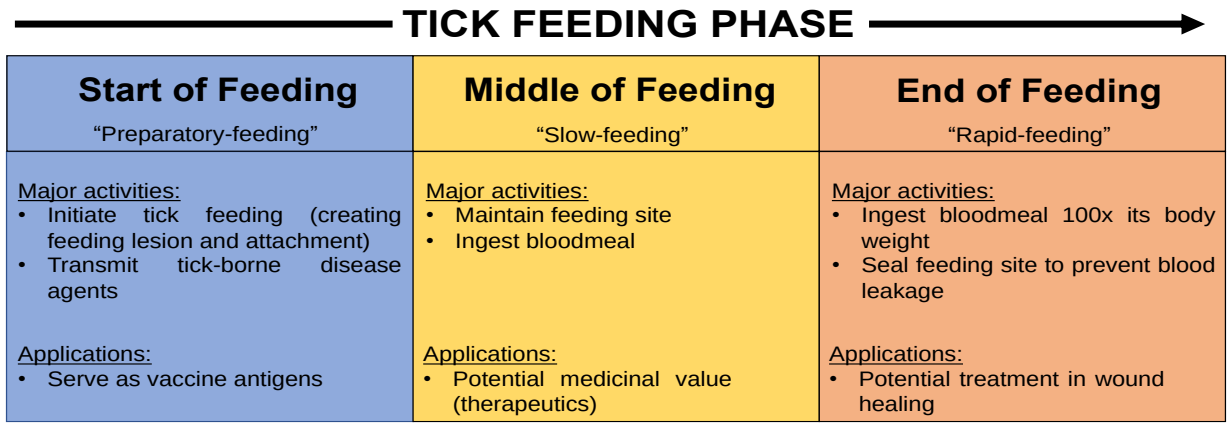

Figure 1. Mapping TSPs to broad tick feeding phases.